UNIVERSIDAD NACIONAL DE COLOMBIA

MASTER'S THESIS

Short distance constraints from HLbL contribution to the muon anomalous magnetic moment

---

Author:
Daniel Gerardo MELO PORRAS

Supervisors:
Prof. Dr. Angelo Raffaele FAZIO
Dr. Edilson Alfonso REYES ROJAS

A thesis submitted in fulfillment of the requirements
for the degree of Master in Science

in the

Grupo de Campos y Partículas
Departamento de Física

January 30, 2023

UNIVERSIDAD NACIONAL DE COLOMBIA

Resumen

Facultad de Ciencias

Departamento de Física

Magíster en Ciencias

Límites de corta distancia de la contribución HLbL al momento magnético anómalo del muon

por Daniel Gerardo MELO PORRAS

La dispersión HLbL no es la contribución hadrónica más grande para el momento magnético anómalo del muon, pero esta tiene la incertidumbre relativa más grande de todas las contribuciones a ese observable. Con la tensión entre la valor predicho por el Modelo Estándar y las mediciones actualmente en 4.2 σ, los físico teóricos se han centrado en reducir la incertidumbre de la contribución HLbL para reducir la tensión o llevarla más allá del umbral de descubrimiento. En tal escenario, la contribución de alta energía de la dispersión HLbL al momento magnético anómalo del muon juega un papel importante. El objetivo de la investigación desarrollada en esta tesis es estudiar la contribución HLbL de primer orden en la región de alta energía máximamente simétrica muy por encima del límite del umbral hadrónico. Esto se logra al realizar una expansión de productos de operadores del tensor HLbL, la cual realizamos sistemáticamente con el método de campos de fondo. Consideramos nuestra aproximación al problema muy eficiente, entre otras razones, porque esta permite la renormalización directa de los resultados de teoría de campos. Nuestro método es también original y, hasta nuestro mejor conocimiento, no se encuentra en la literatura. El quark loop sin masa es el primer término de la expansión y lo calculamos sin dejar de lado su estructura tensorial. Para lograrlo, usamos un método de descomposición tensorial de integrales de loop que no introduce singularidades cinemáticas. Las integrales escalares de loop resultantes con dimensiones modificadas son calculadas considerando toda su dependencia de la masa y utilizando la representación de Mellin-Barnes. Nuestro método original de cálculo para el quark loop proporciona una verificación independiente de los resultados publicados recientemente en la literatura. Más aún, al conservar la estructura tensorial completa de la amplitud, podemos llevar a cabo una verificación explícita de una descomposición libre de singularidades cinemáticas para la dispersión HLbL que juega un papel central en los cálculos dispersivos del régimen de baja energía.

Palabras clave: Momento magnético anómalo del muon; HLbL; Mellin-Barnes; OPE; Series hipergeométricas; Residuos multivariables; Singularidades cinemáticas.

UNIVERSIDAD NACIONAL DE COLOMBIA

Abstract

Facultad de Ciencias

Departamento de Física

Master in Science

Short distance constraints from HLbL contribution to the muon anomalous magnetic moment

by Daniel Gerardo MELO PORRAS

Hadronic Light by Light (HLbL) scattering is not the biggest hadronic contribution to the muon's anomalous magnetic moment, but it has the biggest relative uncertainty of all the contributions to that observable. With the tension between the Standard Model value prediction and the measurement at 4.2 σ, theoretical physicists have set their sights on reducing the HLbL contribution's uncertainty to reduce the tension or push it beyond the discovery threshold. In such scenario, the high energy contribution of HLbL scattering to anomalous magnetic moment of the muon plays an important role. The aim of the research developed in this thesis is to study the HLbL leading order contribution in the maximally symmetric high energy region well above the hadronic threshold limit. This is achieved by performing an operator product expansion of the HLbL tensor, which we do systematically in the background field method. We consider our approach very efficient, also because it allows a straightforward renormalization of the field theoretical results. Our approach is also original and at the best of our knowledge not available in literature. The massless quark loop is the leading term and we compute it without neglecting its tensor structure. To this end, we use a tensor–loop–integral decomposition that does not introduce kinematic singularities. The resulting scalar loop integrals with shifted dimensions are computed with their full mass–dependence using a Mellin–Barnes representation. Our original method of computation for the quark loop provides an independent check of recent literature results. Furthermore, by conserving the full tensor structure of the amplitude, we are able to perform an explicit check of a proposed kinematic–singularity–free tensor decomposition for the HLbL scattering amplitude that plays a central role in the dispersive computation in the low–energy regime.

Keywords: Anomalous magnetic moment of the muon; HLbL; Mellin-Barnes; OPE; Hypergeometric series; Multivariate residues; Kinematic singularities.

Acknowledgements

Primero que todo quiero agradecer al Profesor Angelo Raffaele Fazio, quien fue mi director de proyecto de maestría. Fruto de su generosa dedicación, sus clásicos cursos de teoría cuántica de campos continúan retando e iluminando a sus estudiantes. Como director, le agradezco su acompañamiento constante que, junto con su amplio conocimiento, han sido claves para la terminación de este proyecto. Al Profesor Edilson Reyes, codirector de esta tesis, quiero agradecerle su invaluable apoyo en el desarrollo de los scripts de cálculo simbólico. Su experiencia y claridad sobre este tema han sido de gran ayuda para dar el salto desde la programación tradicional.

Finalmente, quiero agradecer a mi familia por su apoyo constante desde que tengo memoria. A Luis Alberto, mi padre, por su ejemplo y por esas primeras clases de álgebra cuando apenas sabía dividir. A Carmen Elena, mi madre, por su dedicación sin reservas y por creer siempre en mí. A Luis Alberto, mi hermano, por ser mi confidente y escudero y por siempre estar dispuesto a tener una discusión bizantina conmigo.

Contents

List of Figures

List of Tables

Introduction

The Standard Model (SM) is the current theoretical paradigm for particle physics at its most fundamental level. This fact is rooted in the SM's mathematical consistency and specially in its highly accurate predictions for precision experiments. In fact, one of the most precisely verified theoretical predictions in the history of physics and in particular the true triumph of quantum field theory is the SM magnetic moment of the electron [1–3] $\vec{\mu} = g\left(\frac{e}{2m}\right)\vec{S}$, being m the electron mass and $\vec{S}$ its spin operator. The so called anomalous part is expressed by the quantity $a = \frac{g-2}{2}$, quantifying the deviation of the Landé factor from the classical value $g = 2$, and is entirely due to quantum-mechanical phenomena: the "cloud" of virtual particles with which the electron is constantly interacting, slightly changes the way it interacts with a classical magnetic field (see figure 1). Therefore, the measurement of the anomalous part of a particle's magnetic moment makes possible to test which kind of other particles it interacts with and what is the strength of the interaction. Consequently, this quantity is of the utmost interest for theoretical physicists when testing the SM itself and also theories so called Beyond the Standard Model (BSM). For the electron this anomalous part has been computed to $O(\alpha^5)$ in QED, for weak contributions the uncertainty is $\sim 10^{-16}$ and for hadronic contributions it is $\sim 10^{-14}$ [3]. The discrepancy with measurements is $8.76 \cdot 10^{-13}$ [2] or 2.42 times the standard uncertainty (often represented as σ), which is still far enough from the discovery threshold.

For the muon, the tension between the SM theoretical prediction for the anomalous magnetic moment a_μ and its experimental measurement is bigger. Therefore, it has attracted very much attention since the Brookhaven National Laboratory (BNL) experiment results shed light on the issue in 2004 [4]. There has been an enduring effort, on both the experimental and theoretical sides, to solve this tension or verify if such a discrepancy goes beyond the $5\,\sigma$ and thus to discern if it is a signal of New Physics (NP). To this end it is necessary to reduce the uncertainty on both the measurements and the SM theoretical value. Currently, the tension stands at 4.2σ if the 2021 results from Fermilab (FNAL) [5] are taken into account in addition to the BNL ones:

$$a_\mu^{BNL} = 116\,592\,089(63) \cdot 10^{-11}\,, \tag{1}$$

$$a_\mu^{Fermilab} = 116\,592\,040(54) \cdot 10^{-11}\,, \tag{2}$$

$$a_\mu^{exp} = \left(\frac{a_\mu^{BNL}}{\sigma_{BNL}^2} + \frac{a_\mu^{Fermilab}}{\sigma_{Fermilab}^2}\right)\left(\frac{1}{\sigma_{Fermilab}^2} + \frac{1}{\sigma_{BNL}^2}\right)^{-1}\,, \tag{3}$$

where σ represents the standard deviation of the corresponding value. As usual the combination of the two measurements is obtained from the principle of maximum likelihood which, mathematically realized by the method of least squares due to the Gaussian probability distribution, provides the above weighted average.

Consequently, the tension between the SM value and the measurement is:

$$\Delta a_\mu = a_\mu^{exp} - a_\mu^{SM} = 251(59) \cdot 10^{-11} \text{ or } 4.2\ \sigma\,. \tag{4}$$

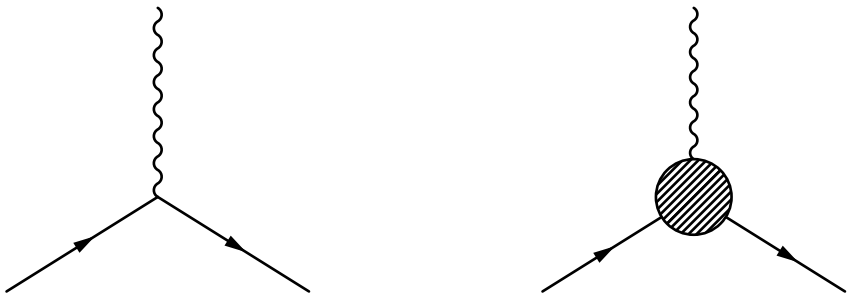

FIGURE 1: Interaction of a fermion with a classical electromagnetic field at tree level (left) vs. corrections due to virtual particles (right).

The most recent consensus SM prediction a_μ^{SM} has been obtained by the "Muon $g-2$ Theory Initiative" and is described in [6]. A review of recent developments can be found in [7]. The need for improvement in the SM values becomes more urgent in light of the projected uncertainty for the FNAL experiment: $16 \cdot 10^{-11}$ [8].

From the three fundamental interactions considered in the SM, only the strong force contribution currently has an uncertainty that is relevant with respect to the tension's value [6]. Therefore these strong contributions to a_μ are the main focus of the theoretical work towards reducing uncertainty. Hadronic contributions affect a_μ in two ways: the so called Hadronic Vacuum Polarization (HVP) and Hadronic Light by Light Scattering (HLbL).

The topology of diagrams from which the HVP contribution to a_μ arises can be seen in figure 2. This contribution is much larger than the HLbL one and moreover it can be computed from experimental measurements in the well–known approach of dispersive integrals [6]. More specifically, the contribution from HVP amounts to $6845 \cdot 10^{-11}$ and from HLBL it is $92 \cdot 10^{-11}$. HVP is essentially an hadronic correction to the photon propagator, then, because of analyticity of Green functions and the unitarity of the theory, it can be computed from the cross section of a virtual photon decaying into hadrons. This cross section can be extracted from $e^+e^- \longrightarrow Hadrons$ data in experiments such as $DA\Phi NE$, $BEPCII$, and $VEPP-2000$. The method of determination of the HVP amplitude by dispersive relation approach (dispersive method) involves integrals of the imaginary part of the amplitude expressed by the optical theorem in terms of the total cross section [9, 10]. Those integrals are performed in the center of mass energy variable, $\sqrt{s}$, by consequence it is necessary to know the $e^+e^- \longrightarrow Hadrons$ cross section at different values of s. This can be achieved either by directly changing the energy of the e^- and e^+ beams, called *direct scan* [11, 12], or by fixing it and letting the (measured) initial–state radiation do the work of varying the energy of the virtual photon which then decays into hadrons, called *radiative return* [13, 14]. There are also alternative methods of measuring HVP by τ decay experiments [15] and by measuring the hadronic contribution to the running of the fine structure constant $\alpha = e^2/4\pi$ from $\mu^- e^-$ elastic cross sections, called the MUonE project [16–18]. From the experimental side, efforts seek to tackle issues such as the lack of data on some hadronic channels or very close to the threshold and the tensions between current data. Instead, the theoretical work focuses on providing estimates on the contribution of unmeasured channels at low energy and directly computing contributions at high energy through perturbative QCD. Also there is interest in achieving a proper modelling of final–state radiation in multi–hadronic systems, for some experiments neglect these data and it is therefore necessary to put it back in before using it in the dispersion integrals [6]. Of course there are the constantly improving results of lattice QCD, which have very recently become comparable to the dispersive ones in terms of uncertainty [19].

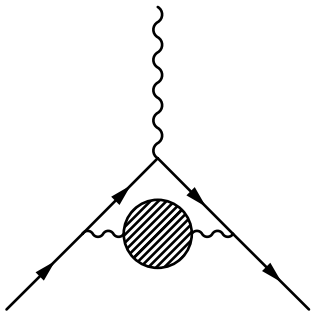

FIGURE 2: Hadronic vacuum polarization contribution to the anomalous magnetic moment of the muon. The blob contains only strongly interacting virtual particles.

In fact, this recent lattice computation is in tension with prior data–drive results, but it could by itself bring the tension with the experiment down to $1.5\,\sigma$. Currently, there is a search for new lattice works of similarly small uncertainty to confirm the tension and meaningful progress has been achieved already [20].

Now we go on to the HLbL scattering. The diagrams through which it contributes to a_μ can be seen in figure 3. The HLbL contribution has the typical size of the electroweak corrections to the a_μ, the latter amounting to $(156.1 \pm 1) \cdot 10^{-11}$ [6]. That size is what is expected from new physics (NP) and the amount requested experimentally to include BSM effects since the order of magnitude of what might be the contribution of new physics to the muon anomaly is expected to be: $a_\mu(EW)\left(\frac{M_W}{M_{NP}}\right)^2 \times$ couplings with $M_{NP} \gg M_W$ [21]. In contrast with HVP, the theoretical side of the HLbL scattering computation had been much less understood until recently. The added complexity is due to the fact that four currents are involved, instead of only two. This introduces several difficulties. First of all, HLbL scattering cannot be as cleanly related to e^+e^- annihilation or other experiments. Furthermore, the HLbL amplitude has a much more complex tensor decomposition: it is a linear combination of 43 tensors, even after gauge invariance constraints have been considered. Moreover, it is necessary to expand this set to a redundant one with 54 elements in order to avoid kinematic, meaning spurious or in general no-dynamical, singularities, that spoil the dispersive approach. In the end, for the purpose of computing a_μ^{HLbL}, it is only necessary to know 7 of these scalar coefficients, since the rest are related to them by crossing symmetry of Mandelstam's variables. Meanwhile, for HVP one initially has two tensor structures which are then reduced to one due to gauge invariance. In fact, this dispersion–fit tensor decomposition for HLbL was only recently found for the first time [22, 23]. This multiplicity of scalar coefficients makes the dispersive approach much more complex for HLbL than it is for HVP, because each coefficient requires its own dispersive integral. In spite of this, contribution of intermediate states with masses up to around 1 GeV have been quite successfully computed from this approach. These include pseudoscalar poles, box topologies and rescattering diagrams [6]. Particular applications with pions can be found in [23–25]. Before recent breakthroughs with the dispersive method, the low energy regime of the HLbL scattering was studied mostly with hadronic models, whose uncertainty was harder to assess. An advantage on the computation of the HLbL contribution with respect to the HVP one is that the first one appears at one further order of α than the second one and thus its computation requires slightly less accuracy. Finally, a common feature for both HLbL and HVP is that they are dominated by very different degrees of freedom at low and high energies, namely, hadrons and then quarks

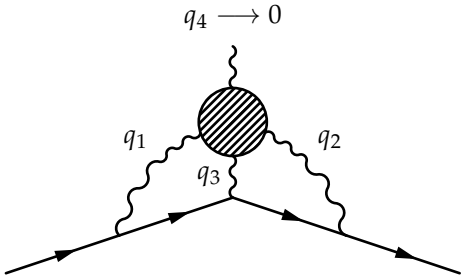

FIGURE 3: Hadronic light–by–light scattering contribution to the anomalous magnetic moment of the muon. The blob contains only strongly interacting virtual particles.

and gluons[1], respectively. The fact that HVP and HLbL amplitudes enter the muon vertex as an insertion of one and two loops, respectively, makes it necessary to properly "sew" the contributions from different approaches at different kinematic regions.

As mentioned previously, the HLbL amplitude at low photon virtualities (see figure 3) was obtained from low–energy QCD models (scalar QED for the pion, Nambu Jona-Lasinio model and vector meson dominance, for example) [26, 27] or, more recently, from dispersive integrals on hadronic production from multiple virtual photons [28]. Of course, these methods have a certain high energy limit of validity, be it conceptual or practical. For the dispersive approach it is the latter case. Extension to heavier intermediate states has been hindered by a lack of data on the necessary subprocesses and the increasing complexity of unitarity diagrams with multiple particles. Fortunately, heavy intermediate states contributions are suppressed in dispersive integrals by a narrower phase space and thus one can consider states up to certain mass and still obtain a useful result. Nevertheless, to assess or reduce the uncertainty coming from the neglected heavier states it is necessary to resort to tools that complement, replace or evaluate the dispersive approach at high energies. These tools are called *short distance constraints* (SDC). For example, in the high energy regions of dispersive integrals, data for an hadronic form factor can be replaced by the expression for its known asymptotic behaviour. One can also evaluate the asymptotic behaviour of HLbL scattering amplitude itself and use it to evaluate how well the set of intermediate states considered in the dispersive approach resembles such behaviour. For a finite number of intermediate states it is not possible to completely mimic such behaviour [29, 30], but this fact can be used to measure how well a set of intermediate states represent high energy contributions. Such studies are a key complement of dispersive computations and play a central role in uncertainty assessment [31–33]. There are two loop momenta configurations that lead to a high energy regime in HLbL scattering: $|q_1^2| \sim |q_2^2| \sim |q_3^2| \gg \Lambda_{QCD}^2$ and $|q_1^2| \sim |q_2^2| \gg \Lambda_{QCD}^2$, where q_1, q_2 and q_3 are the virtual photon momenta, q_4 is the real soft photon momentum representing the electromagnetic external field (see figure 3) and Λ_{QCD} is the QCD hadronic regime threshold. The main purpose of this research is to compute the HLbL scattering amplitude by the methods of perturbative QCD in the regime in which the absolute values of the three virtualities, q_1^2, q_2^2, q_3^2, are much larger than the hadronic threshold. In particular, we perform an operator product expansion (OPE) in an electromagnetic background for the HLbL scattering amplitude following [34–36], but we fully harness the background field method to provide an original and, in our view, more systematic framework, to include the hadronic contributions in the same spirit of QCD sum rules. The main result of the work is nevertheless the computation of the quark loop amplitude that constitutes the leading contribution of the HLbL scattering amplitude at high energies. Our computation can be considered an extension of the literature's

[1] In principle, the dispersive approach could be used at high energies (virtualities of the photons) as well, but then many more hadronic degrees of freedom are excited and it is not feasible to consider them all.

result, because we obtain and study the full tensor structure of the amplitude and obtain a complete series expansion of ligth quark mass corrections up to arbitrary order. The computation is implemented using original *Mathematica* scripts in combination with state–of–the–art packages, *FeynCalc* [37–39] and *MBConicHulls* [40], for computations in high energy physics.

The structure of this thesis is as follows. In the first chapter we present the basics of the computation of the HLbL contribution to a_μ with special focus on the dispersive approach. We also present a tensor decomposition of the HLbL amplitude suitable for a Mandelstam representation (that is, such that the scalar coefficient have not kinematic zeroes or singularities) and the projectors associated to its scalar coefficients. We also arrive to the master formula that provides the basis to compute the quark loop contribution to a_μ in terms of the Mandelstam decomposition scalar coefficients. In the second chapter we perform the OPE of the HLbL scattering amplitude considering operators of up to six mass dimensions. To avoid singularities related to the static limit for the soft external photon we introduce the latter as an external electromagnetic background field. We study the background field method for HLbL scattering and in that framework perform systematically the OPE computation. This allows us to introduce the renormalization of the OPE expansion and Wilson coefficients in a natural way from the perspective of background operators renormalization.

Chapter 3 contains the main original results of this work. In it we present the full computation of the quark loop (from the OPE Wilson coefficient), without using projectors. In contrast with the literature's approach, we compute the quark loop amplitude with its full tensor structure, i.e. without the use of projectors to obtain relevant amplitudes. This allows us to provide an explicit check of the generality of the kinematic–singularity–free decomposition of the HLbL scattering amplitude that is the base for dispersive computations. To this end, we present alternative loop tensor decomposition tools that do not introduce kinematic singularities [41]. We also compute the resulting scalar integrals keeping their full mass dependence by means of Mellin–Barnes integrals in multiple variables [42]. Lastly, we compute the quark loop contribution to a_μ and discuss the impact of such results. Finally, we give our conclusions and consider outlooks of future work. There are two appendices in this thesis. The first one presents the Gegenbauer polynomial method for computing the angular part of loop integrals, which plays a role in the derivation of the master formula for the HLbL scattering contribution to a_μ. The second appendix contains complements for the derivation of some of the second chapter's results.

Chapter 1

HLbL contribution to a_μ

In this chapter we review the basics of the computation of the HLbL contribution to a_μ with special focus on the dispersive approach. We present a tensor decomposition of the HLbL amplitude suitable for a Mandelstam representation (that is, such that the scalar coefficient have no kinematic zeroes or singularities) and the projectors associated to its scalar coefficients. We also arrive to the master formula which provides the basis to compute the quark loop contribution to a_μ in terms of the Mandelstam decomposition scalar coefficients.

1.1 Basics

In this section we present the basics of the anomalous magnetic moment of a fermion.

The magnetic moment of a particle is defined through its scattering amplitude on a classical magnetic field. More specifically, for a particle with spin s and magnetic moment μ interacting with a classical magnetic field $\boldsymbol{B}$, the matrix element of the interaction hamiltonian H_{int} between an initial state $\psi_{\boldsymbol{p}\sigma}$ with momentum $\boldsymbol{p}$ and spin projection σ and final state $\psi_{\boldsymbol{p}'\sigma'}$ is:

$$\langle \psi_{\boldsymbol{p}'\sigma'} | H_{int} | \psi_{\boldsymbol{p}\sigma} \rangle = -\frac{\mu}{s} (\boldsymbol{J}^{(s)})_{\sigma'\sigma} \cdot \boldsymbol{B}\ \delta^3(\boldsymbol{p}' - \boldsymbol{p}) \times 2m\ , \tag{1.1}$$

where δ^3 represents the Dirac delta in three dimensions, m stands for the particle's mass and $\boldsymbol{J}^{(s)}$ is the little group generator associated to a massive particle of spin s. It is worth noting that the factor $2m$ appears only due to the relativistic normalization of the states:

$$\langle \psi_{\boldsymbol{p}'\sigma'} | \psi_{\boldsymbol{p}\sigma} \rangle = 2p^0 \delta_{\sigma\sigma'} \delta^3(\boldsymbol{p}' - \boldsymbol{p})\ . \tag{1.2}$$

For a relativistic charged particle, the corresponding matrix element is:

$$\langle \psi_{\boldsymbol{p}'\sigma'} | H_{int} | \psi_{\boldsymbol{p}\sigma} \rangle = -e_q j_\mu A^\mu\ , \tag{1.3}$$

where A_μ is the classical electromagnetic potential, j_μ is the matrix element of the particle's current operator and e_q represents its electric charge. For the muon we have $s = 1/2$, $e_q = -e$[1] and:

$$j_\mu(x) = e^{i(p-p')x} \langle \mu^-_{\boldsymbol{p}'\sigma'} | J^\mu(0) | \mu^-_{\boldsymbol{p}\sigma} \rangle = e^{i(p-p')x} \overline{u}_{\boldsymbol{p}'\sigma'} \Gamma_\mu(p', p) u_{\boldsymbol{p}\sigma}\ , \tag{1.4}$$

[1] e represents the absolute value of the electric charge of the electron.

Dirac matrices' basis element	Available structures
1	P^μ, q^μ
γ^μ	γ^μ, $q^\mu \not{q}$, $q^\mu \not{P}$, $P^\mu \not{q}$, $P^\mu \not{P}$, $\epsilon^{\mu\nu\lambda\rho}\gamma_\nu P_\lambda q_\rho$
γ^5	$P^\mu\gamma^5$, $q^\mu\gamma^5$
$\gamma^\mu\gamma^5$	$\gamma^\mu\gamma^5$, $q^\mu \not{q}\gamma^5$, $q^\mu \not{P}\gamma^5$, $P^\mu \not{q}\gamma^5$, $P^\mu \not{P}\gamma^5$, $\epsilon^{\mu\nu\lambda\rho}\gamma_\nu\gamma^5 P_\lambda q_\rho$
$\sigma_{\mu\nu}$	$P^\alpha q^\beta \sigma_{\alpha\beta} P^\mu$, $P^\alpha q^\beta \sigma_{\alpha\beta} q^\mu$, $\sigma^{\mu\nu}P_\nu$, $\sigma^{\mu\nu}q_\nu$, $\epsilon^{\mu\nu\lambda\rho}\sigma_{\nu\lambda}P_\rho$, $\epsilon^{\mu\nu\lambda\rho}\sigma_{\nu\lambda}q_\rho$

TABLE 1.1: A priori available structures in the covariant decomposition of the muon electromagnetic on–shell vertex Γ^μ (see equation (1.4) and figure 1). We use $\sigma_{\mu\nu} = \frac{i}{2}[\gamma^\mu, \gamma^\nu]$

where J^μ represents the electromagnetic current Heisenberg operator of the muon, Γ_μ (in QFT) is the amplitude of the full on–shell vertex diagram to the right of Figure 1 and u_{ps} and $\overline{u}_{p's'}$ are the spinors associated to the incoming and outgoing muon, respectively.

Considering the fact that j_μ has to behave as a four vector under Lorentz transformations and it may contain elements of Dirac matrices, then Γ_μ must be a linear combination of the four–momenta, the Levi–Civita symbol $\epsilon^{\mu\nu\lambda\rho}$ and Dirac bilinears, which are listed in the first column of table 1.1. The tensor rank of these three types of objects can be lowered by contraction with each other and raised by multiplication among themselves, which broadens the number of spinor matrix elements that transform as a vector and thus a priori form a vector basis for j_μ. The complete set of independent structures that can be built in this way is written in the second column of table 1.1, where we have used the basis of total momentum $P^\mu \equiv p^\mu + p'^\mu$ and exchanged momentum $q^\mu \equiv p'^\mu - p^\mu$. However, such set can be greatly reduced. For example, from the available structures in the second column and second row of table 1.1, four elements are rendered trivial via the on–shell character of the spinors in (1.4). The remaining structures after using the Dirac equation of motion are written in table 1.2. Some cancellations require Dirac algebra and are worth mentioning:

$$[\not{p}, \not{p}'] = -2\not{p}'\not{p} + 2p\cdot p' \,, \tag{1.5}$$

$$[\not{p}, \gamma^\mu] = -2\not{p}\gamma^\mu + 2p^\mu \,, \qquad [\not{p}', \gamma^\mu] = 2\not{p}'\gamma^\mu - 2p'^\mu \,, \tag{1.6}$$

$$\gamma_5\gamma_\beta\epsilon^{\beta\mu\rho\tau}P_\rho q_\tau = \frac{i}{6}(\gamma^\mu[\gamma^\rho,\gamma^\tau] + [\gamma^\rho,\gamma^\tau]\gamma^\mu - \gamma^\rho\gamma^\mu\gamma^\tau + \gamma^\tau\gamma^\mu\gamma^\rho)P_\rho q_\tau \,, \tag{1.7}$$

$$\gamma_5\gamma_\beta\epsilon^{\beta\mu\rho\tau}\gamma_\rho q_\tau = \frac{i}{6}(\gamma^\mu[\gamma^\rho,\gamma^\tau] + [\gamma^\rho,\gamma^\tau]\gamma^\mu - \gamma^\rho\gamma^\mu\gamma^\tau + \gamma^\tau\gamma^\mu\gamma^\rho)\gamma_\rho q_\tau \,, \tag{1.8}$$

$$\gamma_5\gamma_\beta\epsilon^{\beta\mu\rho\tau}\gamma_\rho P_\tau = \frac{i}{6}(\gamma^\mu[\gamma^\rho,\gamma^\tau] + [\gamma^\rho,\gamma^\tau]\gamma^\mu - \gamma^\rho\gamma^\mu\gamma^\tau + \gamma^\tau\gamma^\mu\gamma^\rho)\gamma_\rho P_\tau \,. \tag{1.9}$$

The last three equations can be obtained by writing γ_5 as $\frac{i}{4!}\epsilon^{\mu\nu\lambda\rho}\gamma_\mu\gamma_\nu\gamma_\lambda\gamma_\rho$ (with $\epsilon_{0123} \equiv 1$) and then using the identity for the product of two Levi-Civita symbols. It is worth noting that γ^5 can be put at either side of these three equations and then they can be used to simplify to different structures of table 1.1.

By applying gauge invariance of the muon electromagnetic vertex, we can conclude that the most general tensor structure of $\overline{u}_{p'\sigma'}\Gamma_\mu(p',p)u_{p\sigma}$ is:

$$\overline{u}_{p'\sigma'}\Gamma_\mu(p',p)u_{p\sigma} = \overline{u}_{p'\sigma'}\Big(A_1(q^2)\gamma_\mu + P^\mu A_2(q^2) + (\gamma^\mu - \frac{2mq^\mu}{q^2})\gamma^5 A_3(q^2) + P^\mu\gamma^5 A_4(q^2)\Big)u_{p\sigma} \,.$$

Dirac matrices' basis element	Available structures
1	P^μ, q^μ
γ^μ	γ^μ
γ^5	$P^\mu\gamma^5$, $q^\mu\gamma^5$
$\gamma^\mu\gamma^5$	$\gamma^\mu\gamma^5$
$\sigma_{\mu\nu}$	None

TABLE 1.2: Remaining structures in the covariant decomposition of the muon electromagnetic on–shell vertex Γ^μ (see equation (1.4) and figure 1) after using Dirac's equation of motion.

However, it is more common to rewrite this via the Gordon identity:

$$\overline{u}_{\boldsymbol{p}'\sigma'}\gamma^\mu u_{\boldsymbol{p}\sigma} = \frac{1}{2m}\overline{u}_{\boldsymbol{p}'\sigma'}\{P^\mu + i\sigma^{\mu\nu}q_\nu\}u_{\boldsymbol{p}\sigma}\ , \tag{1.10}$$

$$\begin{aligned}\implies \overline{u}_{\boldsymbol{p}'\sigma'}\Gamma_\mu(p',p)u_{\boldsymbol{p}\sigma} = \overline{u}_{\boldsymbol{p}'\sigma'}\Big(&F_1(q^2)\gamma_\mu + i\sigma^{\mu\nu}\frac{q_\nu}{2m}F_2(q^2) + (\gamma^\mu - \frac{2mq^\mu}{q^2})\gamma^5 F_3(q^2)\\ &+ \sigma^{\mu\nu}\frac{q_\nu}{2m}\gamma^5 F_4(q^2)\Big)u_{\boldsymbol{p}\sigma}\ .\end{aligned} \tag{1.11}$$

This convention is used because $\sigma_{\mu\nu} \equiv \frac{i}{2}[\gamma^\mu, \gamma^\nu]$ is the generator of Lorentz transformations for covariant wave functions of Dirac fermions and therefore σ_{ij} generates rotations and little group transformations. Hence the parallel with (1.1) becomes straightforward. In (1.11) F_1, F_2, F_3 and F_4 are Lorentz invariant coefficients, also called "form factors". The first two are associated to parity conserving contributions and are also known as electric and magnetic form factor, respectively. On the other hand, F_3 and F_4 are related to parity violating and CP violating contributions, respectively, and are also known as anapole moment and electric dipole moment.[2]

Since the anomalous magnetic moment is related to a non–relativistic interaction, it is therefore necessary to evaluate the muon vertex in the limit of zero exchanged momentum, that is $q \to 0$. In such limit we have $F_1(0) = 1$ in order to define e as the physical electric charge measured in the interaction with a classical Coulomb field. Also we have $F_3(0) = 0$ in this limit. On the other hand, $F_2(0)$ and $F_4(0)$ are not constrained.

In the limit of zero exchanged momentum and a slowly varying magnetic field (1.3) and (1.4) become:

$$\langle\psi_{\boldsymbol{p}'\sigma'}|H_{int}|\psi_{\boldsymbol{p}\sigma}\rangle = 2m \times \frac{e}{m}(1 + F_2(0))(\boldsymbol{J}^{(1/2)})_{\sigma'\sigma}\cdot\boldsymbol{B}\ \delta^3(\boldsymbol{p'} - \boldsymbol{p})\ , \tag{1.12}$$

which means:

$$\mu = \frac{e}{2m}(1 + F_2(0))\ . \tag{1.13}$$

The number one that appears along with $F_2(0)$ is in fact $F_1(0)$. At tree level we have $\Gamma_\mu = \gamma_\mu$ and thus $\mu = \frac{e_q}{2m}$, which of course agrees with Pauli's equation and Dirac's equation in the non–relativistic limit. Then, quantum corrections to this classical value can be singled out by the

[2]These coefficients have to behave as a Lorentz scalar because the covariant vector transformation have already been taken into account in the tensor elements of the decomposition. Also, they can only depend on q^2, just as Γ^μ, because of translation invariance.

gyromagnetic factor g:

$$\mu \equiv g\frac{e_q}{2m}s \implies a \equiv \frac{1}{2}(g-2) = F_2(0)\ , \tag{1.14}$$

where a is called the anomalous part of the magnetic moment of such particle. For the muon we will use the symbols a_μ and g_μ.

1.2 Computing a_μ from Feynman amplitudes

The purpose of this section is to present an explicit formula to compute a_μ from the Feynman amplitudes of the muon electromagnetic vertex.

As seen in equation 1.11 and 1.14, a_μ can be computed from the amplitude of the electromagnetic vertex of the muon. However, we are only interested in the magnetic form factor F_2. The obvious path is to compute the amplitude of the relevant Feynman diagrams up to certain order and then rearrange the result according to 1.11 to finally read F_2 off. However, the rearrangement of the result becomes unbearably complex at higher perturbative orders. Therefore, it is more efficient to project F_2 out of the on–shell vertex in 1.4.

The projector needed for the electric and magnetic form factors are, respectively [43]:

$$P_1^\mu \equiv \frac{1}{(q^2-4m^2)^2}\Big(\frac{\gamma^\mu}{4}(q^2-4m^2)+\frac{3m}{2}P^\mu)\Big)\ , \tag{1.15}$$

$$P_2^\mu \equiv -\frac{m^2}{q^2(q^2-4m^2)}\Big(\gamma^\mu+\frac{q^2+2m^2}{m(q^2-4m^2)}P^\mu\Big)\ , \tag{1.16}$$

which are to be used in the following way:

$$F_i(q^2) = \mathrm{Tr}\{(\not{p}+m)P_{i\mu}(\not{p}'+m)\Gamma^\mu\}\ , \tag{1.17}$$

where the trace acts on the gamma matrices space. Thus, for our case of interest we have:

$$a_\mu = F_2(0) = -\lim_{q\to 0}\mathrm{Tr}\{(\not{p}+m)\frac{m^2}{q^2(q^2-4m^2)}\Big(\gamma_\mu+\frac{q^2+2m^2}{m(q^2-4m^2)}P_\mu\Big)(\not{p}'+m)\Gamma^\mu\}\ . \tag{1.18}$$

Note that it is not possible to explicitly take the $q\to 0$ limit straight away because of the $1/q^2$ factor in $P_{2\mu}$. Although expanding Γ^μ around $q=0$ is inevitable, we can cap the expansion at first order if we first reorganize P_2 a bit using a slightly different version of the Gordon identity for the on-shell vertex

$$(\not{p}'+m)\gamma^\mu(\not{p}+m) = \frac{1}{2m}(\not{p}'+m)\{P^\mu+i\sigma^{\mu\nu}q_\nu\}(\not{p}+m)\ , \tag{1.19}$$

$$\implies (\not{p}+m)P_2^\mu(\not{p}'+m) = (\not{p}+m)\frac{-m}{2(q^2-4m^2)}\Big(-i\sigma^{\mu\nu}\frac{q_\nu}{q^2}+\frac{3}{(q^2-4m^2)}P^\mu\Big)(\not{p}'+m)\ . \tag{1.20}$$

We see that the divergent term in the projector is of order $1/q$, so, as claimed, we only need to expand Γ^μ to first order in q to retain all the relevant terms in the $q\to 0$ limit:

$$\Gamma^\mu(q^2) = \Gamma^\mu(0) + q_\nu \underbrace{\partial^\nu\Gamma^\mu(q^2)|_{q=0}}_{\equiv\Gamma^{\mu\nu}}\ . \tag{1.21}$$

By inserting (1.21) as well as (1.20) into (1.18) with the substitutions $p' = \frac{1}{2}(P+q)$ and $p = \frac{1}{2}(P-q)$ we evaluate the corresponding expression at $q=0$ obtaining after some algebra:

$$\begin{aligned} a_\mu &= \lim_{q\to 0} \frac{-m}{2(q^2-4m^2)} \operatorname{Tr}\Big\{ (\frac{1}{2}\{\not{P}-\not{q}\}+m)\Big(-i\sigma_{\mu\nu}\frac{q^\nu}{q^2} + \frac{3}{(q^2-4m^2)}P_\mu\Big) \\ &\qquad \times (\frac{1}{2}\{\not{P}+\not{q}\}+m)(\Gamma^\mu(0)+q_\beta\Gamma^{\mu\beta})\Big\} \qquad (1.22) \\ &= \lim_{q\to 0} \frac{im}{2(q^2-4m^2)} \operatorname{Tr}\Big\{ (\frac{1}{2}\{\not{P}-\not{q}\}+m)\sigma_{\mu\nu}\frac{q^\nu}{q^2}(\frac{1}{2}\{\not{P}+\not{q}\}+m)\Gamma^\mu(0)\Big\} \\ &+ \lim_{q\to 0} \frac{im}{2(q^2-4m^2)} \operatorname{Tr}\Big\{ (\frac{1}{2}\not{P}+m)\sigma_{\mu\nu}\frac{q^\nu q_\beta}{q^2}(\frac{1}{2}\not{P}+m)\Gamma^{\mu\beta}\Big\} \\ &\qquad - \frac{3}{16m^3}\operatorname{Tr}\Big\{ (\not{p}+m)p_\mu(\not{p}+m)\Gamma^\mu(0)\Big\} \qquad (1.23) \\ &= \lim_{q\to 0} \frac{im}{2(q^2-4m^2)} \operatorname{Tr}\Big\{ \Big(-\frac{1}{2}\not{q}\sigma_{\mu\nu}\frac{q^\nu}{q^2}(\frac{1}{2}\not{P}+m) + (\frac{1}{2}\not{P}+m)\sigma_{\mu\nu}\frac{q^\nu}{q^2}(\frac{1}{2}\not{P}+m) \\ &\qquad + (\frac{1}{2}\not{P}+m)\sigma_{\mu\nu}\frac{q^\nu}{q^2}\frac{1}{2}\not{q}\}\Big)\Gamma^\mu(0)\Big\} \\ &+ \lim_{q\to 0} \frac{im}{2(q^2-4m^2)} \operatorname{Tr}\Big\{ (\frac{1}{2}\not{P}+m)\sigma_{\mu\nu}\frac{q^\nu q_\beta}{q^2}(\frac{1}{2}\not{P}+m)\Gamma^{\mu\beta}\Big\} - \frac{3}{8m^2}\operatorname{Tr}\Big\{ p_\mu(m+\not{p})\Gamma^\mu(0)\Big\}\,, \qquad (1.24) \end{aligned}$$

where we have neglected any terms of order q or higher and we have explicitly evaluated the limit for the part of the projector which has no $1/q^2$ factor. We still have divergent terms together with linear and bilinear tensor dependence on q^μ. To get rid of them we will harness the fact that $F_2(q^2)$ is a Lorentz scalar coefficient in a covariant tensor decomposition. Thus, before taking the $q\to 0$ limit we are allowed to perform Lorentz transformations on q^μ.

In particular, we can perform spatial rotations, thus, we carry out an angular average over the spatial components of q^μ taking P as reference, that is, leaving it fixed. The results are:

$$\begin{aligned} \int \frac{d\Omega}{4\pi} q^\mu &= 0\,, \\ \int \frac{d\Omega}{4\pi} q^\mu q^\nu &= \frac{q^2}{3}\Big(g^{\mu\nu} - \frac{P^\mu P^\nu}{P^2}\Big)\,. \end{aligned} \qquad (1.25)$$

The first result is obvious[3] by the oddness of the integrand. For the second result it was necessary to invoke Lorentz covariance to perform a tensor decomposition into $g^{\mu\nu}$ and $P^\mu P^\nu$ and then we turn to trace and contraction with P to find the corresponding coefficients.

By inserting the angular averages (1.25) inside (1.24) we obtain:

$$\begin{aligned} a_\mu &= \frac{-i}{48m}\operatorname{Tr}\Big\{ \Big(-\gamma_\alpha\sigma_{\mu\nu}(\not{p}+m) + (\not{p}+m)\sigma_{\mu\nu}\gamma_\alpha\}\Big)\Big(g^{\alpha\nu} - \frac{p^\alpha p^\nu}{m^2}\Big)\Gamma^\mu(0)\Big\} \\ &\qquad - \frac{i}{24m}\operatorname{Tr}\Big\{ (\not{p}+m)\sigma_{\mu\nu}\Big(g^\nu_\beta - \frac{p^\nu p_\beta}{m^2}\Big)(\not{p}+m)\Gamma^{\mu\beta}\Big\} - \frac{3}{8m^2}\operatorname{Tr}\Big\{ p_\mu(m+\not{p})\Gamma^\mu(0)\Big\} \\ &= \frac{-i}{48m}\operatorname{Tr}\Big\{ \Big(3i\{(\not{p}+m),\gamma_\mu\} + \frac{i}{m}\{(p_\mu - m\gamma_\mu),(\not{p}+m)\}\Big)\Gamma^\mu(0)\Big\} \\ &\qquad - \frac{i}{24m}\operatorname{Tr}\Big\{ (\not{p}+m)\sigma_{\mu\beta}(\not{p}+m)\Gamma^{\mu\beta}\Big\} - \frac{3}{8m^2}\operatorname{Tr}\Big\{ p_\mu(m+\not{p})\Gamma^\mu(0)\Big\} \end{aligned}$$

[3] Perhaps it is worth noting that $q^0 = \sqrt{\boldsymbol{p}'^2+m^2} - \sqrt{\boldsymbol{p}^2+m^2}$, too, is odd since p and p' have the same mass.

$$
\begin{aligned}
&= \frac{1}{48m}\,\mathrm{Tr}\left\{\left(6p_\mu + 4m\gamma_\mu + \frac{2}{m}p_\mu \not{p}\right)\Gamma^\mu(0)\right\} \\
&\quad + \frac{1}{48m}\,\mathrm{Tr}\left\{(\not{p}+m)[\gamma_\mu,\gamma_\beta](\not{p}+m)\Gamma^{\mu\beta}\right\} - \frac{3}{8m^2}\,\mathrm{Tr}\left\{p_\mu(m+\not{p})\Gamma^\mu(0)\right\} \\
&= \mathrm{Tr}\left\{\left(\frac{1}{12}\gamma_\mu - \frac{1}{4}\frac{p_\mu}{m} - \frac{1}{3}\frac{1}{m^2}p_\mu\not{p}\right)\Gamma^\mu(0)\right\} + \frac{1}{48m}\,\mathrm{Tr}\left\{(\not{p}+m)[\gamma_\mu,\gamma_\beta](\not{p}+m)\Gamma^{\mu\beta}\right\}, \qquad (1.26)
\end{aligned}
$$

where we have used multiple times the on-shell relation $(\not{p}+m)\not{p} = \not{p}(\not{p}+m) = m(\not{p}+m)$. The issues about the limit $q \to 0$ limit in Γ^μ and $\Gamma^{\mu\nu}$ will be addressed in section 1.5.

1.3 Computing a_μ from HLbL scattering amplitudes

In this section we specialize the result obtained in section 1.2 to compute a_μ from HLbL scattering amplitudes.

From all the SM interactions that can occur in the muon vertex shown in figure 1 and, thus, contribute to a_μ, in this work we are only interested in the ones coming from hadronic light–by–light scattering, whose diagrams are shown in Figure 3. The term "light–by–light" makes reference to the subdiagram appearing in figure 3, which has four external photons (three virtual and attached to the muon line and one representing and external field). The term "hadronic" is due to the fact that only strongly interacting particles (quarks and gluons) or hadrons (mesons and various resonances) are allowed to appear in the blob of figure 3, either as virtual exchanged particles or as poles of the amplitude, for the HLbL contributions.

The first step is to isolate the HLbL subdiagram amplitudes from the muon electromagnetic vertex ones. Making use of the Feynman rules for QED it is possible to read the result off the Feynman diagram in figure 3:

$$
\begin{aligned}
& i\mathcal{M}^\mu = -ie\overline{u}_{p'\sigma'}\Gamma^\mu u_{p\sigma}\,, \\
\Longrightarrow\ & \mathcal{M}^{\mu_4} = -e\overline{u}_{p'\sigma'}\Gamma^{\mu_4}u_{p\sigma} \\
&\quad = \overline{u}_{p'\sigma'}\int\frac{d^4q_1}{(2\pi)^4}\int\frac{d^4q_2}{(2\pi)^4}\frac{-i}{q_1^2}\frac{-i}{q_2^2}\frac{-i}{q_3^2}(-ie\gamma_{\mu_1})i\frac{\not{p}'+\not{q}_1+m}{(p'+q_1)^2-m^2} \\
&\qquad \times(-ie\gamma_{\mu_3})i\frac{\not{p}-\not{q}_2+m}{(p-q_2)^2-m^2}(-ie\gamma_{\mu_2})\mathcal{M}_{HLbL}^{\mu_1\mu_2\mu_3\mu_4}(q_1,q_2,q_3)u_{p\sigma}\,, \qquad (1.27)
\end{aligned}
$$

where $\mathcal{M}^\mu$ represents the Feynman amplitude of the muon electromagnetic vertex and $\mathcal{M}_{HLbL}^{\mu_1\mu_2\mu_3\mu_4}$ represents the Feynman amplitude of the hadronic blob inside figure 3. Let us present the matrix element related to this Feynman amplitude:

$$
\mathcal{M}_{HLbL}^{\mu_1\mu_2\mu_3\mu_4} = e^4 \times \underbrace{-i\int d^4x\int d^4y\int d^4z e^{-i(q_1x+q_2y+q_3z)}\langle\Omega|J_q^{\mu_1}(x)J_q^{\mu_2}(y)J_q^{\mu_3}(z)J_q^{\mu_4}(0)|\Omega\rangle}_{\equiv\Pi^{\mu_1\mu_2\mu_3\mu_4}}\,, \qquad (1.28)
$$

where $|\Omega\rangle$ represents the vacuum of the QCD and J_q stands for electromagnetic quark currents.[4] In the literature, $\Pi^{\mu_1\mu_2\mu_3\mu_4}$ is referred to as "fourth rank vacuum polarization tensor" [44–46] or

[4] More generally speaking, these represent electromagnetic currents of strongly interacting particles, but are reduced to quarks since gluons do not share interaction vertices with photons.

"HLbL tensor" [28, 34]. Introducing this new convention into (1.27) we obtain:

$$\Gamma^{\mu_4}_{HLbL} = -e^6 \int \frac{d^4q_1}{(2\pi)^4} \int \frac{d^4q_2}{(2\pi)^4} \frac{1}{q_1^2}\frac{1}{q_2^2}\frac{1}{q_3^2} \gamma_{\mu_1} \frac{\not{p}' + \not{q}_1 - m}{(p'+q_1)^2 - m^2} \gamma_{\mu_3} \frac{\not{p} - \not{q}_2 - m}{(p-q_2)^2 - m^2} \gamma_{\mu_2} \times \Pi^{\mu_1\mu_2\mu_3\mu_4}(q_1, q_2, q_3) \,. \tag{1.29}$$

The next step towards finding the HLbL contribution to a_μ, labelled a_μ^{HLbL} is to insert (1.29) into (1.26). Before doing that, though, it is useful to note that $\Pi^{\mu_1\mu_2\mu_3\mu_4}|_{q_4\to 0} = 0$ and therefore $\Gamma^{\alpha}_{HLbL}|_{q_4\to 0} = 0$. This can be deduced from the analysis of cross sections in the soft–photon limit presented in [47], which concludes that the cross section of a process in the limit in which an external photon becomes soft is equal to a sum of terms proportional to the amplitude of the process without the soft photon or its derivative plus vanishing contributions proportional to the soft photon momentum. In the context of HLbL scattering, the previous statement reads:

$$\Pi^{\mu_1\mu_2\mu_3\mu_4}(q_1, q_2, q_3, q_4) \sim \Pi^{\mu_1\mu_2\mu_3} A^{\mu_4} + \partial\Pi^{\mu_1\mu_2\mu_3} B^{\mu_4} + O(q_4) \,, \tag{1.30}$$

where $\Pi^{\mu_1\mu_2\mu_3}$ represents the three–photon scattering amplitude, A_{μ_4} and B_{μ_4} are two vectors of order $O(1/q_4)$ and $O(q_4^0)$, respectively, and ∂ represents derivative with respect to some kinematic variable of the problem. From Furry's theorem the three–photon amplitude is equal to zero and therefore $\Pi^{\mu_1\mu_2\mu_3\mu_4}$ vanishes (at least) linearly in the static field limit.[5] In the end we get:

$$a_\mu^{HLbL} = \frac{1}{48m} \mathrm{Tr}\left\{ (\not{p} + m)[\gamma_\mu, \gamma_\beta](\not{p} + m)\Gamma^{\mu\beta}_{HLbL} \right\} . \tag{1.31}$$

From (1.29) we find:

$$\frac{\partial\Gamma^{\mu_4}_{HLbL}}{\partial q_{4\nu_4}} = -e^6 \int \frac{d^4q_1}{(2\pi)^4} \int \frac{d^4q_2}{(2\pi)^4} \frac{1}{q_1^2}\frac{1}{q_2^2}\frac{1}{q_3^2} \gamma_{\mu_1} \frac{\not{p} + \not{q}_1 + m}{(p+q_1)^2 - m^2} \gamma_{\mu_3} \frac{\not{p} - \not{q}_2 + m}{(p-q_2)^2 - m^2} \gamma_{\mu_2} \times \Big(-\frac{2q_4^{\nu_4}}{q_3^2} + \frac{\partial}{\partial q_{4\nu_4}} \Big) \Pi^{\mu_1\mu_2\mu_3\mu_4} \,, \tag{1.32}$$

$$\frac{\partial\Gamma^{\mu_4}_{HLbL}}{\partial q_{4\nu_4}}\Big|_{q_4\to 0} = e^6 \int \frac{d^4q_1}{(2\pi)^4} \int \frac{d^4q_2}{(2\pi)^4} \frac{1}{q_1^2}\frac{1}{q_2^2}\frac{1}{q_3^2} \gamma_{\mu_1} \frac{\not{p} + \not{q}_1 + m}{(p+q_1)^2 - m^2} \gamma_{\mu_3} \frac{\not{p} - \not{q}_2 + m}{(p-q_2)^2 - m^2} \gamma_{\mu_2} \times \frac{\partial}{\partial q_{4\mu_4}} \Pi^{\mu_1\mu_2\mu_3\nu_4}\Big|_{q_4\to 0} \,, \tag{1.33}$$

where we have used the antisymmetry between μ_4 and ν_4 of $\partial^{\mu_4}\Pi^{\mu_1\mu_2\mu_3\nu_4}|_{q_4\to 0}$, which can be deduced by differentiating the Ward identity twice with respect to q_4. Finally turning back to a_μ^{HLbL} one obtains:

$$a_\mu^{HLbL} = \frac{e^6}{48m} \int \frac{d^4q_1}{(2\pi)^4} \int \frac{d^4q_2}{(2\pi)^4} \frac{1}{q_1^2}\frac{1}{q_2^2}\frac{1}{q_3^2} \frac{1}{(p+q_1)^2 - m^2} \frac{1}{(p-q_2)^2 - m^2} \times \mathrm{Tr}\left\{ (\not{p} + m)[\gamma_{\mu_4}, \gamma_{\nu_4}](\not{p} + m)\gamma_{\mu_1}(\not{p} + \not{q}_1 + m)\gamma_{\mu_3}(\not{p} - \not{q}_2 + m)\gamma_{\mu_2} \right\} \times \frac{\partial}{\partial q_{4\mu_4}} \Pi^{\mu_1\mu_2\mu_3\nu_4}|_{q_4\to 0} \,. \tag{1.34}$$

From here there are only three steps left to compute a_μ^{HLbL}: compute the Dirac trace, compute

[5] It is worth noting that it is not possible to arrive at this conclusion using Weinberg's eikonal factor since the external soft photon may be emitted by an internal line in the strongly–interacting blob.

$\partial^{\mu_4}\Pi^{\mu_1\mu_2\mu_3\nu_4}|_{q_4\to 0}$ and compute the two–loop integral. The trace can be performed straightforwardly. On the other hand, the computation of the HLbL amplitude is very complex and it is therefore necessary to study it in depth before advancing further.

1.4 Mandelstam representation for the HLbL amplitude

In this section we will present the dispersive approach for computing $\Pi^{\mu_1\mu_2\mu_3\mu_4}$ and the associated Mandelstam representation.

In the previous section we expressed a_μ in terms of the HLbL scattering amplitude $\Pi^{\mu_1\mu_2\mu_3\mu_4}$ which corresponds to the strong interactions appearing inside the blob of figure 3. It is well known that the strong interaction coupling α_s becomes larger and approaches 1 at low energies. The asymptotic freedom, therefore, invalidates the perturbation theory for the S–matrix at a lower energy scale than Λ_{QCD} $\sim$1 GeV. Since the amplitude $\Pi^{\mu_1\mu_2\mu_3\mu_4}(q_1, q_2)$ appears inside a two loop integral on q_1 and q_2, it is necessary to compute it at different energy regions involving perturbative and non–perturbative regimes. Furthermore, high energy contributions are also used as constraints for the asymptotic behaviour of the low energy contributions and it is therefore useful that computations in both regimes are performed in a unified framework. In this chapter we present one of the state of the art the dispersive frameworks for the computation of the low energy contribution to a_μ^{HLbL}, which will be the one used in chapters 2 and 3.

There are few tools that allow for the computation of amplitudes in non–perturbative regimes. The main two are: QFT in the lattice and the dispersive approach. The first one tries to solve the QFT equations in a finite spacetime cube of side length L with discrete Euclidean spacetime coordinates of spacing a. The observables of interest are then computed for different values of large L and $1/a$ and these results are then extrapolated to $L, 1/a \to \infty$ in order to recover the standard QCD results. Using a very different perspective, the dispersive approach [22–24, 28] relies on the analyticity properties of the scattering amplitudes and the unitarity of the S–matrix (probability conservation) to relate the scattering amplitudes of a process with the cross sections of its sub–processes. For those reasons we speak about data driven approach because it is based on the match with the poles of the found resonances. QFT computations in the lattice have very high numerical complexity due to the very large number of degrees of freedom involved.[6] Therefore, even for the simpler case of HVP only till very recently have its results become competitive with the dispersive ones in terms of uncertainty [19, 48, 49]. Furthermore, for HLbL the first lattice computations are relatively new are still not competitive with dispersive ones. Although the dispersive approach for the computation of the HLbL contribution to a_μ also has its drawbacks, the main one relating to the Mandelstam representation of $\Pi^{\mu_1\mu_2\mu_3\mu_4}$ have been recently overcome. This has allowed to obtain the most reliable accounts of a_μ^{HLbL} in recent years [6].[7] In this work we focus on the dispersive approach for the computation of a_μ^{HLbL}. It is based on four fundamental pillars: unitarity of the S–matrix, the Sugawara–Kanazawa theorem for functions of a complex variable and the Schwarz reflection theorem. We will review such pillars in order.

[6] There are essentially two main sources of complexity: the spacetime square side length L and the inverse of the spacetime coordinate discrete spacing $1/a$. These two need to be large in order to reduce the uncertainty coming from the extrapolation to $L, 1/a \to \infty$.

[7] Although the approach proposed in [22, 23, 28] has been the standard scheme in recent estimations of a_μ^{HLbL}, there exist alternate dispersive frameworks. For example, in [50–54] a dispersive equation is applied directly to the magnetic form factor F_2 instead of the HLbL Feynman amplitude.

1.4.1 Unitarity of the S–matrix

A key concept in relativistic quantum theories of fundamental interactions[8] is conservation of probability. In the context of transition rates, this concept appears as a feature of the S–matrix: its unitarity. Let us explore the consequences of such feature for the transition matrix T:

$$S^\dagger = S^{-1} \implies (1+iT)(1-iT^\dagger) = 1 \implies TT^\dagger = i(T^\dagger - T)\,. \tag{1.35}$$

If we evaluate a certain matrix element of S and insert a complete set of momentum eigenstates in last equation we obtain [55]:

$$\begin{aligned} 2\mathrm{Im}\mathcal{M}(i\to f) = \sum_n \Big(\Pi_{i=1}^n \int \frac{d^3\boldsymbol{q}_i}{(2\pi)^3}\frac{1}{2E_i}\Big)\mathcal{M}^*(f\to\{q_i\})\mathcal{M}(i\to\{q_i\}) \\ \times (2\pi)^4\delta^4(P_i - \sum_i q_i)\,, \end{aligned} \tag{1.36}$$

where $\mathcal{M}$ stands for a Feynman amplitude, i represents the initial state, f the final one and q_i the on–shell intermediate–states, which come from the insertion of the identity resolved in terms of the momentum eigenstates. If the initial and final states are the same then the right hand side turns into the total cross section for the transition between the initial states and all possible physical states of the theory, in which case we obtain the optical theorem.[9]

Equation (1.36) can only be applied in principle to the complete electromagnetic vertex amplitude. However, it is possible to identify and simplify terms in both sides of the equation such that it applies just as well to the HLbL subdiagram. The process may be regarded as two initial virtual photons scattering into two final virtual photons. At this point (1.36) does not seem to be of much help. We are now entitled to compute one amplitude in terms of infinitely many and infinitely complex different amplitudes. Additionally, it only provides us with the imaginary part of $\Pi^{\mu_1\mu_2\mu_3\mu_4}$. However, to compute observables such as a_μ^{HLbL} in (1.26) we need the complete amplitude. We will answer the first issue later. To deal with the second one we need to make use of the Nagawara–Kanazawa theorem, which reconstructs a complex variable function based on its analyticity (poles and branch cuts) properties. We will introduce it in the following.

1.4.2 Sugawara–Kanazawa theorem and Schwarz reflection identity

Consider a function of a complex variable z with (possibly) two branch cuts along the real axis: one to the right starting at c_1 and extending (possibly) to positive infinity and one to the left starting at $-c_2$ and extending (possibly) to negative infinity. Based on the following three requirements:

- $f(z)$ has finite limits in the positive real infinity direction above and below the right–hand cut.
- The limit of $f(z)$ in the negative real infinity direction above and below the left–hand cut exists.
- If $f(z)$ is divergent in certain infinite direction, such a divergence is weaker than a polynomial with finite power N such that $N \geq 1$.

[8] Not any quantum theory conserves probability. Non–relativistic systems with (non–hermitian) absorptive potentials are an example.

[9] This is the case for the HVP subdiagram in figure 2

then the Sugawara–Kanazawa theorem [56] claims that $f(z)$ may be represented as:[10]

$$f(z) = \sum_i \frac{R_i}{z - x_i} + \frac{1}{\pi}\Big(\int_{c_1}^{\infty} + \int_{-\infty}^{-c_2} \Big) \frac{\Delta_x f(x)}{x - z}\, dx + \lim_{x\to\infty} \overline{f}(x) \tag{1.37}$$

$$\Delta_x f(x) = \frac{1}{2i}\{f(x + i\epsilon) - f(x - i\epsilon)\} \tag{1.38}$$

$$\overline{f}(x) = \frac{1}{2}\{f(x + i\epsilon) + f(x - i\epsilon)\}\,, \tag{1.39}$$

where R_i represents the residue of $f(z)$ in x_i which lies on the real interval $[-c_2, c_1]$. The two integrals in (1.37) are performed along the real axis. This representation of $f(z)$ is usually called "dispersion relation". The last term is referred to as the "subtraction constant" and accounts for possible divergences of $f(z)$ in the infinity, which enter the equation as the contribution of the circumference of a Cauchy integration path at infinity. Except in the case of one–one scattering, amplitudes have independent variables, therefore applying (1.37) would require to fix all the other variables except one. In our specific case $\Pi^{\mu_1\mu_2\mu_3\mu_4}$ may be regarded as a function of the usual Mandelstam variables s, t and u for two–two scattering although only two of them are independent. Therefore, the Sugawara–Kanazawa theorem has to be applied twice; one for each independent variable. Then, for HLbL or any two–two scattering in general, the complete amplitude $\mathcal{M}$ requires a double dispersive integral representation (also known as Mandelstam representation [57]). The first step to build it is to write a single dispersive representation for, say, s, which we will consider to be unsubtracted for simplicity:

$$\mathcal{M}(s,t) = \sum_i \frac{R_i^s(t)}{s - x_i^s} + \frac{1}{\pi}\Big(\int_{c_1^s}^{\infty} + \int_{-\infty}^{-c_2^s} \Big) \frac{\Delta_{s'}\mathcal{M}(s',t)}{s' - s}\, ds'\,. \tag{1.40}$$

Since we are expecting $\mathcal{M}$ to "contain" the amplitudes for the three s–, t– and u– channel processes, it must be invariant under crossing. As such, given that t has a fixed value, we expect to have:

$$\mathcal{M}(s,t) = \sum_i \frac{R_i^s(t)}{s - x_i^s} + \frac{1}{\pi}\int_{c_1}^{\infty} \frac{\Delta_{s'}\mathcal{M}(s',t)}{s' - s}\, ds' + \frac{1}{\pi}\int_{c_1}^{\infty} \frac{\Delta_{u'}\mathcal{M}(u',t)}{u' - u}\, du'\,. \tag{1.41}$$

Now we perform an analytic continuation on t to whichever value we require. The t dependence of the residues is usually well–known via interaction form factors. However, the dependence of $\Delta\mathcal{M}$ is not. To deal with this once again we apply (1.37), but this time for $\Delta_s\mathcal{M}$ and for a fixed s' and the same for u:

$$\begin{aligned}
\Delta_{s'}\mathcal{M}(s',t) &= \frac{1}{\pi}\int_{c_2(s')}^{\infty} \frac{\Delta_{t'}\Delta_{s'}\mathcal{M}(s',t')}{t' - t}\, dt' + \frac{1}{\pi}\int_{c_2(s')}^{\infty} \frac{\Delta_{u'}\Delta_{s'}\mathcal{M}(s',u')}{u' - \overline{u}}\, du' \\
\Delta_{u'}\mathcal{M}(u',t) &= \frac{1}{\pi}\int_{c_2(u')}^{\infty} \frac{\Delta_{s'}\Delta_{u'}\mathcal{M}(s',u')}{s' - \overline{s}}\, ds' + \frac{1}{\pi}\int_{c_2(u')}^{\infty} \frac{\Delta_{t'}\Delta_{u'}\mathcal{M}(t',u')}{t' - t}\, dt'\,,
\end{aligned} \tag{1.42}$$

where $\overline{s}$ is the Mandelstam variable associated to u' and t, while $\overline{u}$ is the Mandelstam variable associated to s' and t. Inserting this into the single dispersion relation we obtain:

$$\begin{aligned}
\mathcal{M}(s,t) = &\sum_i \frac{R_i^s(t)}{s - x_i^s} \\
&+ \frac{1}{\pi^2}\int_{c_1}^{\infty} ds' \int_{c_2(s')}^{\infty} dt' \frac{\Delta_{t'}\Delta_{s'}\mathcal{M}(s',t')}{(s' - s)(t' - t)} + \frac{1}{\pi^2}\int_{c_1}^{\infty} ds' \int_{c_2(s')}^{\infty} du' \frac{\Delta_{u'}\Delta_{s'}\mathcal{M}(s',u')}{(s' - s)(u' - \overline{u})}
\end{aligned}$$

[10] There is also another result to this theorem that essentially claims that $f(z)$ has the same limit at infinity in any direction with positive (negative) imaginary part as it has along and above (under) the right (left) cut.

$$+\frac{1}{\pi^2}\int_{c_1}^{\infty}du'\int_{c_2(u')}^{\infty}ds'\frac{\Delta_{s'}\Delta_{u'}\mathcal{M}(s',u')}{(u'-u)(s'-\bar{s})}+\frac{1}{\pi^2}\int_{c_1}^{\infty}du'\int_{c_2(u')}^{\infty}dt'\frac{\Delta_{t'}\Delta_{s'}\mathcal{M}(t',u')}{(u'-u)(t'-t)}\,. \quad (1.43)$$

It is possible to combine the second and fourth terms by noting that $s'-\bar{s}=s'-s+u'-u=u'-\bar{u}$. The final result is:

$$\mathcal{M}(s,t)=\sum_i\frac{R_i^s(t)}{s-x_i^s} \quad (1.44)$$

$$+\frac{1}{\pi^2}\int_{c_1}^{\infty}ds'\int_{c_2(s')}^{\infty}dt'\frac{\Delta_{t'}\Delta_{s'}\mathcal{M}(s',t')}{(s'-s)(t'-t)}+\frac{1}{\pi^2}\int_{c_1}^{\infty}ds'\int_{c_2(s')}^{\infty}du'\frac{\Delta_{u'}\Delta_{s'}\mathcal{M}(s',u')}{(s'-s)(u'-u)}$$

$$+\frac{1}{\pi^2}\int_{c_1}^{\infty}du'\int_{c_2(u')}^{\infty}dt'\frac{\Delta_{t'}\Delta_{s'}\mathcal{M}(t',u')}{(u'-u)(t'-t)}\,. \quad (1.45)$$

Equation (1.45) is known as the Mandelstam representation of $\mathcal{M}$ and the objects $\Delta_i\Delta_j\mathcal{M}$ are called the double spectral functions of $\mathcal{M}$. The constant c_1 and the function c_2 have a physical meaning that will be explained in the next part of the section.

There is a caveat: the theorem applies for scalar functions of a complex variable, but $\Pi^{\mu_1\mu_2\mu_3\mu_4}$ is not one. Therefore, it is necessary to perform a tensor decomposition on it such the scalar coefficients of the tensor structures appearing in such decomposition will be treated by the Sugawara–Kanazawa theorem. The requirements on this tensor decomposition will be discussed later in the chapter.

1.4.3 Schwarz reflection principle

There is a subtlety that does not let us use (1.36) and (1.37) to compute $\Pi^{\mu_1\mu_2\mu_3\mu_4}$ just yet. $\Delta f(z)$ is not the imaginary part of $f(z)$, but its discontinuity across the right hand cut. The tool that allows us to overcome this problem is the Schwarz reflection principle, which states that if a function $f(z)$ of a complex variable z is real along certain finite segment Γ of the real axis, then:

$$f^*(z)=f(z^*)\,, \quad (1.46)$$

in a domain D of the z complex plane that contains Γ and in which $f(z)$ is analytic. For any physically allowed value of the kinematic variables that characterize a process (for example, the well known Mandelstam variables s, t and u for two–two scattering) there is always at least one possible intermediate state: the initial one. Intermediate states lighter than the initial one are always accessible, too. However, we can analytically continue the amplitude to unphysical values of its kinematic variables. At a sufficiently low center–of–mass (CM) energy no intermediate state is allowed and, thus, the amplitude becomes real. Therefore, the Schwarz reflection principle applies for any Feynman amplitude.

This theorem, along with the fact that a physical region in which the imaginary part of the amplitude is not null, implies the existence of a discontinuity across the physical region of the real axis of each kinematic variable. Let z be a kinematic variable of an amplitude $\mathcal{M}$, then:

$$2i\mathrm{Im}\mathcal{M}(z+i\epsilon)=\mathcal{M}(z+i\epsilon)-\mathcal{M}^*(z+i\epsilon)=\mathcal{M}(z+i\epsilon)-\mathcal{M}(z-i\epsilon) \quad (1.47)$$

$$=\Delta\mathcal{M}(z)\,. \quad (1.48)$$

Now, we can apply this tool to change $\mathrm{Im}\mathcal{M}$ for $\Delta\mathcal{M}$, which was the result we needed. Connecting this result with (1.36) we see that the constant c_1 of the previous section is in fact the CM–frame energy of the lightest multiparticle intermediate state. One–particle intermediate

states are already taken into account by poles. Analogously, this helps us understand the meaning of c_2. For a physical value of s and t, $\Delta\mathcal{M}$ is just $\mathrm{Im}\mathcal{M}$ and is hence real. However, if we analytically continue $\Delta\mathcal{M}$ beyond the physically permissible boundaries of t, it may (and does) become complex, betraying the existence of a discontinuity. $c_2(s)$ is the point where this happens. Note that this is true even if s takes a physically allowed value, as is the case in the initial fixed–t single dispersive integral of $\mathcal{M}$.

We can see that the presence of an infinite number of amplitudes in the equation for $\mathrm{Im}\mathcal{M}$ is not too problematic, because the contribution of heavier intermediate states will be suppressed by the reduced region in which they contribute to the dispersive integrals.

In summary, from this theoretical framework it is possible to compute scattering amplitudes (in particular $\Pi^{\mu_1\mu_2\mu_3\mu_4}$) with (1.37) in which $\Delta\mathcal{M}$ is replaced with $\mathrm{Im}\mathcal{M}$ thanks to the Schwarz reflection principle and in turn we obtain $\mathrm{Im}\mathcal{M}$ from (1.36).[11] This last step requires theoretical or experimental input to determine the scattering amplitudes of the intermediate states appearing in (1.36).

1.4.4 Tensor decomposition of $\Pi^{\mu_1\mu_2\mu_3\mu_4}$

We previously mentioned that it was necessary to decompose $\Pi^{\mu_1\mu_2\mu_3\mu_4}$ into tensor structures with scalar coefficients to apply the dispersive approach to these scalar functions. Nevertheless, the Mandelstam hypothesis cannot be considered to apply in general for these scalar coefficients as well. The key point behind this is that the tensor structures of the decomposition may have kinematic singularities and/or zeroes.[12] Since the complete amplitude does not have these, then the associated scalar coefficient must have corresponding kinematic zeroes and/or singularities such that they cancel the former. In such cases, zeroes (singularities) change the asymptotic (analytic) behaviour of the coefficients and this has an impact on the dispersion relation in the form of subtraction constants in (1.37). Such input has to be determined experimentally and its presence in (1.37) further hinders the computations.[13] In order to avoid these issues it is necessary to perform a tensor decomposition of the amplitude such that none of the tensor structures have kinematic singularities and/or zeroes. That is called a Bardeen–Tarrach–Tung (BTT) decomposition and it was found recently for $\Pi^{\mu_1\mu_2\mu_3\mu_4}$. Let us review the main steps in the computation of such decomposition [22].

The only covariant objects which we can work with are the metric and the momenta of the four photons. There are 138 possible combinations of said objects. The most general structure is therefore:

$$\begin{aligned}\Pi^{\mu_1\mu_2\mu_3\mu_4} = {} & g^{\mu_1\mu_2}g^{\mu_3\mu_4}\Pi^1 + g^{\mu_1\mu_3}g^{\mu_2\mu_4}\Pi^2 + g^{\mu_1\mu_4}g^{\mu_3\mu_2}\Pi^3 \\ & + \sum_{k,l} g^{\mu_1\mu_2}q_k^{\mu_3}q_l^{\mu_4}\Pi^4_{kl} + \sum_{j,l} g^{\mu_1\mu_3}q_j^{\mu_2}q_l^{\mu_4}\Pi^5_{jl} + \sum_{j,k} g^{\mu_1\mu_4}q_k^{\mu_3}q_j^{\mu_2}\Pi^6_{jk} \\ & + \sum_{i,l} g^{\mu_3\mu_2}q_i^{\mu_1}q_l^{\mu_4}\Pi^7_{il} + \sum_{i,k} g^{\mu_4\mu_2}q_k^{\mu_3}q_i^{\mu_1}\Pi^8_{ik} + \sum_{i,j} g^{\mu_3\mu_4}q_i^{\mu_1}q_j^{\mu_2}\Pi^9_{ij} \\ & + \sum_{i,j,k,l} q_i^{\mu_1}q_j^{\mu_2}q_k^{\mu_3}q_l^{\mu_4}\Pi^{10}_{ijkl}\,,\end{aligned} \tag{1.49}$$

[11] This sentence implicitly claims that the analytic properties of an amplitude can be obtained entirely from its dynamics, that is, from the intermediate states it allows. This claim is known as the "Mandelstam hypothesis" and it is related to the causality requirement of the theory.

[12] Kinematic zeroes are defined as zeros of denominators arising when a tensor decomposition is performed.

[13] It may even introduce ambiguities in the soft photon limit of $\mathrm{Im}\Pi^{\mu_1\mu_2\mu_3\mu_4}$ and its derivatives. See [28].

where the indices are $i \in \{2,3,4\}$, $j \in \{1,3,4\}$, $k \in \{1,2,4\}$ and $l \in \{1,2,3\}$.[14] There are no kinematic singularities in the scalar coefficients till this point. However there are kinematic zeroes coming from two constraints that we have not yet explicitly accounted for: gauge invariance and crossing symmetry.

Gauge invariance may be explicitly imposed by projecting each one of the Lorentz indices of the amplitude onto the orthogonal space of the associated virtual photon momentum. To this end the following projectors maybe used [59]:

$$\begin{aligned} I_{12}^{\mu\nu} &= g^{\mu\nu} - \frac{q_1^\mu q_2^\nu}{q_1 \cdot q_2} \\ I_{34}^{\mu\nu} &= g^{\mu\nu} - \frac{q_3^\mu q_4^\nu}{q_3 \cdot q_4} \end{aligned} \tag{1.50}$$

which are to be used by taking advantage of gauge invariance of $\Pi^{\mu_1\mu_2\mu_3\mu_4}$ and the projectors' properties:

$$\begin{aligned} I_{12}^{\mu_2\mu_2'}\Pi_{\mu_1\mu_2'\mu_3\mu_4} &= \Pi_{\mu_1}{}^{\mu_2}{}_{\mu_3\mu_4} & I_{12}^{\mu_1'\mu_1}\Pi_{\mu_1'\mu_2\mu_3\mu_4} &= \Pi^{\mu_1}{}_{\mu_2\mu_3\mu_4} \\ I_{34}^{\mu_3'\mu_3}\Pi_{\mu_1\mu_2\mu_3'\mu_4} &= \Pi_{\mu_1\mu_2}{}^{\mu_3}{}_{\mu_4} & I_{34}^{\mu_4\mu_4'}\Pi_{\mu_1\mu_2\mu_3\mu_4'} &= \Pi_{\mu_1\mu_2\mu_3}{}^{\mu_4} \end{aligned} \tag{1.51}$$

$$\Pi^{\mu_1\mu_2\mu_3\mu_4} = I_{12}^{\mu_1'\mu_1} I_{12}^{\mu_2\mu_2'} I_{34}^{\mu_3'\mu_3} I_{34}^{\mu_4\mu_4'} \Pi_{\mu_1'\mu_2'\mu_3'\mu_4'} \,. \tag{1.52}$$

Of course these are not the only projectors suitable for the job. We could have given each momentum its own projector, like, for example:

$$g^{\mu_1\mu_2} - \frac{q_1^{\mu_1} q_1^{\mu_2}}{q_1^2} \qquad \text{or} \qquad g^{\mu_1\mu_2} - \frac{q_2^{\mu_1} q_2^{\mu_2}}{q_2^2} \,.$$

However, by applying any transverse projectors to $\Pi^{\mu_1\mu_2\mu_3\mu_4}$ we are introducing kinematic singularities of the type $1/q_i \cdot q_j$. Thus, the less projectors we introduce and the simpler they are, the less types of kinematic singularities will be introduced.

Returning to (1.52) we find:

$$\begin{aligned} \Pi^{\mu_1\mu_2\mu_3\mu_4} = {} & I_{12}^{\mu_2\mu_1} I_{34}^{\mu_4\mu_3}\Pi^1 + I_{12\mu_3'}{}^{\mu_1} I_{34}^{\mu_3\mu_3'} I_{12}{}^{\mu_2}{}_{\mu_4'} I_{34}^{\mu_4\mu_4'}\Pi^2 + I_{12\mu_4'}{}^{\mu_1} I_{34}^{\mu_4\mu_4'} I_{12}{}^{\mu_2}{}_{\mu_3'} I_{34}^{\mu_3'\mu_3}\Pi^3 \\ & + \sum_{\substack{k=1,2 \\ l=1,2}} I_{12\mu_2'}{}^{\mu_1} I_{12}^{\mu_2\mu_2'} I_{34}^{\mu_3'\mu_3} q_{k\mu_3'} I_{34}^{\mu_4\mu_4'} q_{l\mu_4'}\Pi_{kl}^4 + \sum_{\substack{j=3,4 \\ l=1,2}} I_{12\mu_3'}{}^{\mu_1} I_{34}^{\mu_3'\mu_3} I_{12}^{\mu_2\mu_2'} q_{j\mu_2'} I_{34}^{\mu_4\mu_4'} q_{l\mu_4'}\Pi_{jl}^5 \\ & + \sum_{\substack{j=3,4 \\ k=1,2}} I_{12\mu_4'}{}^{\mu_1} I_{34}^{\mu_4\mu_4'} I_{12}^{\mu_2\mu_2'} q_{j\mu_2'} I_{34}^{\mu_3\mu_3} q_{k\mu_3'}\Pi_{jk}^6 + \sum_{\substack{i=3,4 \\ l=1,2}} I_{12}^{\mu_1'\mu_1} q_{i\mu_1'} I_{12}{}^{\mu_2}{}_{\mu_3'} I_{34}^{\mu_3'\mu_3} I_{34}^{\mu_4\mu_4'} q_{l\mu_4'}\Pi_{il}^7 \\ & + \sum_{\substack{i=3,4 \\ k=1,2}} I_{12}^{\mu_1'\mu_1} q_{i\mu_1'} I_{12}{}^{\mu_2}{}_{\mu_4'} I_{34}^{\mu_4\mu_4'} I_{34}^{\mu_3'\mu_3} q_{k\mu_3'}\Pi_{ik}^8 + \sum_{\substack{i=3,4 \\ j=3,4}} I_{12}^{\mu_1'\mu_1} q_{i\mu_1'} I_{12}^{\mu_2\mu_2'} q_{j\mu_2'} I_{34\mu_4'}{}^{\mu_3} I_{34}^{\mu_4\mu_4'}\Pi_{ij}^9 \\ & + \sum_{\substack{i=3,4 \\ k=1,2}} \sum_{\substack{j=3,4 \\ l=1,2}} I_{12}^{\mu_1'\mu_1} q_{i\mu_1'} I_{12}^{\mu_2\mu_2'} q_{j\mu_2'} I_{34}^{\mu_3'\mu_3} q_{k\mu_3'} I_{34}^{\mu_4\mu_4'} q_{l\mu_4'}\Pi_{ijkl}^{10} \end{aligned}$$

[14] Each index may be any three–element subset of the four photons momenta this choice in particular is due to [58] and has special crossing symmetric properties that are useful to determine constraints coming from such symmetry.

which has only 43 tensor structures, which means that we have taken into account 95 constraints coming from gauge invariance. At this point, due to the poles in the projectors, we see that the scalar coefficients have kinematic zeroes. Each projector introduces a term with no kinematic (the metric) and another one with a pole in $q_1 \cdot q_2$ or $q_3 \cdot q_4$. Therefore, two appearances of I_{12} and two of I_{34} in the tensor structures lead us to poles associated to all the possible combinations of $q_1 \cdot q_2$ and $q_3 \cdot q_4$ with up to two repetitions of each.

To take these zeroes out of the scalar coefficients it is necessary to eliminate the singularities from the tensor structures. This can be achieved by building linear combinations of these singular tensor structures such that the poles cancel. The precise procedure proposed by [59] deals with the poles by decreasing singularity order. In the first step poles of the form $(q_1 \cdot q_2)(q_3 \cdot q_4)$ are eliminated, first by linear combinations and, once this is not possible, by multiplying them by $q_1 \cdot q_2$ or $q_3 \cdot q_4$. The next step is to deal in the same way with the single–double poles, that is, $(q_1 \cdot q_2)(q_3 \cdot q_4)^2$ and $(q_1 \cdot q_2)^2(q_3 \cdot q_4)$. Single–single poles then come an so forth until there are no kinematic singularities left.

After following the previously mentioned procedure a 43–element basis [22] that contains no kinematic singularities or zeroes is found. However the Mandelstam representation of the amplitude is not yet possible: the basis found is actually not linearly independent in $q_1 \cdot q_2 = 0$ or $q_4 \cdot q_4 = 0$ nor it actually spans the complete space of possible gauge invariant tensors for the HLbL amplitude. This stems from the fact that there are 11 linear combinations of the basis elements that are proportional to $q_1 \cdot q_2$ and/or $q_3 \cdot q_4 = 0$ and some new tensor structure. Therefore, when $q_1 \cdot q_2 = 0$, the basis we found ceases to be linearly independent and said new tensor structure is no longer in the span of it.[15] Thus, it is necessary to add these 11 eleven new structures to the 43–element basis that has been just found in order to have a set that spans all relevant gauge–invariant tensor structures even at $q_1 \cdot q_2 = 0$ and $q_3 \cdot q_4 = 0$ [22]. Of course, since the set is not linearly independent, there is redundancy on the definition of the scalar coefficients associated to each tensor.

It is not surprising that our 43–element basis does not work as expected in $q_1 \cdot q_2 = 0$ and $q_3 \cdot q_4 = 0$; we found it after using projectors (1.50) and so assuming those terms were not zero. However it is not clear explicitly how we missed these 11 new structures. To see this it is necessary to impose gauge invariance directly from the definition, that is, without using singular projectors. To present the process we will work with gauge invariance in the first index of $\Pi^{\mu_1\mu_2\mu_3\mu_4}$:

$$\begin{aligned} q_{1\mu_1'}\Pi^{\mu_1'\mu_2\mu_3\mu_4} = 0 = {} & q_1^{\mu_2} g^{\mu_3\mu_4}\Pi^1 + q_1^{\mu_3} g^{\mu_2\mu_4}\Pi^2 + q_1^{\mu_4} g^{\mu_3\mu_2}\Pi^3 \\ & + \sum_{k,l} q_1^{\mu_2} q_k^{\mu_3} q_l^{\mu_4}\Pi^4_{kl} + \sum_{j,l} q_1^{\mu_3} q_j^{\mu_2} q_l^{\mu_4}\Pi^5_{jl} + \sum_{j,k} q_1^{\mu_4} q_k^{\mu_3} q_j^{\mu_2}\Pi^6_{jk} \\ & + \sum_{i,l} g^{\mu_3\mu_2}(q_1 \cdot q_i) q_l^{\mu_4}\Pi^7_{il} + \sum_{i,k} g^{\mu_4\mu_2} q_k^{\mu_3}(q_1 \cdot q_i)\Pi^8_{ik} + \sum_{i,j} g^{\mu_3\mu_4}(q_1 \cdot q_i) q_j^{\mu_2}\Pi^9_{ij} \\ & + \sum_{i,j,k,l} (q_1 \cdot q_i) q_j^{\mu_2} q_k^{\mu_3} q_l^{\mu_4}\Pi^{10}_{ijkl} \,. \end{aligned} \tag{1.53}$$

We must collect the factors of linearly independent tensor structures, which consequently must be zero, therefore constituting constraints between the scalar coefficients. To illustrate the point

[15] This was first mentioned by Tarrach [60] for the BTT decomposition of the $\gamma\gamma \to \pi\pi$ process.

we will work with constraints from the $g^{\mu_3\mu_2}q_1^{\mu_4}$ tensor:

$$\begin{aligned}0 = {} & q_1^{\mu_2} g^{\mu_3\mu_4}\Pi^1 + q_1^{\mu_3} g^{\mu_2\mu_4}\Pi^2 + q_1^{\mu_4} g^{\mu_3\mu_2}(\Pi^3 + \sum_{i=2,3,4}(q_1\cdot q_i)\Pi^7_{i1}) \\ & + \sum_{k,l} q_1^{\mu_2} q_k^{\mu_3} q_l^{\mu_4}\Pi^4_{kl} + \sum_{j,l} q_1^{\mu_3} q_j^{\mu_2} q_l^{\mu_4}\Pi^5_{jl} + \sum_{j,k} q_1^{\mu_4} q_k^{\mu_3} q_j^{\mu_2}\Pi^6_{jk} \\ & + \sum_{i,l\neq 1} g^{\mu_3\mu_2}(q_1\cdot q_i) q_l^{\mu_4}\Pi^7_{il} + \sum_{i,k} g^{\mu_4\mu_2} q_k^{\mu_3}(q_1\cdot q_i)\Pi^8_{ik} + \sum_{i,j} g^{\mu_3\mu_4}(q_1\cdot q_i) q_j^{\mu_2}\Pi^9_{ij} \\ & + \sum_{i,j,k,l}(q_1\cdot q_i) q_j^{\mu_2} q_k^{\mu_3} q_l^{\mu_4}\Pi^{10}_{ijkl}\,,\end{aligned} \tag{1.54}$$

$$\implies 0 = \Pi^3 + (q_1\cdot q_2)\Pi^7_{21} + (q_1\cdot q_3)\Pi^7_{31} + (q_1\cdot q_4)\Pi^7_{41}\,. \tag{1.55}$$

There are several conclusions that can be drawn from this example. In this case Π^3 may be written in terms of the other Π^7_{i1} without any assumptions on the value of the momenta scalar products. However, any other option to solve the equation requires to assume $q_1\cdot q_i \neq 0$ for some i. Note that after applying the transverse projectors the coefficient Π^7_{21} is cancelled, which, from the perspective of our constraint, means that equation (1.55) has been solved for Π^7_{21}. Another way to see this is to notice that solving (1.55) for Π^7_{21} introduces a $1/q_1\cdot q_2$ in the tensor structures that multiply Π^3 and the other Π^7_{i1}, which is exactly the problem we encountered when following the BTT procedure. But how can this fact affect linear independence of the 43–element basis that we found earlier? Note that, as far as constraint (1.55) is concerned, setting $q_1\cdot q_2 = 0$ in (1.55) renders Π^7_{21} linearly independent from Π^3 and the other Π^7_{i1}, while the latter are no longer independent. Therefore, the tensor structures that we find by using these replacements no longer span the space of relevant structures neither remain linearly independent in the problematic limits. The number of constraints remains the same, the problem is solely based on the intrinsic equation solving that we choose by using the projectors in (1.50). There is nothing special about the limit $q_1\cdot q_2$: other types of projectors or constraint solving procedures (like using $g^{\mu\nu} - q_1^\mu q_4^\nu/q_1\cdot q_4$ or solving for Π^7_{41} instead) would have introduced analogous and meaningless degeneracies in our gauge–invariant basis. As a final remark on this issues, let us address the possibility to solve the constraints in such a way that no assumptions on scalar products of momenta has to be made. We said that we could solve (1.55) for Π^3 without assumptions. A quick survey concludes that the remaining constraints can be solved for Π^1, Π^2, Π^4_{kl}, Π^5_{jl} and Π^6_{jk} without assumptions. However, when we turn to the constraints imposed by gauge invariance with respect to q_2, we find that solving for Π^5_{jl} and Π^6_{jk} involves assumptions on momenta scalar products. Analogously, Π^4_{kl} must be discarded when considering the constraints related to gauge invariance with respect to q_3. In the end, gauge invariance constraints can be safely solved only for Π^1, Π^2 and Π^3. There are 95 such constraints, so these coefficients are not enough. Note that this analysis applies regardless of which values the indices i,j,k,l take and, thus, is generally valid.

Finally, it is necessary to consider the crossing symmetries of $\Pi^{\mu_1\mu_2\mu_3\mu_4}$. Thanks to the choice of the i,j,k,l in (1.49), the crossing symmetries of the 54 tensor structures that span the amplitude are explicit and they have be checked in [22]. They are such that the "basis"[16] is crossing invariant as a set of tensor, although most elements are not.[17] In fact, only 7 of the 54 tensor are actually independent in terms of crossing symmetries.

[16] It is a basis in the sense that it spans the tensor structures of the amplitude, but it is not linearly independent.

[17] There are some elements that are actually crossing antisymmetric, but the corresponding kinematic zero does not affect the computation of a_μ [22].

1.5 Master formula for the HLbL contribution to a_μ

In the last three sections we have presented the formula that extracts the so called HLbL contribution to the anomalous magnetic moment of a muon and performed a tensor decomposition of the corresponding tensor, $\Pi^{\mu_1\mu_2\mu_3\mu_4}$, whose scalar coefficients are suitable for a Mandelstam representation. Now we have to combine these three results in order to relate a_μ^{HLbL} directly to the scalar coefficients of the tensor decomposition and therefore to the experimental data (in the low energy regime) via dispersion relations.

Since the tensor structures of $\Pi^{\mu_1\mu_2\mu_3\mu_4}$ are manifestly gauge invariant, therefore they must implement the soft photon zeroes mentioned earlier, that is, $T^{\mu_1\mu_2\mu_3\mu_4}|_{q_4\to 0} = 0$. This fact, together with absence of kinematic zeroes in the associated scalar coefficients leads us to:

$$\begin{aligned} a_\mu^{HLbL} = \frac{e^6}{48m}\int\frac{d^4q_1}{(2\pi)^4}\int\frac{d^4q_2}{(2\pi)^4}\frac{1}{q_1^2}\frac{1}{q_2^2}\frac{1}{q_3^2}\frac{1}{(p+q_1)^2-m^2}\frac{1}{(p-q_2)^2-m^2} \\ \times \mathrm{Tr}\left\{(\not{p}+m)[\gamma_{\nu_4},\gamma_{\mu_4}](\not{p}+m)\gamma_{\mu_1}(\not{p}+\not{q}_1+m)\gamma_{\mu_2}(\not{p}-\not{q}_2+m)\gamma_{\mu_2}\right\} \\ \times \sum_i^{54}\left(\frac{\partial}{\partial q_{4\nu_4}}T_i^{\mu_1\mu_2\mu_3\mu_4}|_{q_4\to 0}\right)\Pi_i|_{q_4\to 0}\,. \end{aligned} \tag{1.56}$$

From the 54 $T_i^{\mu_1\mu_2\mu_3\mu_4}$ tensor structures it is possible to perform a change of base to $\hat{T}_i^{\mu_1\mu_2\mu_3\mu_4}$ (which has no kinematic zeroes or singularities, too) such that only the derivatives of 19 of the elements do not vanish in the $q_4\to$ limit. In such basis we have:

$$a_\mu^{HLbL} = e^6\int\frac{d^4q_1}{(2\pi)^4}\int\frac{d^4q_2}{(2\pi)^4}\frac{1}{q_1^2}\frac{1}{q_2^2}\frac{1}{(q_1+q_2)^2}\frac{1}{(p+q_1)^2-m^2}\frac{1}{(p-q_2)^2-m^2}\times\sum_i^{19}\hat{T}_i\hat{\Pi}_i\,, \tag{1.57}$$

$$\begin{aligned} \hat{T}_i \equiv \frac{1}{48m}\mathrm{Tr}\left\{(\not{p}+m)[\gamma_{\nu_4},\gamma_{\mu_4}](\not{p}+m)\gamma_{\mu_1}(\not{p}+\not{q}_1+m)\gamma_{\mu_2}(\not{p}-\not{q}_2+m)\gamma_{\mu_2}\right\} \\ \times\left(\frac{\partial}{\partial q_{4\nu_4}}T_i^{\mu_1\mu_2\mu_3\mu_4}|_{q_4\to 0}\right)\,. \end{aligned} \tag{1.58}$$

The objects $\hat{T}_i$ act as kernels for the two loop integral. Their number can be further reduced to 12 by harnessing the symmetry of the integral and some of the kernels under the $q_1\leftrightarrow -q_2$ exchange. Therefore, some pairs of kernels actually give the same result and can be absorbed into one.

At this point a_μ^{HLbL} depends on five scalar products: q_1^2, q_2^2, $q_1\cdot q_2$, $q_1\cdot p$ and $q_2\cdot p$. We know by momentum conservation that F_2 (and therefore a_μ^{HLbL}) depends only on the exchanged momentum q_4, which we have already fixed. Thus, we should be able to remove the appearance of p in the expression for a_μ^{HLbL}. To achieve this let us start by performing a change of variables in which all the time components of the momenta are multiplied by i, also called a Wick rotation. This is essentially equivalent to rendering said time components imaginary. This causes all scalar products to acquire a minus sign and renders the corresponding metric euclidean. This transformation has non–trivial consequences for loop integrals, because it amounts to a rotation of the real axis of integration into the imaginary one. In case that the region swept by such rotation contains singularities, the resulting contributions have to be taken into account accordingly. However, for a_μ there no such issues [22] and the Wick rotation may be performed without problems. The Wick–rotated version of the momenta is represented by Q_1, Q_2 and P.[18] After the

[18] This capital "P" still represents the initial momentum of the muon. It should not be confused with $p+p'$, as was represented in previous sections.

Wick rotation is performed, the two–loop integrals may be transformed into two set of integrals over a four–dimensional hypersphere. Then it is possible to remove the spurious dependence on P by performing a four–dimensional angular average on P. To perform such integral average the Gegenbauer polynomials are a very useful tool [61].[19] The key point is to take advantage of the resemblance of the Wick–rotated propagators and the Gegenbauer polynomials' generating function to represent each propagator as a linear combination of polynomials and finally make use of their orthogonality properties. The procedure starts by expanding the scalar product in the propagator under study:

$$\frac{1}{(P \pm Q_i)^2 + m^2} = \frac{t_i}{|Q_i||P|} \frac{1}{t_i(|Q_i| \pm 2\hat{Q}_i \cdot \hat{P})} \,. \tag{1.59}$$

Then we require t_i to fulfill the following identity:

$$\frac{t_i}{|Q_i||P|} \frac{1}{t_i(|Q_i| \pm 2\hat{Q}_i \cdot \hat{P})} \equiv \frac{1}{1 \pm 2t_i\hat{Q}_i \cdot \hat{P} + t_i^2} \,, \tag{1.60}$$

where $\hat{P}$ and $\hat{Q}_i$ represent the unit vectors associated to the Euclidean vectors P_μ and $Q_{i\mu}$, while $|P|$ $|Q_i|$ represent their norm. Thus, we find:

$$t_i = \frac{1}{2} \frac{|Q_i|}{|P|} (1 - \sigma_i^E) \,, \tag{1.61}$$

where we have used the following notation:

$$\begin{aligned} \sigma_i^E \equiv & \sqrt{1 + \frac{m^2}{Q_i^2}} \,, \qquad Q_1 \cdot Q_2 \equiv |Q_1||Q_2|\tau \,, \qquad x \equiv \sqrt{1 - \tau^2} \,, \\ R_{12} \equiv & |Q_1||Q_2|x \,, \qquad z \equiv \frac{|Q_1||Q_2|}{4m^2}(1 - \sigma_1^E)(1 - \sigma_2^E) \,. \end{aligned} \tag{1.62}$$

Finally, by using the expression of the generating polynomial of the Gegenbauer polynomials we obtain:

$$\frac{1}{(P \pm Q_i)^2 + m^2} = \frac{t_i}{|Q_i||P|} \sum_{n=0}^{\infty} (-t_i)^n C_n(\pm \hat{Q}_i \cdot \hat{P}) \,, \tag{1.63}$$

where C_n represents the n–th Gegenbauer polynomial.

Then, a_μ is averaged over the four dimensional directions of p in order to take advantage of the orthogonality properties of these polynomials [62]. The absence of P in the scalar coefficients allows us to explicitly evaluate such average taking into account the dependence of the $\hat{T}_i$ on P. Since the kernels T_i are at most quadratic in P, only the following integrals are relevant:

$$\int \frac{d\Omega_4(P)}{2\pi^2} \frac{1}{(P + Q_1)^2 + m^2} \frac{1}{(P - Q_2)^2 + m^2} = \frac{1}{R_{12}m^2} \arctan\left(\frac{zx}{1 - z\tau}\right) \,, \tag{1.64}$$

$$\int \frac{d\Omega_4(P)}{2\pi^2} \frac{1}{(P + Q_1)^2 + m^2} = -\frac{1 - \sigma_1^E}{2m^2} \,, \tag{1.65}$$

$$\int \frac{d\Omega_4(P)}{2\pi^2} \frac{1}{(P - Q_2)^2 + m^2} = -\frac{1 - \sigma_2^E}{2m^2} \,, \tag{1.66}$$

[19] Some properties of the Gegenbauer polynomials and derivation of relevant integrals can be found in appendix A

$$\int \frac{d\Omega_4(P)}{2\pi^2} \frac{P\cdot Q_2}{(P+Q_1)^2+m^2} = Q_1\cdot Q_2 \frac{(1-\sigma_1^E)^2}{8m^2}\,, \tag{1.67}$$

$$\int \frac{d\Omega_4(P)}{2\pi^2} \frac{P\cdot Q_1}{(P-Q_2)^2+m^2} = -Q_1\cdot Q_2 \frac{(1-\sigma_2^E)^2}{8m^2}\,. \tag{1.68}$$

After performing the corresponding average, it is possible to perform five of the six four–dimensional angular integrals on Q_1 and Q_2 and the final result is:

$$a_\mu^{HLbL} = \frac{2\alpha^3}{3\pi^2}\int_0^\infty dQ_1 \int_0^\infty dQ_2 \int_{-1}^1 d\tau \sqrt{1-\tau^2}|Q_1|^3|Q_2|^3 \times \sum_i^{12} T_i \overline{\Pi}_i\,. \tag{1.69}$$

There are three aspects of this last step that are worth noting:

- The integral over Q_2 in spherical coordinates is considered in the first place. It is possible to take any four–momentum as a reference for the angular integral; it does not matter because the integrals will go over all the possible values anyway. We take Q_1 as a reference.
- The integrand is only dependent on one angle (in $\tau = \hat{Q}_1\cdot\hat{Q}_2$) and it is therefore convenient to assign τ as one of the three euclidean angles over which the angular integrals of the four momentum Q_2 is performed. It is relevant which of these three angle we are referring to because it will determine which term of the Jacobian will appear. In the master formula there is a term $1-\tau^2$, a sine squared, which means τ does not represent neither polar nor the azimuthal angle of the three dimensional sphere embedded in the four dimensional space. Thus, the angular integral on Q_2 yields:

  $$\int d\tau\sqrt{1-\tau^2}\int d\theta d\phi \sin\theta = 4\pi\int d\tau\sqrt{1-\tau^2}\,, \tag{1.70}$$

  where θ and ϕ represent the three–dimensional polar and azimuthal angles of the four–dimensional Q_2 space.
- Once the angular integrals on Q_2 have been performed there is no dependence on τ or another angle left on the integrand. This means that we can perform the four–dimensional solid angle integral on Q_1 which yields $2\pi^2$.

1.6 Review of low energy contributions to a_μ^{HLbL}

Up to this point we have presented an approach to compute low–energy contributions to a_μ^{HLbL} based on a dispersive description of the HLbL scattering amplitude. Now let us review the results obtained when such approach is put to use.

As we stated in section 1.4, the dispersive calculation of an amplitude offers a way to establish a hierarchy of contributions for the intermediate states that enter the computation via the unitarity relation of (1.36). Heavier intermediate states induce cuts that appear further to the right of the dispersive integration region compare to their lighter counterparts and therefore the contributions from heavier intermediate states are expected to be smaller. The $1/(s-s')$, $1/(t-t')$ or $1/(u-u')$ weights further suppress such contributions. Thus, in the context of HLbL low energy scattering, the most relevant intermediate states are expected to be the lightest one– or two–hadron intermediate states.

1.6.1 One–particle intermediate states contribution to a_μ

The lightest mesons with masses up to ~ 1 GeV are π^0, $\pi^\pm$, $K^\pm$, K^0, η and η'[20]. Charge conservation obviously prohibits the appearance of charged pions and kaons as one–particle intermediate states of HLbL. Furthermore, the neutral kaon is also not an allowed single–particle intermediate state since strong interactions conserve strangeness. Therefore, only π^0, η and η' may contribute to a_μ^{HLbL} as single–particle states up to ~ 1 GeV.

Baryons are not suitable single–particle intermediate states of the HLbL scattering amplitude due to baryonic number conservation. Thus, they can only contribute from two–particle intermediate states on, however, since the proton, the lightest baryon, has a mass of $\sim$ 938.3 MeV [63], its corresponding two–particle state has a mass of about 1.9 GeV, which is already in the perturbative regime of QCD. Perturbative computations are much more straight forward than dispersive ones and have a huge advantage over them in terms of required experimental inputs. As such, perturbative computations should always be used when possible and therefore baryon contributions to a_μ^{HLbL} are not considered in dispersive computations.

The contributions from the π^0, η and η' intermediate states to a_μ^{HLbL} are of the form:

$$a_\mu^{P-\text{Pole}} = \frac{2\alpha^3}{3\pi^2}\int_0^\infty dQ_1 \int_0^\infty dQ_2 \int_{-1}^{1} d\tau \sqrt{1-\tau^2}|Q_1|^3|Q_2|^3 \times \left(T_1 \overline{\Pi}_1^{P-\text{pole}} + T_2 \overline{\Pi}_2^{P-\text{pole}}\right), \quad (1.71)$$

$$\overline{\Pi}_1^{P-\text{pole}} = -\frac{\mathcal{F}_{P\gamma^*\gamma^*}(-Q_1^2,-Q_2^2)\mathcal{F}_{P\gamma^*\gamma^*}(-Q_3^2,0)}{Q_3^2+M_P^2}, \quad (1.72)$$

$$\overline{\Pi}_2^{P-\text{pole}} = -\frac{\mathcal{F}_{P\gamma^*\gamma^*}(-Q_1^2,-Q_3^2)\mathcal{F}_{P\gamma^*\gamma^*}(-Q_2^2,0)}{Q_2^2+M_P^2}, \quad (1.73)$$

where P states for the corresponding meson in the one–particle intermediate state, M_P is the meson's mass and $\mathcal{F}_{P\gamma^*\gamma^*}$ represents the doubly virtual transition form factor of the meson, which is defined by:

$$i\int d^4x\, e^{-iq_1x}\langle 0|T\{J_\mu(x)J_\nu(0)\}|P(q_1+q_2)\rangle = \epsilon_{\mu\nu\lambda\rho}q_1^\lambda q_2^\rho \mathcal{F}_{P\gamma^*\gamma^*}(q_1^2,q_2^2)\,. \quad (1.74)$$

The main hurdle for the computation of $a_\mu^{P-\text{pole}}$ is to obtain reliable values for the transition form factor, specially for the double virtual sector, for which there is little experimental data available [64]. Furthermore, data available below 1 GeV is particularly scarce, which means that a fit extrapolation is required in order to obtain the transition for factors at that range. This is specially troublesome because the main contribution to (1.71) comes actually from the low energy region. For the neutral pion, however, the negative effects of these issues have been addressed by a dispersive reconstruction of the transition form factor [24, 65, 66] which starts from (1.74) and uses very much the same framework presented in section 1.4. When $\mathcal{F}_{\pi^0\gamma^*\gamma^*}$ is computed in this fashion, the corresponding contribution to a_μ^{HLbL} is:

$$a_\mu^{\pi^0-\text{pole}}(dispersive) = 63.0^{+2.7}_{-2.1}\times 10^{-11}\,. \quad (1.75)$$

There are of course alternate approaches for evaluating $\mathcal{F}_{\pi^0\gamma^*\gamma^*}$ such as the Canterbury Approximants (CA) [64, 67, 68], which reproduces the low energy behaviour of the transition form factor

[20] η and η' are actually not stable in QCD and therefore it does appear in the unitary relation (1.36) as a one-particle intermediate state, however, its decay width is small enough to be considered as a one.

approximating it via rational functions of polynomials in Q_1^2 and Q_2^2.[21] The CA computation of the pion transition form factor yields the result [6] $a_\mu^{\pi^0-\text{pole}}(CA) = 63.2(2.7) \times 10^{-11}$, which is very much compatible with the dispersive one.

For the η and η' there is however not yet available a dispersive computation of the corresponding form factor in its doubly virtual region, although the framework has been established for the singly–virtual one [69]. Furthermore, progress has been made in the doubly–virtual case as well [70, 71]. In any case, until a full dispersive computation of the transition form factor is obtained the CA approach offers an option whose reliability is supported by the excellent compatibility with the dispersive results in the case of the neutral pion pole. For the η and η' pole contributions the CA approach concludes [64]:

$$a_\mu^{\eta-\text{pole}}(CA) = 16.3(1.4) \times 10^{-11} \,, \tag{1.76}$$

$$a_\mu^{\eta'-\text{pole}}(CA) = 14.5(1.9) \times 10^{-11} \,. \tag{1.77}$$

It is clear that the neutral pion contribution is by far the largest from the on–particle intermediate states. Since the π^0 is lighter than the η and it in turn is lighter than the η', these results for the contribution of each of these intermediate states agrees with the expected hierarchy of contributions mentioned at the beginning of this section. In summary, the one–particle intermediate states contribution to a_μ is [6]:

$$a_\mu^{\pi^0+\eta+\eta'} = 93.8^{+4.0}_{-3.6} \times 10^{-11} \,. \tag{1.78}$$

1.6.2 Two–particle intermediate states contribution to a_μ

The lightest two–meson intermediate states with mass up to ~ 1 GeV from lightest to heaviest are $\pi^0\pi^0$, $\pi^+\pi^-$, $\eta\pi^0$, K^+K^- and $K^0\overline{K}^0$. Note that, again due to the strangeness conservation in QCD, no intermediate states with a single kaon is allowed.

The dispersive frame work for the computation of the two–pions contribution has been studied in [22]. In there, by performing the unitarity cut across the s–channel, this amplitude is split into two $\gamma\gamma \to \pi\pi$; one with two virtual photons and one with one virtual and one real soft photon. Then, this two amplitudes are split again by performing the unitary cut across the t–channel, which is the application of a second dispersion relation that leads to the Mandelstam representation that was described in section 1.4. Although in this second cut there is the possibility for multi–pion intermediate states to appear, the biggest contribution is expected to come from the pion pole (lightest intermediate state) as well. This introduces the pion–box topology as an intermediate state.[22] Since the four pieces in which the original HLbL is split are essentially pion electromagnetic vertices, it is reasonable to expect the pion–box topology contribution to a_μ to be proportional to four pion electromagnetic vector form factors $\mathcal{F}_\pi^V(q_i^2)$. Furthermore in [22] this relation is taken further and via explicit computation of the double spectral functions associated to the pion–box contribution it was shown that the pion–box contribution to $\Pi^{\mu\nu\lambda\rho}$ is in fact equal to the scalar QED pion loop amplitude multiplied by four pion vector form factors

[21] For the singly–virtual transition form factor the Padé Approximants approach is used, which are essentially the univariate version of the CA.

[22] It is worth noting that due to angular momentum conservation and Bose symmetry, a photon does not couple to two neutral pions and therefore the $\gamma^*\gamma^* \to \pi^0\pi^0$ does not allow a neutral pion intermediate state across the t–channel.

due to each of the four off-shell photons. The mathematical expression of these statements is:

$$\begin{aligned}\Pi_i^{\pi-\text{box}} &= \mathcal{F}_\pi^V(q_1^2)\mathcal{F}_\pi^V(q_2^2)\mathcal{F}_\pi^V(q_3^2)\mathcal{F}_\pi^V(q_4^2)\\ &\times\frac{1}{\pi^2}\left(\int_{c_1}^\infty ds'\int_{c_2(s')}^\infty dt'\frac{\Delta_{t'}\Delta_{s'}\mathcal{M}^{\text{sQED}}(s',t')}{(s'-s)(t'-t)}+\int_{c_1}^\infty ds'\int_{c_2(s')}^\infty du'\frac{\Delta_{u'}\Delta_{s'}\mathcal{M}^{\text{sQED}}(s',u')}{(s'-s)(u'-u)}\right.\\ &\left.+\int_{c_1}^\infty du'\int_{c_2(u')}^\infty dt'\frac{\Delta_{t'}\Delta_{s'}\mathcal{M}^{\text{sQED}}(t',u')}{(u'-u)(t'-t)}\right),\end{aligned}\tag{1.79}$$

where $\mathcal{M}^{\text{sQED}}$ is the scalar QED one loop amplitude with pions. The corresponding double spectral functions can of course be obtained used Cutkosky's rules to perform unitary cuts to loops, however, it is much more efficient to compute the light by light scattering amplitude directly in perturbative scalar QED and then insert into the master formula (1.69) with the appropriate vector form factors. This allows for the contribution of the pion box to be written in terms of compact and well known Feynman parameters integrals. In conclusion, the pion box contribution to a_μ^{HLbL} reads:

$$\begin{aligned}a_\mu^{\pi-\text{box}} &= \frac{2\alpha^3}{3\pi^2}\int_0^\infty dQ_1\int_0^\infty dQ_2\int_{-1}^1 d\tau\sqrt{1-\tau^2}|Q_1|^3|Q_2|^3\\ &\times\mathcal{F}_\pi^V(-Q_1^2)\mathcal{F}_\pi^V(-Q_2^2)\mathcal{F}_\pi^V(-Q_3^2)\sum_i^{12}T_i\overline{\Pi}_i^{sQED} &(1.80)\\ &= -15.9(2)\times10^{-11}\,, &(1.81)\end{aligned}$$

where $\overline{\Pi}_i^{sQED}$'s are the scalar coefficients of the BTT decomposition of the scalar QED one–loop light–by–light scattering amplitude, which obviously is a subset of the HLbL BTT structures. In the previous equation only three vector form factors appear, instead of four, because one of the photons of this HLbL process is actually on–shell.

Regarding intermediate states heavier than one pion in the t–channel cut of the $\gamma\gamma\to\pi\pi$ subprocess, they can be classified in two: one with one pion–pole contribution in one subamplitude and a multiparticle cit in the other and one where both subprocesses contain multiparticle cuts. The computation of this contributions can be performed through a partial wave expansion of the amplitude. One of the advantages of this approach is that the unitarity relation (1.36) is diagonal in the helicity partial wave basis, that is, helicity partial waves of HLbL $h^J_{\lambda_1\lambda_2\lambda_3\lambda_4}$ are only connected by unitarity with the $\gamma^*\gamma^*\to\pi\pi$ partial waves $h^J_{\lambda_i\lambda_j}$ with the same total angular momentum J and photon helicities λ_i:

$$\text{Im}^{\pi\pi}\,h^J_{\lambda_1,\lambda_2,\lambda_3,\lambda_4} = \frac{\sigma_\pi}{16\pi S}h^J_{\lambda_1\lambda_2}h^{*J}_{\lambda_3\lambda_4}\,,\tag{1.82}$$

$$H_{\lambda_1\lambda_2\lambda_3\lambda_4} = \sum_J(2J+1)d^J_{m_1m_2}(z)h^J_{\lambda_1\lambda_2\lambda_3\lambda_4}\,,\tag{1.83}$$

$$H_{\lambda_i\lambda_j} = \sum_J(2J+1)d^J_{m0}(z)h^J_{\lambda_i\lambda_j}\,,\tag{1.84}$$

$$m=|\lambda_i-\lambda_j|\,,\qquad m_1=|\lambda_1-\lambda_2|\,,\qquad m_2=|\lambda_3-\lambda_4|\,,\tag{1.85}$$

$$\sigma_\pi=\sqrt{1-\frac{4M_\pi^2}{s}}\,,\tag{1.86}$$

where $H_{\lambda_1\lambda_2\lambda_3\lambda_4}$ and $H_{\lambda_i\lambda_j}$ are helicity amplitudes for the HLbL and the $\gamma^*\gamma^*\to\pi\pi$ processes, respectively, which are obtained by contracting polarization vectors of a given helicity with the

corresponding process amplitude. Furthermore, $d^J_{m_1 m_2}$ are Wigner's matrices, z is the scattering angle and M_π represents the pion's mass. Helicity partial waves are however not suitable for a double Mandelstam representation, because they contain kinematic singularities (see section 3 of chapter 7 in [72]). To retain the advantages of the partial wave expansion, but solve the kinematic singularities issues it is necessary to relate them to the BTT basis described in section 1.4. This is done by first inverting the linear relation that is obtained between helicity amplitudes and BTT scalar functions via its definition from contraction with photon polarization vectors. Then helicity partial waves are projected out of the corresponding helicity amplitude by using orthogonality properties of Wigner's matrices. As we mentioned in section 1.4 [57], the BTT decomposition of $\Pi^{\mu_1\mu_2\mu_3\mu_4}$ actually trades linear independence in order to span the whole amplitude, therefore introducing redundancies. This redundancies are constrained in the soft limit ($q_4 \to 0$) by using dispersive sum rules derived from the asymptotic properties of the scalar coefficients [23]. Finally, the S–wave contribution to the two pion HLbL intermediate states with one pion as and intermediate state in one $\gamma^*\gamma^* \to \pi\pi$ subprocess and a multiparticle cut in the other is [23]:

$$a_\mu^{\pi\pi,\ \pi-\text{pole LHC}} = -8(1) \times 10^{-11}\ , \tag{1.87}$$

where "LHC" stands for "left hand cut". Contributions from higher angular momentum partial waves is difficult due to the lack of experimental input for the doubly virtual subprocess $\gamma^*\gamma^* \to \pi\pi$. Furthermore, heavier singularities in the left hand cut have to be taken into account for the computation of higher angular momentum partial waves, but in such case some assumptions that simplified the computation of (1.87) are no longer valid. Therefore, the dispersive framework developed in [23] would have to be studied from a more general perspective.

In [6] it is proposed that the comparison between the size of the $\gamma\gamma \to \pi\pi$ cross section and $\gamma\gamma \to MM$ cross section for some given processes gives input to determine which two–particle intermediate state contribution MM may be relevant beyond the $\pi\pi$ contribution. Following this approach, the relevant heavier intermediate states are $\pi^0\eta$ and K^+K^-, which are actually the next two–particle intermediate states in terms of mass. For the two kaon contribution, the same arguments of the pion box apply and therefore, via the scalar QED kaon loop and using vector meson dominance to obtain the electromagnetic form factor, the corresponding contribution has bee computed [6]:

$$a_\mu^{KK\text{–loop}} = -0.5(1) \times 10^{-11}\ . \tag{1.88}$$

For the $\pi^0\eta$ the real version of the process a dispersive framework has been developed [73] and the results performed well against data of the $\eta \to \pi^0\gamma\gamma$ crossed process. Work on the singly and doubly virtual processes is still under way [74].

1.6.3 Intermediate states with more than two particles and heavier than KK

The dispersive computation of contributions heavier than the ones we presented previously, that is, with masses between 1 GeV and 2 GeV, is more difficult due to the more complex unitarity diagrams than come into play. Perhaps the most straightforward upgrade is the contribution from D–[23] and higher waves from the two pion contribution, for which there is a pretty much developed framework [25]. Contributions from states heavier that two pions are expected to be small. For example, the K^+K^- intermediate state has mass $\sim$ 1 GeV and its contribution

[23] Each pion has isospin equal to one, therefore the possible values for total isospin are $|1-1| = 0$ and $1+1 = 2$. This means that only even partial waves are allowed.

to a_μ is already below 10^{-11}. Consequently, heavier intermediate states contributions are expected to be non–negligible only if they are associated to resonant helicity partial waves. To estimate such contributions a narrow–width resonance approximation is followed in [75] (updated in [76]) and [77], which essentially means that narrow resonances are treated as dispersive poles. In summary, the contributions considering the $f_0(980\text{ MeV})$, $a_0(980\text{ MeV})$, $f_0(1370\text{ MeV})$, $a_0(1450\text{ MeV})$, $f_0(1500\text{ MeV})$, $f_2(1270\text{ MeV})$, $f_2(1565\text{ MeV})$, $a_2(1320\text{ MeV})$ and $a_2(1700\text{ MeV})$ [24] is:

$$a_\mu^{\text{scalars+tensor}} = -1(3) \times 10^{-11} \,, \tag{1.89}$$

which introduces a significant uncertainty due to the unknown error introduced by the narrow–width resonance approximation. In principle, such approximation may be tested in the lightest scalar and tensor resonances against the $\pi\pi$ and KK contributions described previously. However, only a full tower of resonant poles satisfy the sum rules found in [23], which is a necessary condition for a tensor–basis independent contribution.

Axial vector mesons (meson bound states with total angular momentum equal to 1, but even parity) have not been considered in the previous paragraphs, because[25] the lightest associated resonances are actually heavy compared with other states: $a_1(1260\text{ MeV})$, $f_1(1285\text{ MeV})$ and $f_1(1420\text{ MeV})$. They contribute to a_μ as resonant poles and their respective transition form factors are obtained from experimental data using a non–relativistic quark model computation [78–81] which simplifies the tensor structure of the $\gamma^*\gamma^* \to A$ amplitude, as described in [75]. The current agreed contribution (see [6]) is obtained from the mean of three results [75, 77, 82] that consider the three lightest axial vector mesons:

$$a_\mu^{\text{axial vectors}} = 6(6) \times 10^{-11} \,. \tag{1.90}$$

1.7 Conclusions

In this chapter we have presented the basics of the computation of a_μ and in particular a_μ^{HLbL}, which led to the (1.69) master formula, which is based on a BTT tensor decomposition of the HLbL amplitude with 54 elements such that its scalar coefficients are free of kinematic singularities and zeroes. The tensor "basis" is actually not linearly independent in the whole phase space due to 11 structures that need to be added by hand in order to span the amplitude at some kinematic points $q_1 \cdot q_2 = 0$ or $q_3 \cdot q_4 = 0$. Furthermore, in four space–time dimensions there are two additional linear relations among the 138 tensors of (1.49) [83] which the 54 BTT structures inherite. Of course, the linear dependence of the set of structures introduces redundancies in the definition of the associated scalar coefficients. Although it is clear that a_μ^{HLbL} cannot be affected by these redundancies, the mathematical mechanism that ensures that is not apparent. In [25] a set of scalar coefficients is built such that each one is invariant under these redundancies, provided that they satisfy a set of sum rules derived assuming: 1) that the HLbL tensor behaves as s,t, u for large values of the Mandelstam variables, 2) that this behaviour is uniform across all the elements of its tensor decomposition and 3) that the BTT scalar coefficients satisfy unsubstracted dispersion relations. The first two assumptions fix the asymptotic behaviour of the scalar functions by explicitly requiring them to complement the asymptotic behaviour of its corresponding tensor structures. The third assumption requires the new redundancy–free coefficients to be

[24] In [75] and its updated version [76] the first three (scalar) resonances and the last four (tensor) resonances are considered. In [77] considers all the scalar resonances mentioned.

[25] note that the Landau-Yang theorem only forbids the coupling of two real photons to axial vector mesons, therefore in virtual HLbL it is allowed.

transformed into the original BTT coefficients set by a matrix that cannot be arbitrarily singular at infinity. From these three assumptions the asymptotic behaviour of the BTT coefficients is obtained. Those coefficients that fall quicker than s^{-1}, t^{-1} or u^{-1} for large values of these Mandelstam variables are subject to dispersive identities called "sum rules" that are beyond the usual double spectral representation. Such identities are obtained by noting that if $\hat{\Pi}_i$ satisfies an unsubtracted dispersion relation, so should $s\hat{\Pi}_i$ or $s^2\hat{\Pi}_i$ and so on, depending on how fast does $\hat{\Pi}_i$ fall. Therefore, for contributions that cannot more or less satisfy these physical sum rules it is hard to compare their results between dispersive and alternate approaches, as we mentioned in the previous section for the resonant poles in narrow–width resonance approximation.

We presented a quick survey of low–energy contributions to a_μ^{HLbL}. From these, the dispersive approach has allowed for an unambiguous definition of contributions from intermediate states with contributions that follow a systematic hierarchy in terms of their mass. The pion–pole computation was data driven, while the η and η' resonances where computed using Canterbury approximants due to a lack of experimental data for their transition form factors. Heavier pseudoscalar mesons are not considered since they are already above the 1.8 GeV threshold. Possible upgrades on the pseudoscalar sector are now essentially on the experimental side. Two–particle intermediate states up to $\sim$ 1 GeV are considered. Pion and kaon box topologies have been accurately computed by exploiting a relation between unitary boxes and one–loop scalar QED. Contributions with heavier intermediate states in the $\gamma^*\gamma^* \to \pi\pi$ subamplitudes have been considered up to the S–wave. Scalar and tensor contributions are in general $\gtrsim$ 1 GeV threshold[26] and are computed using a narrow–with resonance approximation and therefore treated like poles. Axials vector mesons contributions are also treated as poles and their transition form factors are based on a phenomenological model for the $\gamma^*\gamma* \to A$ [78–81] amplitude. The scalar, tensor and axial vector mesons contributions, which covers the 1 GeV – 2 GeV region, cannot satisfy the sum rules from [25] and, thus, they suffer from tensor basis ambiguity, which makes it difficult to distinguish them from other high energy contributions, also called short–distance constraints (SDC). This ambiguity, together with the difficult assessment of the uncertainty that their intrinsic approximations convey, causes the high energy region of HLbL to be the main source of uncertainty to a_μ^{HLbL}.

In this chapter we discussed contributions of intermediate states with masses up to $\sim$ 2 GeV, which are expected to give the man contribution to a_μ^{HLbL}. However, it is as well necessary to understand the behaviour of the HLbL tensor beyond that threshold. The high energy regime of the HLbL contribution has been already reached from the light intermediate states when the high energy part of the integral in (1.69) has been carried out for high virtuality values of the transition and vector form factors. Although these penetrations into the high energy regime are expected to take into most of the contribution, in this regime heavier states with more complex topologies that are not taken into account dispersively can also contribute. It is those contributions and other uses for computations in the high energy regime of the QCD in the context of a_μ with which the next chapters will deal.

[26] Some lighter scalar resonances such as $f_0(500\text{ MeV})$ are already taken into account in the $\pi\pi$ intermediate states.

Chapter 2

Operator Product Expansion

Computations in the high energy regime of QCD play several important roles in the determination of a_μ. First, for data–driven computations they are used as input for transition and electromagnetic form factors at high energies where there is not enough experimental data available, which is always an issue given that the integral in the master formula (1.69) is extended on regions of indefinitely high virtual photon momenta. Examples of short distance constraints (SDC) for hadronic form factors can be found in [84–89] and an implementation of this SDC for the specific case of pion in the context of dispersive computations can be found in [90, 91]. Second, there are SDC that apply to the high virtuality regimes of the HLbL tensor and are used to evaluate how much of the asymptotic behaviour of the tensor is recovered by the finite set of intermediate states considered in the dispersive approach and consequently to account for the high energy contributions that the dispersive computations miss. This happens even though intermediate states of the dispersive approach contribute to the high virtuality regions of the master formula (1.69), because there are heavier intermediate states with topologically more complex unitarity diagrams that are ignored in the dispersive approach but start contributing to a_μ^{HLbL} in those high energy regions. The conclusions deduced from this second approach are key both for the computation of a_μ^{HLbL} and for its uncertainty assessment.

In this work we are interested in the SDC for the HLbL tensor. There are two high energy regimes for the HLbL process with one real soft photon, representing the background electromagnetic field: one where all three Euclidean virtualities are similarly high ($Q_1^2 \sim Q_2^2 \sim Q_3^2 \gg \Lambda_{QCD}^2$), (we refer to the Euclidean virtualities $q_i^2 = -Q_i^2$) and one where two are similarly high and much greater than the third Euclidean virtuality ($Q_1^2 \sim Q_2^2 \gg Q_3^2 \sim \Lambda_{QCD}^2$ and crossed versions). It is worth to remind that we refer to the Euclidean virtualities, because the considered photons are far off-shell since when the space-time separation goes to zero the corresponding momenta q_i become space-like. Each of these regimes impose asymptotic behaviour constraints on different subsets of BTT scalar coefficients and therefore they allow for the independent evaluation of the sets of intermediate states that contribute to one subset of scalar coefficients but not to the other. In this chapter we will focus on the $Q_1^2 \sim Q_2^2 \sim Q_3^2 \gg \Lambda_{QCD}^2$ regime of the HLbL tensor, which we will study by performing and Operator Product Expansion (OPE) where the soft photon is introduced by a background electromagnetic field.

2.1 OPE of $\Pi^{\mu_1\mu_2\mu_3\mu_4}$

A product of operators carrying very high momenta can be expressed in terms of a linear combination of local operators carrying zero momentum with singular coefficients that carry the

momentum dependence of the original operator. The mathematical expression of this statement for the product of two operators O_1 and O_2 is:

$$\int d^4x e^{-iqx} O_1(x) O_2(0) = \sum_n C_n^{12}(q^2) O_n(0) \,, \tag{2.1}$$

where C_n^{12} is a c–number function that decreases for large Q^2 and is known as "Wilson coefficient". The operator basis $\{O_n\}$ of the expansion only admits elements with the same quantum numbers and symmetries of the original operator product. The generalization for higher numbers of operators with arbitrary tensor structures is straightforward. Such identity is called operator product expansion (OPE) and was originally introduced by Kenneth Wilson [92]. By engineering dimensional analysis it can be noticed that the Wilson coefficients vanish increasingly quicker for O_n of higher mass dimensions. In other words, the OPE has an implicit and useful hierarchy of contributions in which simpler operators O_n (with less derivatives and fields) give bigger contributions than more complex operators. Since the operators on both sides of (2.1) are renormalized at some scale μ, a more careful study finds that dimensional analysis must be done considering the anomalous dimensions of the operators O_n, but for asymptotically free theories such as QCD, at high energy the simple power counting suffices. It is also worth noting that the relation in (2.1) is given in terms of operators, that is, it does not depend on specific matrix elements an therefore Wilson coefficients do not either. For further details see chapter 20 of volume II in [93] and chapter 20 in [55].

To perform the OPE in (2.1) it is first necessary to fix the maximum number of mass dimensions of the operators that are going to be considered and then the task is to find all operators compatible with quantum numbers and symmetries of the original operator product. Once the complete set of relevant operators O_n is known, each Wilson coefficient is found by choosing an appropriate matrix element of the original operator product $O_1 O_2$ and then transforming it into the corresponding element of the operator basis O_n. Such transformation is done by expanding the correlation function and leaving the elements that form O_n uncontracted. For example, to find the Wilson coefficient associated with a local operator of two fermions, then the appropriate matrix element would be one with two external fermions. The result of the contraction of the rest of the parts of the original product and the fields in the correlation function vertices constitutes the Wilson coefficient of the element O_n for the operator basis.

From the definition of the OPE it is evident that it constitutes a very well suited framework for the evaluation of the HLbL tensor in the $Q_1^2 \sim Q_2^2 \sim Q_3^2 \gg \Lambda_{QCD}^2$ regime. However, it is important to note that the limit $q_4 \to 0$ implies that it does not make sense to include the fourth current of (1.28) in the OPE. One could in principle start the construction of such OPE for the four currents of $\Pi_{HLbL}^{\mu_1\mu_2\mu_3\mu_4}$, but it does not work for our particular problem. For example, the computation of the Wilson coefficients associated to the identity operator involves the computation of the HLbL tensor in perturbative QCD, which of course requires renormalization and therefore implies an expansion in terms of the strong coupling constant and the usual large logarithms for increasing powers n:

$$\alpha_s^n(\mu) \ln^n \left\{ \frac{Q_4^2}{\mu^2} \right\} , \tag{2.2}$$

where μ represents the renormalization subtraction point in the $\overline{MS}$ scheme. In order for the logarithms not to blow up it is necessary to have $\mu \sim Q_4$, but in such case α_s would enter the non–perturbative domain of QCD and the expansion would be spoiled anyway. Wilson coefficients for higher dimensional operators also suffer from infrared singularities since they depend upon the $1/q_4^2$ propagator. One could argue that such problems arise because of trying

to include the fourth current J^{μ_4} into the OPE even though its momentum is not large and this is true, but that is not the only problem. Even if the OPE were performed only for the three currents with high momenta, there would still be matrix elements of the type $\langle 0|O_n J^{\mu_4}(q_4)|0\rangle$, which cannot be perturbatively computed in QCD. In general, these issues are different consequences of the fact that perturbative QCD is not the correct framework to describe the soft interaction that is required by a_μ. It is therefore necessary to perform the OPE of the three high–momentum currents only and also take the fourth one into account properly. This can be done by letting the soft photon be introduced by an external electromagnetic field instead of a quark current and not by analytically continuing the result of large Q^2 to $Q^2 \to 0$. This approach was first used in [94] in the context of the computation of the magnetic moment of nucleons, then it was used in [95] for the hadronic corrections to the electroweak contribution to a_μ and finally it was again picked up in [34–36] for the study of the asymptotic behaviour of the HLbL tensor in the $Q_1^2 \sim Q_2^2 \sim Q_3^2 \gg \Lambda_{QCD}^2$ high energy regime. A pedagogical review of the framework is presented in [96]. References [35, 94, 96] will be the main guideline throughout the rest of this chapter.

2.2 OPE of $\Pi^{\mu_1\mu_2\mu_3\mu_4}$ in an electromagnetic background field: A first look

As mentioned previously, it is necessary to build an OPE for the three high–momenta currents in the HLbL tensor with the soft photon introduced by an external (background) electromagnetic field insertion. Consequently, a new object suitable for such an OPE is defined:

$$\begin{aligned}\Pi^{\mu_1\mu_2\mu_3} &= \frac{1}{e}\int d^4x \int d^4y\, e^{-i(q_1 x + q_2 y)} \langle 0|T\, J^{\mu_1}(x) J^{\mu_2}(y) J^{\mu_3}(0)|\gamma(q_4)\rangle \\ &= -\epsilon_{\mu_4}(q_4)\Pi^{\mu_1\mu_2\mu_3\mu_4}(q_1, q_2, q_3)\ ,\end{aligned} \tag{2.3}$$

where the soft photon $q_4 \to 0$ is included implicitly in the initial state. In addition, J^μ this times makes reference to the electromagnetic current of the three lightest quarks, namely, up, down and strange or u, d and s and thus:

$$J^\mu = \overline{\Psi}\hat{Q}\gamma^\mu\Psi \qquad\qquad \hat{Q} = \mathrm{diag}\Big(\frac{2}{3}, -\frac{1}{3}, -\frac{1}{3}\Big)\ , \tag{2.4}$$

where $\hat{Q}$ is the charge matrix and now Ψ is a vector of bispinors with quark flavor and color indices, which are summed upon and suppressed in the current.

When performing the OPE of the three currents, the elements in the operator basis of the OPE will be evaluated at their matrix elements in $\langle 0|...|\gamma(q_4)\rangle$, that is, with one soft photon interaction with the background electromagnetic field A_μ. Since $\Pi^{\mu_1\mu_2\mu_3}$ is gauge invariant, then it must be proportional to a gauge invariant matrix elements and only $F_{\mu\nu}$, its corresponding field–strength tensor, gives a first order contribution in q_4. Thus, only operators that have the same quantum numbers and symmetries of $F_{\mu\nu}$ are relevant for the OPE of $\Pi^{\mu_1\mu_2\mu_3}$. In summary, this means that in the static and uniform limit $q_4 \to 0$ and at the first order in the external electromagnetic field we have for the regime of high virtualities at hands

$$\begin{aligned}\Pi^{\mu_1\mu_2\mu_3} &\equiv i\Pi_F^{\mu_1\mu_2\mu_3\mu_4\mu_5}(q_1, q_2)\langle 0|F_{\mu_4\mu_5}(0)|\gamma(q_4)\rangle \\ &= q_{4\mu_4}\epsilon_{\mu_5}(q_4)\Pi_F^{\mu_1\mu_2\mu_3[\mu_4\mu_5]}\ .\end{aligned} \tag{2.5}$$

We will see in the following sections that it is possible to find a gauge in which A_μ can be expanded in terms of $F_{\mu\nu}$, thus making this relation more straightforward. As a result of this relation one finds[1]:

$$\left.\frac{\partial \Pi^{\mu_1\mu_2\mu_3\mu_4}}{\partial q_{4\mu_5}}\right|_{q_4\to 0} = \Pi_F^{\mu_1\mu_2\mu_3[\mu_4\mu_5]} \,. \tag{2.6}$$

Therefore the real object of interest for a_μ^{HLbL} is actually $\Pi_F^{\mu_1\mu_2\mu_3[\mu_4\mu_5]}$, which is explicitly free of any q_4 dependence and therefore does no suffer from the singularity $q_4^2 \to 0$. To compute $\Pi_F^{\mu_1\mu_2\mu_3[\mu_4\mu_5]}$ it is necessary to find the Wilson coefficients in the OPE for $\Pi^{\mu_1\mu_2\mu_3}$, which in turn requires us to specify the symmetries that the elements of the operator basis must fulfill and then use this to find all relevant operators. The starting point for the OPE is equation (2.5), which upon comparison with the definition of the OPE in (2.1) fixes the operator basis elements to have the same Lorentz structure and symmetries of $F_{\mu_1\mu_2}$, that is:

- second rank antisymmetric tensor;
- odd charge–conjugation parity, remember in this regard the famous Furry's theorem for which the sum of all Feynman diagrams with an odd number of external photon lines (off or on the photon mass shell) and no other external lines vanishes.

In [35] operators with these features and mass dimension up to 6 are taken into account and the rest are neglected. This choice is ultimately supported by the fact the contribution of higher dimensional operators turns out to be at least two orders of magnitude smaller than the leading order. It is however also true that the non perturbative matrix elements of the dimension seven operators are less known than the above mentioned up to dimension 6. We focus here, for simplicity of reading at this step of our analysis, to the case of only one flavour and therefore on the following list of operators

$$\begin{aligned}
S_{1,\mu\nu} &\equiv ee_f F_{\mu\nu} \,, \\
S_{2,\mu\nu} &\equiv \overline{\Psi}\sigma_{\mu\nu}\Psi \,, \\
S_{3,\mu\nu} &\equiv ig_S\overline{\Psi}G_{\mu\nu}\Psi \,, \\
S_{4,\mu\nu} &\equiv ig_S\overline{\Psi}\,\overline{G}_{\mu\nu}\gamma_5\Psi \,, \\
S_{5,\mu\nu} &\equiv \overline{\Psi}\Psi\; ee_f F_{\mu\nu} \,, \\
S_{6,\mu\nu} &\equiv \frac{\alpha_s}{\pi}G_a^{\alpha\beta}G_{\alpha\beta}^a\; ee_f F_{\mu\nu} \,, \\
S_{7,\mu\nu} &\equiv g_S\overline{\Psi}(G_{\mu\lambda}D_\nu + D_\nu G_{\mu\lambda})\gamma^\lambda\Psi + g_S\overline{\Psi}(G_{\nu\lambda}D_\mu + D_\mu G_{\nu\lambda})\gamma^\lambda\Psi \,, \\
S_{\{8\},\mu\nu} &\equiv \alpha_s(\overline{\Psi}\Gamma\Psi\overline{\Psi}\Gamma\Psi)_{\mu\nu} \,,
\end{aligned} \tag{2.7}$$

where Ψ represents again a quark field in a given flavour of electric charge ee_f, the colour indices indices are implicitly summed upon, Γ represents a combination of Dirac gamma matrices, D_ν represents the gauge–covariant derivative, $G_{\mu\nu}^a$ represents the gluon field strength tensor, $G_{\mu\nu} \equiv it^a G_{\mu\nu}^a$ and $\overline{G}_{\mu\nu} \equiv \frac{i}{2}\epsilon^{\mu\nu\alpha\beta}G_{\alpha\beta}$. Since the largest non–perturbative QCD energy scale is the perturbative threshold Λ_{QCD}, then the contributions from matrix elements with mass dimension d are expected to be suppressed like $\left(\frac{\Lambda_{QCD}}{Q_i}\right)^d$, in agreement with the order of magnitude of the

[1] In chapter 1 we had already seen that the derivative of the HLbL tensor in the limit $q_4 \to 0$ was antisymmetric by differentiating the Ward identities twice.

error of replacing the cut–off regularized dimension six operators proposed in [35], amounting to $O\left(\frac{\Lambda_{QCD}^6}{Q_i^6}\right)$.[2] When included in the high–energy integration region of the master formula (1.69), the integration domain should be used coherently in agreement with the obtained OPE.

To include operators other than $S_{1,\mu\nu}$ may seem superfluous since when renormalized in QED their vacuum expectation value and even their $\langle 0|...|\gamma\rangle$ matrix element are zero. Due to the quantum numbers of the $S_{i,\mu\nu}$ operators we will be able to factorize the plane wave of the external electromagnetic field times the vacuum expectation value in the full QCD vacuum of a Lorentz, gauge invariant and charge-conjugation even operator with non-zero vacuum expectation value in the true QCD vacuum, so called a condensate. The nature of this non–perturbative dynamics is parameterized in coefficients X_i^S so called "vacuum condensates" that are defined as:

$$\langle 0|S_{i,\mu\nu}|\gamma\rangle \equiv X_i^S \langle 0|F_{\mu\nu}|\gamma\rangle \ . \tag{2.8}$$

Now that the operator basis is known up to dimension six, the next step is to obtain the Wilson coefficients of those operators in the OPE of the high virtualities $\Pi^{\mu_1\mu_2\mu_3}(q_1, q_2, q_3)$ in a static background $q_4 \to 0$ electromagnetic field. To parameterize the non–perturbative interactions of the strongly interacting fields with the QCD vacuum, they are expanded around their (QCD) vacuum expectation value:

$$A_\mu(x) = a_\mu(x) + A'_\mu(x) \ , \tag{2.9}$$

$$A^a_\mu(x) = a^a_\mu(x) + A'^a_\mu(x) \ , \tag{2.10}$$

$$\Psi^f_l(x) = \psi^f_l(x) + \psi'^f_l(x) \ , \tag{2.11}$$

where A^μ, A^a_μ and Ψ^f_l represent the complete photon, gluon and quark fields, respectively. f and l stand for the flavor and color of the quark, respectively and the unprimed variables are classical background fields that represent the effects of the non-perturbative QCD vacuum on the perturbative dynamics dictated by the asymptotic freedom. It is not needed to include the specific form of the QCD vacuum fields but just to parameterize them as external fields, as it is for instance done in the Coleman-Weinberg approach. Concerning the photon field decomposition at the order $\sqrt{\alpha}$ in which we are interested in, only the background part corresponding in this case to the classical external field of the measurement apparatus, is relevant for us. When translating these separation to the product of three currents in $\Pi^{\mu_1\mu_2\mu_3}$ we obtain the following:

$$\begin{aligned}&\langle 0|TJ^{\mu_1}(x)J^{\mu_2}(y)J^{\mu_3}(0)|\gamma\rangle = \\ &\langle 0|T(\overline{\psi}_x + \overline{\psi}'_x)\hat{Q}\gamma^{\mu_1}(\psi_x + \psi'_x)(\overline{\psi}_y + \overline{\psi}'_y)\hat{Q}\gamma^{\mu_2}(\psi_y + \psi'_y)(\overline{\psi}_0 + \overline{\psi}'_0)\hat{Q}\gamma^{\mu_3}(\psi_0 + \psi'_0)|\gamma\rangle \ ,\end{aligned} \tag{2.12}$$

where we have used the shorthand notation $\psi(x) \equiv \psi_x$. Note that at this point we have not introduced interaction vertices yet, but when we do, the quark fields coming from them are also split into classical and quantum parts, while gluon fields are only quantum fluctuations. Classical background photon and gluon fields come from the fermion "free" propagators that are modified as usual by external classical gauge fields. In principle there are 64 different combinations in (2.12), but only 27 do contribute since connected diagrams appear exclusively in cases in which at most one of the two fermionic fields of each current are classical. From a kinematical point of view, it does not make sense for a hard virtual photon to produce two soft quarks.

[2] Note that the mass dimensions of the matrix element $\langle 0|...|\gamma\rangle$ of an operator with mass dimension d actually has mass dimension $d-1$.

Furthermore, most of these matrix elements are related by complex conjugation and vertex permutation and therefore they can all be represented by only six different Feynman diagrams, which are shown in Figure 2.1. A representative set of matrix elements related to each of those six diagrams is

$$\begin{aligned}
&\langle 0|T\overline{\psi}'_x\hat{Q}\gamma^{\mu_1}\psi'_x\overline{\psi}'_y\hat{Q}\gamma^{\mu_2}\psi'_y\overline{\psi}'_0\hat{Q}\gamma^{\mu_3}\psi_0|\gamma\rangle\,, \qquad &&\langle 0|T\overline{\psi}'_x\hat{Q}\gamma^{\mu_1}\psi'_x\overline{\psi}'_y\hat{Q}\gamma^{\mu_2}\psi'_y\overline{\psi}'_0\hat{Q}\gamma^{\mu_3}\psi'_0|\gamma\rangle\,,\\
&\langle 0|T\overline{\psi}'_x\hat{Q}\gamma^{\mu_1}\psi'_x\overline{\psi}_y\hat{Q}\gamma^{\mu_2}\psi'_y\overline{\psi}'_0\hat{Q}\gamma^{\mu_3}\psi_0|\gamma\rangle\,, \qquad &&\langle 0|T\overline{\psi}_x\hat{Q}\gamma^{\mu_1}\psi'_x\overline{\psi}'_y\hat{Q}\gamma^{\mu_2}\psi_y\overline{\psi}'_0\hat{Q}\gamma^{\mu_3}\psi_0|\gamma\rangle\,,\\
&\langle 0|T\overline{\psi}'_x\hat{Q}\gamma^{\mu_1}\psi'_x\overline{\psi}_y\hat{Q}\gamma^{\mu_2}\psi'_y\overline{\psi}'_0\hat{Q}\gamma^{\mu_3}\psi_0|\gamma\rangle\,, \qquad &&\langle 0|T\overline{\psi}'_x\hat{Q}\gamma^{\mu_1}\psi_x\overline{\psi}'_y\hat{Q}\gamma^{\mu_2}\psi_y\overline{\psi}'_0\hat{Q}\gamma^{\mu_3}\psi_0|\gamma\rangle\,.
\end{aligned} \tag{2.13}$$

Note that some matrix elements in (2.13) have an odd number of quark fluctuations. These nevertheless give non–zero contributions, because they can be complemented by soft quark–gluon vertices coming from the Dyson series, as can be seen in diagrams of figure 2.1 with soft quarks coming out of the shaded blob. In any case, this means that these matrix elements either do not contribute to the leading order of the Wilson coefficients that we need or they contribute to operators with mass dimension higher that six and therefore they are of no interest for us.

2.3 OPE of $\Pi^{\mu_1\mu_2\mu_3\mu_4}$ in an electromagnetic background field: Theoretical framework

The need for the introduction of the expansion of the background fields around a spacetime point, for instance $x = 0$, stems from the fact that local operators that form any OPE are of course evaluated at $x = 0$, since any momentum or coordinate dependence is supposed to be carried by the Wilson coefficients. However, from the fields in the currents and vertices that we might introduce, we will get in general field variables that are explicitly dependent on the coordinates (the only incidental exception might be from the third current in $\Pi^{\mu_1\mu_2\mu_3}$). To obtain the local operators that we require it is therefore necessary to Taylor–expand the background fields:

$$\psi(x) = \psi(0) + x^{\mu_1}\partial_{\mu_1}\psi(0) + \frac{1}{2!}x^{\mu_1}x^{\mu_2}\partial_{\mu_1}\partial_{\mu_2}\psi(0) + \dots\,, \tag{2.14}$$

$$a^a_\alpha(x) = a^a_\alpha(0) + x^{\mu_1}\partial_{\mu_1}a^a_\alpha(0) + \frac{1}{2!}x^{\mu_1}x^{\mu_2}\partial_{\mu_1}\partial_{\mu_2}a^a_\alpha(0) + \dots\,, \tag{2.15}$$

$$a_\alpha(x) = a_\alpha(0) + x^{\mu_1}\partial_{\mu_1}a_\alpha(0) + \frac{1}{2!}x^{\mu_1}x^{\mu_2}\partial_{\mu_1}\partial_{\mu_2}a_\alpha(0) + \dots\,. \tag{2.16}$$

Since the OPE has been cut off at dimension six operators, then the same is required for these Taylor expansions and matrix elements of derivatives of the fields at $x = 0$ will thus have to be related to the original $S_{i,\mu\nu}$ operators. However, this task is hindered by the fact that the terms in the Taylor expansion are not even gauge covariant while the $S_{i,\mu\nu}$ are invariant. These issues render the usual approach to the computations of the Wilson coefficients very complex particularly for the gluon operators, as can be seen in [97, 98]. To work around these problems it is convenient to choose the radial gauge, also known as Fock–Schwinger gauge [99], which imposes the condition:

$$(x^\mu - x_0^\mu)a_\mu(x) = 0\,. \tag{2.17}$$

The advantages of this gauge for the OPE are related to the Taylor expansion expressed in terms of gauge covariant fields [100]. In our context, imposing the radial gauge for the photon and

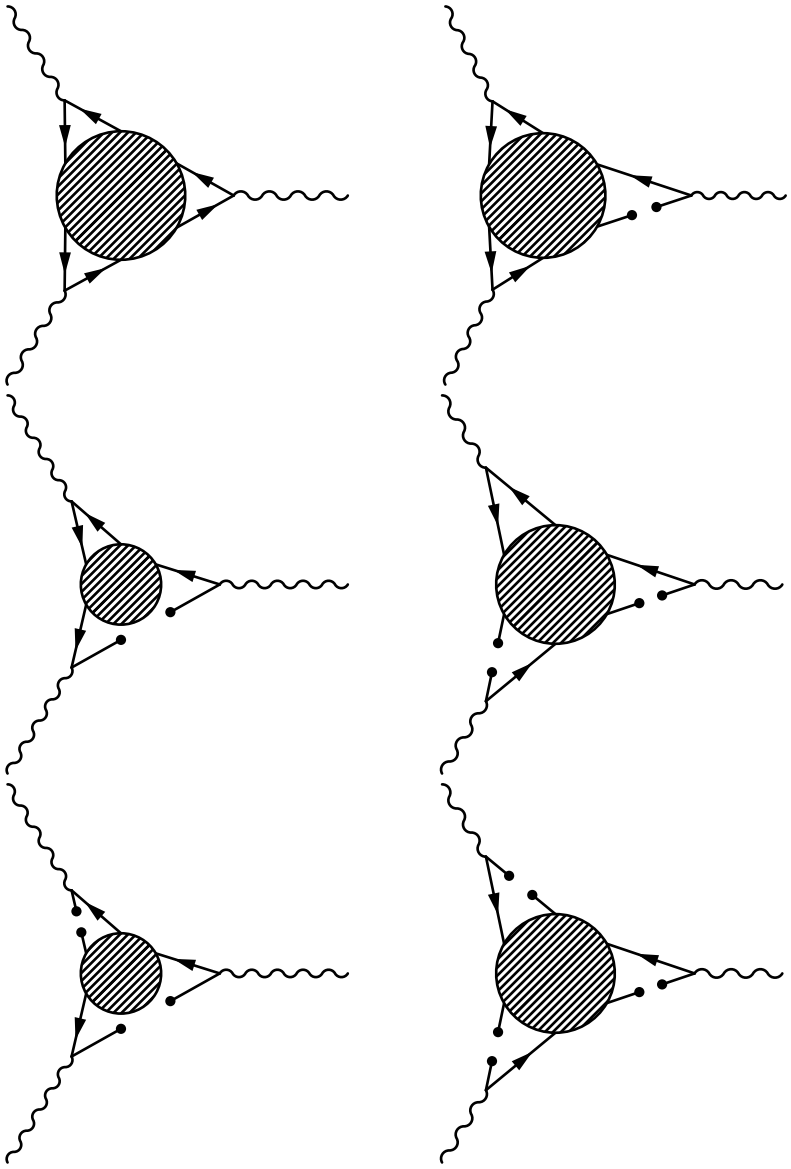

FIGURE 2.1: These diagrams represent the six truly different types of matrix elements (see (2.13)) contributing to $\Pi^{\mu_1\mu_2\mu_3}$. Black circles at the end of a line represent annihilation/creation of the corresponding particle by interaction with the non–perturbative fields in vacuum.

gluon fields backgrounds we have:

$$\psi(x) = \psi(0) + x^{\mu_1} D_{\mu_1}\psi(0) + \frac{1}{2!}x^{\mu_1}x^{\mu_2}D_{\mu_1}D_{\mu_2}\psi(0) + \dots ,$$
$$a^a_\alpha(x) = \frac{1}{2\times 0!}x^{\mu_1} f^a_{\mu_1\alpha}(0) + \frac{1}{3\times 1!}x^{\mu_1}x^{\mu_2}D_{\mu_1}f^a_{\mu_2\alpha}(0) + \dots ,$$
$$a_\alpha(x) = \frac{1}{2\times 0!}x^{\mu_1} f_{\mu_1\alpha}(0) + \frac{1}{3\times 1!}x^{\mu_1}x^{\mu_2}D_{\mu_1}f_{\mu_2\alpha}(0) + \dots ,$$

$$f^a_{\mu\nu} \equiv \partial_\mu a^a_\nu - \partial_\nu a^a_\mu + g_S f^{abc} a^b_\mu a^c_\nu ,$$
$$f_{\mu\nu} \equiv \partial_\mu a_\nu - \partial_\nu a_\mu .$$

These expansions hold for $x_0 = 0$, by using the expansion at a generic x_0, one can prove that the final results are x_0 independent, due to the gauge invariance of the theory. Due the presence of a background in general the translational invariance is lost in general and this is reflected on a non translational invariant propagator. That translational invariance is of course recovered in the static limit at hands $q_4 \to 0$. The separation of soft and hard parts of the fields that was introduced previously in this chapter allows us to have the radial gauge advantages in the construction of the basis elements of the OPE, while not having to deal with the complexity of its propagator in the computation of the Wilson coefficients. That is the main reason behind the use of this approach for the OPE. Otherwise it would have been enough to consider only the photon field as background.

After having motivated the purpose of the background field method for the OPE that we are interested in, we will present in detail the theoretical framework that supports it. The lagrangian for the HLbL interaction may be written as:

$$\mathcal{L}^{HLbL} = -\frac{1}{4}(G^a_{\mu\nu})^2 - \frac{1}{4}(F_{\mu\nu})^2 + \overline{\Psi}_l(i\not{D}_{lk} - \delta_{lk}m)\Psi_k - \frac{1}{2\xi}f^a f^a - \mathcal{L}_{ghosts} , \tag{2.18}$$
$$D^\mu_{lk} = \delta_{lk}\partial^\mu - ie\hat{Q}\delta_{lk}A^\mu - ig_S t^a_{lk}A^{a\mu} , \tag{2.19}$$
$$\mathcal{L}_{ghosts} = w^*_a \mathcal{F}_{ab} w_b , \tag{2.20}$$
$$\mathcal{F}_{ab} = \frac{\delta f^a_\epsilon}{\delta \epsilon^b} , \tag{2.21}$$

where the indices in the quark fields and the covariant derivative represent the quark color, the rest of Latin indices represent gluon color and greek indices represent Lorentz degrees of freedom as usual. Flavor indices are suppressed. With respect to the fields, w^a are ghosts fields associated to the Faddeev–Popov gauge fixing procedure for the gluon[3], f^a is the associated gauge fixing function and f^a_ϵ is its gauge–transformed version. In the definition of $\mathcal{F}_{ab}$ the deltas represent a functional derivative. Under gauge transformations of A^a_μ the background field transforms as a gauge field, while the fluctuation part transforms as a matter field in the adjoint representation:

$$\begin{aligned}\delta a^a_\mu &= \langle 0|\delta A^a_\mu|0\rangle = \langle 0|\partial_\mu\epsilon^a + g_S f^{abc}A^b_\mu\epsilon^c|0\rangle \\ &= \partial_\mu\epsilon^a + g_S f^{abc}a^b_\mu\epsilon^c , \end{aligned}\tag{2.22}$$
$$\begin{aligned}\delta A'^a_\mu &= \delta A^a_\mu - \delta a^a_\mu \\ &= g_S f^{abc}A'^b_\mu\epsilon^c . \end{aligned}\tag{2.23}$$

[3]The gauge fixing term for the photon field does not appear here because we are only interested for the aims of our computations in its classical part.

The transformation laws for all other fields are the usual:

$$\begin{aligned} \delta\psi_l &= ig_S\epsilon^a t^a_{lk}\psi_k \,, & \delta\psi'_l &= ig_S\epsilon^a t^a_{lk}\psi'_k \,, \\ \Longrightarrow\ \delta\Psi_l &= \delta\psi_l + \delta\psi'_l & & \\ &= ig_S\epsilon^a t^a_{lk}(\psi' + \psi)_k \,, & & \\ \delta w^{*a} &= f^{abc}\epsilon^c w^{*b} \,, & \delta w^a &= f^{abc}\epsilon^c w^b \,. \end{aligned} \tag{2.24}$$

These are called background gauge transformations. After the separation of the background and fluctuation parts of the gauge fields, the true integration variables for the path integral are the fluctuations, and since they transform as matter fields under the gauge transformation of A^a_μ, then this redundancy no longer requires a gauge fixing term in the classical action of the path integral. However, A'^a_μ is still a gauge field for another local transformation of the lagrangian, which we denote by δ':

$$\delta' A'^a_\mu = \partial_\mu\epsilon^a(x) + g_S f^{abc}\epsilon^c(a^b_\mu + A'^b_\mu) \,, \qquad \delta' a^a_\mu = 0 \,, \tag{2.25}$$

$$\delta'\psi'_l = ig_S\epsilon^a t^a_{lk}(\psi + \psi')_k \,, \qquad \delta'\psi_l = 0 \,, \tag{2.26}$$

$$\delta' w^{*a} = f^{abc}\epsilon^c w^{*b} \,, \qquad \delta' w^a = f^{abc}\epsilon^c w^b \,. \tag{2.27}$$

This redundancy does require a gauge fixing term to render the quadratic terms in A'^a_μ of the lagrangian invertible. To maintain background gauge invariance we choose

$$f^a = \overline{D}^\mu A'^a_\mu \equiv \partial^\mu A'^a_\mu + g_S f^{abc} a^b_\mu A^{c'\mu} \tag{2.28}$$

instead of the usual choice $\partial_\mu A^\mu$. $\overline{D}$ acts as a background–gauge covariant derivative. A disadvantage of this choice is however that the gluon propagator depends on the background fields in a rather involved way, as will be shown later. The background–gauge invariance of such gauge fixing term can be checked easily by recalling that A'^b_μ transforms covariantly under such transformations, therefore $\overline{D}^\mu A'^a_\mu$ must too (see B.1) and consequently:

$$\delta f^a = g_S f^{abc}\epsilon^c \overline{D}^\mu A'^b_\mu \,, \tag{2.29}$$

$$\Longrightarrow\ \delta(f^a f^a) = 2g_S\epsilon^c f^{abc}\overline{D}^\mu A'^a_\mu \overline{D}^\mu A'^b_\mu = 0 \,. \tag{2.30}$$

Since the ghost part of the lagrangian depends only on A'^a, not on the complete field, then it also has to be checked for background gauge invariance. For the f^a gauge fixing term that was chosen we have:

$$\mathcal{L}_{ghost} = w^*_a \overline{D}_\mu \{\overline{D}^\mu w_a + f_{abc} w_c A'^\mu_b\} \,. \tag{2.31}$$

The ghost fields transform just as the gluon fluctuations under the background gauge transformation, therefore by the same procedure followed with $\overline{D}_\mu A'^a_\mu$ it can be shown that $\overline{D}^\mu w_a$ and $\overline{D}_\mu \overline{D}^\mu w_a$ transform covariantly as well. Consequently, invariance under background gauge transformations for $\mathcal{L}_{ghost}$ is conserved.

Now we have successfully imposed the radial gauge prescription on the background gluon field without imposing it on the quantum fluctuation part. However, to achieve this we have chosen f^a to have a non–standard functional. It is therefore necessary to check that the term $f^a f^a$ actually fixes the gauge of the quantum field fluctuation:

$$\delta' f^a = \overline{D}_\mu \overline{D}^\mu \epsilon^a + g_S f^{abc} A'^{b\mu} \overline{D}_\mu \epsilon^c + g_S f^{abc}\epsilon^c \overline{D}_\mu A'^{b\mu} \,, \tag{2.32}$$

$$\begin{aligned}\implies \delta' f^a f^a &= 2\overline{D}_\nu A^{a'\nu}\{\overline{D}_\mu \overline{D}^\mu \epsilon^a + g_S f^{abc} A'^{b\mu}\overline{D}_\mu \epsilon^c + g_S f^{abc}\epsilon^c \overline{D}_\mu A'^{b\mu}\} \\ &= 2\overline{D}_\nu A^{a'\nu}\{\overline{D}_\mu \overline{D}^\mu \epsilon^a + g_S f^{abc} A'^{b\mu}\overline{D}_\mu \epsilon^c\} \\ &\neq 0\,. \end{aligned} \tag{2.33}$$

As a final comment it is worth noting that the background fields should not depend on the coordinates since the QCD vacuum is translation–invariant, but they do because the background gauge prescription breaks that symmetry for gauge non–invariant matrix elements.

Now that we have presented the theoretical framework of the separation of fields that we will use and have checked its consistency, we are ready to obtain the computational tools that we will need to build the OPE. Let us read in detail the Feynman rules from the lagrangian $\mathcal{L}^{HLbL}$ after the separation of the fields in classical background and quantum parts:

$$\begin{aligned}\mathcal{L}^{HLbL} = &-\frac{1}{4}(f^a_{\mu\nu} + \overline{D}_\mu A'^a_\nu - \overline{D}_\nu A'^a_\mu + g_S f^{abc} A'^b_\mu A'^c_\nu)^2 - \frac{1}{4}(f_{\mu\nu} + \partial_\mu A'^a_\nu - \partial_\nu A'^a_\mu)^2 \\ &+ (\overline{\psi}_l + \overline{\psi}'_l)(\{i\partial\!\!\!/ - m\}\delta_{lk} + e\hat{Q}\delta_{lk}A\!\!\!/ + g_S t^a_{lk} A'\!\!\!/^a)(\psi_l + \psi'_l) \\ &+ (\overline{\psi}_l + \overline{\psi}'_l)(e\hat{Q}\delta_{lk}A\!\!\!/' + g_S t^a_{lk} A'\!\!\!/^a)(\psi_k + \psi'_k) \\ &- \frac{1}{2\xi}\overline{D}^\mu A'^a_\mu \overline{D}^\mu A'^a_\mu - \mathcal{L}_{ghosts}\,. \end{aligned} \tag{2.34}$$

This lagrangian can be simplified very much. First, the parts with only background field variables are constant from the point of view of the path integral and therefore they may be adsorbed by its normalization constant. From a diagramatical point of view, these terms represent amplitudes of disconnected diagrams, which again are contained in the normalization of the path integral in the usual way. In addition, since HLbL scattering only involves vertices from strong interactions, the quantum fluctuation part of the photon field is not relevant. In second place, it is necessary to recall that the classical background field parts of quark and gluon fields minimize the classical action and therefore obey the classical equations of motion.[4] This fact allows us to disregard the background part of the quark fields in the second line in the lagrangian. For the gluon fields it is not as apparent how this fact can be used to simplify the parts of the lagrangian that are relevant for the action, because the gluon equations of motion are not as easy to read off the lagrangian. Since the background fields minimize the action, therefore the first functional derivative of the action with respect to each field fluctuation vanishes, which means that terms of the lagrangian that are linear in the gluon field fluctuations do not contribute to the dynamics. Finally for the gauge fixing parameter we choose $\xi = 1$. In summary, the parts of the lagrangian that are relevant to our case is:

$$\begin{aligned}\mathcal{L}^{HLbL} = &-\frac{g_S}{2} f^{a\mu\nu} f^{abc} A'^b_\mu A'^c_\nu - \frac{1}{2}\left(\overline{D}^\mu A'^{a\nu}\overline{D}_\mu A'^a_\nu + \overline{D}^\mu A'^a_\mu \overline{D}^\nu A'^a_\nu - \overline{D}^\mu A'^{a\nu}\overline{D}_\nu A'^a_\mu\right) \\ &- g_S f^{a\bar{b}\bar{c}} A'^{\bar{b}\mu} A'^{\bar{c}\nu}\overline{D}_\mu A'^a_\nu - \frac{1}{4} g_S^2 f^{abc} f^{a\bar{b}\bar{c}} A'^b_\mu A'^c_\nu A'^{\bar{b}\mu} A'^{\bar{c}\nu} \\ &+ \overline{\psi}'_l(\{i\partial\!\!\!/ - m\}\delta_{lk} + e\hat{Q}\delta_{lk}A\!\!\!/ + g_S t^a_{lk} A'\!\!\!/^a)\psi'_k \\ &+ \overline{\psi}_l(e\hat{Q}\delta_{lk}A\!\!\!/' + g_S t^a_{lk} A'\!\!\!/^a)\psi'_k + \overline{\psi}'_l(e\hat{Q}\delta_{lk}A\!\!\!/' + g_S t^a_{lk} A'\!\!\!/^a)\psi_k \\ &+ \overline{\psi}'_l(e\hat{Q}\delta_{lk}A\!\!\!/' + g_S t^a_{lk} A'\!\!\!/^a)\psi'_k\,. \end{aligned} \tag{2.35}$$

[4] The classical background fields actually minimize the quantum effective action, which in absence of external sources and to leading order is equivalent to the same statement on the classical action. For quark and gluon fields the vacuum expectation values of course do not receive perturbative contributions since tadpole perturbative diagrams are zero at all orders.

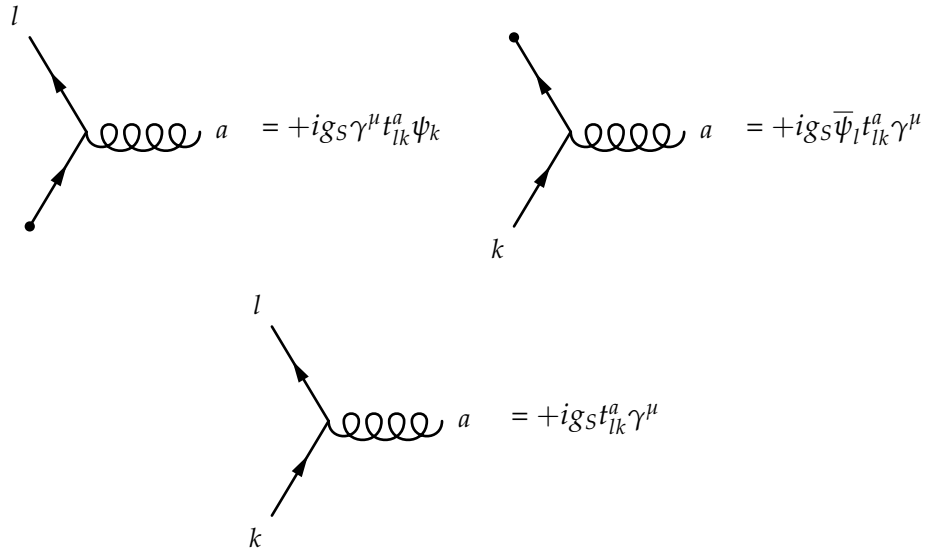

FIGURE 2.2: These figures show the three different types of quark interactions with a quantum gluon. In the two diagrams at the top one quark line is non–pertubatively annihilated by the vacuum. l and k represent the colour of the quarks, a represents the colour of the gluon and trivial quark flavor indices are suppressed.

As usual, the kernel of quadratic terms in one specific fluctuation variable (first and third line in (2.35)) are the inverse of corresponding free propagator, while the terms with a different number of fluctuations (second and fourth line in (2.35)) are interaction vertices. Vertices are very similar to the ones in a theory with no background fields, the only difference being that any one line can now be created or annihilated by the vacuum. Feynman rules for quark–gluon vertices are summarized in figure 2.2, while the ones for gluon self interactions can be found in figure 2.3. It is worth noting that no background gluons appear in any of those graphs since they contribute only to the fermion and gluon propagators that will be presented in the following.

The quark free propagator is modified by the background fields in the usual way:

$$(\{i\partial\!\!\!/ - m\}\delta_{l'l}\delta^{f'f} + e\hat{Q}^{f'f}\delta_{l'l}A\!\!\!/ + g_S\delta^{f'f}t^a_{l'l}A\!\!\!/^a)S^{fs}_{lk}(x,y) = i\delta^4(x-y)\delta^{f's}\delta_{l'k}\,, \tag{2.36}$$

therefore it can be computed recursively by supposing that the strength of the background gauge fields is much smaller than the characteristic momentum of the process of interest, which is a reasonable hypothesis in our context. Note that the new indices $f'f$ represent quark flavor and had been suppressed previously. In the approximation of weak external electromagnetic field, an expansion to $O(e)$ is enough. For the background gluon field it is necessary to go to $O(g_S^2)$ in agreement with the highest mass dimension of the local operators that were chosen for the OPE. In summary, the free quark propagator (in the presence of background gluon and photon fields)

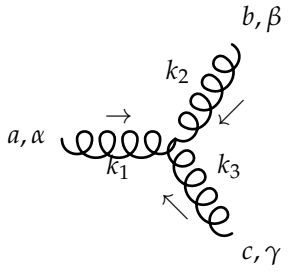

$$= -g_S f^{abc}\Big(g^{\alpha\beta}(k_1-k_2)^{\gamma} + g^{\beta\gamma}(k_2-k_3)^{\alpha} + g^{\gamma\alpha}(k_3-k_1)^{\beta}\Big)$$

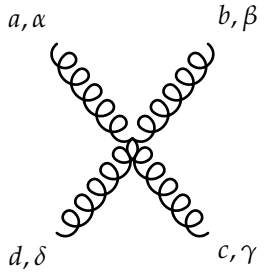

$$= -ig_S^2\Big(f^{abe}f^{cde}(g^{\alpha\gamma}g^{\beta\delta}-g^{\alpha\delta}g^{\beta\gamma}) + f^{ace}f^{bde}(g^{\alpha\beta}g^{\gamma\delta}-g^{\alpha\delta}g^{\beta\gamma}) + f^{ade}f^{bce}(g^{\alpha\beta}g^{\gamma\delta}-g^{\alpha\gamma}g^{\beta\delta})\Big)$$

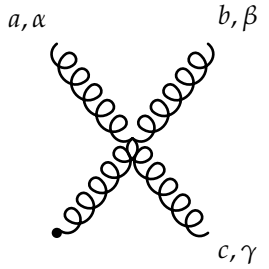

$$= -ig_S^2\Big(f^{abe}f^{cde}(g^{\gamma\alpha}a^{d\beta}-g^{\gamma\beta}a^{d\alpha}) + f^{ace}f^{bde}(g^{\beta\alpha}a^{d\gamma}-g^{\beta\gamma}a^{d\alpha}) + f^{ade}f^{bce}(g^{\alpha\beta}a^{d\gamma}-g^{\alpha\gamma}a^{d\beta})\Big)$$

FIGURE 2.3: These figures show the three different types of gluon self–interactions. The first two diagrams are the the same as the usual diagrams with no backgrounds, while in the last one one of the gluons is annihilated in the vacuum. a, b, c and d represent the colour of the gluons.

at $O(eg_S^2)$ is:

$$\begin{aligned}
S^{fs}_{lk}(x,y) = {} & S^0(x-y)\delta^{fs}\delta_{lk} + i\int_{x_1} S^0(x-x_1)\{e\hat{Q}^{fs}\delta_{lk}\not{A}_{x_1} + g_S t^a_{lk}\delta^{fs}\not{A}^a_{x_1}\}S^0(x_1-y) \\
& - e\hat{Q}^{fs}g_S t^a_{lk}\int_{x_1} S^0(x-x_1)\not{A}_{x_1}\int_{x_2} S^0(x_1-x_2)\not{A}^a_{x_2}S^0(x_2-y) \\
& - e\hat{Q}^{fs}g_S t^a_{lk}\int_{x_1} S^0(x-x_1)\not{A}^a_{x_1}\int_{x_2} S^0(x_1-x_2)\not{A}_{x_2}S^0(x_2-y) \\
& - g_S^2 t^a_{ll'}t^b_{l'k}\delta^{fs}\int_{x_1} S^0(x-x_1)\not{A}^a_{x_1}\int_{x_2} S^0(x_1-x_2)\not{A}^b_{x_2}S^0(x_2-y) \\
& - ie\hat{Q}^{fs}g_S^2 t^a_{lk'}t^b_{k'k}\int_{x_1} S^0(x-x_1)\not{A}_{x_1}\int_{x_2} S^0(x_1-x_2)\not{A}^a_{x_2}\int_{x_3} S^0(x_2-x_3)\not{A}^b_{x_3}S^0(x_3-y) \\
& - ie\hat{Q}^{fs}g_S^2 t^a_{ll'}t^b_{l'k}\int_{x_1} S^0(x-x_1)\not{A}^a_{x_1}\int_{x_2} S^0(x_1-x_2)\not{A}_{x_2}\int_{x_3} S^0(x_2-x_3)\not{A}^b_{x_3}S^0(x_3-y) \\
& - ie\hat{Q}^{fs}g_S^2 t^a_{ll'}t^b_{l'k}\int_{x_1} S^0(x-x_1)\not{A}^a_{x_1}\int_{x_2} S^0(x_1-x_2)\not{A}^b_{x_2}\int_{x_3} S^0(x_2-x_3)\not{A}_{x_3}S^0(x_3-y)\ ,
\end{aligned} \tag{2.37}$$

where $S^0(x-y)$ represents the free quark propagator without background fields:

$$S^0(x-y) = \int \frac{d^4q}{(2\pi)^4} e^{-iq(x-y)} i\frac{\not{q}+m}{q^2-m^2+i\epsilon}\ . \tag{2.38}$$

Due to the presence of a background the propagator is not traslational invariant. This of course also breaks momentum conservation along the propagator in its Fourier transformed version, therefore there are in general three different types of momentum–space quark propagators:

$$S^{fs}_{lk}(p_1,p_2) \equiv \int d^4x \int d^4y\ e^{ip_1x}e^{-ip_2y}S^{fs}_{lk}(x,y)\ , \tag{2.39}$$

$$S^{fs}_{lk}(p_1) \equiv \int d^4x\ e^{ip_1x}S^{fs}_{lk}(x,0) = \int \frac{d^4p_2}{(2\pi)^4}S^{fs}_{lk}(p_1,p_2)\ , \tag{2.40}$$

$$\tilde{S}^{fs}_{lk}(p_2) \equiv \int d^4x\ e^{-ip_2x}S^{fs}_{lk}(0,x) = \int \frac{d^4p_1}{(2\pi)^4}S^{fs}_{lk}(p_1,p_2)\ , \tag{2.41}$$

By Taylor expanding the gauge fields we have intrinsically assumed that they are soft, but not even that restores translation invariance of the propagator. The expression for the momentum

space propagator is:

$$
\begin{aligned}
S^{fs}_{lk}(p_1,p_2) &= (2\pi)^4\delta^4(p_1-p_2)S^0_{p_1}\delta^{fs}\delta_{lk} \\
&+ iS^0_{p_1}\int_{q_1}\{e\hat{Q}^{fs}\delta_{lk}\not{A}_{q_1}+g_S t^a_{lk}\delta^{fs}\not{a}^a_{q_1}\}S^0_{p_1+q_1}(2\pi)^4\delta^4(p_1-p_2+q_1) \\
&- e\hat{Q}^{fs}g_S t^a_{lk}S^0_{p_1}\int_{q_1}\not{A}_{q_1}S^0_{p_1+q_1}\int_{q_2}\not{a}^a_{q_2}S^0_{p_1+q_1+q_2}(2\pi)^4\delta^4(p_1-p_2+q_1+q_2) \\
&- e\hat{Q}^{fs}g_S t^a_{lk}S^0_{p_1}\int_{q_1}\not{a}^a_{q_1}S^0_{p_1+q_1}\int_{q_2}\not{A}_{q_2}S^0_{p_1+q_1+q_2}(2\pi)^4\delta^4(p_1-p_2+q_1+q_2) \\
&- g_S^2 t^a_{ll'}t^b_{l'k}\delta^{fs}S^0_{p_1}\int_{q_1}\not{a}^a_{q_1}S^0_{p_1+q_1}\int_{q_2}\not{a}^b_{q_2}S^0_{p_1+q_1+q_2}(2\pi)^4\delta^4(p_1-p_2+q_1+q_2) \\
&- ie\hat{Q}^{fs}g_S^2 t^a_{ll'}t^b_{l'k}\Big(S^0_{p_1}\int_{q_1}\not{A}_{q_1}S^0_{p_1+q_1}\int_{q_2}\not{a}^a_{q_2}S^0_{p_1+q_1+q_2}\int_{q_3}\not{a}^b_{q_3}S^0_{p_1+q_1+q_2+q_3} \\
&\qquad + S^0_{p_1}\int_{q_1}\not{a}^a_{q_1}S^0_{p_1+q_1}\int_{q_2}\not{A}_{q_2}S^0_{p_1+q_1+q_2}\int_{q_3}\not{a}^b_{q_3}S^0_{p_1+q_1+q_2+q_3} \\
&\qquad + S^0_{p_1}\int_{q_1}\not{a}^a_{q_1}S^0_{p_1+q_1}\int_{q_2}\not{a}^b_{q_2}S^0_{p_1+q_1+q_2}\int_{q_3}\not{A}_{q_3}S^0_{p_1+q_1+q_2+q_3}\Big) \\
&\qquad\qquad \times(2\pi)^4\delta^4(p_1-p_2+\sum_{i=1,2,3}q_i)\,.
\end{aligned}
\tag{2.42}
$$

Note that the Dirac delta is always under the effect of the integrals to its left. Additionally, we have defined:

$$
S^0(p) = i\frac{\not{p}+m}{p^2-m^2+i\epsilon} \equiv S^0_p\,. \tag{2.43}
$$

Note that we have kept the momentum–conservation delta of the y vertex explicitly for $S(p_1,p_2)$ in order to make the relation with $S(p)$ and $\tilde{S}(p)$ more evident in the sense that the effect of the integration over q_1 or q_2 is to simply remove the momentum "conservation" delta. At this point, we can use the expansions of the gauge fields in (2.18). Since the local operators considered for the OPE contain no derivatives of the photon fields and contain only up to one derivative of the gluon field, it is enough to retain the first term of the expansion for the photon field and two terms for the gluon, therefore in the momentum representation we can do the replacement:[5]

$$
\begin{aligned}
a^\mu(q) &= \frac{i}{2}(2\pi)^4 f^{\nu\mu}(0)\frac{\partial}{\partial q^\nu}\delta^4(q) = -\frac{i}{2}(2\pi)^4\delta^4(q)f^{\nu\mu}(0)\frac{\partial}{\partial q^\nu} \\
a^{a\mu}(q) &= \frac{i}{2}f^{a\nu\mu}(0)\frac{\partial}{\partial q^\nu}(2\pi)^4\delta^4(q) - \frac{1}{3}D^\tau f^{a\nu\mu}(0)\frac{\partial}{\partial q^\nu}\frac{\partial}{\partial q^\tau}(2\pi)^4\delta^4(q) \\
&= (2\pi)^4\delta^4(q)\Big(-\frac{i}{2}f^{a\nu\mu}(0)\frac{\partial}{\partial q^\nu} - \frac{1}{3}D^\tau f^{a\nu\mu}(0)\frac{\partial}{\partial q^\nu}\frac{\partial}{\partial q^\tau}\Big)\,,
\end{aligned}
\tag{2.44}
$$

[5]Note that these expressions were derived for soft insertions where momentum is leaving the diagram. From the distributional point of view the derivatives are supposed to act on test-functions [101].

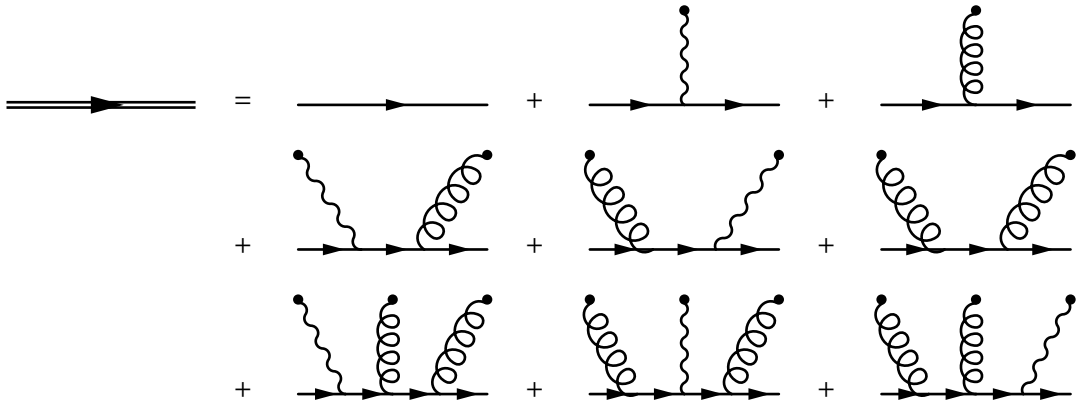

FIGURE 2.4: This figure shows the expansion of the free quark propagator in a background of gauge fields in terms of diagrams with interactions with gluons and photons that are created/annihilated in the vacuum. The order in which diagrams appear in the sum corresponds to the order of terms in equation (2.45).

which yields the following result:

$$
\begin{aligned}
S^{fs}_{lk}(p_1,p_2) = (2\pi)^4 \Bigg(& S^0_{p_1}\delta^{fs}\delta_{lk}\delta^4(p_1-p_2) \\
& + \frac{1}{2}\{e\hat{Q}^{fs}\delta_{lk}f^{\mu_1\nu_1}(0) + g_S t^a_{lk}\delta^{fs}f^{a\mu_1\nu_1}(0)\}\frac{\partial}{\partial q_1^{\mu_1}} S^0_{p_1}\gamma_{\nu_1}S^0_{p_1+q_1}\delta^4(p_1-p_2+q_1) \\
& - \frac{i}{3}g_S t^a_{lk}\delta^{fs}\overline{D}^{\tau}f^{a\mu_1\nu_1}\frac{\partial}{\partial q_1^{\tau}}\frac{\partial}{\partial q_1^{\mu_1}} S^0_{p_1+q_1}S^0_{p_1}\gamma_{\nu_1}\delta^4(p_1-p_2+q_1) \\
& + \frac{1}{4}e\hat{Q}^{fs}g_S t^a_{lk}\Big(f^{\mu_1\nu_1}f^{a\mu_2\nu_2} + f^{a\mu_1\nu_1}f^{\mu_2\nu_2}\Big) \\
& \qquad \times \frac{\partial}{\partial q_1^{\mu_1}}\frac{\partial}{\partial q_2^{\mu_2}}\Big(S^0_{p_1}\gamma_{\nu_1}S^0_{p_1+q_1}\gamma_{\nu_2}S^0_{p_1+q_1+q_2}\delta^4(p_1-p_2+q_1+q_2)\Big)\Big|_{q_{1,2}=0} \\
& + \frac{1}{4}g_S^2 t^a_{ll'}t^b_{l'k}\delta^{fs}\Big(f^{a\mu_1\nu_1}f^{b\mu_2\nu_2}\Big) \\
& \qquad \times \frac{\partial}{\partial q_1^{\mu_1}}\frac{\partial}{\partial q_2^{\mu_2}}\Big(S^0_{p_1}\gamma_{\nu_1}S^0_{p_1+q_1}\gamma_{\nu_2}S^0_{p_1+q_1+q_2}\delta^4(p_1-p_2+q_1+q_2)\Big)\Big|_{q_{1,2}=0} \\
& + \frac{1}{8}e\hat{Q}^{fs}g_S^2 t^a_{lk'}t^b_{k'k}\Big(f^{\mu_1\nu_1}f^{a\mu_2\nu_2}f^{b\mu_3\nu_3} + f^{a\mu_1\nu_1}f^{\mu_2\nu_2}f^{b\mu_3\nu_3} + f^{a\mu_1\nu_1}f^{b\mu_2\nu_2}f^{\mu_3\nu_3}\Big) \\
& \qquad \times \frac{\partial}{\partial q_1^{\mu_1}}\frac{\partial}{\partial q_2^{\mu_2}}\frac{\partial}{\partial q_3^{\mu_3}}\Big(S^0_{p_1}\gamma_{\nu_1}S^0_{p_1+q_1}\gamma_{\nu_2}S^0_{p_1+q_1+q_2}\gamma_{\nu_3}S^0_{p_1+q_1+q_2+q_3} \\
& \qquad\qquad \times \delta^4(p_1-p_2+\sum_{i=1,2,3}q_i)\Big)\Big|_{q_{1,2,3}=0}\Bigg) .
\end{aligned}
\tag{2.45}
$$

This expression for the free quark propagator can be understood as an expansion in terms of diagrams (see figure 2.4) with increasing number of (background) gauge bosons.

At the order that we are interested in there appear no gluon propagators, nevertheless, for the sake of completeness we present the result up to relevant terms for the operators in (2.7):

$$D_{F,\mu\nu}(q) = \frac{-i}{q^2}g_{\mu\nu} + 2ig_S\frac{f_{\mu\nu}}{q^4} - 4\frac{g_S}{q^6}q_\alpha D^\alpha f_{\mu\nu} + g_S\frac{2}{3}\frac{g_{\mu\nu}}{q^6}q^\alpha D^\beta f_{a\beta\alpha} + i\frac{2g_S}{q^8}g_{\mu\nu}q^\alpha q^\beta D_\beta D^{\mu'} f_{\mu'\alpha}$$
$$+ 2i\frac{g_S}{q^6}D^2 f_{\mu\nu} - \frac{8i}{q^8}g_S q_\alpha q_\beta D^\beta D^\alpha f_{\mu\nu} + i\frac{g_S^2}{2}\frac{g_{\mu\nu}}{q^6}f_{\alpha\mu'}f^{\mu'\alpha} + i\frac{g_S^2}{q^8}g_{\mu\nu}q^\alpha q^\beta f_\beta{}^{\mu'} f_{\mu'\alpha}$$
$$- 4i\frac{g_S^2}{q^6}f_{\mu\mu'}f^{\mu'}{}_{\nu}\,.$$

The details of the computation are presented in the appendix B.2.

2.4 Computation of un–renormalized Wilson coefficients

In the previous section we obtained expressions for the quark and gluon fluctuations propagators which contained background insertions of vacuum expectation values (VEV) such as $f^{a\mu\nu}$ and $f^{\mu\nu}$. Furthermore we saw that vertices from the Dyson series also introduce VEVs of quark operators, thus giving us all the tools required to build the OPE of $\Pi^{\mu_1\mu_2\mu_3}$ with background fields and find the Wilson coefficients that require to compute $\Pi_F^{\mu_1\mu_2\mu_3\mu_4\mu_5}$. There is, however, a subtlety that has not been addressed: we are assuming that the product of background fields, that is, the product of VEVs is somehow equivalent to the VEVs of the product of the corresponding fields. For example, we are letting $\overline{\psi}\sigma_{\mu\nu}\psi$ take the role of $\langle\overline{\Psi}\sigma_{\mu\nu}\Psi\rangle$. The justification for such equivalence lies at the core of the background field method definition in terms of the quantum one-particle irreducible effective action [102]. Let us represent a generating functional for a general theory as:

$$Z[J_n] = \int\prod_n \mathcal{D}\Phi_n \exp i\Big(S[\Phi_n] + J_n\Phi_n\Big)\,, \tag{2.46}$$

where Φ represents different types of fields (fermion, vector, scalar, etc.) and n is a collective index that is meant to label all color, flavor, Lorentz, and other degrees of freedom. Complementary one can define a background generating functional:

$$\mathcal{Z}[J_n,\phi_n] = \int\prod_n \mathcal{D}\phi'_n \exp i\Big(S[\phi_n+\phi'_n] + J_n\phi'_n\Big)\,, \tag{2.47}$$

where primed and unprimed variables represent quantum fluctuations and background fixed fields just as in the previous sections. From these objects one can obtain the corresponding quantum effective action by performing a Legendre transform on the generator of connected diagrams:

$$W[J_n] = -i\ln Z[J_n]\,, \qquad \Gamma[\langle\Phi_n\rangle_J] = W[J_n] - \int d^4x\, J_n(x)\langle\Phi_n\rangle_J(x)\,,$$
$$\mathcal{W}[J_n,\phi_n] = -i\ln\mathcal{Z}[J_n,\phi_n]\,, \qquad H[\langle\phi'_n\rangle_J,\phi_n] = \mathcal{W}[J_n] - \int d^4x\, J_n(x)\langle\phi'_n\rangle_J(x)\,,$$

where $\langle\Phi_n\rangle_J$ and $\langle\phi'_n\rangle_J$ represent the VEVs of Φ_n and ϕ'_n in the presence of sources J_n:

$$\langle\Phi_n\rangle_J \equiv \frac{\delta Z}{\delta J_n}\,, \qquad \langle\phi'_n\rangle_J \equiv \frac{\delta\mathcal{Z}}{\delta J_n}\,.$$

Furthermore, by shifting the integration variable in $\mathcal{Z}$ it is possible to conclude that these objects, although defined for different generating functionals, are related to each other:

$$\begin{aligned} \langle \phi'_n \rangle_J = \langle \Phi_n \rangle_J - \phi_n \qquad &\Longrightarrow \qquad H[\langle \phi'_n \rangle_J, \phi_n] = \Gamma[\langle \phi'_n \rangle_J + \phi_n] \,, \\ \phi_n = \langle \Phi_n \rangle_J \qquad &\Longrightarrow \qquad H[0, \phi_n] = \Gamma[\phi_n] \,. \end{aligned}$$

The last equation states that the quantum effective action of a theory can be computed from its corresponding background effective action by turning off the VEV of the fluctuations. Moreover, since one–particle irreducible (1PI) diagrams are obtained by functional differentiation of the quantum effective action one can conclude that: 1) $H[0, \phi_n]$ diagrams contain no external lines of quantum fluctuations, 2) matrix elements in the original theory (represented by $Z[J_n]$) can be computed by functionally differentiating vacuum–to–vacuum diagrams in the background theory with respect to the background fields, which is the result we required at the start of this section.[6]

Concerning the actual computation of Wilson coefficients, let us start by considering the one related to $S_{1,\mu\nu} = e e_f F_{\mu\nu}$. This term represents the configuration in which hard momenta travels through all internal lines of the diagrams, thus, there are no cut lines. The leading order contribution for this configuration is given by the quark loop (see figure 2.5), where different contributions are obtained by inserting the soft photon in different sides of the triangle and/or inverting the orientation of the loop. Since $S_{1,\mu\nu}$ is the operator with the lowest dimension in the OPE, its Wilson coefficient is expected to give the most relevant contribution to $\Pi_F^{\mu_1\mu_2\mu_3\mu_4\mu_5}$ and therefore to a_μ. With respect to the background field expansion of (2.12), this contribution comes from the matrix element that contains only quantum fluctuations in (2.13) and so:

$$\begin{aligned} \Pi^{\mu_1\mu_2\mu_3} = \frac{1}{e} \sum_{f_1 f_2 f_3} e_{f_1} e_{f_2} e_{f_3} \int d^4x \int d^4y \, e^{-i(q_1 x + q_2 y)} \\ \times \Bigg(\langle 0| \operatorname{Tr} \left\{ \gamma^{\mu_1} S^{f_1 f_2}(x,y) \gamma^{\mu_2} S^{f_2 f_3}(y,0) \gamma^{\mu_3} S^{f_3 f_1}(0,x) \right\} |\gamma\rangle \\ + \langle 0| \operatorname{Tr} \left\{ S^{f_3 f_1}(y,x) \gamma^{\mu_1} S^{f_1 f_3}(x,0) \gamma^{\mu_3} S^{f_3 f_2}(0,y) \gamma^{\mu_2} \right\} |\gamma\rangle \Bigg) \,, \end{aligned} \tag{2.48}$$

where the trace acts on Dirac and color indices of the quarks. Note that the two terms between big parentheses can be obtained from one another by permuting indices and momentum between the x and y vertices. They represent two different orientations of the quark loop. Furthermore, the insertion of the soft photon can be performed on any one of the fermion propagators, therefore it is necessary to permute the position of such soft vertex as well. In the end, the result in momentum space is:

$$\begin{aligned} \Pi_{S_1}^{\mu_1\mu_2\mu_3} = \frac{N_c}{2} \int \frac{d^4p}{(2\pi)^4} \sum_f e_f^4 \langle 0| F_{\nu_4\mu_4} |\gamma\rangle \frac{\partial}{\partial q_{4\nu_4}} \sum_{\sigma(1,2,4)} \operatorname{Tr} \Big\{ \gamma^{\mu_3} S^0(p + q_1 + q_2 + q_4) \\ \times \gamma^{\mu_4} S^0(p + q_1 + q_2) \gamma^{\mu_1} S^0(p + q_2) \gamma^{\mu_2} S^0(p) \Big\} \Big|_{q_4 = 0} \,, \end{aligned} \tag{2.49}$$

where N_c is the number of quark colors, f represents quark flavor and $\sigma(1,2,4)$ represents a permutation over the set $\{(q_i, \mu_i) \,|\, i \in \{1,2,4\}\}$. The derivative with respect to the soft photon

[6] The gauge fixing procedure requires one to be careful not to break the symmetries of the "original" $Z[J_n]$ when building $\mathcal{Z}[J_n, \phi_n]$ in order for this conclusions to hold, which is just what we did in the previous section.

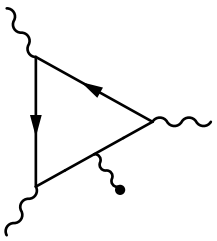

FIGURE 2.5: Representative diagram of the leading order contribution to the Wilson coefficient of $S_{1,\mu\nu}$ in the OPE of $\Pi^{\mu_1\mu_2\mu_3}$. The black dot represents creation/annihilation of a line by the background fields in the vacuum.

momentum can be traced back to (2.45). Note that propagator depends implicitly on the quark flavor through the masses, assumed to be all equal for the light flavours considered. Consequently, the contribution from the Wilson coefficient of $S_{1,\mu\nu}$ to $\Pi_F^{\mu_1\mu_2\mu_3\mu_4\mu_5}$ is:

$$\Pi_{F(S_1)}^{\mu_1\mu_2\mu_3\mu_4\nu_4} = i\frac{N_c}{2}\int\frac{d^4p}{(2\pi)^4}\sum_f e_f^4\frac{\partial}{\partial q_{4\nu_4}}\sum_{\sigma(1,2,4)}\mathrm{Tr}\left\{\gamma^{\mu_3}S^0(p+q_1+q_2+q_4)\gamma^{\mu_4}\right.$$
$$\left.\times S^0(p+q_1+q_2)\gamma^{\mu_1}S^0(p+q_2)\gamma^{\mu_2}S^0(p)\right\}\Big|_{q_4=0}, \tag{2.50}$$

where the effect of the derivative on the propagators is to duplicate them:

$$\lim_{q_4\to 0}\frac{\partial}{\partial q_{\nu_4}}S(p+q_4) = i\lim_{q_4\to 0}S^0(p+q_4)\gamma^{\nu_4}S(p+q_4) = iS^0(p)\gamma^{\nu_4}S^0(p)\,. \tag{2.51}$$

Contributions with one cut quark line and at most one soft gauge boson insertion ($S_{2-5,\mu\nu}$ and $S_{7,\mu\nu}$) are obtained at leading order from the diagrams in figure 2.6. Their corresponding amplitudes are computed from matrix elements in (2.13) that contain two soft quark fields and require no vertices from the Dyson series expansion. Soft gluon or photon insertions on quark hard lines, if necessary, come from propagators of quark fluctuations as seen in the previous section.

Except for $S_{1,\mu\nu}$, contributions from all operators to $\Pi_F^{\mu_1\mu_2\mu_3\mu_4\mu_5}$ depend on the susceptibilities X_i^S. By definition these are non–perturbative quantities which are usually computed either by lattice, models and/or educated guesses. Since we are mainly focused on the bigger contribution coming from $S_{1,\mu\nu}$, they are not of interest for us in this work. The most well–known one is X_5,[7] because it is related to the quark condensate which is a common subject of study in lattice computations. A more recent version of the review cited in [35] can be found in [103], where figure 14, table 22 and references therein represent a thorough compilation of results for the quark condensate. The rest of the susceptibilities are not so well–known and their numerical values are estimated in [35] by a combination of models and educated guesses whose details are not very relevant for this work and hence we do not discuss them here.

[7] Note that we have suppressed the S index. This was done because, as we will see in the next section, the elements of the OPE need renormalization and therefore a new set of susceptibilities X_i is defined in terms of the renormalized operators.

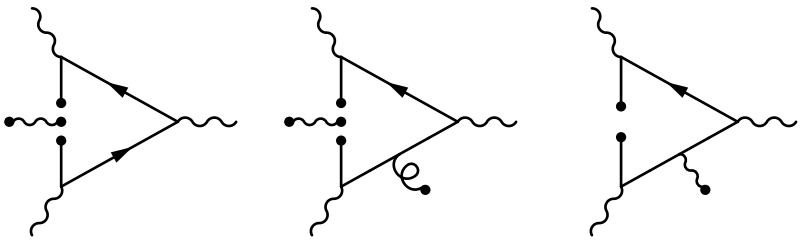

FIGURE 2.6: Representative diagrams of the leading order contribution to the Wilson coefficient of $S_{2,\mu\nu}$ (first diagram), $S_{3,4,7,\mu\nu}$ (second diagram) and $S_{5,\mu\nu}$ (third diagram) in the OPE of $\Pi^{\mu_1\mu_2\mu_3}$. The black dot represents creation/annihilation of a line by the background fields in the vacuum.

Although operators $S_{2-5,\mu\nu}$ and $S_{7,\mu\nu}$ may seem quite different at first, their contributions to $\Pi^{\mu_1\mu_2\mu_3}$ can actually be computed together with a very compact formula:

$$\Pi^{\mu_1\mu_2\mu_3}_{S_{2,3,4,5,7}} = \frac{1}{e}\sum_{\substack{f,A,p,n\\ \sigma(1,2,3)}} e_f^3(-1)^n\langle 0|\overline{\Psi}D_{\nu_1}...D_{\nu_n}c_A\Gamma^A\Psi|\gamma(q_4)\rangle \\ \times \mathrm{Tr}\left\{\gamma^{\mu_3}\Gamma^A\gamma^{\mu_1}S^0(-q_1)\gamma^{\nu_1}S^0(-q_1)...\gamma^{\nu_p}S^0(-q_1)\gamma^{\nu_2}S^0(q_3)\gamma^{\nu_{p+1}}S^0(q_3)...\gamma^{\nu_n}S^0(q_3)\right\}, \tag{2.52}$$

where f represents quark flavor, Γ^A is an element of a basis of Dirac matrices and

$$c_A \equiv 1/\,\mathrm{Tr}\{\Gamma^A\Gamma^A\}\,. \tag{2.53}$$

Broadly speaking, this formula is obtained by: 1) expanding the soft quark bilinears as:

$$\overline{\psi}_j\psi_i = \sum_A c_A\Gamma^A_{ij}\overline{\psi}\Gamma^A\psi\,, \tag{2.54}$$

where i, j are bispinor indices, 2) Taylor expanding the soft quark and gauge field using (2.18) up to operators with relevant dimensions and 3) Fourier–transforming the result of the previous two steps. Since the Fourier representation of the x polynomials that come from Taylor expansions is a derivative in the momentum space, a corresponding number of new vertices and propagators arise by iterative use of (3.8). Details of the derivation of (2.52) can be found in appendix D of [35].

Although equation (2.52) is very compact, its disadvantage is that it is expressed in terms of a basis of operators $\overline{\Psi}\Gamma D_{\nu_1}...D_{\nu_n}\Psi$ that is different from the one we have in (2.7). Even more important: the relation between such basis elements and $\langle F_{\mu\nu}\rangle$ is quite obscure and it makes the computation of Π_F harder. Thus, it is necessary to perform a basis change between the matrix elements in (2.52) and (2.7). Only operators with the same symmetries as $F_{\mu\nu}$, namely, odd charge conjugation parity, give non–trivial transformation coefficients, which greatly narrows the options down. Then, Lorentz covariance, quark equations of motion and Dirac matrices identities can be used to obtain the desired transformation matrix, up to matrix elements of total gauge–covariant derivatives, which are trivially zero due the soft nature of the background photon. Classifying matrix elements by the number of covariant derivatives, the non–trivial transformation coefficients between both bases are given in the following list, while the derivation of these results can be found in B.3.

- Matrix elements with zero covariant derivatives:

$$\langle 0|\overline{\Psi}\sigma^{\alpha\beta}\Psi|\gamma(q_4)\rangle \equiv \langle\overline{\Psi}\sigma^{\alpha\beta}\Psi\rangle = X_2^S\langle ee_f F^{\alpha\beta}\rangle \,. \tag{2.55}$$

None of the other Dirac bilinears have the correct Lorentz structure and consequently do not contribute.

- Matrix elements with one covariant derivative:

$$\langle\overline{\Psi}D^\nu\gamma^\alpha\gamma_5\Psi\rangle = -\frac{im_f}{4}X_2^S\epsilon^{\nu\alpha\tau\rho}\langle ee_f F_{\tau\rho}\rangle \,. \tag{2.56}$$

Lorentz covariance allows one to discard $\sigma^{\mu\nu}$, γ_5 and $\mathbb{1}$ from appearing and γ^μ is rejected due to its charge conjugation parity. Note that the parity violation of this matrix element is compensated by the appearance of $\gamma^\alpha\gamma_5$ again in the Dirac trace of (2.52).

- Matrix elements with two covariant derivatives:

$$\langle\overline{\Psi}D^{\nu_1}D^{\nu_2}\Psi\rangle = -\frac{i}{2}\langle ee_f F^{\nu_1\nu_2}\rangle\Big(X_5^S - X_3^S\Big) \,, \tag{2.57}$$

$$\langle\overline{\Psi}D^{\nu_1}D^{\nu_2}\gamma_5\Psi\rangle = -\frac{1}{4}X_4^S\epsilon^{\nu_1\nu_2\alpha\beta}\langle ee_f F_{\alpha\beta}\rangle \,, \tag{2.58}$$

$$\begin{aligned}\langle\overline{\Psi}D^{\nu_1}D^{\nu_2}\sigma^{\alpha\beta}\Psi\rangle &= A_1 g^{\nu_1\nu_2}\langle ee_f F^{\alpha\beta}\rangle \\ &\quad + ee_f A_2\Big(g^{\nu_1\alpha}\langle F^{\nu_2\beta}\rangle + g^{\nu_2\alpha}\langle F^{\nu_1\beta}\rangle - g^{\nu_1\beta}\langle F^{\nu_2\alpha}\rangle - g^{\nu_2\beta}\langle F^{\nu_1\alpha}\rangle\Big) \,,\end{aligned} \tag{2.59}$$

where

$$\begin{aligned}A_1 &= \frac{1}{3}\Big(-m_f^2X_2^S - X_S^4 + \frac{1}{2}(X_5^S - X_3^S)\Big) \,, \\ A_2 &= \frac{1}{12}(m_f^2X_2^S + X_S^4 + X_5^S - X_3^S) \,.\end{aligned} \tag{2.60}$$

Lorentz covariance allows one to discard γ^μ and $\gamma^\mu\gamma_5$ from appearing and none is rejected due to its charge conjugation parity.

- Matrix elements with three covariant derivatives:

$$\begin{aligned}\langle\overline{\Psi}D^{\nu_1}D^{\nu_2}D^{\nu_3}\gamma^\alpha\Psi\rangle &= ee_f A_3\Big(g^{\nu_1\nu_2}\langle F^{\nu_3\alpha} - g^{\nu_3\nu_2}\langle F^{\nu_1\alpha}\rangle\Big) \\ &\quad + ee_f A_4\Big(g^{\nu_1\alpha}\langle F^{\nu_2\nu_3}\rangle - g^{\nu_3\alpha}\langle F^{\nu_2\nu_1}\rangle\Big) \\ &\quad + ee_f A_5 g^{\nu_2\alpha}\langle F^{\nu_1\nu_3}\rangle \,,\end{aligned} \tag{2.61}$$

$$\begin{aligned}\langle\overline{\Psi}D^{\nu_1}D^{\nu_2}D^{\nu_3}\gamma^\alpha\gamma_5\Psi\rangle &= ee_f A_6 g^{\nu_1\nu_3}\langle\overline{F}^{\nu_2\alpha}\rangle \\ &\quad + ee_f A_7\Big(g^{\nu_1\nu_2}\langle\overline{F}^{\nu_3\alpha}\rangle + g^{\nu_2\nu_3}\langle\overline{F}^{\nu_1\alpha}\rangle\Big) \\ &\quad + ee_f A_8\Big(g^{\nu_1\alpha}\langle\overline{F}^{\nu_2\nu_3}\rangle - g^{\nu_3\alpha}\langle\overline{F}^{\nu_1\nu_2}\rangle\Big) \,,\end{aligned} \tag{2.62}$$

where $\overline{F}_{\mu\nu} \equiv \frac{i}{2}\epsilon^{\mu\nu\alpha\beta}F_{\alpha\beta}$ is the dual of the electromagnetic field–strength tensor and the coefficients are found to be:

$$\begin{aligned}
A_3 &= \frac{1}{24}\Big(-5X^S_{8,1} + 2X^S_7 - 5m_f X^S_4 + 2m_f X^S_3 \Big) \,, \\
A_4 &= \frac{1}{24}\Big(-5X^S_{8,1} + X^S_7 - 3m_f X^S_5 - m_f X^S_4 + 4m_f X^S_3 \Big) \,, \\
A_5 &= \frac{1}{24}\Big(-2X^S_{8,1} - X^S_7 - 3m_f X^S_5 - 2m_f X^S_4 + 2m_f X^S_3 \Big) \,, \\
A_6 &= \frac{1}{24}\Big(-6X^S_{8,1} + X^S_7 - m_f X^S_5 - 2m_f X^S_4 + 2m_f X^S_3 + 2m^3_f X^S_2 \Big) \,, \\
A_7 &= \frac{1}{24}\Big(-X^S_{8,1} + X^S_7 - m_f X^S_5 + m_f X^S_4 + 2m_f X^S_3 + 2m^3_f X^S_2 \Big) \,, \\
A_8 &= \frac{1}{24}\Big(-6X^S_{8,1} + 3m_f X^S_4 \Big) \,.
\end{aligned} \tag{2.63}$$

Lorentz covariance allows one to discard: $\mathbb{1}$, $\sigma^{\mu\nu}$ and γ_5 from appearing and none is rejected due to its charge conjugation parity.

These transformation relations together with (2.52) allow one to compute the leading order Wilson coefficients of the operators in (2.7) with one cut quark line for the OPE that we are interested in and even some contributions with two cut quark lines.

Let us now consider operators with four quark background insertions ($S_{8,\mu\nu}$). Diagrams that contribute to the Wilson coefficients of this operator correspond to the quark loop with two cut quark lines, therefore the diagram is divided in two parts, which have to be connected by a gluon (see figure 2.7). There are six different ways in which the virtual gluon line can connect the two parts of the diagram and all have to be accounted for. The corresponding two gluon–quark vertices are responsible for the α_S coefficient of $S_{8,\mu\nu}$. There are only two combinations of operators with four quark fields that are not trivial:

$$\begin{aligned}
S^{\mu\nu}_{8,1} &= -\frac{g_S^2}{2}\epsilon^{\mu\nu\lambda\rho}\sum_{A,B}\overline{\Psi}_A\gamma_\lambda t^a\Psi_A\, e_B^3\,\overline{\Psi}_B\gamma_\rho\gamma_5 t^a\Psi_B \,, \\
S^{\mu\nu}_{8,2} &= -\frac{g_S^2}{2}\epsilon^{\mu\nu\lambda\rho}\sum_{A,B} e_A^2\,\overline{\Psi}_A\gamma_\lambda t^a\Psi_A\, e_B\,\overline{\Psi}_B\gamma_\rho\gamma_5 t^a\Psi_B \,.
\end{aligned} \tag{2.64}$$

Note that the only difference between the two operators are the charge matrix elements. Their corresponding contribution to the OPE is:

$$\begin{aligned}
\Pi^{\mu_1\mu_2\mu_3} = \frac{i}{e}\frac{g_S^2}{16}\sum_{A,B}\Big\langle e_A^2\,\overline{\Psi}_A\Gamma^{\alpha P}t^a\Psi_A\, e_B\,\overline{\Psi}_B\Gamma^{\beta Q}t^a\Psi_B\Big\rangle \\
\times\sum_{\sigma(1,2,3)}\frac{1}{q_3^2}\,\mathrm{Tr}\Big[\Gamma_{\beta Q}\Big(\gamma^{\mu_3}S^0(-q_3)\gamma^\lambda + \gamma^\lambda S^0(q_3)\gamma^{\mu_3}\Big)\Big] \\
\times\,\mathrm{Tr}\Big[-\Gamma_{\alpha P}\Big(\gamma^{\mu_1}S^0(-q_1)\gamma^{\mu_2}S^0(q_3)\gamma_\lambda + \gamma_\lambda S^0(-q_3)\gamma^{\mu_1}S^0(q_2)\gamma^{\mu_2} \\
+\gamma^{\mu_1}S^0(-q_1)\gamma_\lambda S^0(q_2)\gamma^{\mu_2}\Big)\Big] \,,
\end{aligned} \tag{2.65}$$

where $\Gamma^{\alpha P} \in \{\gamma^\alpha, \gamma^\alpha\gamma_5\}$ and $\Gamma^\alpha_P \in \{\gamma^\alpha, -\gamma^\alpha\gamma_5\}$. Note that the factor $1/16$ comes from the trace

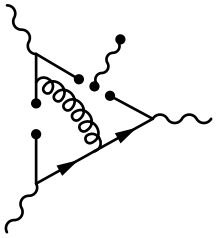

FIGURE 2.7: Representative diagram of the leading order contribution to the Wilson coefficient of $S_{8,\mu\nu}$ in the OPE of $\Pi^{\mu_1\mu_2\mu_3}$. The black dot represents creation/annihilation of a line by the background fields in the vacuum.

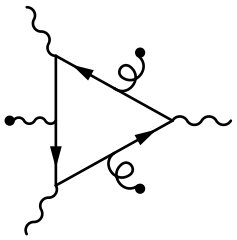

FIGURE 2.8: Representative diagram of the leading order contribution to the Wilson coefficient of $S_{6,\mu\nu}$ in the OPE of $\Pi^{\mu_1\mu_2\mu_3}$. The black dot represents creation/annihilation of a line by the background fields in the vacuum.

of gamma matrices in the expansion of spinor products that we mentioned previously. The same goes for the minus sign in $-\Gamma_{\alpha P}$. There are two independent traces because there are two disconnected fermionic lines in the diagram of figure 2.7. Note that charge conjugation antisymmetry requires P and Q to be different. Furthermore, some terms in the series can be neglected up to mass corrections, due to the vanishing trace of an odd number of gamma matrices.

Let us now consider the operator with two cut gluon lines, that is, $S_{6,\mu\nu}$. Diagrams contributing to this operator are very similar to the quark loop of $S_{1,\mu\nu}$, but they have two soft gluon insertions (see figure 2.8). As with the first quark loop, these insertions must be permuted in all possible ways (for example, all three may be in the same quark line or there may be just one on each side of the triangle) to obtain the full contribution. This leads to an expression similar but more complex than the one in (2.50):

$$\begin{aligned}\Pi^{\mu_1\mu_2\mu_3}_{S_6} = \frac{1}{16}\sum_f e_f^4 g_S^2 \,\mathrm{Tr}\{t^a t^b\} F_{\nu_4\mu_4}\langle G_{a\nu_5\mu_5} G_{b\nu_6\mu_6}\rangle \int \frac{d^d p}{(2\pi)^d}\frac{\partial}{\partial q_{4\nu_4}}\frac{\partial}{\partial q_{5\nu_5}}\frac{\partial}{\partial q_{6\nu_6}} \\ \times \sum_{\sigma(1,2,4,5,6)} \mathrm{Tr}\Big\{\gamma^{\mu_3} S^0(p+q_1+q_2+q_4+q_5+q_6)\gamma^{\mu_1} \\ \times S^0(p+q_2+q_4+q_5+q_6)\gamma^{\mu_2} S^0(p+q_4+q_5+q_6)\gamma^{\mu_4} \\ \times S^0(p+q_5+q_6)\gamma^{\mu_5} S^0(p+q_6)\gamma^{\mu_6} S^0(p)\Big\}\Big|_{q_{4,5,6}=0}.\end{aligned} \tag{2.66}$$

Note that three derivatives appear instead of one because of the three soft insertions. Replacing $\mathrm{Tr}\{t^a t^b\} = \frac{1}{2}\delta^{ab}$ and $\alpha_S = g_S^2/4\pi$ we obtain:

$$\begin{aligned}\Pi^{\mu_1\mu_2\mu_3\mu_4\nu_4}_{F(S_6)} = i\frac{\pi^2}{8}\sum_f e_f^4 \frac{1}{d(d-1)}\langle\frac{\alpha_S}{\pi}G^{c\mu\nu}G_{c\mu\nu}\rangle\left(g_{\nu_5\nu_6}g_{\mu_5\mu_6}-g_{\nu_5\mu_6}g_{\mu_5\nu_6}\right)\\ \times\int\frac{d^dp}{(2\pi)^d}\frac{\partial}{\partial q_{4\nu_4}}\frac{\partial}{\partial q_{5\nu_5}}\frac{\partial}{\partial q_{6\nu_6}}\sum_{\sigma(1,2,4,5,6)}\mathrm{Tr}\Big\{\gamma^{\mu_3}S^0(p+q_1+q_2+q_4+q_5+q_6)\gamma^{\mu_1}\\ \times S^0(p+q_2+q_4+q_5+q_6)\gamma^{\mu_2}S^0(p+q_4+q_5+q_6)\gamma^{\mu_4}\\ \times S^0(p+q_5+q_6)\gamma^{\mu_5}S^0(p+q_6)\gamma^{\mu_6}S^0(p)\Big\}\Big|_{q_{4,5,6}=0},\end{aligned} \tag{2.67}$$

where we have used that:

$$\langle G^{a\nu_5\mu_5}G^{b\nu_6\mu_6}\rangle = \langle G^{c\mu\nu}G_{c\mu\nu}\rangle\frac{1}{8d(d-1)}\delta^{ab}\left(g^{\nu_5\nu_6}g^{\mu_5\mu_6}-g^{\nu_5\mu_6}g^{\mu_5\nu_6}\right), \tag{2.68}$$

where d is the space–time dimension. We leave the space time dimension d, for renormalization purposes as will be made clear later.

Up to this point we have presented all unrenormalized Wilson coefficients associated with operators in (2.7) and, more importantly, their contribution to $\partial^{\mu_5}\Pi^{\mu_1\mu_2\mu_3\mu_4}$. It is possible to include these high energy contributions to a_μ in the same framework of the low energy dispersive computations by projecting them onto the different scalar form factors $\overline{\Pi}_i$ of the Mandelstam decomposition that appear in the master formula (1.69). Such projectors can be found in references [35, 36][8] and are unique up to the freedom given by gauge invariance of the HLbL tensor.

Computation of the Wilson coefficients is however not yet complete, for renormalization of the OPE elements has not been taken into account. In contrast to the usual situation in perturbative computations, we have not encountered ultraviolet divergences in the Wilson coefficients of this section. In fact, except for $S_{1,\mu\nu}$ and $S_{6,\mu\nu}$ all of their leading order contributions are at tree level. As we will see in the next chapter for the quark loop, the Wilson coefficients of these two operators, although finite, have infrared divergences that are regularized by the quark masses. Such singularities scale as logarithms and negative powers of m_f. These singular terms are problematic in a twofold way. From a computational perspective these singular factors may spoil convergence of the perturbative computation when the momenta of the process, namely Q_i, get much bigger that the mass scale of the quarks, which is actually our situation. From a conceptual point of view it is also questionable to have Wilson coefficients with infrared contributions: in the OPE framework they are meant to represent the contribution from the parts of the diagram through which the external very high momenta travel. In the next section we will present how renormalization of the the product of background fields "cures" these infrared divergences and thus completes the separation of low and high energy contributions of the OPE.

2.5 OPE of $\Pi^{\mu_1\mu_2\mu_3\mu_4}$ in an electromagnetic background field: Renormalization

In this section we will present the renormalization program for the operators that form the OPE for $\Pi^{\mu_1\mu_2\mu_3}$ in the $\overline{MS}$ scheme.

[8] Note that the projectors in [35, 36] refer to the tensor structures of [23] instead of the ones in [22].

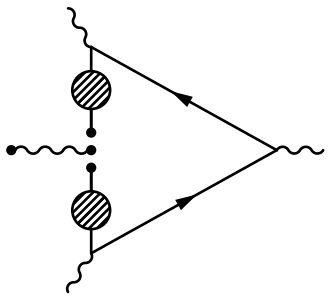

FIGURE 2.9: Diagram with infrared divergences affecting the Wilson coefficient of $S_{2,\mu\nu}$ in the OPE of $\Pi^{\mu_1\mu_2\mu_3}$. The black dot represents creation/annihilation of a line by the background fields in the vacuum. The shaded blob represents self–energy corrections to the soft quark line.

The Wilson coefficients that were presented in the previous section do not suffer from ultraviolet divergences at the computed order, but do have infrared divergences that are regularized by the quarks masses. As mentioned at the end of the previous section, these singularities may spoil the convergence of the perturbative expansion with terms like $1/m_f^2$ or logarithms $\ln\{Q_i^2/m_f^2\}$ that compare the scales of the external momenta Q_i and the quark masses. Moreover, Wilson coefficients should not have infrared contributions in the first place, therefore it should be possible to safely to compute them in the massless quarks limit. There is an additional kind of low energy effects that may affect Wilson coefficients: the ones arising from diagrams where soft quark and gluon[9] lines receive self–energy corrections. For example, figure 2.9 shows how such divergences can arise in diagrams that contribute to the Wilson coefficient of $S_{2,\mu\nu}$. The gray blob of figure 2.9 involves a perturbative series in α_S at zero momentum, which of course does not converge since the processes it is trying to describe belong to the non–perturbative domain. These diagrams however do not appear at the order we are considering and therefore we will not discuss them in detail this section.

The prescription of a renormalization program in this context is not very surprising considering that the OPE is built from composite operators which are known to require counterterms of their own to be renormalized. Therefore, one could expect that after carrying out the renormalization of these composite operators the infrared divergences of the Wilson coefficients are cancelled. In [35], renormalization was done in the full–field framework by dressing operators $S_{i.\mu\nu}$, that is, by inserting them into the Dyson series expansion. For example, for $S_{2,\mu\nu}$ the dressing procedure involved the replacement:

$$\overline{\Psi}\sigma_{\mu\nu}\Psi \longrightarrow \overline{\Psi}\sigma_{\mu\nu}\Psi e^{i\int d^4x\mathcal{L}_{int}}(x)\ , \tag{2.69}$$

where $\mathcal{L}_{int}$ is the HLbL interaction lagrangian. Then, operator mixing[10] was obtained by appropriately contracting some of the fields.

However, from the point of view of the background field method that we have followed in the previous sections, these operators are simply products of classical background fields, so at first it may seem rather odd to assert that they require renormalization. Nevertheless, this is not at all surprising if we trace the step back to the analysis at the start of the previous section. There it was argued that Green functions in the "original" theory could be obtained from the background theory by functionally differentiating vacuum–to–vacuum amplitudes with respect to background fields. Thus, products of background fields were converted into Green functions.

[9] This does not apply for photon soft lines since we do not consider photon fluctuations.

[10] It is well known that in general composite operators mix under renormalization, that is, they do not obey multiplicative renormalization but rather require counterterms proportional to other local operators with equal or lower mass dimension.

We will proceed by computing such amplitudes and by expanding the background fields around $x = 0$ to obtain the local products we required. This means that we computed the corresponding Green function and then took the limit where all fields were evaluated at the same point. Although it is a rather ad–hoc way to insert composite operators into Green functions, it gives correct results. Nevertheless, it does not give us the required framework for renormalization. For this, it is necessary to take a more formal approach: insertions of composite operators are taken into account by the inclusion a source term in the generating functional:

$$Z[J_n] = \int \prod_n \mathcal{D}\Phi_n \exp i\Big(S[\Phi_n] + J_n\Phi_n + L_i O_i(\{\Phi\})\Big) \,, \tag{2.70}$$

where $O_i(\Phi)$ is the classical value of a composite operator whose insertions one is interested in, $\{\Phi\}$ is the set of fields which appear inside it and L_i is its corresponding source. This term allows for the definition of counterterms, which, as we will later see, may include operators different than the one that is being renormalized due to operator mixing. For the relation

$$H[0, \phi_n] = \Gamma[\phi_n] \tag{2.71}$$

between the effective action and its background counterpart to remain valid including composite operator insertions the corresponding expression for the background generating functional must be:

$$\mathcal{Z}[J_n, \phi_n] = \int \prod_n \mathcal{D}\phi'_n \exp i\Big(S[\phi_n + \phi'_n] + J_n\phi'_n + L_i O_i(\{\phi + \phi'\})\Big) \,. \tag{2.72}$$

Note the big difference: while the source terms for elemental fields involve only fluctuations, the ones for composite operators involve the sum of backgrounds and fluctuations, therefore the insertion of, say, $S_{2,\mu\nu}$ in the background actually involves:

$$(\overline{\psi} + \overline{\psi}')\sigma_{\mu\nu}(\psi + \psi') \tag{2.73}$$

instead of just:

$$\overline{\psi}\sigma_{\mu\nu}\psi \,. \tag{2.74}$$

This does not mean that computation of Wilson coefficients of the previous section is wrong, for the operators in (2.74) is the one that is related to the matrix element we are interested in. We will later see that they can be related to the renormalized composite operator in a straightforward manner. Instead, this means that operator mixing is naturally ingrained in the background field formalism. This also means that it is the operator in (2.73) the one that needs renormalization even though it ends up curing divergences in the Wilson coefficients of the operator in (2.74) as well.

After justifying the need for renormalization in the background theory, now we can proceed to apply to the operators in (2.7). In our renormalization program composite operators are inserted in Green's functions, which then are computed using dimensional regularization to preserve gauge invariance. Finally, the relation between singular terms and counterterms is defined by modified minimal subtraction $\overline{MS}$. As was mentioned earlier, counterterms required for renormalization of composite operators are a linear combination that includes other composite operators with singular coefficients. This is referred to as "operator mixing". For simplicity, we will compute Green's functions with an insertion of each composite operator and no other fields involved, for otherwise additional singularities renormalized by the lagrangian's counterterms would appear. However, not any operators can mix under renormalization. Only operators with the same quantum numbers can. Furthermore, since the background field method does

not break background gauge invariance, then this means that mixing also respects gauge invariance[11] [104–106]. In the end, this means that the operators that form the OPE of $\Pi^{\mu_1\mu_2\mu_3}$ mix among themselves under renormalization

In our context this means that the renormalization of the elements of our OPE will have the following shape:

$$\begin{aligned} \boldsymbol{Q}^0_{\mu\nu} &= \hat{Z}\boldsymbol{Q}_{\mu\nu} \\ Q^0_{i,\mu\nu} &= Q^0_{i,\mu\nu}(\psi+\psi', a^{a\mu}+A'^{a\mu}, a^\mu)\ , \end{aligned} \tag{2.75}$$

where $\boldsymbol{Q}^0_{\mu\nu}$ represents the vector whose components are the bare elements of the OPE of (2.7) and it is a function of the full fields, that is, the sum of the background and fluctuation parts. $\boldsymbol{Q}_{\mu\nu}$ contains its renormalized versions. Consequently, $\hat{Z}$ is a 8×8 matrix containing constants with regularized ultraviolet divergences. As we will see in the following, the vector of operators $\boldsymbol{Q}_{\mu\nu}$ does not coincide with the $\boldsymbol{S}_{\mu\nu}$ that we defined earlier, but they are related by a constant matrix whose elements contain regularized infrared divergences. Consequently one can define:

$$\boldsymbol{Q}_{\mu\nu} = \hat{U}\boldsymbol{S}_{\mu\nu} \implies \boldsymbol{Q}^0_{\mu\nu} = \hat{Z}\hat{U}\boldsymbol{S}_{\mu\nu}\ . \tag{2.76}$$

Renormalization is used to separate contributions coming from different energy scales and in this case such objective is achieved since the elements in $\hat{U}$ are just the required ones to cancel the infrared contributions of the Wilson coefficients. Furthermore, it is important to note that we could not have avoided singular terms in the Wilson coefficients by using $\boldsymbol{Q}^0_{\mu\nu}$ instead of $\boldsymbol{S}_{\mu\nu}$, since in such case we would have traded infrared for ultraviolet contributions. Instead it is necessary to use renormalization to successfully separate low and high energy contributions and find $\boldsymbol{Q}_{\mu\nu}$. The renormalized Wilson coefficients $\boldsymbol{C}$ are free of infrared contributions and are defined in terms of the bare ones $\boldsymbol{C}_S$ as:

$$\Pi^{\mu_1\mu_2\mu_3} = \boldsymbol{C}_S^{\mu_1\mu_2\mu_3\mu_4\mu_5}\cdot\langle 0|\boldsymbol{S}_{\mu\nu}|\gamma\rangle \tag{2.77}$$

$$= \boldsymbol{C}_S^{\mu_1\mu_2\mu_3\mu_4\mu_5}\cdot\hat{U}^{-1}\langle 0|\boldsymbol{Q}_{\mu\nu}|\gamma\rangle \tag{2.78}$$

$$\equiv \boldsymbol{C}^{\mu_1\mu_2\mu_3\mu_4\mu_5}\cdot\langle 0|\boldsymbol{Q}_{\mu\nu}|\gamma\rangle \tag{2.79}$$

$$\implies \boldsymbol{C}^{\mu_1\mu_2\mu_3\mu_4\mu_5} = (\hat{U}^{-1})^T\boldsymbol{C}_S^{\mu_1\mu_2\mu_3\mu_4\mu_5}\ . \tag{2.80}$$

Note that renormalized susceptibilities $\boldsymbol{X}$ can also be defined for $\boldsymbol{Q}_{\mu\nu}$ and can be related to the unrenormalized ones $\boldsymbol{X}^S_i$ in a straightforward way:

$$\boldsymbol{Q}_{\mu\nu} \equiv \boldsymbol{X}F_{\mu\nu} \implies \boldsymbol{X} = \hat{U}\boldsymbol{X}^S\ . \tag{2.81}$$

As always, it is of course necessary to specify an order at which renormalization constants will be truncated. The appearance of non–perturbative matrix elements in the OPE introduces non–perturbative expansion parameters (Λ_{QCD}/Q) besides the perturbative ones (g_S and e). In terms of the latter, the cut–off is placed at $O(e^{-1}g_S^2)$. With respect to the former we have $O(\Lambda^6_{QCD}/Q^6)$, which, in addition to gauge invariance conservation of the background field theory, essentially means that operators $S_{i,\mu\nu}$ only mix among themselves. Since we are considering the three lightest quarks, its masses' effects can be regarded as perturbations as well therefore introducing another expansion parameter m_f/Λ_{QCD}. Nevertheless, we can obtain the full dependence of the mixing coefficients on the quarks' masses.

[11] Only if the Green's function in which it is inserted has only background quark and gauge fields.

It is important to note that perturbative and non–perturbative parameters must not be regarded independently: the mixing matrix $\hat{U}$ is meant to modify the Wilson coefficients as shown in the previous equation, therefore each element must be expanded up to the order of the Wilson coefficients which it modifies. This introduces an interplay between the dimension of the operators that are mixing and the order of their Wilson coefficients. The precise implications of this assertion should become clearer throughout the rest of this section.

Now we are ready to put the renormalization program we just described to use. For $S_{1,\mu\nu}$ renormalization is at its simplest. Since the photon field does not have quantum fluctuations, then $Q^0_{1,\mu\nu}$ is just equal to $S_{1,\mu\nu}$ and hence it cannot mix with any other operator.

2.5.1 Mixing of the $Q^0_{2,\mu\nu}$ operator

The first and most non–trivial case is $Q_{2,\mu\nu}$. A Green's function with a full–field insertion of this composite operator is given by:

$$\langle 0|Q^0_{2,\mu\nu}|\gamma\rangle = \overline{\psi}\sigma_{\mu\nu}\psi + \langle 0|\overline{\psi}\sigma_{\mu\nu}\psi'|\gamma\rangle + \langle 0|\overline{\psi}'\sigma_{\mu\nu}\psi|\gamma\rangle + \langle 0|\overline{\psi}'\sigma_{\mu\nu}\psi'|\gamma\rangle \ , \tag{2.82}$$

where we are evaluating the matrix element of a Heisenberg operator and therefore the Dyson series of interaction vertices has to be inserted. Mixing with $S_{1,\mu\nu}$ can only come from the fourth term and it requires the contraction of both quark fluctuations and a soft insertion of the photon field in the resulting propagator. As we will see later in this section, further soft insertions lead to mixing with other operators. Since the Wilson coefficient of $S_{2,\mu\nu}$ is $O(e^{-1}g_S^0)$ and the mixing coefficient is $O(e^0 g_S^0)$, then the net mixing contribution is of order $O(e^{-1}g_S^0)$, already the same as the Wilson coefficient of $S_{1,\mu\nu}$. Therefore we can cut off the mixing coefficient at this point. The result is:

$$\begin{aligned}
\langle 0|\overline{\psi}'\sigma_{\mu\nu}\psi'|\gamma\rangle &= -\operatorname{Tr}\{S^{ff}_{ll}(0,0)\sigma_{\mu\nu}\} \\
&= \frac{e\mu^{2\epsilon}}{2} f^{\mu_1\nu_1}\int \frac{d^dp_1}{(2\pi)^d}\frac{\partial}{\partial q_1^{\mu_1}}\operatorname{Tr}\{S^0_{p_1}\gamma_{\nu_1}S^0_{p_1+q_1}\sigma_{\mu\nu}\}\Big|_{q_1=0} \\
&= \frac{N_c e\mu^{2\epsilon}e_f m_f}{2} f^{\mu_1\nu_1}\int \frac{d^dp_1}{(2\pi)^d}\frac{\partial}{\partial q_1^{\mu_1}}\frac{\operatorname{Tr}\{\gamma_{\nu_1}\not{q}_1\sigma_{\mu\nu}\}}{[p_1^2-m_f^2][(p_1+q_1)^2-m_f^2]}\Big|_{q_1=0} \\
&= \frac{N_c e\mu^{2\epsilon}e_f m_f}{2} f^{\mu_1\nu_1} 4i\int \frac{d^dp_1}{(2\pi)^d}\frac{\partial}{\partial q_1^{\mu_1}}\frac{(-g_{\nu_1\mu}q_{1\nu}+g_{\nu_1\nu}q_{1\mu})}{[p_1^2-m_f^2][(p_1+q_1)^2-m_f^2]}\Big|_{q_1=0} \\
&= 4iN_c e\mu^{2\epsilon}e_f m_f f_{\mu\nu}\int \frac{d^dp_1}{(2\pi)^d}\frac{1}{[p_1^2-m_f^2]^2} \\
&= -\frac{N_c e e_f}{4\pi^2} m_f f_{\mu\nu}\Gamma(\epsilon)\Big(\frac{4\pi\mu^2}{m_f^2}\Big)^{\epsilon} \ ,
\end{aligned} \tag{2.83}$$

where $d \equiv 4-2\epsilon$ is the shifted dimension, μ is the mass parameter that carries the mass dimension of e in the regularized theory and we have used the well–known formula:

$$\int \frac{d^dp}{(2\pi)^d}\frac{1}{[p^2-\Delta]^n} = \frac{(-1)^n}{(4\pi)^{d/2}} i\frac{\Gamma(n-\frac{d}{2})}{\Gamma(n)}\Big(\frac{1}{\Delta}\Big)^{n-\frac{d}{2}} \ . \tag{2.84}$$

Note that the derivation of this formula involves a Wick rotation of the integration variable, therefore it is necessary to ensure that Δ is positive, as it is of course in (2.83). Otherwise the integrand acquires a discontinuity when the norm of the spatial momentum $\boldsymbol{p}^2$ becomes smaller than the absolute value $|\Delta|$. This can be accounted for by giving the pole a vanishing imaginary part: $\Delta \longrightarrow \Delta - i0^+$, which plays a role analogous to the Feynman prescription for free propagators.

Turning back to (2.83), it is necessary to expand the result around $\epsilon = 0$ to expose the singular terms. The result when one discards terms that vanish when $\epsilon \longrightarrow 0$ is:

$$\langle 0|\overline{\psi}'\sigma_{\mu\nu}\psi'|\gamma\rangle = -\frac{N_c e e_f}{4\pi^2} m_f f_{\mu\nu}\left(\frac{1}{\epsilon} + \ln\left\{\frac{4\pi\mu^2}{m_f^2}\right\} - \gamma_E\right) , \tag{2.85}$$

where $\gamma_E \approx 0.5772$ is the Euler–Mascheroni constant and we have use the expansion of the gamma function around $\epsilon \longrightarrow 0$:

$$\Gamma(\epsilon) = \frac{1}{\epsilon} - \gamma_E + O(\epsilon) . \tag{2.86}$$

As was mentioned previously, we define the singular term to be subtracted in the $\overline{MS}$ scheme:

$$\frac{1}{\hat{\epsilon}} \equiv \frac{1}{\epsilon} + \ln\{4\pi\} - \gamma_E \tag{2.87}$$

and therefore the final result of the $S_{1,\mu\nu}$–$S_{2,\mu\nu}$ mixing reads:

$$\langle 0|\overline{\psi}'\sigma_{\mu\nu}\psi'|\gamma\rangle = -\frac{N_c}{4\pi^2} m_f\left(\frac{1}{\hat{\epsilon}} + \ln\left\{\frac{\mu^2}{m_f^2}\right\}\right) S_{1,\mu\nu} . \tag{2.88}$$

This equation states two facts about the insertions of the operator $Q_{2,\mu\nu}$: 1) a part of their singular ultraviolet behaviour can be effectively renormalized by mixing with $S_{1,\mu\nu}$ and 2) they involve a low–energy contribution from $S_{1,\mu\nu}$, which is represented by the mass logarithm. This second conclusion explains the appearance of the mass-regularized infrared divergences in the Wilson coefficients that appeared in the previous section, but most importantly it shows a path to their elimination by building linear combinations of the operators $S_{1,2,\mu\nu}$ that cancel each other's infrared contributions, just as it is conventionally done with ultraviolet singularities. This is not particular of $S_{1,\mu\nu}$ and $S_{2,\mu\nu}$, but rather applies for all other mixing coefficients as well. In fact this is an explicit example of the appearance of the $\hat{Z}$ and $\hat{U}$ matrices that were defined in (2.76).

The leading order contribution to the mixing of $Q_{2,\mu\nu}$ with $S_{3,4,5,\mu\nu}$ and $S_{7,\mu\nu}$ is given by the second and third terms at the right hand side of (2.82). However, they require the introduction two quark–gluon vertices: one completely made up of fluctuations and the other with a soft quark line. Then a soft gluon or photon could be inserted in a quark or even gluon propagator. However, Wilson coefficients of these operators are all $O(e^{-1})$, so the mixing coefficient cannot receive perturbative corrections from interaction vertices at the relevant order and therefore it is equal to zero. The same analysis of course applies the other way around, thus, $S_{2-5,\mu\nu}$ and $S_{7,\mu\nu}$ do not mix with each other under renormalization at leading order of their Wilson coefficients.

The mixing of $Q_{2,\mu\nu}$ with $S_{6,\mu\nu}$ can of course only come from the fourth term in (2.82). Just as with the mixing with $S_{1,\mu\nu}$ we can contract both fluctuations without introducing interaction vertices

and then three soft insertions can be performed on the propagator. The corresponding result is:

$$\begin{aligned}\langle 0|\overline{\psi}'\sigma_{\mu\nu}\psi'|\gamma\rangle &= -\operatorname{Tr}\{S^{ff}_{ll}(0,0)\sigma_{\mu\nu}\}\\ &= -\frac{ee_f g_S^2}{8}\operatorname{Tr}\{t^a t^b\}\Big(f^{\mu_1\nu_1}f^{a\mu_2\nu_2}f^{b\mu_3\nu_3}+f^{a\mu_1\nu_1}f^{\mu_2\nu_2}f^{b\mu_3\nu_3}+f^{a\mu_1\nu_1}f^{b\mu_2\nu_2}f^{\mu_3\nu_3}\Big)\\ &\times\int\frac{d^4p}{(2\pi)^4}\frac{\partial}{\partial q_1^{\mu_1}}\frac{\partial}{\partial q_2^{\mu_2}}\frac{\partial}{\partial q_3^{\mu_3}}\operatorname{Tr}\{S^0_p\gamma_{\nu_1}S^0_{p+q_1}\gamma_{\nu_2}S^0_{p+q_1+q_2}\gamma_{\nu_3}S^0_{p+q_1+q_2+q_3}\sigma_{\mu\nu}\}\Big|_{q_{1,2,3}=0}\Big)\\ &= -\frac{ee_f g_S^2}{16}\frac{1}{18\pi^2 m_f^3}f^{\mu\nu}f^{a\alpha\beta}f_{a\alpha\beta}\\ &= -\frac{1}{72m_f^3}S_{6,\mu\nu}\,.\end{aligned} \tag{2.89}$$

Finally, the mixing coefficient of $Q_{2,\mu\nu}$ with $S_{8,\mu\nu}$ is evidently beyond the perturbative order that we are interested in.

2.5.2 Mixing of the $Q^0_{3,\mu\nu}$ operator

For this operator we have:

$$\begin{aligned}\langle 0|Q^0_{3,\mu\nu}|\gamma\rangle = &-g_S\langle 0|\overline{\psi}t^aG^a_{\mu\nu}(a+A')\psi|\gamma\rangle - g_S\langle 0|\overline{\psi}t^aG^a_{\mu\nu}(a+A')\psi'|\gamma\rangle\\ &- g_S\langle 0|\overline{\psi}'t^aG^a_{\mu\nu}(a+A')\psi|\gamma\rangle - g_S\langle 0|\overline{\psi}'t^aG^a_{\mu\nu}(a+A')\psi'|\gamma\rangle\,,\end{aligned} \tag{2.90}$$

where $G^a_{\mu\nu}(a+A')$ is the gluon field strength tensor separated between fluctuation and background parts, namely:

$$G^a_{\mu\nu}(a+A') = f^a_{\mu\nu}+\overline{D}_\mu A'^a_\nu - \overline{D}_\nu A'^a_\mu + g_S f^{abc}A'^b_\mu A'^c_\nu\,, \tag{2.91}$$

as it was introduced in the previous sections. All the Wilson coefficients of the previous section were computed up to $O(e^{-1}g_S^0)$, therefore no terms with gluon quantum fluctuations give relevant contributions to the mixing and we can replace $G^a_{\mu\nu}\longrightarrow f^a_{\mu\nu}$ in $\langle Q^0_{3,\mu\nu}\rangle$. This means that at the order that is relevant for us $Q^0_{3,\mu\nu}$ can only mix with operators that have at least one soft insertion of $f^{a\mu\nu}$. From (2.7) the only compatible one is $S_{6,\mu\nu}$.[12] The leading order contribution to that mixing coefficient is given by the term in (2.90) with two quark fluctuations when they are contracted with each other and one soft gluon and one soft photon insertion are performed on

[12] In principle $S_{7,\mu\nu}$ is compatible as well, but to obtain terms with covariant derivatives it is necessary to introduce additional g_S^2 factors that take the mixing beyond the established cutoff.

the resulting quark propagator:

$$\begin{aligned}
-\langle 0|\overline{\psi}' t^a f^a_{\mu\nu}\psi'|\gamma\rangle &= g_S \,\mathrm{Tr}\{S^{ff}_{kl}(0,0)\}t^a_{lk}f^a_{\mu\nu} \\
&= \frac{1}{4}ee_f f^a_{\mu\nu} g_S^2 \,\mathrm{Tr}\{t^a t^b\}\left(f^{\mu_1\nu_1}f^{b\mu_2\nu_2} + f^{b\mu_1\nu_1}f^{\mu_2\nu_2}\right) \\
&\qquad \times \int \frac{d^4p}{(2\pi)^4}\frac{\partial}{\partial q_1^{\mu_1}}\frac{\partial}{\partial q_2^{\mu_2}}\,\mathrm{Tr}\left\{S^0_p\gamma_{\nu_1}S^0_{p+q_1}\gamma_{\nu_2}S^0_{p+q_1+q_2}\right\}\Big|_{q_{1,2}=0} \\
&= \frac{1}{8}ee_f g_S^2 f^{a\alpha\beta}f_{a\alpha\beta}f_{\mu\nu}\frac{1}{18m_f\pi^2} \\
&= \frac{1}{36m_f}S_{6,\mu\nu}\ .
\end{aligned} \tag{2.92}$$

2.5.3 Mixing of the $Q^0_{4,\mu\nu}$ operator

For $Q^0_{4,\mu\nu}$ we have:

$$\begin{aligned}
\langle 0|Q^0_{4,\mu\nu}|\gamma\rangle = &-g_S\langle 0|\overline{\psi}t^a\overline{G}^a_{\mu\nu}(a+A')\gamma_5\psi|\gamma\rangle - g_S\langle 0|\overline{\psi}t^a\overline{G}^a_{\mu\nu}(a+A')\gamma_5\psi'|\gamma\rangle \\
&- g_S\langle 0|\overline{\psi}'t^a\overline{G}^a_{\mu\nu}(a+A')\gamma_5\psi|\gamma\rangle - g_S\langle 0|\overline{\psi}'t^a\overline{G}^a_{\mu\nu}(a+A')\gamma_5\psi'|\gamma\rangle\ ,
\end{aligned} \tag{2.93}$$

where $\overline{G}^{a\mu\nu}(a+A')$ is the dual of $G^{a\mu\nu}(a+A')$, that is: $\overline{G}^{a\mu\nu} = \frac{i}{2}\epsilon^{\mu\nu\alpha\beta}G^a_{\alpha\beta}$. The analysis of the relevant mixing coefficients at the order of interest is essentially the same as for $Q^0_{3,\mu\nu}$, therefore there is mixing only with $S^0_{6,\mu\nu}$ and the corresponding coefficient is:

$$\begin{aligned}
-\langle 0|\overline{\psi}' t^a \overline{f}^a_{\mu\nu}\gamma_5\psi'|\gamma\rangle &= g_S \,\mathrm{Tr}\{S^{ff}_{kl}(0,0)\gamma_5\}t^a_{lk}\overline{f}^a_{\mu\nu} \\
&= \frac{1}{4}ee_f \overline{f}^a_{\mu\nu} g_S^2 \,\mathrm{Tr}\{t^a t^b\}\left(f^{\mu_1\nu_1}f^{b\mu_2\nu_2} + f^{b\mu_1\nu_1}f^{\mu_2\nu_2}\right) \\
&\qquad \times \int \frac{d^4p}{(2\pi)^4}\frac{\partial}{\partial q_1^{\mu_1}}\frac{\partial}{\partial q_2^{\mu_2}}\,\mathrm{Tr}\left\{S^0_p\gamma_{\nu_1}S^0_{p+q_1}\gamma_{\nu_2}S^0_{p+q_1+q_2}\gamma_5\right\}\Big|_{q_{1,2}=0} \\
&= \frac{1}{8}ee_f g_S^2 \frac{i}{12}\epsilon_{\mu\nu}{}^{\mu_2\nu_2}f^{a\alpha\beta}f_{a\alpha\beta}f^{\mu_1\nu_1}\epsilon_{\mu_1\mu_2\nu_1\nu_2}\frac{-i}{4m_f\pi^2} \\
&= \frac{1}{8}ee_f g_S^2 \frac{i}{12}f^{a\alpha\beta}f_{a\alpha\beta}f_{\mu\nu}\frac{-i}{m_f\pi^2} \\
&= \frac{1}{24m_f}S_{6,\mu\nu}\ .
\end{aligned} \tag{2.94}$$

2.5.4 Mixing of the $Q^0_{5,\mu\nu}$ operator

For $Q^0_{5,\mu\nu}$ we have:

$$\begin{aligned}
\langle 0|Q^0_{5,\mu\nu}|\gamma\rangle = &\langle 0|\overline{\psi}\psi ee_f F_{\mu\nu}|\gamma\rangle + \langle 0|\overline{\psi}\psi' ee_f F_{\mu\nu}|\gamma\rangle + \langle 0|\overline{\psi}' ee_f F_{\mu\nu}\psi|\gamma\rangle \\
&+ \langle 0|\overline{\psi}'\psi' ee_f F_{\mu\nu}|\gamma\rangle\ .
\end{aligned} \tag{2.95}$$

In a similar fashion as with $Q_{3,\mu\nu}$ and $Q_{4,\mu\nu}$, the soft photon insertion allows only for mixing with $S_{1,\mu\nu}$ and $S_{6,\mu\nu}$. The leading order contribution to both mixing coefficients is once again given by the term in (2.95) with two quark fluctuations:

$$\langle 0|\overline{\psi}'\psi' ee_f F_{\mu\nu}|\gamma\rangle = -\operatorname{Tr}\{S^{ff}_{ll}(0,0)\}ee_f f_{\mu\nu} \,. \tag{2.96}$$

Mixing with $S_{1,\mu\nu}$ is obtained by performing no soft insertions in the quark propagator:

$$\begin{aligned}\langle 0|\overline{\psi}'\psi' ee_f F_{\mu\nu}|\gamma\rangle &= -\mu^{2\epsilon} ee_f f_{\mu\nu}\int \frac{d^d p}{(2\pi)^d}\frac{4m_f}{p^2-m_f^2} \\ &= -\frac{m_f^3}{4\pi^2}\Big(\frac{1}{\hat{\epsilon}}+\ln\Big\{\frac{\mu^2}{m_f^2}\Big\}+1\Big)S_{1,\mu\nu} \,,\end{aligned} \tag{2.97}$$

where we used again formula (2.84). As mentioned in [35], this mixing coefficient can be used to subtract the low–energy contributions to the $O(m_f^4)$ correction to the massless part of the quark loop. On the other hand, mixing with $S_{6,\mu\nu}$ is obtained by inserting two soft gluons on the quark propagator:

$$\begin{aligned}\langle 0|\overline{\psi}'\psi' ee_f F_{\mu\nu}|\gamma\rangle &= -\frac{1}{4}ee_f f_{\mu\nu} g_S^2 \operatorname{Tr}\{t^a t^b\} f^{a\mu_1\nu_1} f^{b\mu_2\nu_2} \\ &\qquad \times \int \frac{d^4 p}{(2\pi)^4}\frac{\partial}{\partial q_1^{\mu_1}}\frac{\partial}{\partial q_2^{\mu_2}} \operatorname{Tr}\Big\{S^0_p \gamma_{\nu_1} S^0_{p+q_1}\gamma_{\nu_2} S^0_{p+q_1+q_2}\Big\}\Big|_{q_{1,2}=0} \\ &= -\frac{1}{8}ee_f f_{\mu\nu} g_S^2 f^{a\alpha\beta} f_{a\alpha\beta}\frac{1}{6m_f\pi^2} \\ &= -\frac{1}{12m_f}S_{6,\mu\nu} \,.\end{aligned} \tag{2.98}$$

2.5.5 Mixing of the $Q^0_{6,\mu\nu}$ operator

For this operator it can be performed the same separation of the gluon field strength tensor that was described for $Q_{3,\mu\nu}$ and $Q_{4,\mu\nu}$. However, since this operator is $O(eg_S^2)$ and all other Wilson coefficients are $O(e^{-1}g_S^0)$, then its mixing coefficients are equal to zero at the order that is relevant for us. For example, the leading mixing contribution is given by contracting the two fluctuation parts of the gluon condensate $G^{a\alpha\beta}G_{a\alpha\beta}$, but the resulting mixing with $S_{1,\mu\nu}$ gives a contribution $O(e^{-1}g_S^2)$, which is quite beyond the perturbative order of the quark loop.

2.5.6 Mixing of the $Q^0_{7,\mu\nu}$ operator

With respect to $Q^0_{7,\mu\nu}$ we have:

$$\begin{aligned}\langle 0|Q^0_{7,\mu\nu}|\gamma\rangle &= ig_S\langle 0|\overline{\psi}(t^a G^a_{\mu\lambda}D_\nu + D_\nu t^a G^a_{\mu\lambda})\gamma^\lambda\psi|\gamma\rangle - (\mu\longleftrightarrow\nu) \\ &+ ig_S\langle 0|\overline{\psi}(t^a G^a_{\mu\lambda}D_\nu + D_\nu t^a G^a_{\mu\lambda})\gamma^\lambda\psi'|\gamma\rangle - (\mu\longleftrightarrow\nu) \\ &+ ig_S\langle 0|\overline{\psi}'(t^a G^a_{\mu\lambda}D_\nu + D_\nu t^a G^a_{\mu\lambda})\gamma^\lambda\psi'|\gamma\rangle - (\mu\longleftrightarrow\nu) \\ &+ ig_S\langle 0|\overline{\psi}'(t^a G^a_{\mu\lambda}D_\nu + D_\nu t^a G^a_{\mu\lambda})\gamma^\lambda\psi'|\gamma\rangle - (\mu\longleftrightarrow\nu) \,,\end{aligned} \tag{2.99}$$

where this time both the field strength tensor and the covariant derivative are implicitly divided into background and fluctuation parts. Since this operator is already $O(e^0 g_S)$, it can only mix with $S_{3,\mu\nu}$, $S_{4,\mu\nu}$ and $S_{6,\mu\nu}$. Mixing with the first two is relevant only up to terms that do not introduce higher orders of g_S, therefore only the first term in (2.99) may contribute. With respect to the product of the gluon field strength tensor and a covariant derivative, the relevant terms would be:

$$t^a G^a_{\mu\lambda} D_\nu + D_\nu t^a G^a_{\mu\lambda} = t^a f^a_{\mu\lambda} \overline{D}_\nu + \overline{D}_\nu t^a f^a_{\mu\lambda} + O(g_S) \; . \tag{2.100}$$

This would give just the background version $S_{7,\mu\nu}$ of $Q_{7,\mu\nu}$. Therefore there is no relevant mixing of $Q_{7,\mu\nu}$ with $S_{3,\mu\nu}$ and $S_{4,\mu\nu}$ at the order we are working on. With respect to the mixing with $S_{6,\mu\nu}$, the leading contribution comes from the last term in (2.99) when both quark fluctuations are contracted. For this mixing only terms that introduce at most another order of g_S are relevant. These can come from the product of a field strength tensor and a covariant derivative:

$$\begin{aligned} t^a G^a_{\mu\lambda} D_\nu + D_\nu t^a G^a_{\mu\lambda} = t^a f^a_{\mu\lambda} \overline{D}_\nu + \overline{D}_\nu t^a f^a_{\mu\lambda} + t^a (\partial_\mu A'^a_\lambda - \partial_\lambda A'^a_\mu)(-i g_S t^b A'^b_\nu) \\ + (-i g_S t^b A'^b_\nu) t^a (\partial_\mu A'^a_\lambda - \partial_\lambda A'^a_\mu) + O(g_S^2) \end{aligned} \tag{2.101}$$

or from soft gluon insertions on the quark propagator. The last two terms of the previous equations introduce a higher order in g_S, but there is no soft gluon insertion, which then must come from the gluon or quark propagator with a corresponding additional factor g_S, which renders it irrelevant for our case. Therefore only the first two terms contribute to the mixing with $S_{6,\mu\nu}$ and the additional soft gluon and photon insertions must come from the quark propagator. In the end, the mixing coefficient between $Q_{7,\mu\nu}$ and $S_{6,\mu\nu}$ is:

$$\begin{aligned} i g_S \langle 0 | \overline{\psi}' (t^a G^a_{\mu\lambda} D_\nu + D_\nu t^a G^a_{\mu\lambda}) \gamma^\lambda \psi' | \gamma \rangle &= -2 i g_S t^a_{lk} f^a_{\mu\lambda} \overline{D}_\nu \, \mathrm{Tr}\{ S^{ff}_{kl} \gamma^\lambda \} \\ &= \frac{i}{2} \mu^{2\epsilon} e e_f g_S^2 \, \mathrm{Tr}\{ t^a t^b \} f^a_{\mu\lambda} \left(f^{\mu_1\nu_1} f^{b\mu_2\nu_2} + f^{b\mu_1\nu_1} f^{\mu_2\nu_2} \right) \\ &\quad \times \int \frac{d^d p}{(2\pi)^d} i p_\nu \frac{\partial}{\partial q_1^{\mu_1}} \frac{\partial}{\partial q_2^{\mu_2}} \, \mathrm{Tr} \left\{ S^0_p \gamma_{\nu_1} S^0_{p+q_1} \gamma_{\nu_2} S^0_{p+q_1+q_2} \gamma^\lambda \right\} \Big|_{q_{1,2}=0} \\ &= \frac{i}{4} \frac{6}{(2-\epsilon)(3-2\epsilon)} e e_f g_S^2 f^{a\alpha\beta} f_{a\alpha\beta} f_{\mu\nu} \frac{i}{6\pi^2} \left(\frac{1}{\hat{\epsilon}} + \ln \left\{ \frac{\mu^2}{m_f^2} \right\} \right) \\ &= -\frac{1}{6} \left(\frac{1}{\hat{\epsilon}} + \ln \left\{ \frac{\mu^2}{m_f^2} \right\} + \frac{7}{6} \right) S_{6,\mu\nu} \; , \end{aligned} \tag{2.102}$$

where we have implicitly included the $(\mu \longleftrightarrow \nu)$ permutation.

2.5.7 Mixing of the $Q^0_{8,\mu\nu}$ operator

Finally, it is worth mentioning that operator $Q^0_{8,\mu\nu}$ is already $O(e^0 g_S^2)$ and therefore its mixing coefficients are not relevant for the Wilson coefficients at the computed order. Note that the order $O(e^0 g_S^2)$ of the operator $Q^0_{8,\mu\nu}$ is not arbitrary, but rather depends on the way in which it appears in $\Pi^{\mu_1\mu_2\mu_3}$. As shown at the end of the first section in (2.13), at most three soft quark lines can be obtained from the original three currents of $\Pi^{\mu_1\mu_2\mu_3}$, therefore we need to introduce two interaction vertices from the Dyson series to complete the two cut quark lines (see figure 2.7).

2.6 Conclusion

In this chapter we have followed [35] to present the computation of the HLbL tensor $\Pi^{\mu_1\mu_2\mu_3\mu_4}$ in the high energy regime via an OPE in the presence of an electromagnetic background field. We have generalized such approach to include gluon and quark background fields as well. In the OPE there is a separation of perturbative contributions (which are bigger) and non–perturbative ones coming matrix elements of strongly interacting operators. All contributions are computed at leading order up to dimension six operators. Infrared contributions to the Wilson coefficients of the OPE represented both conceptual and computational problems, but they were dealt with by performing renormalization of the composite operators of the OPE. The need for a renormalization program in the background field method context, when composite operators are represented by products of background classical quark, gluon and photon fields, is not evident and it must be justified. We presented the rationale behind the renormalization scheme and performed all necessary computations within the background field method framework.

The main contribution to $\Pi^{\mu_1\mu_2\mu_3\mu_4}$ (and, thus, to a_μ) comes from the Wilson coefficient of the electromagnetic field–strength tensor $F_{\mu\nu}$,[13] which is the quark loop (see figure 2.5) and its expression is given in (2.50). In the next chapter we present our computation of this contribution, which we do in an alternate way to [35]. This gives us computational advantages such as the avoidance of spurious kinematic singularities and also an expansion in the quark masses is obtained straightforwardly.

[13] After renormalization there are actually contributions from non–perturbative operators. However, such mixing contributions only affect the mass corrections of the quark loop.

Chapter 3

High energy contribution to a_μ^{HLbL}

In the previous chapter we presented the OPE formalism with a static background field used in [35] to compute the HLbL tensor $\Pi_{HLbL}^{\mu_1\mu_2\mu_3\mu_4}$ in a highly symmetric of high virtuality regime. A tensor $\Pi_F^{\mu_1\mu_2\mu_3\mu_4\nu_4}$, built from non-perturbative quantities called "magnetic susceptibilities" and the perturbative Wilson coefficients of the OPE was found to be proportional to the derivative of the HLbL tensor $\partial_{\nu_4}\Pi_{HLbL}^{\mu_1\mu_2\mu_3\mu_4}$ in the static limit of zero momentum of one external leg. In chapter 1 we discussed that this object contains all the necessary information to compute the HLbL contribution to a_μ. In the chapter 2 we also found the renormalized Wilson coefficients of the OPE and concluded that (up to renormalization mixing contributions) the Wilson coefficient of the lowest dimensional element of the OPE was proportional to a quark loop with a soft photon insertion (see equation (2.50) and figure 2.5). Due to the low distance suppression of the others OPE contributions the quark loop gives the dominant contribution to a_μ, the observable we are computing for HLbL. Consequently, in this chapter we focus on the computation of the quark loop contribution to a_μ from the high energy integration regions of the master formula (1.69). From chapter 1 we know exactly how $\partial_{\nu_4}\Pi_{HLbL}^{\mu_1\mu_2\mu_3\mu_4}$ and thus $\Pi_F^{\mu_1\mu_2\mu_3\mu_4\nu_4}$ contributes to a_μ without recurring to a specific tensor basis. However, it is convenient to express the result in the tensor basis used for the master formula in order to benefit from the Gegenbauer polynomials framework that allowed to simplify a full two loop integral, containing eight integrals, into a threefold one. Consequently, in [35] the quark loop amplitude is not directly computed but rather a set of projectors is applied to it in order to extract its contributions for each $\hat{\Pi}_i$ of the master formula (1.69). Then, the resulting scalar integrals reduced in terms of a set of well–known master integrals. After the three remaining integrals over the two virtual photon momenta magnitudes $|Q_1|$ and $|Q_2|$ and the angle between them τ is performed the quark loop is found to give the largest contribution to a_μ than any other Wilson coefficient of the OPE by at least two orders of magnitude.

In this chapter we follow an alternative approach with respect to [35]. Instead of projecting the quark loop amplitude onto the form factors of the master formula as a first step, we compute the amplitude in its tensor form. At intermediate stages of the computation we have to deal with tensor loop integrals, which we are able to write in terms of scalar ones by means of a kinematic–singularity–free tensor decomposition method first presented in [41]. Once the tensor decomposition is performed we finally project on to the $\hat{\Pi}_i$ form factors of the master formula. In this way we are able to verify that there are no quark loop contributions neglected by the projection procedure, which is an implicit check of the generality of the tensor structures of the HLbL tensor found in [22, 23] that we discussed in chapter 1. Finally, we compute the scalar integrals found in the tensor decomposition by means of their Mellin–Barnes representation [42]. The series representation of Mellin–Barnes integrals provide a full systematic expansion of the

chiral corrections to the massless part of the quark loop. Finally, we perform a numeric evaluation of the master formula (1.69) considering the quark loop contribution to the form factors $\hat{\Pi}_i$ and we discuss the results.

3.1 Computation of the quark loop by the method of Bijnens

In this section we present and consider the computational approach used in [35] to obtain the quark loop contribution to a_μ. As we discussed in the previous chapter, the static limit derivative of the HLbL tensor in the regime of high virtual photon momenta receives contributions from the quark loop amplitude with an soft photon insertion, which is given in (2.50):

$$\begin{aligned}\frac{\partial}{\partial q_{4\nu_4}}\Pi^{\mu_1\mu_2\mu_3\mu_4}_{(S_1)}\bigg|_{q_4\to 0} = i\frac{N_c}{2}\int\frac{d^4p}{(2\pi)^4}\sum_f e_f^4\frac{\partial}{\partial q_{4\nu_4}}\sum_{\sigma(1,2,4)}\mathrm{Tr}\Big\{\gamma^{\mu_3}S^0(p+q_1+q_2+q_4)\gamma^{\mu_4}\\ \times S^0(p+q_1+q_2)\gamma^{\mu_1}S^0(p+q_2)\gamma^{\mu_2}S^0(p)\Big\}\bigg|_{q_4=0}.\end{aligned} \tag{3.1}$$

In [35] the computation was performed by applying projectors which extract the relevant contributions to the $\overline{\Pi}_i$ of the master formula (1.69) out of the amplitude

$$\hat{\Pi}_i = P_i^{\mu_1'\mu_2'\mu_3'\mu_4'\nu_4'}\Pi_{F\,\mu_1'\mu_2'\mu_3'\mu_4'\nu_4'}\,. \tag{3.2}$$

Some denominator cancellations can be performed on the resulting scalar loop integrals such that they are written in terms of scalar tadpole, self-energy and triangle integrals. Note that no scalar box integrals arise due to the soft $q_4\to$ limit, which guarantees that, after applying the soft derivative, only three different propagators appear in the quark loop. These three scalar master integrals are then expanded as a function of the squared of the infinitesimal (in the considered regime) quark mass m_f^2. Finally, the infrared divergences that appear as $\ln(Q_3^2/m_f^2)$ in the mass–suppressed corrections are cancelled via mixing with $S_{2,\mu\nu}$ as discussed in the previous chapter. The final result can be written as:

$$\hat{\Pi}_m^{\overline{MS}} = \hat{\Pi}_m^0 + m_f^2\hat{\Pi}^{m_f^2}_{\overline{MS},m} + O(m_f^4)\,, \tag{3.3}$$

$$\hat{\Pi}_m^0 = \frac{N_c e_q^4}{\pi^2}\sum_{i,j,k,n}\Big[c_{ijk}^{(m,n)} + f_{ijk}^{(m,n)}F + g_{ijk}^{(m,n)}\ln\Big(\frac{Q_2^2}{Q_3^2}\Big) + h_{ijk}^{(m,n)}\ln\Big(\frac{Q_1^2}{Q_2^2}\Big)\Big]\lambda^{-n}Q_1^{2i}Q_2^{2j}Q_3^{2k}\,, \tag{3.4}$$

$$\begin{aligned}\hat{\Pi}^{m_f^2}_{\overline{MS},m} = \frac{N_c e_q^4}{\pi^2}\sum_{i,j,k,n}\lambda^{-n}Q_1^{2i}Q_2^{2j}Q_3^{2k}\\ \times\Big[d_{ijk}^{(m,n)} + p_{ijk}^{(m,n)}F + q_{ijk}^{(m,n)}\ln\Big(\frac{Q_2^2}{Q_3^2}\Big) + r_{ijk}^{(m,n)}\ln\Big(\frac{Q_1^2}{Q_2^2}\Big) + s_{ijk}^{(m,n)}\ln\Big(\frac{Q_3^2}{\mu^2}\Big)\Big]\,,\end{aligned} \tag{3.5}$$

where $c_{ijk}^{(m,n)}$, $f_{ijk}^{(m,n)}$, $g_{ijk}^{(m,n)}$, $h_{ijk}^{(m,n)}$, $d_{ijk}^{(m,n)}$, $p_{ijk}^{(m,n)}$, $q_{ijk}^{(m,n)}$, $r_{ijk}^{(m,n)}$ and $s_{ijk}^{(m,n)}$ are constant coefficients and their values are given in appendix C.1 of [35]. λ is the Källen function of the three virtual photon momenta:

$$\lambda(q_1^2,q_2^2,q_3^2) \equiv q_1^4+q_2^4+q_3^4-2q_1^2q_2^2-2q_1^2q_3^2-2q_2^2q_3^2\,, \tag{3.6}$$

where we have used the standard notation $q^{2n} \equiv (q^2)^n$. In addition, μ represents the subtraction point of the $\overline{MS}$ renormalization scheme, which we introduced in the previous chapter. Finally, $F = F(Q_1^2, Q_2^2, Q_3^2)$ is the massless triangle integral:

$$F(Q_1^2, Q_2^2, Q_3^2) \equiv (4\pi)^2 i \int \frac{d^4p}{(2\pi)^4} \frac{1}{p^2} \frac{1}{(p-q_1)^2} \frac{1}{(p-q_1-q_2)^2} \,. \tag{3.7}$$

Note that the expressions of the form factors $\hat{\Pi}_i$ have several terms with negative powers of λ, which constitute spurious kinematic singularities in the $\lambda \to 0$ limit. These were introduced by the projectors that were used to extract the form factors from the quark loop amplitude, but they are explicitly cancelled in contributions from all other Wilson coefficients. In the case of the quark loop however there is implicit dependence on λ coming from the massless triangle integral $F(Q_1^2, Q_2^2, Q_3^2)$, which thus obscures the cancellation of these singularities. When F is Taylor expanded around $\lambda = 0$ all negative powers of λ cancel.[1] Such expansion is necessary in the integration regions of the master formula in which two virtual photon momenta have a similar size and are much bigger than the third one, namely $Q_1 \sim Q_2 \gg Q_3 \gg \Lambda_{QCD}$ and crossed versions. This regime is not quite the same as the $Q_1 \sim Q_2 \sim Q_3 \gg \Lambda_{QCD}$ that was considered at the beginning of the previous chapter, but the OPE remains valid anyway as long as we remain in the perturbative QCD domain and the logarithms $\ln(Q_i/Q_j)$ do not become too large and spoil the convergence of the perturbative series.

3.2 Computation of the quark loop amplitude in this thesis

In this section we describe the alternative approach that we followed for the computation of the quark loop amplitude in (2.50) and present its results. We also highlight the advantages and downsides of our approach with respect to the ones discussed in the previous section. Our whole computation of the quark loop amplitude was done using the software *Mathematica* and we also made extensive use of version 9.3.1 of *FeynCalc* package [37–39] to compute Dirac traces and for intermediate steps involving tensors.

3.2.1 First stages of the quark loop computation

In contrast to the procedure followed in [35], we did not use projectors to extract the contribution to each form factor $\hat{\Pi}_i$ as our first step. Instead we wanted to obtain the full tensor structure of quark loop amplitude to be able to compare it to the $\frac{\partial}{\partial q_{4\nu_4}} \hat{T}_i^{\mu_1\mu_2\mu_3\mu_4}$ tensor basis that is used in the master formula (1.69). This is an indirect check of the completeness and generality of the kinematic–singularity–free tensor decomposition that we discussed for the HLbL tensor in chapter 1. To this end it was convenient to postpone the use of any projector until all tensor structures in the amplitude were written in terms of the metric tensor and the virtual photon momenta q_1, q_2 and q_3.

[1] In principle, this cancellation happens whether $F(Q_1^2, Q_2^2, Q_3^2)$ is expanded around $\lambda = 0$ or not, but the integrals in the master formula are performed numerically and therefore the computation may become unstable around $\lambda = 0$.

The first step in our computation was to perform the differentiation and take the limit with respect to $q_4^{\nu_4}$, whose effect is to duplicate the propagator that they act upon:[2]

$$\lim_{q_4\to 0}\frac{\partial}{\partial q_{\nu_4}}S(p+q_4) = i\lim_{q_4\to 0}S(p+q_4)\gamma^{\nu_4}S(p+q_4) = iS(p)\gamma^{\nu_4}S(p)\,.$$

It is convenient to perform this differentiation and limit before computing the trace and the loop integral because by doing so we reduce the number of different propagators and external momenta from four to three. Although in this way one of the propagators acquires a power of two, having only three types of propagators greatly simplifies Dirac trace computation and enhances the cancellation of denominators in the loop integrals that arise from it.

After the Dirac trace was computed, several denominator simplifications were performed to reduce the complexity of the structure of the remaining tensor loop integrals. This lead to the appearance of integrals with only one and two different types of propagators in addition to the obvious ones with three. From these, the one with the most complex tensor structure was a fifth rank tensor with five propagators (but only three of them different from each other).

3.2.1.1 Tensor loop integrals decomposition

In general, computation of tensor loop integrals involves decomposing them in a linear combination of their external momenta and the metric tensor in which coefficients are given in terms of scalar loop integrals. Because of the obvious analogy with the tensor decomposition presented in chapter 1, these coefficients are usually called form factors. The linear combination of tensors is fixed by Lorentz covariance, and so differences between algorithms focus on the shape of their form factors. A standard procedure to achieve this is the Passarino–Veltman decomposition.[3] Scalar coefficients of this decomposition are obtained by contracting the tensor integral with each element of the tensor basis in which it is being decomposed. This yields a system of equations involving scalar integrals and form factors scalar products of the external momenta of the integral. Such an approach always introduces spurious kinematic singularities in the form factors at the kinematic points where the tensor basis chosen for the decomposition ceases to span the complete tensor structure of the tensor loop integral.[4] In linear algebra jargon: the form factors of the Passarino–Veltman decomposition always contain negative powers of the determinant of the Gram matrix of tensors used as a basis. These singularities may be difficult to handle when the integrals of the (1.69) master formula are performed. Moreover, we will later see that there are other unavoidable spurious kinematic singularities which we will have to deal with and it is therefore very inconvenient to introduce more of those singularities in our dispersive integrals.

Since the Passarino-Veltman decomposition is technically inconvenient for our computation, we preferred to use an approach proposed by Davydychev in [41] for tensor decomposition into scalar integrals which does not introduce kinematic singularities in the coefficients, at the cost of shifting the (space-time) dimension of the scalar integrals. Let us describe this decomposition procedure before continuing with the discussion of the quark loop computation. First, we need

[2] Note that there is a difference in this formula with respect to the one cited in [35]. It is due to a difference in the used convention for the quark propagator.

[3] See appendices D, E and F of the original reference [107] and appendix A of [108] for typographical corrections to the results.

[4] Note that this is essentially the same problem faced when looking for the Mandelstam decomposition of the HLbL amplitude in chapter 1.

to introduce suitable notation. Tensor loop integrals are represented as:

$$I^{(N)}_{\mu_1\ldots\mu_M}(d;\nu_1,\ldots,\nu_N) \equiv \int \frac{d^dp}{(2\pi)^d}\frac{p_{\mu_1}\ldots p_{\mu_M}}{D_1^{\nu_1}\ldots D_N^{\nu_N}}\,, \tag{3.8}$$

where $D_i = (q_i+p)-m_i^2+i\epsilon$ represents the usual scalar (possibly massive) propagator, ν_i is the power of propagator D_i in the integral, q_i is an arbitrary external momentum and the Feynman prescription is implemented by $\epsilon\to 0^+$. Correspondingly, scalar integrals are represented as:

$$I^{(N)}(d;\nu_1,\ldots,\nu_N) \equiv \int \frac{d^dp}{(2\pi)^d}\frac{1}{D_1^{\nu_1}\ldots D_N^{\nu_N}}\,. \tag{3.9}$$

With this convention, the decomposition formula for tensor loop integrals in terms of scalar ones with shifted dimensions can be written as[5] [41]:

$$\begin{aligned} I^{(N)}_{\mu_1\ldots\mu_M}(d;\nu_1,\ldots,\nu_N) = &\sum_{\substack{\lambda,\kappa_1,\ldots,\kappa_N\\ 2\lambda+\sum_i\kappa_i=M}}\Big(-\frac{1}{2}\Big)^\lambda\{[g]^\lambda[q_1]^{\kappa_1}\ldots[q_N]^{\kappa_N}\}_{\mu_1\ldots\mu_M}\\ &\times(\nu_1)_{\kappa_1}\ldots(\nu_N)_{\kappa_N}(4\pi)^{M-\lambda}I^{(N)}(d+2(M-\lambda);\nu_1+\kappa_1,\ldots,\nu_N+\kappa_N)\,, \end{aligned} \tag{3.10}$$

where $(\nu)_\kappa \equiv \Gamma(\nu+\kappa)/\Gamma(\nu)$ is the Pochhammer symbol. The structure between brackets represents the symmetrized tensor structure in which $g^{\mu_1\mu_2}$ appears λ times, and each $q_i^{\mu_j}$ appears κ_i times. Consequently, the restriction $2\lambda+\sum_i\kappa_i = M$ ensures that the tensor rank of the integral is conserved. The sum extends to all non–negative values of $\lambda,\kappa_1,\ldots,\kappa_N$. The proof of this formula rests mainly on the Schwinger representation of scalar loop integrals and recurrence formulas obtained by differentiation of such integrals with respect to each external momentum q_i. Finally, the result is generalized by induction. The proof of (3.10) is described in great detail in [41] and we will not repeat it here. Nevertheless, there are some features of the formula which are worth to be motivated. First, note that the number of times that a tensor element $q_i^{\mu_j}$ appears in the decomposition is related to the power with which its associated denominator D_i appears. This is in fact reminiscent of the external momentum derivatives which where used to obtain the formula. For example, the starting point of the proof of the formula for the vector integral $I^{(N)}_\mu(d;\nu_1,\ldots,\nu_N)$ is the following differential identity:

$$\frac{1}{2\nu_1}\frac{\partial}{\partial q_1^\mu}I^{(N)}(d;\nu_1,\ldots,\nu_N) = -I^{(N)}_\mu(d;\nu_1+1,\ldots,\nu_N) - p_{1\mu}I^{(N)}(d;\nu_1+1,\ldots,\nu_N)\,. \tag{3.11}$$

The difference in the powers of the ν_1 in the derivative term and the two terms to the right is solved by using the Schwinger representation for scalar integrals, namely:

$$\begin{aligned} I^{(N)}(d;\nu_1,\ldots,\nu_N) = &\,\pi^{d/2}\,i^{1-d}\,\Gamma\Big(\sum_i\nu_i-\frac{d}{2}\Big)\Big[\prod_i\Gamma(\nu_i)\Big]^{-1}\\ &\times\int_0^1\ldots\int_0^1\prod\beta^{\nu_i-1}d\beta_i\,\delta\Big(\sum_i\beta_i-1\Big)\Big(\sum_{j<l}\sum\beta_j\beta_l(p_j-p_l)^2-\sum_i\beta_i m_i^2\Big)^{d/2-\sum_i\nu_i}\,, \end{aligned} \tag{3.12}$$

which is valid for $Re\{\nu_i\} > 0$ and it is equivalent to the more usual representation in terms of Feynman parameters. There one can see how a shift in the sum of powers of denominators

[5] Note that there is a difference in the equation we cite here and the one written in [41] with respect to the factor of 4π due to the difference in the normalization convention for loop integrals.

$\sum \nu_i$ may be offset by a twofold shift in the scalar integral's dimension. In the case of the metric tensor, its appearance is related to a reduction of the shift in the dimension of the scalar integral. This is due to the fact that metric tensors enter this decomposition from terms in which an external momentum derivative acts on its corresponding momentum, not on the scalar integral that is multiplying it, therefore it requires no additional offset and its dimensional shift is not increased. An explicit example of this situation can bee seen when taking a second derivative of the vector integral $I_\mu^{(N)}$ in (3.11).

Finally, it is very important to note that although the dimension of the scalar integrals is increased in (3.10) with respect to the original tensor one, its superficial degree of divergence (index) is not. A general tensor integral $I^{(N)}_{\mu_1\ldots\mu_M}(d;\nu_1,\ldots,\nu_N)$ has superficial degree of divergence equal to $d+M-2\sum_i \nu_i$ while for the scalar integrals in which it is decomposed it is equal to $d+M-2\sum_i \nu_i-\sum_i \kappa_i$. Therefore the original degree of divergence is only recovered for the scalar integral corresponding to the term in which the tensor structure of the loop integral is fully saturated by metric tensors, if it exists. For the rest of the terms the ultraviolet asymptotic behaviour is less singular than the original. This result is a standard feature of decomposition algorithms for tensor loop integrals, but for scalar integrals decomposition algorithms it is not always true.

We applied (3.10) to the tensor integrals appearing in our computation of the quark loop amplitude, thus its tensor structure was explicitly written in terms of the external momenta and the metric. As such, it was then possible to compare this structure to the $\partial_{q_4}^{\nu_4}\hat{T}_i^{\mu_1\mu_2\mu_3\mu_4}$ tensor basis that is used for the (1.69) master formula. To do this we extracted the quark loop contributions to the form factors $\hat{\Pi}_i$ with the help of the projectors of [35]. We found that all form factors received non–zero contributions from the quark loop. Furthermore, when we subtracted such contributions from the amplitude itself the result was equal to zero, which means that the quark loop amplitude contains no spurious parts that do not contribute to a_μ. This implies that the first principles arguments presented in chapter 1 to justify the decomposition of the HLbL tensor completely characterize the tensor structure of the quark amplitude, at least with respect to the soft derivative part of the decomposition.

It is worth noting that the tensor basis used for $\partial_{q_4}^{\nu_4}\Pi_{HLbL}^{\mu_1\mu_2\mu_3\mu_4}$ in [22] is built from derivatives of the elements of the set

$$\{T_i^{\mu_1\mu_2\mu_3\mu_4}|\, i=1,\ldots,11,13,14,16,17\}\cup\{T_{39}+T_{40},T_{42},T_{43},T_{50}-T_{51}\}\,, \tag{3.13}$$

while in [35] they use the set

$$\{T_i^{\mu_1\mu_2\mu_3\mu_4}|\, i=1,\ldots,11,13,14,16,17,39,50,51,54\}\,, \tag{3.14}$$

which was proposed in [23]. The choice of any of these two sets is of course irrelevant for a_μ and in this work we use the latter, because we are interested in using the projectors of [35].

3.2.1.2 Computation of scalar integrals with shifted dimensions: first approach

After tensor decomposing loop integrals and applying projectors on the quark loop amplitude, the form factors $\hat{\Pi}_i$ are given in terms of scalar integrals with shifted dimensions coming from (3.10). It is necessary to compute them in order to perform the $|Q_1|$, $|Q_2|$ and τ integrals of the master formula. Just like tensor integrals discussed earlier these scalar ones appear with one, two, and three different propagators in the quark loop amplitude. Due to the topologies

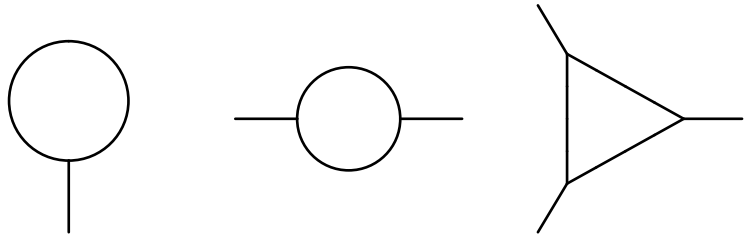

FIGURE 3.1: Three different basic topologies of one–loop diagrams with up to three external lines. These and the scalar integrals that appear in their amplitudes are often referred to as tadpole (left), self–energy (center) and triangle (right).

of Green functions in which they may appear, these integrals are called one–, two– and three–point scalar integrals. From the point of view of the diagrams in which they arise, they are also called tadpole, self–energy and triangle scalar integrals (see figure 3.1). One–point integrals can be computed analytically and the result can be put in a closed form, which is the formula we presented in (2.84) for arbitrary dimensions.

The case for the two point function is considerably more complex[6]. However it is simple enough to be explained in detail and it gives one a natural introduction to the framework of hypergeometric functions and their corresponding Mellin–Barnes representation, which plays a central role in our work. Therefore we fully derive the self–energy result and cite the general formula for the triangle.

The tadpole formula (2.84) can be used to compute self–energy integrals with the help of a well–known integral representation for products of propagators in terms of so-called "Feynman parameters", namely:

$$\frac{1}{D_1^{\nu_1}...D_N^{\nu_N}} = \int_0^1 \delta\Big(\sum_1^N x_i - 1\Big) \prod_i dx_i \, \frac{\prod_i x_i^{\nu_i - 1}}{\{x_1 D_1 + ... + x_N D_N\}^{\sum_i \nu_i}} \frac{\Gamma(\sum_i \nu_i)}{\prod_i \Gamma(\nu_i)} \,. \tag{3.15}$$

This formula applies for a set of arbitrary complex numbers D_i and ν_i, as long as $Re\{\nu_i\} > 0$ for every $i = 1, .., N$. When this formula is used for the propagators in a self–energy integral one can turn the term $x_1 D_1 + ...x_N D_N$ into the shape of a single new propagator whose external momentum and masses are a linear combination of the original ones. For the general case with different masses one has:[7]

$$\begin{aligned} I^{(2)}(d;\nu_1,\nu_2) &= \int \frac{d^d p}{(2\pi)^d} \frac{1}{\{(p+q_1)^2 - m_1^2\}^{\nu_1}} \frac{1}{\{p^2 - m_2^2\}^{\nu_2}} \\ &= \int \frac{d^d p}{(2\pi)^d} \int_0^1 dx_1 \frac{x_1^{\nu_1 - 1} x_2^{\nu_2 - 1}}{\{p^2 + 2x_1 p\cdot q_1 + x_1(q_1^2 - m_1^2) - x_2 m_2^2\}^{\nu_1+\nu_2}} \frac{\Gamma(\nu_1+\nu_2)}{\Gamma(\nu_1)\Gamma(\nu_2)} \\ &= \frac{\Gamma(\nu_1+\nu_2)}{\Gamma(\nu_1)\Gamma(\nu_2)} \int_0^1 dx_1 \, x_1^{\nu_1 - 1} x_2^{\nu_2 - 1} \int \frac{d^d p}{(2\pi)^d} \frac{1}{\{p^2 - \Delta(x_1)\}^{\nu_1+\nu_2}} \,, \end{aligned} \tag{3.16}$$

where $\Delta(x_1) = x_1^2 q_1^2 - x_1(q_1^2 - m_1^2) + x_2 m_2^2$ and we have performed an integration–variable shift in the last step. For brevity it is always assumed that $x_2 = 1 - x_1$ due to the delta function in (3.15). Note that in this case the caveat presented in chapter 2 about the role of the Feynman

[6] Two–point integrals in four dimensions can be put in a relatively simple closed form (see section 5.1 in [109]), but we are interested in dimension–shifted integrals.

[7] Note that one can set one external momentum to zero without loss of generality by shifting the integration variable.

prescription in formula (2.84) becomes relevant, because Δ becomes negative for sufficiently large time–like external momentum. Therefore this is not an issue for us. At this point we can use the expression (2.84) for the tadpole scalar integral to obtain:

$$I^{(2)}(d;\nu_1,\nu_2) = \frac{(-1)^{\frac{1}{2}+\nu_1+\nu_2}}{(4\pi)^{d/2}}\frac{\Gamma(\nu_1+\nu_2-\frac{d}{2})}{\Gamma(\nu_1)\Gamma(\nu_2)}\int_0^1 dx_1\, x_1^{\nu_1-1}x_2^{\nu_2-1} \times \Big(\frac{1}{-x_1(1-x_1)q_1^2+x_1(m_1^2-m_2^2)+m_2^2}\Big)^{\nu_1+\nu_2-\frac{d}{2}}. \tag{3.17}$$

To compute this integral it is necessary to introduce yet another computational trick, the so-called Mellin–Barnes representation

$$\begin{aligned}\frac{1}{(A_1+...+A_N)^\beta} &= \frac{1}{\Gamma(\beta)}\frac{1}{A_N^\beta}\int_{r-i\infty}^{r+i\infty}...\int_{r-i\infty}^{r+i\infty}\prod_j^{N-1}\frac{ds_j}{(2\pi i)}\Gamma(-s_j)\Big(\frac{A_j}{A_N}\Big)^{s_j}\times\Gamma\Big(\beta+\sum_i s_i\Big)\\ &\equiv \frac{1}{\Gamma(\beta)}\frac{1}{A_N^\beta}\int_{\prod_j s_j}\prod_j^{N-1}\Gamma(-s_j)\Big(\frac{A_j}{A_N}\Big)^{s_j}\times\Gamma\Big(\beta+\sum_i s_i\Big),\end{aligned} \tag{3.18}$$

where r and β are real numbers and r is chosen so that the path of integration separates the poles of the $\Gamma(-s_i)$ functions to the left of the poles of the $\Gamma\Big(\beta+\sum_i s_i\Big)$ function. At its core, this seemingly very complex representation is in fact just a Taylor expansion in a geometric series. If we consider the case of a massive scalar propagator, it requires two different Taylor expansions in the infrared and ultraviolet regimes:

$$\begin{aligned}\frac{1}{(p^2-m^2)^\nu} &= \frac{1}{p^{2\nu}}\frac{1}{\Gamma(\nu)}\sum_{n=0}\frac{1}{n!}\Big(\frac{m^2}{p^2}\Big)^n\Gamma(\nu+n) \qquad \text{for} \quad \Big|\frac{m^2}{p^2}\Big|<1,\\ &= \frac{1}{(-m^2)^\nu}\frac{1}{\Gamma(\nu)}\sum_{n=0}\frac{1}{n!}\Big(\frac{p^2}{m^2}\Big)^n\Gamma(\nu+n) \qquad \text{for} \quad \Big|\frac{p^2}{m^2}\Big|<1.\end{aligned} \tag{3.19}$$

The advantage of formula (3.18) is that it contains both series implicitly. The Mellin–Barnes representation for the considered case is

$$\frac{1}{(p^2-m^2)^\nu} = \frac{1}{m^{2\nu}}\frac{1}{\Gamma(\nu)}\int_s\Big(-\frac{p^2}{m^2}\Big)^s\Gamma(-s)\Gamma(\nu+s).$$

To compute this integral we can use the standard framework of residues in complex variable by tracing a semi–circular integration contour with an infinite radius which is closed by a line that lies along the imaginary axis (see figure 3.2). The direction (positive or negative real) to which the semicircle points is restricted by the requirement that its contribution vanishes. Thus by Jordan's lemma one concludes that for $|k^2|<m^2$ the semicircle must point to the right (positive real) and for $m^2<|k^2|$ it must point to the left. In each case the contour of integration encloses the poles of $\Gamma(-s)$ or $\Gamma(\nu+s)$, respectively. Noting that the Euler Gamma function has simple poles at zero and all negative integers, then the sum of residues from Cauchy's theorem gives the correct geometric series of (3.19) in the corresponding regimes. The prescription that the poles of these two functions are divided by the imaginary integration interval ensures that one series representation does not mix with the other. As a final remark, it is worth noting that the Feynman prescription can be straightforwardly taken into account in the Mellin–Barnes representation by including the infinitesimal imaginary part of the momentum: $p^2+i\epsilon$. The consequences of this contribution will be discussed later in this section when we discuss the computation of Mellin–Barnes integrals in detail.

In general, formula (3.18) is very useful to compute non–trivial Feynman parameters integrals; it is just a matter of carefully choosing the A_i's so that each contains only terms with the same power of Feynman parameters. In this way the integral over the x_i becomes straightforward. Inserting this identity into (3.17) one obtains:

$$\begin{aligned} I^{(2)}(d;\nu_1,\nu_2) &= \frac{(-1)^{\frac{1}{2}+\nu_1+\nu_2}}{(4\pi)^{d/2}}\frac{m_2^{d-2\nu_1-2\nu_2}}{\Gamma(\nu_1)\Gamma(\nu_2)}\int_{s_1s_2}\int_0^1 dx_1\, x_1^{s_1+s_2+\nu_1-1}x_2^{s_1+\nu_2-1} \\ &\quad\times\Gamma(-s_1)\Gamma(-s_2)\Gamma\Big(\nu_1+\nu_2+s_1+s_2\Big)\Big(-\frac{q_1^2}{m_2^2}\Big)^{s_1}\Big(\frac{m_1^2}{m_2^2}-1\Big)^{s_2} \\ &= \frac{i^{1-d}}{(4\pi)^{d/2}}\frac{(-m_2^2)^{\frac{d}{2}-\nu_1-\nu_2}}{\Gamma(\nu_1)\Gamma(\nu_2)}\int_{s_1s_2}\frac{\Gamma(s_1+s_2+\nu_1)\Gamma(2s_1+s_2+\nu_1+\nu_2)}{\Gamma(s_1+\nu_2)} \\ &\quad\times\Gamma(-s_1)\Gamma(-s_2)\Gamma\Big(\nu_1+\nu_2+s_1+s_2\Big)\Big(-\frac{q_1^2}{m_2^2}\Big)^{s_1}\Big(\frac{m_1^2}{m_2^2}-1\Big)^{s_2}, \end{aligned} \tag{3.20}$$

where we have used the following formula:

$$\int_0^1\ldots\int_0^1\prod_i dx_i\, x_i^{\rho_i-1}\delta\Big(\sum_i x_i-1\Big)=\frac{\prod_i\Gamma(\rho_i)}{\Gamma(\sum_i\rho_i)} \tag{3.21}$$

to perform the Feynman parameters integral.

To advance any further we need to compute the complex integrals. As usual, this can be done by residues theorem, by considering the semicircular closed path of integration mentioned earlier. However, this time we have multiple nested contours and therefore the situation calls for multivariate residues tools. We will consider this topic in detail later in this section, but we will not come back to this particular integral because we need the simpler case of equal masses. The complete solution of the integral in (3.20) for each kinematic regimes can be found in [110] and further technical details about the hypergeometric functions that appear in the answer can be obtained from [61].

Now we specialize the computation of the two–point integral for our case of interest, namely, $m_1 = m_2 = m$. Note that in such situation one of the Mellin–Barnes integrals in (3.20) is ill–defined,[8] which hints at an over parametrization of the problem. Taking a step back to (3.17) we see that the Mellin–Barnes representation of Δ needs one less integral when all masses are equal and the result is:

$$\begin{aligned} I^{(2)}(d;\nu_1,\nu_2) &= \frac{i^{1-d}}{(4\pi)^{d/2}}\frac{(-m^2)^{\frac{d}{2}-\nu_1-\nu_2}}{\Gamma(\nu_1)\Gamma(\nu_2)}\int_{s_1}\frac{\Gamma(s_1+\nu_1)\Gamma(s_1+\nu_2)}{\Gamma(2s_1+\nu_1+\nu_2)} \\ &\quad\times\Big(-\frac{q_1^2}{m^2}\Big)^{s_1}\Gamma(-s_1)\Gamma\Big(s_1+\nu_1+\nu_2-\frac{d}{2}\Big). \end{aligned} \tag{3.22}$$

[8] Actually hypergeometric functions which are solutions to these Mellin–Barnes integrals have branch points 0, 1 and ∞.

This is in fact the simplest non–trivial case of a general formula for N–point scalar integrals with equal masses, which was first published in [42]:

$$I^{(N)}(d;\nu_1,...,\nu_N) = \frac{i^{1-d}}{(4\pi)^{d/2}} \frac{(-m^2)^{\frac{d}{2}-\sum_i \nu_i}}{\prod_i \Gamma(\nu_i)} \int_{\prod s_{jl}} \prod_{j<l} \left\{ \left(-\frac{q_{jl}^2}{m^2} \right)^{s_{jl}} \Gamma(-s_{jl}) \right\} \\ \times \Gamma\Big(\sum_i \nu_i - \frac{d}{2} + \sum_{j<l}\sum s_{jl} \Big) \Big[\Gamma\Big(\sum_i \nu_i + 2\sum_{j<l}\sum s_{jl} \Big) \Big]^{-1} \prod_{i=1}^{N} \Gamma\Big(\nu_i + \sum_{j<i} s_{ji} + \sum_{l>i} s_{il} \Big) \,, \tag{3.23}$$

where $q_{jl} = q_j - q_l$ are all the distinct differences of external momenta and the indices run over $j < l$ to avoid double counting. Consequently there are $N(N-1)/2$ Mellin-Barnes integrals, one for each distinct difference of external momenta. The two indices in Mellin–Barnes integration variables allow for a quick identification with their respective q_{jl}^2.

For the triangle scalar integral with equal masses, (3.23) yields:

$$I^{(3)}(d;\nu_1,\nu_2,\nu_3) = \frac{i^{1-d}}{(4\pi)^{d/2}} \frac{(-m^2)^{\frac{d}{2}-\sum_i \nu_i}}{\Gamma(\nu_1)\Gamma(\nu_2)\Gamma(\nu_3)} \int_{\substack{s_{12}\\ s_{13}\\ s_{23}}} \left(-\frac{q_{12}^2}{m^2} \right)^{s_{12}} \left(-\frac{q_{13}^2}{m^2} \right)^{s_{13}} \left(-\frac{q_{23}^2}{m^2} \right)^{s_{23}} \\ \times \Gamma(-s_{12})\Gamma(-s_{13})\Gamma(-s_{23}) \\ \times \Gamma\Big(\nu_1 + s_{12} + s_{13}\Big)\Gamma\Big(\nu_2 + s_{12} + s_{23}\Big)\Gamma\Big(\nu_3 + s_{13} + s_{23}\Big) \\ \times \Gamma\Big(\sum_i \nu_i - \frac{d}{2} + s_{12} + s_{13} + s_{23} \Big) \Big[\Gamma\Big(\sum_i \nu_i + 2s_{12} + 2s_{13} + 2s_{23} \Big) \Big]^{-1} . \tag{3.24}$$

Now the task is to compute the integrals in (3.22) and (3.24). This is a complex task even for the self–energy case for both practical and conceptual reasons. From a practical perspective, we see that there are four Gamma functions in (3.22) and seven in (3.24). Each of these introduces its own infinite set of simple poles and each of these may contribute in a different kinematic regime. Furthermore, the triangle integral has a triple nested integral and thus the poles of the Gamma functions are intertwined, which requires one to be even more careful. This issue introduces additionally a conceptual difficulty: the standard complex variable residues framework that is enough for the self–energy case cannot be naively expanded in general by iteration to consider multiple complex variable integrals. There are subtleties that must be accounted for appropriately. Therefore we stop the presentation of our computation of the quark loop to present the tools necessary to afford it.

3.2.2 Mellin–Barnes integrals, multivariate residues and hypergeometric functions

The Davydychev tensor decomposition which has the benefit of not introducing additional kinematic singularities has come at the cost of introducing scalar integrals in shifted dimensions. In (3.22) and (3.24) we have arrived at a representation for the emerging sclar integrals in terms of Mellin–Barnes representation. Analytical expressions to these are often given in terms of hypergeometric–like[9] series in one or more variables, therefore they can give us a complete and systematic expansion of the quark masses effects on the loop. We will present a general framework of computation for Mellin–Barnes integrals from (3.23).

[9]The presence of logarithms and polygamma functions breaks some of the properties required on a power series to be considered a hypergeometric one.

3.2.2.1 General properties of Mellin–Barnes integrals

In particular, we have to deal with P–fold Mellin–Barnes integrals of the form:

$$J(\{\boldsymbol{e}_j\},\boldsymbol{f};\{g_j\},h;u_1,...,u_P)=\int_{-i\infty}^{+i\infty}...\int_{-i\infty}^{+i\infty}\prod_i^P\left\{\frac{ds_i}{2\pi i}(-u_i)^{s_i}\right\}\frac{\prod_{j=1}^k\Gamma(\boldsymbol{e}_j\cdot\boldsymbol{s}+g_j)}{\Gamma(\boldsymbol{f}\cdot\boldsymbol{s}+h)}\,, \tag{3.25}$$

where $\boldsymbol{s}$ is a P–dimensional complex vector containing the integration variables, $\boldsymbol{e}_j$ and $\boldsymbol{f}$ are P–dimensional real vectors, g_j and h are real numbers, and u_i is a complex number. Looking at (3.23), we have $\boldsymbol{f}=(2,...,2)^T$ and $h=\sum_i\nu_i$. The vectors $\boldsymbol{e}_j$ and the numbers g_j do not have a general form, but can be easily read from (3.23). The integral paths are shifted from the origin by a finite real quantity γ_i to prevent them from splitting the poles of a Gamma function in the numerator into subsets or passing through one of them.[10] In general, the Gamma functions in both the numerator and denominator of the integrand may also appear with powers higher than one and there may be multiple gamma functions in the denominator, but we will not consider such cases as they do not happen in (3.23).

There are two quantities upon which some important features of the integral in (3.25) depend:

$$\begin{aligned}&\boldsymbol{\Delta}\equiv\sum_i\boldsymbol{e}_i-\boldsymbol{f}\\&\alpha\equiv\text{Min}_{||\hat{\boldsymbol{y}}||=1}\Big\{\sum_i|\boldsymbol{e}_i\cdot\hat{\boldsymbol{y}}|-|\boldsymbol{f}\cdot\hat{\boldsymbol{y}}|\Big\}\,,\end{aligned} \tag{3.26}$$

where $|.|$ symbolizes real or complex absolute value and $||.||$ represents Euclidean vector norm. In particular, for all integrals of the type (3.10) we have $\boldsymbol{\Delta}=0$. The asymptotic behaviour of the integrand is of course key for Mellin–Barnes integrals and these two quantities characterize it. First, let us see the meaning of α. For this, let us consider the asymptotic behaviour of the integrand in (3.25) when the imaginary part of s_i gets big. Stirling's formula,

$$|z|\to+\infty\ \ ,\ \Gamma(z)\longrightarrow\sqrt{2\pi}z^{z-1/2}e^{-z}\,, \tag{3.27}$$

in the limit of z with big imaginary part yields:

$$\Gamma(r+i\tau)\longrightarrow\sqrt{2\pi}|\tau|^{r-1/2}e^{-\pi|\tau|/2}\qquad\text{for}\quad|\tau|\to\infty\,, \tag{3.28}$$

then evaluating the complex norm of the integrand of (3.25) in the asymptotic regime $s_i=\lim_{|R_i|\to\infty}\gamma_i-x_i+iR_i$, where x_i and R_i are real numbers, and γ_i represents the real shift to the integration paths, we obtain:

$$\begin{aligned}\left|\prod_i^P\Big\{(-u_i)^{s_i}\Big\}\frac{\prod_{j=1}^k\Gamma(\boldsymbol{e}_j\cdot\boldsymbol{s}+g_j)}{\Gamma(\boldsymbol{f}\cdot\boldsymbol{s}+h)}\right|\quad\longrightarrow\quad&\prod_i^P\Big\{|u_i|^{\gamma_i}\Big\}\frac{\prod_{j=1}^k|\boldsymbol{e}_j\cdot\boldsymbol{R}|^{\sum_i\boldsymbol{e}_i\cdot(\boldsymbol{\gamma}-\boldsymbol{x})+g_j-1/2}}{|\boldsymbol{f}\cdot\boldsymbol{R}|^{\boldsymbol{f}\cdot(\boldsymbol{\gamma}-\boldsymbol{x})+h-1/2}}\\&\times\exp\Big\{-\Big(arg\{u_i\}+\pi\Big)R_i\\&\qquad-\Big(\sum_j|\boldsymbol{e}_j\cdot\boldsymbol{R}|-|\boldsymbol{f}\cdot\boldsymbol{R}|\Big)\frac{\pi}{2}\Big\}\,.\end{aligned}$$

[10] If one is computing the integral in dimensional regularization, the former purpose might not be compatible with the limit $\epsilon\to0$. We do not consider this situation here as it is not relevant for this work. Instead we refer the reader to the comprehensive study done in [111].

The first line on the right hand side is a polynomial in R_i, while the other two are exponential. Thus we see that the integral in (3.25) is absolutely convergent for

$$-arg\{-\boldsymbol{u}\}\cdot\boldsymbol{R} < \Big(\sum_j |\boldsymbol{e}_j\cdot\boldsymbol{R}| - |\boldsymbol{f}\cdot\boldsymbol{R}|\Big)\frac{\pi}{2}\,, \tag{3.29}$$

where $arg\{u_i\}$ is the argument of the complex variable u_i and the components of $arg\{-\boldsymbol{u}\}$ are equal to $arg\{u_i\}+\pi$. Since the inequality (3.29) is homogeneous in $\boldsymbol{R}$, then it can be simplified as

$$\text{Max}_{||\hat{\boldsymbol{y}}||=1}|arg\{-\boldsymbol{u}\}\cdot\hat{\boldsymbol{y}}| < \alpha\frac{\pi}{2}\,.$$

Finally, using the well–known Cauchy–Schwartz[11] inequality one concludes that

$$\text{Max}_{||\hat{\boldsymbol{y}}||=1}|arg\{-\boldsymbol{u}\}\cdot\hat{\boldsymbol{y}}| = ||arg\{-\boldsymbol{u}\}|| \tag{3.30}$$

$$||arg\{-\boldsymbol{u}\}|| < \alpha\frac{\pi}{2}\,. \tag{3.31}$$

Therefore, one sees that α characterizes the convergence regions of the Mellin–Barnes integral in (3.25). In particular, it is a necessary condition that $\alpha > 0$ in order for the convergence region of the integral to be non–empty. For the integrals appearing in (3.23) one has $\alpha > \sum_j |(\hat{\boldsymbol{y}})_j| - |\sum_j (\hat{\boldsymbol{y}})_j| > 0$, hence there is always a non–trivial region of convergence.

While α is related to the convergence of the integral as a function of $\boldsymbol{u}$, that is, the asymptotic behaviour of the integrand in imaginary directions, $\boldsymbol{\Delta}$ does the same with respect to the real part of the integration variables $\boldsymbol{s}$. This is key to know the direction to which the contours of integration can be closed. To justify this interpretation we follow a procedure analogous to that of α although this time the Stirling formula is specialized to the case of a big real part:

$$|\Gamma(r+i\tau)| \longrightarrow \sqrt{2\pi}|r|^{r-1/2}e^{-r}\,. \tag{3.32}$$

With such formula we study the integrand in the limit $s_i = \lim_{|x_i|\to\infty}\gamma_i - x_i + iR_i$:

$$\left|\prod_i^P\Big\{(-u_i)^{s_i}\Big\}\frac{\prod_{j=1}^k\Gamma(\boldsymbol{e}_j\cdot\boldsymbol{s}+g_j)}{\Gamma(\boldsymbol{f}\cdot\boldsymbol{s}+h)}\right| \longrightarrow \exp\Big\{-\Big(\sum_j \boldsymbol{e}_j - \boldsymbol{f}\Big)\cdot(\boldsymbol{\gamma}-\boldsymbol{x})\Big\} \times\left|\prod_i^P\Big\{|u_i|^{-x_i}\Big\}\frac{\prod_{j=1}^k|\boldsymbol{e}_j\cdot\boldsymbol{x}|^{e_j\cdot\boldsymbol{x}-1/2}}{|\boldsymbol{f}\cdot\boldsymbol{x}|^{f\cdot\boldsymbol{x}-1/2}}\right|,$$

where $\boldsymbol{x}$ characterizes the direction to which the contour of integration closes and thus we see that for $\boldsymbol{\Delta}\neq 0$ there are preferred directions in the complex plane. Instead, when $\boldsymbol{\Delta}=0$ there are many (infinitely many, as we will discuss later) regions where the integrand decreases depending on the values of $|u_i|$ and as such there are multiple series representations which, if $\alpha>0$, are analytic continuations of one another [112, 113].

Let us introduce useful definitions to shed more light on the meaning of Δ, which is crucial for the computation of Mellin–Barnes integrals. We have found that the exponential increase or decrease of the Mellin–Barnes integrand in infinite real directions of the complex space $\mathbb{C}^P$ depends on a scalar product with $\boldsymbol{\Delta}$. More specifically, we conclude that the integrand increases exponentially for any $\boldsymbol{s}\in\mathbb{C}^P$ with a large real part such that $\boldsymbol{\Delta}\cdot Re\{\boldsymbol{s}\} > \boldsymbol{\Delta}\cdot\boldsymbol{\gamma}$ and the converse statement is valid if $\boldsymbol{\Delta}\cdot Re\{\boldsymbol{s}\} < \boldsymbol{\Delta}\cdot\boldsymbol{\gamma}$. We will later see that one can compute Mellin–Barnes integrals by

[11] Also known as Cauchy–Bunyakovsky or Cauchy–Bunyakovsky–Schwartz inequality.

closing an infinite contour[12] in the region in which the integrand vanishes asymptotically, as one can expect from a naive multivariate generalization of Jordan's lemma. Consequently, we now introduce definition that will come in handy below. Let $l_{\boldsymbol{\Delta}}$ be a hyperplane in the subspace $\mathbb{R}^P$ with normal vector $\boldsymbol{\Delta}$ whose points are defined by the condition $\boldsymbol{\Delta} \cdot Re\{\boldsymbol{s}\} = \boldsymbol{\Delta} \cdot \boldsymbol{\gamma}$. Note that $l_{\boldsymbol{\Delta}}$ constitutes a critical region of the asymptotic behaviour of the Mellin–Barnes integrand. Let $\pi_{\boldsymbol{\Delta}}$ represent the "half" of $\mathbb{R}^P$ for which $\boldsymbol{\Delta} \cdot Re\{\boldsymbol{s}\} < \boldsymbol{\Delta} \cdot \boldsymbol{\gamma}$, which is the region of exponential decrease of the integrand. $\pi_{\boldsymbol{\Delta}}$ can be regarded as the real projection of a section $\Pi_{\boldsymbol{\Delta}}$ of $\mathbb{C}^P$. Since $\boldsymbol{\Delta}$ is a real vector, then such section can be defined as a direct product: $\Pi_{\boldsymbol{\Delta}} \equiv \pi_{\boldsymbol{\Delta}} + i\mathbb{R}^P$. [13] The points of $\Pi_{\boldsymbol{\Delta}}$ are characterized by the condition $Re\{\boldsymbol{\Delta} \cdot \boldsymbol{s}\} < \boldsymbol{\Delta} \cdot \boldsymbol{\gamma}$, therefore, as we just discussed, it should be expected for the integrand poles that belong to $\Pi_{\boldsymbol{\Delta}}$ to play a major role in the computation of Mellin–Barnes integrals.

3.2.2.2 Multivariate generalization of Jordan's lemma for Mellin–Barnes integrals

We have the asymptotic behaviour of Mellin–Barnes integrals. Let us now consider its actual computation. In univariate residues we have the well–known Jordan's lemma:

$$\frac{1}{2\pi i}\int_{-\infty}^{+\infty} dx\, f(x)e^{i\lambda x} = \sum_{a\in S} Res_a f(z)\ , \tag{3.33}$$

where $\lambda > 0$ and S is the set of poles of $f(z)$ in the upper half of the complex plane. This formula is valid if $\lim_{|z|\to\infty} |f(z)| = 0$ for z in the upper half of the complex plane.[14] If $\lambda < 0$ then the upper and lower halves of the complex plane change roles. This formula is only valid for one dimensional Mellin–Barnes integrals, that is, the self–energy ones. It can in principle be applied also for multiple integrals as long as the location of the poles remains univariate. An example of such situation would be a two–fold Mellin–Barnes integrals where such that in the numerator there are two gamma functions $\Gamma(z_1)\Gamma(z_2)$ and a counter example would be $\Gamma(z_1)\Gamma(z_2+z_1)$. In the latter case the poles become entangled and it is necessary to use multivariate residues machinery. It is evident that we face such situations with (3.23).

It is possible to compute integrals (3.25) in the general multivariate case with a formula analogous to (3.33). Such formula is of course more abstract, so, before presenting the result, let us first point at certain features of the univariate formula that should be translated into the multivariate case. The basic idea behind (3.33) is to use the straight path of integration of the original integral as a part of a larger closed contour. The integral along such contour can be computed with residues. The region to which the contour is closed is chosen such that contribution from the part of the contour that is additional to the original straight path vanishes. Since the original integration path is infinite and the contour is closed, then the additional parts are infinite too and must be place in a region where the integrand vanishes, at least asymptotically. Such region is ultimately determined by λ in the univariate case and by $\boldsymbol{\Delta}$ for the multivariate ones of (3.25). Therefore one would expect the relevant poles of the multivariate case to be the ones in $\Pi_{\boldsymbol{\Delta}}$, just as the relevant ones for (3.33) are in the upper half of $\mathbb{C}$ for $\lambda > 0$.

[12] We are perhaps abusing the term "contour", which is more suitable for the single variable case than for multivariate situation, but the analogy stands.

[13] For $P = 1$ $l_{\boldsymbol{\Delta}}$ and $\pi_{\boldsymbol{\Delta}}$ are a point and a line, for $P = 2$ they are a line and a plane, and for $P = 3$ they are a plane and a 3D cube, respectively.

[14] Note that Jordan's lemma is usually taken to be the result regarding the vanishing of the integral of a complex variable function along an infinite semicircle, of which (3.33) is a famous application, but here we adhere to the convention of [114].

Now we need to introduce the definition of multivariate poles and residues. These are slightly different from the univariate case. Let us consider the following general function:

$$f(z) = \frac{\eta(z)}{\phi_1(z)...\phi_n(z)} \,, \tag{3.34}$$

where $z = (z_1, ..., z_n) \in \mathbb{C}^n$. A naive univariate generalization would tell us that $f(z)$ has poles in any z_0 such that $\phi_j(z_0) = 0$ for at least one $j \in \{1, ..., n\}$, as long as $\eta(z_0) \neq 0$. Instead, the correct definition states that $f(z)$ has poles in any z_0 such that $\boldsymbol{\phi}(z_0) = (\phi_1(z_0), ..., \phi_n(z_0)) = 0$, as long as $\eta(z_0) \neq 0$. This definition is not as odd as it may seem: if we could arrange a variable change such that each ϕ_j becomes univariate then we would disentangle the multivariate poles and the closed integral of $f(z)$ would become a product of univariate integrals. For some integration contours such product would be equal to zero if not all ϕ_j had zeros at the same point.

There is one more rather peculiar feature of the definition of poles that we have just given: it leaves space for ambiguities with respect to the way in which singular factors ϕ_j are grouped together. For example, let us consider the following function $f(z_1, z_2)$:

$$f(z_1, z_2) = \frac{\eta(z_1, z_2)}{z_1(z_1 - z_2 + 1)(z_1 + z_2)} \,. \tag{3.35}$$

There is no obvious way to define the singular functions. Three of the possibilities are:

$$\begin{aligned} &\phi_1 = z_1(z_1 - z_2 + 1) \,, && \phi_2 = (z_1 + z_2) \,, \\ &\phi_1 = (z_1 - z_2 + 1) \,, && \phi_2 = z_1(z_1 + z_2) \,, \\ &\phi_1 = z_1 \,, && \phi_2 = (z_1 - z_2 + 1)(z_1 + z_2) \,. \end{aligned}$$

Each of these three combinations has different poles and they may have even different residues in the poles that they share.[15] Furthermore, even if there were only two singular factors, the order in which they are defined introduces a sign ambiguity, as we will see later. Hence any residue formula must clearly specify the singular functions with respect to which its poles are defined. Each set of singular points defined by the condition $\phi_j(z) = 0$ is called a divisor and we represent them with F_j. Consequently, the set $F_1 \cap F_2 \cap ... \cap F_n$ contains the poles of $f(z)$ with respect to a certain set of divisors $\{F_j\}$.

Now let us consider the residues of $f(z)$ in this poles:

$$Res_{\{F_1,...,F_n\},z_0} f(z) = \frac{1}{(2\pi i)^n} \oint_{C_\epsilon} \frac{\eta(z) dz_1 ... dz_n}{\phi_1(z)...\phi_n(z)} \,, \tag{3.36}$$

where $C_\epsilon\{z \in \mathbb{C}^P | \, |\phi_i(z)| = \epsilon_i\}$ is called a cycle and ϵ_i has infinitesimal positive value. The orientation of the integration path C_ϵ is defined such that the change in the argument of every ϕ_j is always possible, which is analogous to the usual clockwise orientation although this time it refers to the functions ϕ_j rather than the integration variables z_j. Note that due to the definition of the orientation of C_ϵ, one sees that residues are skew–symmetric with respect to the permutations of ϕ_j. Equation (3.36) defines local Grothendieck residues, which are a multivariate generalization of the univariate ones and are commonly used in the context of algebraic geometry [116].

[15] An explicit computation of an example of the latter case is given in [115].

Now we are able to state the the formal mathematical generalization of (3.33) for multiple variables, which is called "multidimensional abstract Jordan lemma" [114]. It asserts that for a complex variable function $f(z)$:

$$\frac{1}{(2\pi i)^n}\int_\sigma f(z)dz_1...dz_n = \sum_{a\in\Pi} Res_a f(z)\ . \tag{3.37}$$

Let Π be a polyhedron and σ be the "skeleton" of Π, that is, the structure formed by the vertices and edges of Π. The residues in Π are defined in terms of divisors $\{F_j\}$ such that each of them does not intersect one specific face of the polyhedron, that is, the polyhedron has n faces σ_n and the set of divisors verifies the condition $F_j \cap \sigma_j = \varnothing$ for each $j = 1, ..., n$. This is referred to as "compatibility" between divisors and the polyhedron.

In general, Π may be bounded or not, however, we want to identify the edges in σ with the infinite straight integration paths of (3.25), so we are interested in the unbounded case. In this context there is an additional condition for the validity of (3.37) which is essentially a multivariate generalization of the asymptotic behaviour condition on $f(z)$ when there is an infinite set of poles, which we omitted when discussing (3.33) and we omit for this case, too, because it is not crucial for our analysis [112, 114].

Applying (3.37) to integrals of the type showed in (3.25) one obtains the following result [112, 117]:

$$J(\{\boldsymbol{e}_j\}, \boldsymbol{f}; \{g_j\}, h; u_1, ..., u_P) = \sum_{a\in\Pi_{\boldsymbol{\Delta}}} Res_a J\ . \tag{3.38}$$

In addition, $Res_a J$ represents the residue of the integrand in its pole a. The compatibility condition for the divisors and the polyhedron is of course still required for (3.38) to be valid. For $\boldsymbol{\Delta} = 0$ one sees that there is no preferred region of the $\mathbb{C}^P$ space, hence such integrals are usually called "degenerate". In fact, in such cases formula (3.38) remains valid for any $\Pi_{\boldsymbol{\Delta}}$.

The analogy of this result with the standard one–dimensional Jordan lemma is more apparent in the one–dimensional case of (3.25). In there, $l_{\boldsymbol{\Delta}}$ is just $\gamma + i\mathbb{R}$. Hence when $\Delta > 0$ the sum of residues from the poles enclosed in the negative real half of the complex plane constitute a series representation convergent for any value of u, while the sum of residues from the other half forms a divergent asymptotic expansion [118]. For $\Delta < 0$ the roles of these two halves of the complex plane are inverted, while for $\Delta = 0$ one obtains two different series for each half that converge in non–overlapping complementary regions of the u complex plane. If $\alpha > 0$, then they are an analytical continuation of each other. In this way one can see the analogy of $\boldsymbol{\Delta}$ with the role of the time coordinate and its sign in Fourier transforms. Regarding the compatibility between the divisor and the polyhedron of integration, note that the face of $\Pi_{\boldsymbol{\Delta}}$ is just the integration path $\gamma + i\mathbb{R}$, therefore one sees that such prescription is just the multidimensional generalization of the requirement for (3.33) that no poles lie on the integration path.

Now that we have presented the multivariate generalization of Jordan's lemma, we need to show how to compute Grothendieck residues of the integrand of (3.25) with respect to the poles and divisors that fulfill the requirements of (3.38).

Let us first start with poles. The ones that we are interested in exist at points where P gamma functions become singular, that is, the intersection of P singular hyperplanes of the gamma functions in the numerator. For example, in the case of the three–point function (3.24), we must have an intersection of three two–dimensional planes. Each gamma function in the numerator of the integrand generates a family L^j with countably infinite singular hyperplanes L^j_n defined

as $L_n^j = \{\boldsymbol{s} \in \mathbb{C}^P | \, \boldsymbol{e}_j \cdot \boldsymbol{s} + g_j = -n\}$ for every $n \in \mathbb{N}$. One sees that each $\boldsymbol{e}_j$ is the normal vector of the family of singular hyperplanes of a given gamma function. They give us information about intersection of singular planes an therefore they are key to identify poles of the integrand. If a set of P vectors $\{\boldsymbol{e}_{j_1}, ..., \boldsymbol{e}_{j_P}\}$ is linearly independent, then for any $n_i \in \mathbb{N}$ the set $L_{n_1}^{j_1} \cap ... \cap L_{n_P}^{j_P}$ always has only one element $\boldsymbol{z}_0 \in \mathbb{C}^P$, which constitutes a pole of the Mellin–Barnes integrand. Moreover, if each singular plane L^{j_i} belongs to a different divisor F_{j_i}, then $\boldsymbol{z}_0$ is a relevant pole for (3.38). With this definition of poles, the formula (3.38) requires us to:

- Group the singular planes of the gamma functions in the numerator of (3.25) in P divisors F_j that satisfy the compatibility condition with respect to the faces of Π_Δ.
- Study all possible P combinations of gamma functions in the numerator of (3.25) such that each gamma functions belongs to a different divisor F_j.
- Determine which of these combinations have isolated intersection points, that is, poles.
- Discard all poles that do not belong to $\Pi_{\boldsymbol{\Delta}}$.
- Compute the residues of the integrand of (3.25) for all relevant poles.

In addition, there are situations in which things are more complicated. It is possible, and in fact it happens for the three–point function, that more than P singular hyperplanes coincide at certain points. These cases are the multivariate versions of higher multiplicity poles and they are called "resonant" or "logarithmic" due to the logarithms that appear in the resulting series because of the derivatives of the terms $(-u)^s$ that are involved. Later in the section we present a useful tool to deal with such cases.

There is another subtlety that we have not addressed. The half space $\Pi_{\boldsymbol{\Delta}}$ plays a key role with in the computation, but it seems to be ill–defined for $\boldsymbol{\Delta}$, which is actually true for all the integrals that we need. The solution to this issue is very simple: one may define $\Pi_{\boldsymbol{\Delta}}$ arbitrarily. However, not that the key point for (3.37) and (3.38) is that one computes an integral along the skeleton of a polyhedron in terms of the poles that lie within the polyhedron. Hence the polyhedrons Π that one chooses for the computation must have $\boldsymbol{\gamma}$ as one of its vertices and $\boldsymbol{\gamma} + i\mathbb{R}^P$ as one of its edges. For a given $\boldsymbol{\gamma}$ there are still infinitely many options to define $\Pi_{\boldsymbol{\Delta}}$. Nevertheless, there are still only a finite number of series representations for (3.25) that, since $\alpha > 0$, are analytic continuations of each other for different values of $|u_i|$. Once the residues have been computed and the corresponding series representation has been obtained, one can identify the convergence region of the series obtained by applying Horn's theorem [61, 119, 120]. It is even possible to determine the convergence region of a series before performing the full computation [121] in order to compute only the series representation that converges for the kinematic regime that in one is interested in. We expect to shed more light on these issues with examples later in this subsection.

Now that we have studied the poles that we need to compute (3.25), we have only left to consider how to compute the residues on the right hand side of (3.38). As happens in the single variable case, the formal definition (3.36) usually is not the most appropriate tool.

Let us begin with the simple case in which there is a straightforward connection between univariate residues and multivariate ones. For this, let us consider again the general function $f(\boldsymbol{z})$ of (3.34). If the Jacobian determinant evaluated at the pole $\boldsymbol{z}_0$:

$$det\Big(\frac{\partial \phi_j}{\partial z_i}\Big)\Big|_{z=z_0} \tag{3.39}$$

is not equal to zero then one can perform the variable change $w_i \equiv \phi_i$, which disentangles the poles and hence allows for the multivariate integral to become a product of univariate integrals. The latter can be evaluated by the usual methods. These are called "simple poles" [122]. As we mentioned previously, this is usually not the case for (3.25).

When the Jacobian (3.39) is zero, then one has to use another formula called the "Transformation law" for multivariate residues (see page 20 of [122]), which is valid for residues of any function $f(z)$ irrespective of the value of its Jacobian determinant. For a function $f(z)$ with an isolated pole at $z = z_0$ one has:

$$Res_{z_0} \frac{\eta(z)}{\phi_1(z)...\phi_n(z)} = Res_{z_0} \frac{\eta(z) det \hat{A}}{\rho_1(z)...\rho_n(z)} \,, \tag{3.40}$$

such that:

$$\rho_i(z) = \sum_j a_{ij}(z)\phi_j(z) \qquad \longrightarrow \qquad \boldsymbol{\rho}(z) = \hat{A}(z)\boldsymbol{\phi}(z) \,, \tag{3.41}$$

where the coefficients $a_{ij}(z)$ are holomorphic functions that form the matrix $\hat{A}$ and $\boldsymbol{\rho} = (\rho_1, ..., \rho_n)$. The holomorphy condition for these matrix elements is important to ensure that they do not cancel zeros in any ϕ_j. Another requisite for (3.40) to hold is that all the poles of $\boldsymbol{\rho}$ and $\boldsymbol{\phi}$ are isolated.[16] The transformation law is useful to compute multivariate residues as long as one is able to find a set $\{\rho_j\}$ such that each element is an univariate function, because then one may factorize the integrals and use the standard univariate machinery for residue computation. From this formula it is also easy to see that even a change in the order of the denominators ϕ_j introduces a minus sign from A, which illustrates the importance of properly taking into account the orientation of the cycles in multivariate integrals.

3.2.2.3 Example of the computation of scalar integrals with Mellin–Barnes integrals with one variable.

In this subsection we compute a self–energy scalar integral, that is, a single variable Mellin–Barnes integral.

The general shape of scalar self–energy integrals is (3.22). Since that formula is symmetric with respect to the interchange $\mathbb{N} \setminus \{0\} \ni \nu_1 \leftrightarrow \nu_2$, we can choose without loss of generality $\nu_1 < \nu_2$ such that $\nu_1 \equiv \nu \geq 1$ and $\nu_2 \equiv \nu + n$ where $n \in \mathbb{N}$ is a natural number.[17] For this example we focus on the special case $n = 1$ with space–time dimension $d = 6$ for brevity and we will use it to provide insight about the general case. With that notation, the self–energy integral becomes:

$$I^{(2)}(6;\nu,\nu+1) = \frac{i^{-5}}{(4\pi)^3} \frac{(-m^2)^{2-2\nu}}{\Gamma(\nu)\Gamma(\nu+1)} \int_s \Big(-\frac{q^2}{m^2}\Big)^s \frac{\Gamma(s+\nu)\Gamma(s+\nu+1)}{\Gamma(2s+2\nu+1)} \Gamma(-s)\Gamma\Big(s+2\nu-2\Big) \,. \tag{3.42}$$

For this integral we can use the standard complex calculus tools in one variable. As mentioned previously, we always have $\Delta = 0$ and $\alpha > 0$, therefore the region of the complex plane where we can close the integration contour to obtain a convergent series representation is defined by the asymptotic behaviour of $(|q^2|/m^2)^s$. For the quark loop we are interested in the high energy

[16] In the mathematical literature this result is often presented in terms of ideals noted as $\langle \phi_1, ..., \phi_n \rangle$ and $\langle \rho_1, ..., \rho_n \rangle$. The condition of isolation for the poles is equivalent to the assertion that these two are zero dimensional ideals.

[17] There is actually loss of generality, since formula (3.23) is also valid for integrals with real propagator powers. Nevertheless, for the quark loop computation no such terms appear.

regime, therefore we have $|q^2| \gg m^2$. For such kinematic regime, the integrand of (3.42) is decreasing in the negative real half of the complex plane.

There are three gamma functions in the numerator that have poles in the negative part of the real axis. Using the multidimensional terminology we previously introduced, we can say that there are three families of singular hyperplanes in the negative half of the real plane:

$$\begin{aligned} S_1 &\equiv \{s \in \mathbb{C} |\, s = -p - \nu \quad \text{for } p \in \mathbb{N}\}\,, \\ S_2 &\equiv \{s \in \mathbb{C} |\, s = -p - \nu - 1 \quad \text{for } p \in \mathbb{N}\}\,, \\ S_3 &\equiv \left\{s \in \mathbb{C} \,\middle|\, s = -p + 2 - 2\nu \quad \text{for } p \in \mathbb{N}\right\}. \end{aligned} \tag{3.43}$$

For each of these three sets, the rightmost pole is obtained for $p = 0$, therefore we have $s = -\nu$ for S_1, $s = -\nu - 1$ for S_2 and $s = 2 - 2\nu$ for S_3. Consequently, the rightmost pole of all three sets is $-\nu$ if $2 - \nu < 0$ or $2 - 2\nu$ otherwise.[18] From these two cases, we specialize this computation for the case $\nu > 2$, since it has a wider range of use. There is also a set of poles on the positive real axis, and its leftmost pole is $s = 0$. Therefore γ may be anywhere within the interval $(-\nu, 0)$ in order not to split any of these four sets of poles (see figure 3.2). In multivariate residues language, this means that the polyhedron Π that interests us is defined by $\{s \in \mathbb{C} |\, Re\{s\} < \gamma\}$ and the integration path $\gamma + i\mathbb{R}$ is both its edge and its face. In the single variable case one still does not see much freedom to choose Π even though $\Delta = 0$, because there exist only two polyhedrons for which $\gamma + i\mathbb{R}$ is an edge, namely, the positive and negative real halves.

To expose removable singularities caused by the presence of a gamma function in the denominator we use the duplication formula:

$$\Gamma(2s) = \frac{2^{2s-1}}{\sqrt{\pi}}\Gamma(s)\Gamma(s + \frac{1}{2})\,, \tag{3.44}$$

which, when applied on to the gamma functions in the integral (3.42), yields

$$\sqrt{4\pi}\Big(-\frac{q^2}{4m^2}\Big)^s \frac{\Gamma(s+\nu)\Gamma(s+\nu+1)}{\Gamma(s+\nu+\frac{1}{2})\Gamma(s+\nu+1)}\Gamma(-s)\Gamma(s+2\nu-2)\,. \tag{3.45}$$

Instead for the general d and n case this result reads:

$$\sqrt{4\pi}\Big(-\frac{q^2}{4m^2}\Big)^s \frac{\Gamma(s+\nu)\Gamma(s+\nu+n)}{\Gamma(s+\nu+\frac{n}{2})\Gamma(s+\nu+\frac{n+1}{2})}\Gamma(-s)\Gamma\Big(s+n+2\nu-\frac{d}{2}\Big)\,. \tag{3.46}$$

We have not performed an obvious cancellation of gamma functions to emphasize that in the general n case it is necessary to define if n is odd or even in order to know which of the two Γ in the denominator is removing singularities. Applying basic recurrence formulas to shed light on the actual multiplicity of the remaining poles one obtains a the following expression for the integrand of (3.42):

$$\sqrt{4\pi}\Big(-\frac{q^2}{4m^2}\Big)^s \frac{\Gamma(-s)}{\Gamma(s+\nu+\frac{1}{2})}\frac{\Gamma^2(s+2\nu-2)}{\prod_{j=0}^{\nu-3}(s+\nu+j)}\,. \tag{3.47}$$

We have explicitly extracted the finite set of poles that only belong to the $\Gamma(s+\nu)$ in order the separate them from the rest which are shared with $\Gamma(s+2\nu-2)$ and whose multiplicity equal to two is now evident by the power of the gamma function. Let us first consider the residues of

[18] For arbitrary d and n the condition reads $\frac{d}{2} - \nu - n < 0$.

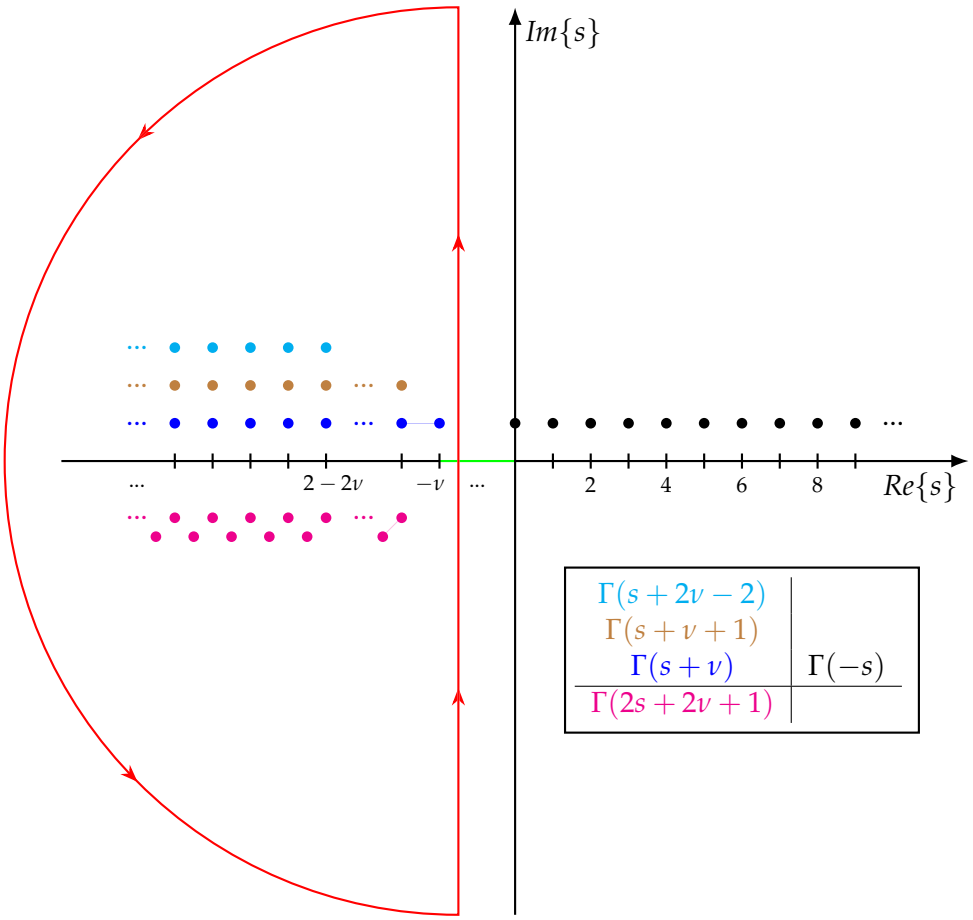

FIGURE 3.2: Graphic representation of the computation of the integral (3.42) with residues in the complex plane of s. The red path represents the contour of integration closed at infinity. The green interval in the real axis represents the possible values that γ can take. Dots represent poles and their color relates them to their corresponding gamma function. All poles are on the real axis, but they are displayed at different heights to expose multiplicity. The gamma functions location inside the legends box is related to the location of their poles in the figure.

the finite set of simple poles:

$$Res_{-\nu-k} I^{(2)} = \sqrt{4\pi}\Big(-\frac{q^2}{4m^2}\Big)^{-\nu-k} \frac{\Gamma(\nu+k)}{\Gamma(-k+\frac{1}{2})} \frac{\Gamma^2(-k+\nu-2)}{\prod_{j=0}^{k-1}(j-k)\prod_{j=k+1}^{\nu-3}(j-k)}\,,$$
$$Res_{-\nu-k} I^{(2)} = \sqrt{4\pi}\Big(-\frac{q^2}{4m^2}\Big)^{-\nu-k} \frac{\Gamma(\nu+k)}{\Gamma(-k+\frac{1}{2})} \frac{\Gamma^2(-k+\nu-2)}{(-1)^k k!(\nu-3-k)!}\,,$$

where $k \in \{0,...,\nu-3\}$ and we have represented the integrand of (3.42) by $I^{(2)}$ for brevity. Thus we see that the total contribution from these simple poles is:

$$\sqrt{4\pi}\Big(-\frac{4m^2}{q^2}\Big)^{\nu} \sum_{k=0}^{\nu-3} \Big(\frac{4m^2}{q^2}\Big)^k \frac{\Gamma(\nu+k)}{\Gamma(-k+\frac{1}{2})} \frac{\Gamma(-k+\nu-2)}{\Gamma(k+1)}\,. \tag{3.48}$$

Second order poles from the gamma function are defined by $s = 2-2\nu-l$ for every $l \in \mathbb{N}$. It is therefore convenient to place them at the origin by the following change of variables: $s \to s+2-2\nu-l$. Then, the singularity is exposed by using the generalized reflection formula for the gamma function:

$$\Gamma(s-n) = (-1)^n \frac{\Gamma(1-s)\Gamma(s+1)}{s\Gamma(n+1-s)} \qquad \text{For } n \in \mathbb{Z} \tag{3.49}$$

and thus the integrand becomes:

$$\sqrt{4\pi}\Big(-\frac{q^2}{4m^2}\Big)^{s+2-2\nu-l} \frac{\Gamma(-s-2+2\nu+l)}{\Gamma(s-\nu-l+\frac{5}{2})} \frac{\Gamma^2(1-s)\Gamma^2(s+1)}{s^2\Gamma^2(l+1-s)\prod_{j=0}^{\nu-3}(s+2-\nu-l+j)}\,. \tag{3.50}$$

This time we need to use the well–known formula for the residue of a complex variable function $f(z)$ in a pole z_0 of arbitrary multiplicity p:

$$Res_{z_0} f(z) = \frac{1}{(p-1)!}\frac{d^{p-1}}{dz^{p-1}}\{(z-z_0)^p f(z)\}\Big|_{z=z_0}\,, \tag{3.51}$$

where $\frac{d^{p-1}}{dz^{p-1}}$ represents the $(p-1)$–th derivative, as usual. Using (3.51) we find the residues of the integrand to be:

$$\begin{aligned} Res_{2-2\nu-l} I^{(2)} &= \sqrt{4\pi}\frac{d}{ds}\Big(-\frac{4m^2}{q^2}\Big)^{2\nu+l-s-2} \frac{\Gamma(-s-2+2\nu+l)}{\Gamma(s-\nu-l+\frac{5}{2})} \frac{\Gamma^2(1-s)\Gamma^2(s+1)}{\Gamma^2(l+1-s)\prod_{j=0}^{\nu-3}(s+2-\nu-l+j)}\Big|_{s=0} \\ &= \sqrt{4\pi}\Big(-\frac{4m^2}{q^2}\Big)^{2\nu+l-2} \frac{\Gamma(-2+2\nu+l)}{\Gamma(-\nu-l+\frac{5}{2})} \frac{(-1)^\nu}{\Gamma(l+1)\Gamma(l+\nu-1)} \\ &\quad \times \Bigg(\ln\Big\{-\frac{q^2}{4m^2}\Big\} - \psi^0(-2+2\nu+l) - \psi^{(0)}(-\nu-l+\frac{5}{2}) - 2\psi^{(0)}(l+1) \\ &\quad - \sum_{j=0}^{\nu-3}\frac{1}{2-\nu-l+j}\Bigg)\,, \end{aligned}$$

where $\Gamma'(z)$ is the first derivative of the gamma function and $\psi^0(z) \equiv \frac{d}{dz}\ln\Gamma(z) = \Gamma'(z)/\Gamma(z)$ is the digamma function. To further simplify the expression we can use the following identity:

$$\psi^{(0)}(p) = \sum_{j=1}^{p-1} \frac{1}{j} \qquad \text{for } p \in \mathbb{N}\setminus\{0\}\,, \tag{3.52}$$

which allows us to conclude that:

$$\sum_{j=0}^{\nu-3} \frac{1}{2-\nu-l+j} = -\psi^0(l+\nu-1) + \psi^{(0)}(l+1) \tag{3.53}$$

and therefore the full contribution from second order poles is:

$$\begin{aligned} &-\sqrt{4\pi}\Big(-\frac{16m^4}{q^4}\Big)^{\nu-1}\sum_{l=0}^{\infty}\Big(-\frac{4m^2}{q^2}\Big)^l \frac{\Gamma(-2+2\nu+l)}{\Gamma(-\nu-l+\frac{5}{2})}\frac{1}{\Gamma(l+1)\Gamma(l+\nu-1)} \\ &\quad\times\left(\ln\Big\{-\frac{q^2}{4m^2}\Big\} - \psi^0(-2+2\nu+l) - \psi^{(0)}(-\nu-l+\frac{5}{2}) - 3\psi^{(0)}(l+1) + \psi^0(l+\nu-1)\right). \end{aligned} \tag{3.54}$$

In conclusion we find that the scalar self–energy integral (3.42), which belongs to a special family of the general type in (3.22) with $\nu_1 \equiv \nu \geq 2$, $\nu_2 \equiv \nu+1$ and $d=6$, is equal to the sum of the expressions in (3.48) and (3.54):

$$\begin{aligned} I^{(2)}(6;\nu,\nu+1) &= \frac{-i}{(4\pi)^{5/2}}\frac{(m^4)^{1-\nu}}{\Gamma(\nu)\Gamma(\nu+1)} \\ &\times\Bigg\{\Big(-\frac{4m^2}{q^2}\Big)^{\nu}\sum_{k=0}^{\nu-3}\Big(\frac{4m^2}{q^2}\Big)^k\frac{\Gamma(\nu+k)}{\Gamma(-k+\frac{1}{2})}\frac{\Gamma(-k+\nu-2)}{\Gamma(k+1)} \\ &-\Big(-\frac{16m^4}{q^4}\Big)^{\nu-1}\sum_{l=0}^{\infty}\Big(-\frac{4m^2}{q^2}\Big)^l\frac{\Gamma(-2+2\nu+l)}{\Gamma(-\nu-l+\frac{5}{2})}\frac{1}{\Gamma(l+1)\Gamma(l+\nu-1)} \\ &\times\left(\ln\Big\{-\frac{q^2}{4m^2}\Big\} - \psi^{(0)}(-2+2\nu+l) - \psi^{(0)}(-\nu-l+\frac{5}{2}) - 3\psi^{(0)}(l+1) + \psi^{(0)}(l+\nu-1)\right)\Bigg\}. \end{aligned} \tag{3.55}$$

Note that this result is quite different from the one cited in equation (18) of [110]. In such case there appear three hypergeometric series and no logarithms or digamma functions. The reason for uch discrepancy is that the result obtained in [110] is valid for "generic" values of ν_1, ν_2 and d, that is, they consider the case in which none of them produces higher multiplicity poles of removable singularities, which does happen in our example. In short, in their computation all gamma functions in the numerator of the integrand have simple poles and none of them is cancelled by the gamma function in the denominator. Consequently, closing the integration contour to the left half of the complex plane only implies summing over three independent sets of simple poles from three gamma functions, thus three hypergeometric series appear.

Several important general properties of the scalar integrals that appear in the quark loop with shifted dimensions are present in this result. First of all, we can see in (3.55) the infrared divergent logarithms $\ln\{\frac{q^2}{m^2}\}$ that we renormalized in the previous chapter. In our computation these came due to the presence of higher multiplicity poles in the integrand. In general, self–energy

integrals have three gamma functions in the numerator with poles in the negative real half of the complex plane (see equation (3.22)), so one might think that poles of order 3 may arise. This would be problematic, since it would introduce further infrared divergent terms like $\ln^2\{\frac{q^2}{m^2}\}$, which we have not taken into account in the renormalization procedure. The absence of such poles is however not a lucky coincidence of the example that we have just considered, but rather a general property of self–energy scalar integrals. At the start of the example we considered the location of the poles of these three gamma functions. In the general d and n case, the sets of poles are:

$$\begin{aligned} S_1 &\equiv \{s \in \mathbb{C} | \, s = -p - \nu \quad \text{for } p \in \mathbb{N} \} \, , \\ S_2 &\equiv \{s \in \mathbb{C} | \, s = -p - \nu - n \quad \text{for } p \in \mathbb{N} \} \, , \\ S_3 &\equiv \left\{ s \in \mathbb{C} \middle| \, s = \frac{d}{2} - p - 2\nu - n \quad \text{for } p \in \mathbb{N} \right\} . \end{aligned} \tag{3.56}$$

If d is an odd integer, then the intersection of S_1 or S_2 with S_3 is empty and no third order poles appear. Now let us consider the case when d is an even integer. Since all of them extend infinitely along the negative integers, the intersection of these sets has an infinite number of elements and, in fact, it is equal to whichever of the three sets starts further to the left in the real axis. Just as we did in the example, for the general case the gamma function in the denominator can be decomposed by means of the duplication formula to get a divisor proportional to $\Gamma(s+\nu+\frac{n+1}{2})\Gamma(s+\nu+\frac{n}{2})$. Since ν and n are always positive integers in the quark loop computation, then one these two gamma function will always remove singularities from the gamma functions in the numerator. Which one of them does it depends on whether n is even or odd and we consider the latter case. In brief we argue that it is a worst–case scenario. The factor $1/\Gamma(s+\nu+\frac{n+1}{2})$ has a set of zeros $\zeta = \{s \in \mathbb{C} | \, s = -p-\nu-\frac{n+1}{2} \quad \text{for } p \in \mathbb{N}\}$. Note that even though the gamma function in the denominator lowers the order of an infinite number of singularities, it is not enough to lower the order of all singularities: singularities which lie to the right of the set of zeros of the factor $1/\Gamma(s+\nu+\frac{n+1}{2})$ do not have their order lowered. Consequently, if the set of zeros of this factor starts further enough to the left[19] such that it does not lower the multiplicity of one or more of the poles in $S_1 \cap S_2 \cap S_3$, then there will appear new infrared singularities of the type $\ln^2\{\frac{q^2}{m^2}\}$. To determine if or when this is possible, we need to show that the rightmost zero in ζ is always further to the right than the rightmost pole of at least one set S_i. It is very easy to show that such is the case for S_2 as long as n is a natural number. Hence, we prove that only simple logarithmic infrared divergences are introduced by self–energy scalar integrals $I^{(2)}(d;\nu_1,\nu_2)$ with any positive integers d, ν_1 and ν_2 in the high energy regime. In fact, it is easy to verify a similar assertion for the low energy regime. In such case one closes the contour of integration to the positive real half of the complex plane, where only the poles of $\Gamma(-s)$ lie, therefore not even simple logarithmic infrared divergences arise.

As a conclusion of our analysis of the result (3.55), we consider the convergence properties of the series representation found. The expression contains two series: one is (3.48), which has a finite number of terms and it is obviously convergent, and the other is (3.54), which has an infinite number of terms and a rather complex structure that requires careful study. The standard tools for the analysis of convergence properties of hypergeometric–like functions of a single variable are d'Alembert's ratio test and Raabe's test [61]. For this example we choose the former. Let us

[19] We refer to right or left in the sense of the real axis with negative numbers to the left and positive ones to the right.

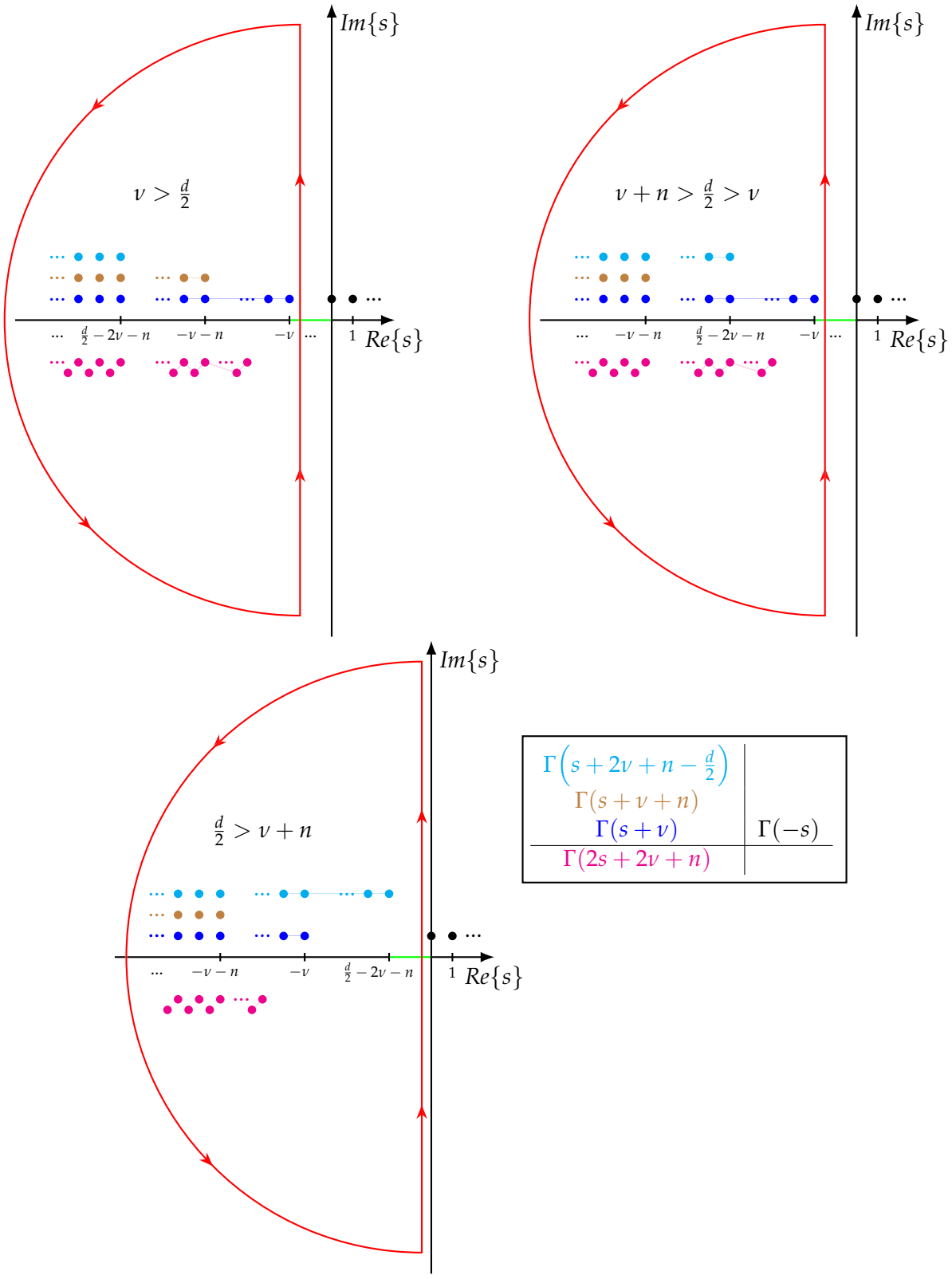

FIGURE 3.3: Graphical representation of the polar structure of a residue computation of the scalar self–energy integral (3.22) for positive propagator powers ν and $\nu + n$ with $n \in \mathbb{N}$ for three illustrative cases. The green interval in the real axis represents the possible values that γ can take. Dots represent singularities and their color shows the gamma function to which they belong, as shown in the legend box. From these figures one sees that no third order poles can possibly arise from the self–energy scalar integral with positive propagator powers.

define:

$$a_l \equiv \Big(-\frac{4m^2}{q^2}\Big)^l \frac{\Gamma(-2+2\nu+l)}{\Gamma(-\nu-l+\frac{5}{2})}\frac{1}{\Gamma(l+1)\Gamma(l+\nu-1)} \times \left(\ln\Big\{-\frac{q^2}{4m^2}\Big\} - \psi^{(0)}(-2+2\nu+l) - \psi^{(0)}(-\nu-l+\frac{5}{2}) - 3\psi^{(0)}(l+1) + \psi^{(0)}(l+\nu-1)\right), \tag{3.57}$$

thus we find:

$$\Big|\frac{a_{l+1}}{a_l}\Big| = \Big(-\frac{4m^2}{q^2}\Big)\frac{(-2+2\nu+l)(-\nu-l+\frac{3}{2})}{(l+1)(l+\nu-1)} \times \left(\frac{\ln\Big\{-\frac{q^2}{4m^2}\Big\} - \psi^{(0)}(-2+2\nu+l+1) - \psi^{(0)}(-\nu-l-1+\frac{5}{2}) - 3\psi^{(0)}(l+2) + \psi^{(0)}(l+\nu)}{\ln\Big\{-\frac{q^2}{4m^2}\Big\} - \psi^{(0)}(-2+2\nu+l) - \psi^{(0)}(-\nu-l+\frac{5}{2}) - 3\psi^{(0)}(l+1) + \psi^{(0)}(l+\nu-1)}\right). \tag{3.58}$$

Taking into account the asymptotic behaviour of the digamma function: $\psi^{(0)}(z) \to \ln z + \frac{1}{2z} + O(\frac{1}{z^2})$, one concludes that:

$$\lim_{l\to\infty}\Big|\frac{a_{l+1}}{a_l}\Big| = \lim_{l\to\infty}\Big(\frac{4m^2}{q^2}\Big)\frac{(-2+2\nu+l)(\nu+l-\frac{3}{2})}{(l+1)(l+\nu-1)} \times \left(\frac{\ln\Big\{-\frac{q^2}{4m^2}\Big\} - \ln\{-2+2\nu+l+1\} - \ln\{-\nu-l-1+\frac{5}{2}\} - 3\ln\{l+2\} + \ln\{l+\nu\}}{\ln\Big\{-\frac{q^2}{4m^2}\Big\} - \ln\{-2+2\nu+l\} - \ln\{-\nu-l+\frac{5}{2}\} - 3\ln\{l+1\} + \ln\{l+\nu-1\}}\right) = \frac{4m^2}{q^2}\,. \tag{3.59}$$

Therefore, we see that the series representation that we found converges absolutely for $q^2 > 4m^2$, that is, above the threshold for particle–antiparticle production.

3.2.3 Final stages of the quark loop computation and analysis

At this point we have all the necessary tools to compute self–energy and tadpole integrals ((3.22) and (3.24)). Nevertheless, in the quark loop expression there appear more than one hundred different scalar integrals of these two types, hence automation is required. For this we have used a *Mathematica* package called *MBConicHulls*[20] [40], which calls upon functions of another package called *MultivariateResidues* [115] that has to be installed as a dependency. In [40] and [121] the authors describe how the computation of Mellin–Barnes integrals with multivariate residues, which we have just reviewed, can be organized in a very compact algorithm that uses very intuitive geometric concepts and allows to understand the practical implications of the rather abstract results of multivariate complex calculus.

A typical Mellin–Barnes integral representing an scalar triangle loop has 16 different series representations, and each of them contains up to six different subseries. Consequently, the assessment of the convergence regions of the series representations found by the *MBConicHulls* package requires automation as well. We have developed a program that evaluates the asymptotic

[20] This package requires *Mathematica* 12 or a more recent version.

behaviour of a given triple series and finds its region of convergence by comparing it with the behaviour of other series whose convergence conditions are already known. The concept of the program is based on Horn's theorem for the convergence of hypergeometric series of up to three variables [120], which is a rather natural extension of D'Alembert's ratio test to the multivariate case. Let us consider the triple series

$$\sum_{n_1,n_2,n_3}^{\infty} C(n_1,n_2,n_3)x^{n_1}y^{n_2}z^{n_3}\,. \tag{3.60}$$

It is considered hypergeometric as long as the coefficients

$$\begin{aligned} f(n_1,n_2,n_3) &= C(n_1+1,n_2,n_3)/C(n_1,n_2,n_3)\\ g(n_1,n_2,n_3) &= C(n_1,n_2+1,n_3)/C(n_1,n_2,n_3)\\ h(n_1,n_2,n_3) &= C(n_1,n_2,n_3+1)/C(n_1,n_2,n_3) \end{aligned} \tag{3.61}$$

are rational functions of n_1, n_2 and n_3. If so, then the convergence region of the integral is given by the intersection of the following five sets:

$$\begin{aligned} C &= \Big\{(|x|,|y|,|z|) \;\Big|\; |x|<\rho(1,0,0)\wedge|y|<\sigma(1,0,0)\wedge|z|<\tau(1,0,0)\Big\}\\ X &= \Big\{(|x|,|y|,|z|) \;\Big|\; \forall(n_2,n_3)\in\mathbb{R}_+^2 \,:\, |x|<\rho(0,n_2,n_3)\vee|y|<\sigma(0,n_2,n_3)\vee|z|<\tau(0,n_2,n_3)\Big\}\\ Y &= \Big\{(|x|,|y|,|z|) \;\Big|\; \forall(n_1,n_3)\in\mathbb{R}_+^2 \,:\, |x|<\rho(n_1,0,n_3)\vee|y|<\sigma(n_1,0,n_3)\vee|z|<\tau(n_1,0,n_3)\Big\}\\ Z &= \Big\{(|x|,|y|,|z|) \;\Big|\; \forall(n_1,n_2)\in\mathbb{R}_+^2 \,:\, |x|<\rho(n_1,n_2,0)\vee|y|<\sigma(n_1,n_2,0)\vee|z|<\tau(n_1,n_2,0)\Big\}\\ E &= \Big\{(|x|,|y|,|z|) \;\Big|\; \forall(n_1,n_2,n_3)\in\mathbb{R}_+^3 \,:\, |x|<\rho(n_1,n_2,n_3)\vee|y|<\sigma(n_1,n_2,n_3)\\ &\qquad\qquad \vee|z|<\tau(n_1,n_2,n_3)\Big\}\,, \end{aligned} \tag{3.62}$$

where $\mathbb{R}_+$ represents the set of positive reals and ρ, σ and τ capture the asymptotic behaviour of f, g and h:

$$\begin{aligned} \rho(n_1,n_2,n_3) &= \Big|\lim_{u\to\infty} f(un_1,un_2,un_3)\Big|^{-1}\\ \sigma(n_1,n_2,n_3) &= \Big|\lim_{u\to\infty} g(un_1,un_2,un_3)\Big|^{-1}\\ \tau(n_1,n_2,n_3) &= \Big|\lim_{u\to\infty} h(un_1,un_2,un_3)\Big|^{-1}\,. \end{aligned} \tag{3.63}$$

The program that we have developed computes ρ, σ and τ for each subseries that form a series representation of a Mellin–Barnes integral and identifies its region of convergence by comparing them to the ρ, σ and τ of series whose convergence conditions are known. Care had to be taken for the program not be misled by redefinitions of the arguments of the series or the presence of logarithms. We have also taken into account the result found in [121] which extends the use of Horn's theorem to series that are not hypergeometric by the definition given previously, because they include polygamma functions. Finally, the program chooses the appropriate series representation according to the kinematic regime indicated beforehand.

The convergence region of some triple series representations of triangle loops in shifted dimensions could not be found in the mathematical literature due to them being quite non–standard. In such cases the approach presented in [123], alternate to [42], was followed. That paper refers

to scalar triangle loop integrals in arbitrary space–time dimension with three different masses, but unit propagator powers:

$$J_3^{(d)} = \int \frac{d^d p}{(2\pi)^d} \frac{1}{(p+p_1+p_2)^2 - m_3^2} \frac{1}{(p+p_1)^2 - m_2^2} \frac{1}{p^2 - m_1^2} \,. \tag{3.64}$$

The first step of the computation is to use Feynman parameters in the standard way, as we described for the self–energy loop when introducing formula (3.23). An appropriate change of variables renders one of the two Feynman parameter integrals straightforward to perform. After using (3.18) on the integrand, the remaining Feynman parameter integral has the one–variable Gaussian hypergeometric function ${}_2F_1$ as its solution. Finally, the Mellin–Barnes integral of ${}_2F_1$ yields the double Appell hypergeometric function F_1. The key point of this result is that F_1 belongs to the well–known family of Gaussian hypergeometric functions and as such its convergence and analytical continuation properties are well–known [119, 124]. We quote here the result for arbitrary space–time dimension d valid in the high energy regime:

$$J_3^{(d)} = \frac{i\Gamma\left(\frac{4-d}{2}\right)}{(4\pi)^{\frac{d}{2}} \lambda_-^{1/2}(p_1^2, p_2^2, p_3^2)} \left\{ J_{123}^{(d)} - (M_3 - i\epsilon)^{\frac{d-4}{2}} J_{123}^{(d=4)} + (1,2,3) \leftrightarrow (2,3,1) + (1,2,3) \leftrightarrow (3,1,2) \right\} , \tag{3.65}$$

where $p_3 = -p_1 - p_2$ and:

$$\begin{aligned} J_{ijk}^{(d)} = {} & \frac{x_{ij}}{(x_k - x_{ij})} (M_{ij} - i\epsilon)^{\frac{d-4}{2}} F_1\left(\frac{1}{2}; 1, \frac{4-d}{2}; \frac{3}{2}; \frac{x_{ij}^2}{(x_k - x_{ij})^2}, -\frac{p_i^2 x_{ij}^2}{M_{ij} - i\epsilon}\right) \\ & - \frac{x_{ij}^2}{2(x_k - x_{ij})^2} (M_{ij} - i\epsilon)^{\frac{d-4}{2}} F_1\left(1; 1, \frac{4-d}{2}; 2; \frac{x_{ij}^2}{(x_k - x_{ij})^2}, -\frac{p_i^2 x_{ij}^2}{M_{ij} - i\epsilon}\right) \\ & - \left\{ x_{ij} \to 1 - x_{ij} \;\; ; \;\; x_k \to 1 - x_k \right\} \end{aligned} \tag{3.66}$$

$$\lambda_-(x,y,z) = x^2 + y^2 + z^2 - 2xy - 2xz - 2yz \qquad\qquad x_{ij} = \frac{p_i^2 + m_i^2 - m_j^2}{2p_i^2} \,. \tag{3.67}$$

M_3 and M_{ij} for $i,j = 1,2,3$ are defined in terms of Cayley and Gramm determinants for the triangle loop. Their definition and properties are given in appendix C. The definition of x_k is rather lengthy and not very relevant, so it is written in the appendix as well. The Appell function F_1 has the convergent series representation:

$$F_1(a; b, b'; c; x, y) = \sum_{n_1, n_2 = 0} \frac{(a)_{n_1+n_2} (b)_{n_1} (b')_{n_2}}{(c)_{n_1+n_2}} \frac{x^{n_1}}{n_1!} \frac{y^{n_2}}{n_2!} \tag{3.68}$$

for $|x| < 1$ and $|y| < 1$. In the high energy regime we have $\left|\frac{x_{ij}^2}{(x_k - x_{ij})^2}\right| = \left|\frac{m_i^2 - M_{ij}}{M_3 - M_{ij}}\right| < 1$ and $\left|\frac{p_i^2 x_{ij}^2}{M_{ij}}\right| = \left|1 - \frac{m_i^2}{M_{ij}}\right| < 1$, therefore this representation is valid for our quark loop computation. From this result, triangle loops with arbitrary propagator powers can be computed from $J_3^{(d)}$ via derivatives with respect to the masses:

$$I^{(N)}(d; \nu_1, ..., \nu_N) = \prod_i \left(\frac{1}{\Gamma(\nu_i)} \left(\frac{\partial}{\partial m_i^2} \right)^{\nu_i - 1} \right) J_3^{(d)} \Bigg|_{m_i = m} \,. \tag{3.69}$$

We are interested in integrals with $d \in \{4, 6, 8, 10, 12\}$. It is not difficult to note that the gamma function pole at $d = 4$ in $J_3^{(d)}$ is of course a spurious singularity. On the other hand for $d \geq 6$ there are actual ultraviolet singularities, as can be checked from their expressions in appendix C. Nevertheless, it is possible to check in a lengthy but straightforward way that singular terms vanish and dependence on the renormalization scale disappears when propagator powers get high enough in $I^{(N)}$. This is relevant for us, because of the loop integrals we find are ultraviolet finite.

After the Mellin–Barnes representation of the scalar integrals with shifted dimensions are computed by the methods described previously[21], the last step is the computation of the integrals over $|Q_1|$, $|Q_2|$ and τ that remain in the master formula.

First, let us remember that even though we followed a kinematic–singularity–free tensor loop decomposition, there are spurious kinematic singularities which have been introduced by the negative powers of λ that are present in the projectors with which one extracts the HLbL form factors from the quark loop. As discussed at the beginning of this chapter, these singularities cancel explicitly for contributions of all Wilson coefficients, except the quark loop. This is expected, since the spurious nature of the singularities implies that they must disappear in tree–level contributions. For self–energy and triangle loop integrals in shifted dimensions we do not arrive in general to closed analytical expression, but rather a series representation. Therefore, spurious kinematic zeros inside these terms do not necessarily show explicitly to cancel singularities. This introduces numerical instability in the region of the master formula's angular integral when $\tau \equiv \hat{Q}_1 \cdot \hat{Q}_2 \to \pm 1$, because that is when λ is equal to or approaches zero:

$$\lambda_+(q_1^2, q_2^2, q_3^2) = (q_3^2 - q_1^2 - q_2^2)^2 - 4q_1^2 q_2^2 = 4Q_1^2 Q_2^2 \Big(\tau^2 - 1\Big) \,, \tag{3.70}$$

where we have switched back to the euclidean versions of the virtual photon momenta $q_i \cdot q_j \to -Q_i \cdot Q_j$. When computing the contribution to the master formula's integral from these regions, it is convenient to expand the integral's series representations around $\tau = \pm 1$ to avoid numerical instability. The fact that we traced the $\lambda_+ = 0$ singularity to a value in τ has useful practical implications. Indeed self–energy and triangle scalar integrals are computed in a single and triple series representation, respectively, where the expansion variable are the differences between external momenta. The external momenta that can appear in quark loop scalar integrals are Q_1 and Q_3 or Q_2 and Q_3, depending on the permutation one is considering. However, only Q_3 depends on τ. Therefore any integral that does not depend on Q_3 does not require special treatments.

To perform the integrals on the euclidean norm of the virtual photons' momenta, it is important to keep in mind that the quark loop was obtained from an OPE in perturbative QCD. Therefore its range of validity starts above Λ_{QCD}, the perturbative threshold. Λ_{QCD} is usually taken to be close to the proton's mass, which is about ~ 940 MeV. In principle, this means that one can compute the quark loop contribution to a_μ starting from $|Q_1| = |Q_2| = 1$ GeV $\equiv Q_{min}$, however, taking into account that the OPE of the previous chapter introduces an implicit counting parameter $\Lambda_{QCD}/|Q|$, one would expect the error coming from neglected higher non-perturbative effects to be large right above Λ_{QCD}. The relation between the size of such error and the values of Q_{min} was studied in [35]. To that end, they computed the quark loop contribution as a function of Q_{min} in the interval $[1\text{ GeV}, 4\text{ GeV}]$ and the contributions from the non–perturbative condensates of the previous chapter were considered as well. Their results showed that massless quark loop contributions fall like $1/Q_{min}^2$ and, in general, contributions from elements of the OPE with dimension d behave like $1/Q_{min}^d$. This is expected from the asymptotic behaviour of the integral

[21] The script that performs the steps that we have described throughout this chapter can be found in this repository.

kernels T_i of the master formula (1.69), which for $|Q_i| \to \infty$ behave like m_μ^2/Q_i^2, except for T_1, which falls like m_μ^4/Q_i^4. Since mass effects become small for large momenta $|Q_i|$ and the massless quark loop contribution does not introduce an energy scale, then it must fall like $1/Q_{min}$. Mass corrections to the quark loop are suppressed by m_f^2/Q_i^2 with respect to the massless part. In addition, contributions from other OPE elements $S_{i,\mu\nu}$ of dimension d are comparatively suppressed as well by a factor $(\Lambda_{QCD}/|Q_i|)^{d-2}$, thus the asymptotic behaviour of their contributions is explained.[22]

For the value of the quarks' masses m_f and the renormalization scale μ we followed the simplified choice of [35], which was:[23]

$$m_u = m_d = 5\,\text{MeV} \qquad m_s = 100\,\text{MeV} \qquad \mu = Q_{min}\,. \tag{3.71}$$

Note that no running of the masses is performed. This is justified by the very small size of mass corrections to the quark loop. With this values we computed the quark loop contribution for $Q_{min} = 1$ or 2 GeV. As discussed previously in this section, we obtained a systematic expansion of the quark loop in terms of the quarks masses. This allowed us to study the mass corrections to the massless quark loop contribution and found them to be very small, even at m_f^2 order. Furthermore, we found the result for $Q_{min} = 1$ GeV to be about four times bigger than the $Q_{min} = 2$ GeV case.

In [35] the massless quark loop was found to be the largest contribution to a_μ by two orders of magnitude and the leading mass corrections were even smaller than the non–perturbative di–quark magnetic susceptibility ($S_{2,\mu\nu}$ in the OPE) by two further orders of magnitude. The complete results of [35] are summarized in table 3.1, where one can see that the dominance of quark loop contributions with respect to the other. Note however that those results do not show the complete picture, because the quark loop contribution, which is the leading perturbative contribution to a_μ^{HLbL}, does not really involve strong interactions and hence it does not depend on α_s. Of course, their higher order corrections do. It could be therefore possible that the perturbative expansion in $\alpha_s(\mu)$ does no fall fast enough for higher orders for the renormalization scale used. Since μ is constrained by the need to avoid large logarithms, then that would mean that the OPE framework of chapter 2 suffers from the same issues that it was meant to avoid in the first place. Nevertheless, in [36] the next–to–leading–order (NLO) gluonic correction to the massless part of the quark loop was computed (see figure 3.4) taking into account the running of $\alpha_s(\mu)$ and its contribution to a_μ^{HLbL} was found to be about 10 % of the leading order and negative.

[22] Asymptotic freedom also plays a role in this result. As we mentioned in the previous chapter, the correction to the naive dimensional counting of the OPE is given by the anomalous dimension of each OPE element, but QCD's asymptotic freedom ensures that, at high enough energy, corrections are small.

[23] In [6], constituent masses are used, because they are more appropriate when comparing with low–energy results.

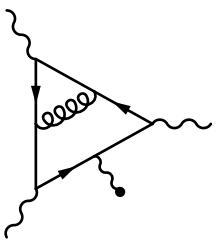

FIGURE 3.4: Representative diagram of the NLO contribution to the Wilson coefficient of $S_{1,\mu\nu}$ in the OPE of $\Pi^{\mu_1\mu_2\mu_3}$. The black dot represents creation/annihilation of a line by the background fields in the vacuum. This diagram represents the first QCD correction to the quark loop.

OPE element	Magnetic susceptibility	Mass order	Contribution to a_μ from Q_{min}	
			1 GeV	2 GeV
$S_{1,\mu\nu}$	1	m^0	$1.73 \cdot 10^{-10}$	$4.35 \cdot 10^{-11}$
		m^2	$-5.7 \cdot 10^{-14}$	$-3.6 \cdot 10^{-15}$
$S_{2,\mu\nu}$	$X_2 = -4 \cdot 10^{-2}$ GeV	m^1	$-1.2 \cdot 10^{-12}$	$-7.3 \cdot 10^{-14}$
		m^3	$6.4 \cdot 10^{-15}$	$1.0 \cdot 10^{-16}$
$S_{3,\mu\nu}$	$X_3 = 3.51 \cdot 10^{-3}$ GeV	m^0	$-3.0 \cdot 10^{-14}$	$-4.7 \cdot 10^{-16}$
$S_{4,\mu\nu}$	$X_4 = 3.51 \cdot 10^{-3}$ GeV		$3.3 \cdot 10^{-14}$	$5.3 \cdot 10^{-16}$
$S_{5,\mu\nu}$	$X_5 = -1.56 \cdot 10^{-2}$ GeV		$-1.8 \cdot 10^{-13}$	$-2.8 \cdot 10^{-15}$
$S_{6,\mu\nu}$	$X_6 = 2 \cdot 10^{-2}$ GeV		$1.3 \cdot 10^{-13}$	$2.0 \cdot 10^{-15}$
$S_{7,\mu\nu}$	$X_7 = 3.33 \cdot 10^{-3}$ GeV		$9.2 \cdot 10^{-13}$	$1.5 \cdot 10^{-14}$
$S_{8,1,\mu\nu}$	$X_{8,1} = -1.44 \cdot 10^{-4}$ GeV		$3.0 \cdot 10^{-13}$	$4.7 \cdot 10^{-15}$
$S_{8,2,\mu\nu}$	$X_{8,2} = -1.44 \cdot 10^{-4}$ GeV		$-1.3 \cdot 10^{-13}$	$-2.0 \cdot 10^{-15}$

TABLE 3.1: Results published in [35] about the contribution of the quark loop and the rest of OPE elements $S_{i,\mu\nu}$ to a_μ as function of the cutoff Q_{min} from which the master formula integral is performed.

At the beginning of the previous chapter we mentioned the different roles that SDC play in the computation of a_μ. Since that was the ultimate purpose of the computation, let us discuss such uses in more detail. The dispersive framework and hadronic models are useful to understand and compute the low energy behaviour of the HLbL tensor $\Pi^{\mu_1\mu_2\mu_3\mu_4}$. However, as one tries to use such tools for higher energies, more degrees of freedom become excited and start to give relevant contributions. In dispersive language this means that at higher energies additional heavier intermediate states with possibly multiple particles are "unlocked" and their contributions have to be taken into account. From a practical perspective, multiple particle states add to the already complex nature of dispersive computations while, from the experimental side, heavier intermediate states are harder to produce and study, and therefore there is a lack of experimental data to feed dispersive integrals with the necessary form factors. Even light intermediate states whose form factors are very well–known at low energy may not have enough data at higher energies. For HLbL, these issues start to show at 1 GeV and become ultimately unbearable at 2 GeV, with a mixed region in between. As usual, a "change of variables" into the relevant degrees of freedom at the new kinematic regime of interest solves many of these issues. This is the underlying motivation of the OPE that we presented in chapter 2. Thus one can identify two uses of high energy frameworks in the computation of a_μ^{HLbL}. First, one can obtain the high–energy asymptotic behaviour of a Green function to learn the asymptotic behaviour of an hadronic form factor, in order to fill the gap of missing or scarce experimental data in the high energy parts of dispersive integrals or the master formula. One can similarly use this approach directly to the HLbL tensor in the high energy regions of the master integral, which is the purpose of the quark loop computation that we did. However, in that case the interplay between low and high energy contributions is not clear cut, because low energy contributions are computed for the full $|Q_1|$ and $|Q_2|$ intervals of the master integral, not only up to 1 or 2 GeV. Thus one sees that some overlapping of contributions is present and there is a risk of double counting. Therefore, for the high energy contributions to be successfully accounted for there remain two questions to be answered [6].

First of all, how well does the new framework really captures the behaviour of $\Pi\mu_1\mu_2\mu_3\mu_4$ at high energy? At first sight, the OPE framework offers a hierarchy such that as energy goes higher, complexity decreases, which solves the practical issue of dispersive computations. Nevertheless, as discussed in the previous chapter, it was necessary to take special care when choosing the background OPE framework, because the standard approach was not really well suited

to account for the soft external photon that defines the magnetic moment of a particle. Moreover, we mentioned how two–loop computations were done in [36] to check that corrections to the leading order were not too big. This analysis elucidates that the background OPE is a suitable framework to understand the high energy behaviour of $\Pi^{\mu_1\mu_2\mu_3\mu_4}$.

Another issue to be clarified after the high energy contribution of $\Pi^{\mu_1\mu_2\mu_3\mu_4}$ to a_μ has been computed is: how much of this has already been taken into account by low–energy computations? This is in fact the key point for the study of asymptotic contributions. The idea is to compare how much the low–energy contributions' asymptotic behaviour resembles the results of the high energy framework. It was argued in [29, 30] that it is impossible to fulfill all QCD SDC with a finite number of resonances. To obtain an estimate of the missing high energy contributions caused by such mismatch, one can use a top–down approach: to constrain hadronic contributions to fulfill SDC and study how much the result differs from when they are constrained by experimental data, that is, by their low–energy behaviour. For example, the mixed virtualities regime $Q_1 \sim Q_2 \equiv Q \gg Q_3 \gg \Lambda_{QCD}$ of the HLbL tensor, first studied in [125], imposes the following constraint:

$$\lim_{Q,Q_3\to\infty} Q^2 Q_3^2 \overline{\Pi}_1 = -\frac{2}{3\pi^2} \tag{3.72}$$

and a similar one for crossed condition for $\overline{\Pi}_2$. In addition, as we already argued, the symmetric regime $Q_1 \sim Q_2 \sim Q_3 \equiv Q \gg \Lambda_{QCD}$, via the massless quark loop, imposes the following asymptotic behaviour:

$$\lim_{Q\to\infty} Q^4 \overline{\Pi}_1 = -\frac{4}{9\pi^2}\,. \tag{3.73}$$

The proposals to ensure that the transition form factors match the mixed virtualities behaviour have ranged from ignoring their momentum dependence [125] to summing an infinite tower of axial and vector resonances in holographic QCD [126, 127]. In [31, 32], a hybrid approach is followed: pseudo scalar pole contributions are computed in a large–N_c Regge model such that they satisfy SDC, but those results are only used in the low–energy region of integration of the master formula. The integral over the remaining part is computed with the quark loop expression, taking advantage of the asymptotic behaviour of the massless quark loop contribution to $\overline{\Pi}_1$, which fulfills the mixed–virtualities SDC as well. This reduces model–dependence with respect to the first two approaches mentioned and allows to clearly separate the effect of SDC on low– and high–energy contributions to lower double counting risks. Nevertheless, such risks still remain with respect to axial vector contributions, lies in a transition region between the perturbative and non–perturbative domain of QCD and is still a significant source of uncertainty for a_μ^{HLbL}. Compared to the data–driven computation, there is an increase in the contribution from pseudo scalar poles:

$$\Delta a_\mu^{LSDC} = \Big[8.7(5.5)_{\text{PS–poles}} + 4.6(9)_{\text{pQCD}}\Big] \times 10^{-11} = 13(6) \times 10^{-11}\,, \tag{3.74}$$

where the superindex *LSDC* illustrates the fact that we are only considering the constraints regarding the asymptotic behaviour of the "longitudinal" part of the HLbL tensor in the mixed virtualities regime. The "transversal" form factors are $\overline{\Pi}_{3-12}$. They are related to the contribution from axial vectors and obey a different SDC in the mixed virtualities regime. This result is in very good agreement with the holographic QCD one [126]. In contrast, it hints at an overestimation from the approach proposed in [125]. When Δa_μ^{LSDC} is computed fully with the large–N_c Regge model, the result is very close to (3.74). In the end, the net increase of the HLbL contribution due to SDC is estimated to be $\Delta a_\mu^{SDC} = 15(10) \cdot 10^{-11}$ [6]. A part of the uncertainty of (3.74) is estimated by varying the matching scale between the Regge model and the quark loop, and

is then added to each element's model or theoretical uncertainty. Therefore higher order corrections to the quark loop can decrease the uncertainty of Δa_μ^{LSDC}. In [33], the SDC contribution was reassessed taking into consideration the perturbative corrections to the quark loop and the result was:

$$\Delta a_\mu^{LSDC} = \Big[8.7(5.3)_{\text{PS–poles}} + 4.2(1)_{\text{pQCD}}\Big] \times 10^{-11} = 13(5) \times 10^{-11} \,, \tag{3.75}$$

which reduces the uncertainty of the previous result. It is worth mentioning that the negative $O(\alpha_s)$ correction to the massless quark loop improves the agreement between the Regge sum of pseudoscalars and the perturbative result. However, further study regarding the matching procedure is still needed.

In recent months two works [128, 129] were published regarding the extension of the background OPE framework to the mixed virtualities regimes of the HLbL tensor. To illustrate the broader range of use of the background field framework that we used in this work, we briefly review their results from chapter 2's perspective. The analogue of $\Pi^{\mu_1\mu_2\mu_3}$ is now:

$$\begin{aligned}\Pi^{\mu_1\mu_2} &= \frac{i}{e^2}\int\frac{d^4q_4}{(2\pi)^4}\int d^4x\int d^4y\, e^{-i(q_1x+q_2y)}\langle 0|T\,J^{\mu_1}(x)J^{\mu_2}(y)|\gamma^*(q_3)\gamma(q_4)\rangle \\ &= -\epsilon_{\mu_3}(q_3)\epsilon_{\mu_4}(q_4)\Pi^{\mu_1\mu_2\mu_3\mu_4}(q_1,q_2,q_3)\,.\end{aligned} \tag{3.76}$$

When the OPE is performed up to operators with mass dimension $D=4$, the quoted result is:

$$\begin{aligned}\Pi^{\mu_1\mu_2} =& -\frac{1}{4}\langle F_{\nu_3\mu_3}F_{\nu_4\mu_4}\rangle\frac{\partial}{\partial q_{3\nu_3}}\frac{\partial}{\partial q_{4\nu_4}}\Pi^{\mu_1\mu_2\mu_3\mu_4}_{\text{quark loop}}\Big|_{q_3=q_4=0} \\ &- \frac{e_f^2}{e^2}\langle\overline{\psi}(0)\Big(\gamma^{\mu_1}S^0(-\hat{q})\gamma^{\mu_2}-\gamma^{\mu_2}S^0(-\hat{q})\gamma^{\mu_1}\Big)\psi(0)\rangle \\ &- \frac{ie_f^2}{e^2\hat{q}^2}\Big(g^{\mu_1\delta}g^{\mu_2}_\beta+g^{\mu_2\delta}g^{\mu_1}_\beta-g^{\mu_1\mu_2}g^\delta_\beta\Big)\Big(g_{\alpha\delta}-2\frac{\hat{q}_\alpha\hat{q}_\delta}{\hat{q}^2}\Big)\langle\overline{\psi}(0)\Big[\overrightarrow{D}^\alpha-\overleftarrow{D}^\alpha\Big]\gamma^\beta\psi(0)\rangle\,,\end{aligned} \tag{3.77}$$

where $\hat{q}\equiv(q_1-q_2)/2$ and the matrix element $\langle ...\rangle$ now includes the virtual photon $\gamma^*(q_3)$ and the real soft one $\gamma(q_4)$. The term $\Pi_{\text{quark loop}}$ is proportional to the quark loop amplitude we found in chapter 2. The origin of the first term is quite clear: it comes from matrix elements with four contracted quark fluctuations in which the resulting two fermion propagators have a total of two soft photon insertions between the two (see figure 3.5), hence the two derivatives and field strength tensors. The second and third terms come instead from terms with two background quark fields and two fluctuations (see figure 3.6), where the background fields are Taylor expanded as usual up to order $O(x_1-x_2)$. The appearance of $\hat{q}$ comes from the fact that only x_1-x_2 is close to zero in the mixed virtualities regimes, in contrast the symmetric regime, where the three currents' coordinates are close. It is worth mentioning that in this case quark operators start at dimension $D=3$ and therefore they are, in principle, the leading term of the OPE instead of the perturbative quark loop.

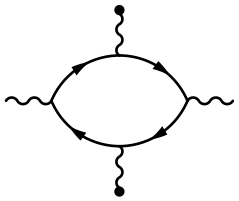

FIGURE 3.5: Representative diagram of the fully perturbative contribution to the OPE of $\Pi^{\mu_1\mu_2}$ in the mixed virtualities regime. A black dot represents creation/annihilation of a line by the background fields in the vacuum. Depending on the value of q_3, one of these photons may be interact perturbatively with vacuum.

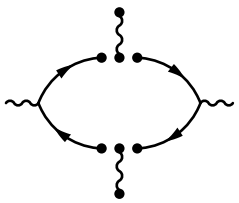

FIGURE 3.6: Representative diagram of the one–cut–quark contributions to the OPE of $\Pi^{\mu_1\mu_2}$ in the mixed virtualities regime. A black dot represents creation/annihilation of a line by the background fields in the vacuum. Depending on the value of q_3, one of these photons may be interact perturbatively with vacuum.

Conclusions

In this thesis we have reviewed the basic framework for the computation of the HLbL contribution to the anomalous magnetic moment of the muon, a_μ^{HLbL}. We have discussed as well relatively recent developments in the kinematic-singularity–free decomposition of the HLbL tensor, $\Pi^{\mu_1\mu_2\mu_3\mu_4}$, that have allowed for the dispersive computation of the low–energy contributions to a_μ^{HLbL}, thanks to the Mandelstam representation admitted by its corresponding scalar form factors. These dispersive computations in the Mandelstam representation have enabled unambiguous computations of hadronic contributions, which has improved the uncertainty estimation with respect to hadronic models. We have also discussed the current consensus of low–energy contributions to a_μ^{HLbL} and the corresponding role of SDC as a means of uncertainty assessment and high energy contribution computation.

In the high energy regime, the HLbL tensor can be decomposed in an OPE, but the external soft photon has to be regarded as a background field in order to avoid the breaking of the perturbative expansion of QCD at low energies and the introduction of infrared–divergent Wilson coefficients. We have studied the background field method, which has allowed us to expand the compute the background OPE found in the literature to include quark and gluon background fields as well. The renormalization procedure of the OPE elements in our framework seems to include operator–mixing in a more natural way than the one found in the literature. The same applies for the derivation of the Wilson coefficients, in which perturbative and non–perturbative contributions are systematically separated and do not require much decision–making from the user. From the OPE of $\Pi^{\mu_1\mu_2\mu_3\mu_4}$, we found that quark loop is leading contribution after infrared divergent logarithms have been subtracted by renormalization, in agreement with the literature.

Finally, we accomplished the computation of the quark loop by an alternative approach. In contrast with previous computations, we did not project the form factors of the HLbL tensor out of the quark loop amplitude, but we rather harnessed its full tensor structure to check the generality of the basis elements of the kinematic–singularity–free tensor decomposition of the HLbL tensor. We concluded that these elements do span the tensor structures of the quark amplitude, thus obtaining an explicit check that we have not found in the literature. To keep the full tensor structure of the quark amplitude we had to deal tensor loop integrals ranging from one to three points and zero to five tensor rank. To avoid introducing further spurious kinematic singularities, we have used a special tensor loop decomposition algorithm which introduces scalar integrals with shifted dimensions. We persisted on keeping the full mass dependence of the amplitude and to that end we used a Mellin–Barnes representation of the scalar integrals in shifted dimensions. This allowed us to obtain a complete series representation of the required integrals that contains all quark mass effects at any order in the high energy regime. To provide a mathematical foundation for this procedure, we wrote a detailed and formal presentation of the fundamentals of single and multiple complex variable residues computation and described the step–by–step. The aforementioned computations were implemented by a *Mathematica* script that used *FeynCalc*, a state–of–the–art high energy physics package. To highlight the importance of the quark loop computation result, we described the use of the quark loop computation as a SDC to the low–energy contributions to a_μ^{HLbL} and its effects in the critical task of lowering the

uncertainty of the anomalous magnetic moment of the muon value in the Standard Model.

There remain several outlooks of future work based on this thesis. In chapter 3 we already mentioned that the $O(\alpha_s)$ correction to the massless quark loop has been performed. In light of the small size of mass corrections, it may not be relevant at the moment to consider mass corrections to such result. Instead, one could perform a more detailed study of non–perturbative contributions to the OPE of $\Pi^{\mu_1\mu_2\mu_3\mu_4}$ and obtain a more carefully obtained value for the magnetic susceptibilities X_i, for which precise values cannot be found currently, only rather crude order–of–magnitude estimations. These power corrections have been proved to be at most a few percent of the massless quark loop contribution, but they hold the key to lower the cutoff at which the OPE results can be used for the master formula of a_μ^{HLbL}, which could lower the uncertainty of the SDC contribution, which currently relies heavily in models such as the Regge sum for pseudoscalar poles.

Perhaps the most natural continuation of this work would be the extension of the OPE for the mixed virtualities regime, in contrast of the symmetric one that we have worked on. Such OPE has been very recently carried out, but it is yet to be formulated from the alternative and, in our view, more systematic approach that we have presented in chapter 2. The OPE in such regime is more complex from a conceptual point of view and, therefore, one could expect our approach's advantages to be highlighted in that regime. At the end of chapter 3, we have already given a very brief overview of the the procedure to be followed. From a more practical point of view, an improvement on SDC coming from the mixed virtualities regime can help to lower the uncertainty from the lower–energy contributions to a_μ^{HLbL} or perhaps provide a better estimation of axial vectors contributions, which continue to be a rather large source of uncertainty.

Appendix A

Angular average integrals

First of all let us recall properties of Gegenbauer polynomials that are relevant for us. Their generating function is [61]:

$$\frac{1}{1-2tx+t^2} = \sum_{n=0}^{\infty} t^n C_n(x) \tag{A.1}$$

and they follow a very useful orthogonality relation [62]:

$$\int \frac{d\Omega_4(\hat{Z})}{2\pi^2} C_i(\hat{X}\cdot\hat{Z}) C_j(\hat{Z}\cdot\hat{Y}) = \frac{\delta_{ij}}{i+1} C_i(\hat{X}\cdot\hat{Y}) \,, \tag{A.2}$$

where $\hat{X}$, $\hat{Y}$ and $\hat{Z}$ represent euclidean unit four vectors. By using the generating function and the geometric series it can be proved easily that:

$$C_i(x=1) = i+1 \,, \tag{A.3}$$

and therefore one obtains a normalization identity:

$$\int \frac{d\Omega_4(\hat{Z})}{2\pi^2} C_i(\hat{X}\cdot\hat{Z}) C_j(\hat{Z}\cdot\hat{X}) = \delta_{ij} \,. \tag{A.4}$$

Let us compute each of the integrals (1.64)–(1.68) by using the Gegenbauer polynomials method. Here we have the first one:

$$\begin{aligned}
&\int \frac{d\Omega_4(\hat{P})}{2\pi^2} \frac{1}{(P+Q_1)^2+m^2} \frac{1}{(P-Q_2)^2+m^2} = \\
&\int \frac{d\Omega_4(\hat{P})}{2\pi^2} \Big(\frac{t_1}{|P||Q_1|} \sum_i (-t_1)^i C_i(\hat{P}\cdot\hat{Q}_1) \Big) \Big(\frac{t_2}{|P||Q_2|} \sum_j (t_2)^j C_j(\hat{P}\cdot\hat{Q}_2) \Big) = \\
&\frac{t_1 t_2}{P^2|Q_1||Q_2|} \sum_{ij} (-t_1)^i (t_2)^j \int \frac{d\Omega_4(\hat{P})}{2\pi^2} C_i(\hat{P}\cdot\hat{Q}_1) C_j(\hat{P}\cdot\hat{Q}_2) = \\
&\frac{t_1 t_2}{P^2|Q_1||Q_2|} \sum_{ij} (-t_1)^i (t_2)^j \frac{\delta_{ij}}{i+1} C_i(\hat{Q}_1\cdot\hat{Q}_2) = \\
&-\frac{1}{m^2|Q_1||Q_2|} \sum_i (\underbrace{-t_1 t_2}_{z})^{i+1} \frac{1}{i+1} C_i(\hat{Q}_1\cdot\hat{Q}_2) = \\
&\frac{-1}{m^2|Q_1||Q_2|} \int dz' \sum_i z^i C_i(\hat{Q}_1\cdot\hat{Q}_2) = \frac{-1}{m^2|Q_1||Q_2|} \int dz' \frac{1}{z'^2-2z'\tau+1} =
\end{aligned} \tag{A.5}$$

$$\frac{1}{m^2 R_{12}} \arctan\Big(\frac{zx}{1-z\tau}\Big) .$$

Let us go on the second integral:

$$\int \frac{d\Omega_4(\hat{P})}{2\pi^2} \frac{1}{(P+Q_1)^2+m^2} = \int \frac{d\Omega_4(\hat{P})}{2\pi^2} \Big(\frac{t_1}{|P||Q_1|} \sum_i (-t_1)^i C_i(\hat{P}\cdot\hat{Q}_1) \Big) = \frac{t_1}{|P||Q_1|} .$$

Now let us remember the following identity:

$$\begin{aligned} t_i &= \frac{m^2+P^2+Q_i^2 - \sqrt{(m^2+P^2+Q_i^2)^2 - 4P^2Q_i^2}}{2|P||Q_i|} \\ &= \frac{Q_i^2(1-\sigma_i^E)}{2|P||Q_i|} . \end{aligned} \tag{A.6}$$

Coming back to the angular integral we get:

$$\int \frac{d\Omega_4(\hat{P})}{2\pi^2} \frac{1}{(P+Q_1)^2+m^2} = -\frac{(1-\sigma_1^E)}{2m^2} . \tag{A.7}$$

Exactly in the same fashion we get the third angular integral:

$$\int \frac{d\Omega_4(\hat{P})}{2\pi^2} \frac{1}{(P-Q_2)^2+m^2} = -\frac{(1-\sigma_2^E)}{2m^2} . \tag{A.8}$$

As for the fourth angular integral we have:

$$\begin{aligned} &\int \frac{d\Omega_4(\hat{P})}{2\pi^2} \frac{P\cdot Q_2}{(P+Q_1)^2+m^2} = \int \frac{d\Omega_4(\hat{P})}{2\pi^2} |P||Q_2| \hat{P}\cdot\hat{Q}_2 \Big(\frac{t_1}{|P||Q_1|} \sum_i (-t_1)^i C_i(\hat{P}\cdot\hat{Q}_1) \Big) = \\ &|Q_2| \frac{t_1}{|Q_1|} \sum_i (-t_1)^i \int \frac{d\Omega_4(\hat{P})}{2\pi^2} \frac{1}{2} C_1(\hat{P}\cdot\hat{Q}_2) C_i(\hat{P}\cdot\hat{Q}_1) = \\ &|Q_2| \frac{t_1}{|Q_1|} \sum_i (-t_1)^i \frac{1}{2} \frac{\delta_{1i}}{1+1} C_1(\hat{Q}_1\cdot\hat{Q}_2) = |Q_2| \frac{t_1}{|Q_1|} (-t_1) \frac{1}{4} 2\hat{Q}_1\cdot\hat{Q}_2 = \\ &-\frac{t_1 t_1}{Q_1^2} \frac{1}{2} Q_1\cdot Q_2 = -\frac{1}{Q_1^2} \frac{Q_1^2(1-\sigma_1^E)}{2|P||Q_1|} \frac{Q_1^2(1-\sigma_1^E)}{2|P||Q_1|} \frac{1}{2} Q_1\cdot Q_2 = \\ &\frac{(1-\sigma_1^E)}{8m^2} (1-\sigma_1^E) Q_1\cdot Q_2 = \frac{(1-\sigma_1^E)^2}{8m^2} Q_1\cdot Q_2 . \end{aligned}$$

Finally, by changing $Q_1 \to Q_2$ and $Q_2 \to -Q_1$ we obtain the last integral:

$$\int \frac{d\Omega_4(\hat{P})}{2\pi^2} \frac{P\cdot Q_1}{(P-Q_2)^2+m^2} = -\frac{(1-\sigma_2^E)^2}{8m^2} Q_1\cdot Q_2 . \tag{A.9}$$

Appendix B

Derivation of relevant results of chapter 2

B.1 Transformation of gauge fixing terms under background field gauge transformations

Under the transformations proposed in (2.24), the Fadeev–Popov gauge–fixing term $f^a f^a$ is invariant. In order to prove that, in this section we will derive the transformation properties of f^a:

$$\begin{aligned} f^a &= \overline{D}^\mu A'^a_\mu = \partial^\mu A'^a_\mu + g_S f^{abc} a^b_\mu A^{c'\mu} \\ \Longrightarrow \delta f^a &= \partial^\mu \delta A'^a_\mu + g_S f^{abc} a^b_\mu \delta A^{c'\mu} + g_S f^{abc} \delta a^b_\mu A^{c'\mu} \\ &= g_S f^{abc} \partial^\mu A'^b_\mu \epsilon^c + g_S^2 f^{abc} f^{c\bar{b}\bar{c}} a^{b\mu} A'^{\bar{b}}_\mu \epsilon^{\bar{c}} + g_S f^{abc} (\partial^\mu \epsilon^b + g_S f^{b\bar{b}\bar{c}} a^{\bar{b}\mu} \epsilon^{\bar{c}}) A'^c_\mu \\ &= g_S f^{abc} \epsilon^c \partial^\mu A'^b_\mu + g_S^2 f^{abc} f^{c\bar{b}\bar{c}} a^{b\mu} A'^{\bar{b}}_\mu \epsilon^{\bar{c}} + g_S^2 f^{abc} f^{b\bar{b}\bar{c}} a^{\bar{b}\mu} A'^c_\mu \epsilon^{\bar{c}} \\ &= g_S f^{abc} \epsilon^c \partial^\mu A'^b_\mu + g_S^2 \epsilon^{\bar{c}} f^{abc} f^{c\bar{b}\bar{c}} (a^{b\mu} A'^{\bar{b}}_\mu - a^{\bar{b}\mu} A'^b_\mu) \,, \end{aligned}$$

where in the last line we have relabelled some indices. Using the Jacobi identity for the structure constants:

$$f^{abc} f^{c\bar{b}\bar{c}} - f^{\bar{b}bc} f^{ca\bar{c}} - f^{a\bar{b}c} f^{cb\bar{c}} = 0 \,, \tag{B.1}$$

we obtain:

$$\begin{aligned} \delta f^a &= g_S f^{abc} \epsilon^c \partial^\mu A'^b_\mu + g_S^2 \epsilon^{\bar{c}} f^{a[bc} f^{c\bar{b}]\bar{c}} (a^{b\mu} A'^{\bar{b}}_\mu - a^{\bar{b}\mu} A'^b_\mu) \\ &= g_S f^{abc} \epsilon^c \partial^\mu A'^b_\mu + \frac{1}{2} g_S^2 \epsilon^{\bar{c}} f^{\bar{b}bc} f^{ca\bar{c}} (a^{b\mu} A'^{\bar{b}}_\mu - a^{\bar{b}\mu} A'^b_\mu) \\ &= g_S f^{abc} \epsilon^c \partial^\mu A'^b_\mu + g_S^2 \epsilon^{\bar{c}} f^{\bar{b}bc} f^{ca\bar{c}} a^{b\mu} A'^{\bar{b}}_\mu \\ &= g_S f^{abc} \epsilon^c (\partial^\mu A'^b_\mu + g_S f^{b\bar{c}\bar{b}} a^{\bar{c}\mu} A'^{\bar{b}}_\mu) \\ &= g_S f^{abc} \epsilon^c \overline{D} A'^b_\mu \,. \end{aligned} \tag{B.2}$$

B.2 Gluon free propagator with a background field

With respect to the gluon, the quadratic kernel of the action for (2.35) yields the following definition for the free propagator $D^{bc}_{F\mu\nu}$ in the vacuum with background fields:

$$\begin{aligned}
&\left(-g_S f^{a\mu\nu'} f^{abc'} + g^{\mu\nu'} (\overline{D}^{\alpha}\overline{D}_{\alpha})^{bc'} - ([\overline{D}^{\nu'}, \overline{D}^{\mu}])^{bc'} \right) D^{c'c}_{F\nu'\nu}(x,y) = \delta^{bc} g_{\mu\nu} \delta^4(x-y) \,, \\
&\left(-2g_S f^{a\mu\nu'} f^{abc'} + g^{\mu\nu'} (\overline{D}^{\alpha}\overline{D}_{\alpha})^{bc'} \right) D^{c'c}_{F\nu'\nu}(x,y) = i\delta^{bc} g_{\mu\nu} \delta^4(x-y) \,.
\end{aligned} \tag{B.3}$$

Following [130] it is possible to invert this equation by taking into account that the gauge covariant derivative is the coordinate space representation of the total momentum operator of the system, which we represent as $\hat{P}^{\alpha} \equiv \hat{p}_{\alpha} + t^a \hat{a}^a_{\alpha} \doteq i\overline{D}_{\alpha}$:

$$\langle x| \left(-2g_S \hat{f}^{\mu\nu'} - g^{\mu\nu'} \hat{P}^{\alpha} \hat{P}_{\alpha} \right) D^{c'c}_{F\nu'\nu} |y\rangle = i\delta^{bc} g_{\mu\nu} \langle x|y\rangle \,, \tag{B.4}$$

$$\begin{aligned}
\implies D_{F,\mu\nu}(q) &\equiv \int d^4x \, e^{iqx} D_{F,\mu\nu}(x,0) = \int d^4x \, e^{iqx} \langle x| D_{F,\mu\nu} |0\rangle \\
&= \int d^4x \, e^{ipx} \langle x| \frac{i}{-2g_S \hat{f}^{\mu\nu} - g^{\mu\nu} \hat{P}^{\alpha} \hat{P}_{\alpha}} |0\rangle \\
&= \int d^4x \langle x| \frac{i}{-2g_S \hat{f}^{\mu\nu} - g^{\mu\nu} \{\hat{P}^{\alpha} + q^{\alpha}\} \{\hat{P}_{\alpha} + q_{\alpha}\}} |0\rangle \,,
\end{aligned}$$

where we have defined $f^{\mu\nu} \equiv f^{abc} f^{a\mu\nu}$ and also suppressed color indices to shorten expressions. Note that the background field strength operator is not affected by the momentum translation operator since it is a function of the coordinates. To invert the operator it is possible to expand it in powers of $1/p^2$ and g_S:

$$\begin{aligned}
&\frac{1}{-2g_S \hat{f}^{\mu\nu} - g^{\mu\nu} \{\hat{P}^{\alpha} + q^{\alpha}\} \{\hat{P}_{\alpha} + q_{\alpha}\}} = \\
&\frac{-1}{q^2} \frac{1}{g^{\mu\nu'} \{g_{\nu'}{}^{\nu} + g_{\nu'}{}^{\nu} \left(\frac{\hat{P}^2}{q^2} + 2\frac{\hat{P}^{\alpha} q_{\alpha}}{q^2} \right) + 2g_S \frac{\hat{f}_{\nu'}{}^{\nu}}{q^2}\}} = \\
&\frac{-1}{q^2} \left(g_{\mu\nu} + \sum_{n=1} (-1)^n \left\{ g_{\mu\nu} \left(\frac{\hat{P}^2}{q^2} + 2\frac{\hat{P}^{\alpha} q_{\alpha}}{q^2} \right) + 2g_S \frac{\hat{f}_{\mu\nu}}{q^2} \right\}^n \right) \,,
\end{aligned} \tag{B.5}$$

where the power of a tensor is defined in the sense of matrix products. Since the OPE that we are interested in contains operators of up to dimension six, then in principle the expansion of the gluon propagator would be relevant up to $O(1/q^8)$. However, the gluon propagator only receives power corrections from the gluon background and gluon operators in the OPE of $\Pi^{\mu_1\mu_2\mu_3}$ are of dimension 2, 3 and 4, then an expansion to $O(1/q^6)$ is enough. The relevant terms of such expansion are:

$$
\begin{aligned}
&\frac{1}{-2g_S\hat{f}^{\mu\nu} - g^{\mu\nu}\{\hat{P}^\alpha + q^\alpha\}\{\hat{P}_\alpha + q_\alpha\}} = \\
&\frac{-1}{q^2}\Bigg(g_{\mu\nu} - \Big\{\frac{g_{\mu\nu}}{q^2}\Big(\hat{P}^2 + 2\hat{P}\cdot q\Big) + 2g_S\frac{\hat{f}_{\mu\nu}}{q^2}\Big\} + \Big\{\frac{g_{\mu\nu}}{q^4}\Big(\hat{P}^4 + 4\hat{P}\cdot q\hat{P}^2 + [\hat{P}^2, \hat{P}\cdot q] + 4(\hat{P}\cdot q)^2\Big) \\
&+ 4\frac{g_S^2}{q^4}\hat{f}_{\mu\mu'}\hat{f}_{\mu'\nu} + 2\frac{g_S}{q^4}\Big(\hat{P}^2\hat{f}_{\mu\nu} + \hat{f}_{\mu\nu}\hat{P}^2\Big) + 4\frac{g_S}{q^4}\Big(\hat{f}_{\mu\nu}\hat{P}\cdot q + \hat{P}\cdot q\hat{f}_{\mu\nu}\Big)\Big\} \\
&- 2\frac{\hat{P}\cdot q}{q^2}\Big\{\frac{g_{\mu\nu}}{q^4}\Big(4\hat{P}\cdot q\hat{P}^2 + [\hat{P}^2, \hat{P}\cdot q] + 4(\hat{P}\cdot q)^2\Big) + 4\frac{g_S}{q^4}\Big(\hat{P}\cdot q\hat{f}_{\mu\nu} + \hat{f}_{\mu\nu}\hat{P}\cdot q\Big)\Big\} \\
&- \frac{4}{q^4}\Big\{g_{\mu\nu}\frac{\hat{P}^2}{q^2} + 2g_S\frac{\hat{f}_{\mu\nu}}{q^2}\Big\}(\hat{P}\cdot q)^2 + 16\frac{g_{\mu\nu}}{q^8}(q\cdot\hat{P})^4\Bigg)\,.
\end{aligned}
\tag{B.6}
$$

For the evaluation of the matrix elements of the operators that appear in the previous expansion, the following results are the most relevant:

$$\int d^4x\langle x|\hat{P}_\alpha|0\rangle = 0\,, \tag{B.7}$$

$$\int d^4x\langle x|\hat{P}_\alpha\hat{P}_\beta|0\rangle = -ig_S t^a\partial_\beta a^a_\alpha(x)|_{x=0} = \frac{i}{2}g_S t^a f^a_{\alpha\beta}|_{x=0}\,, \tag{B.8}$$

$$
\begin{aligned}
\int d^4x\langle x|\hat{P}_\alpha\hat{P}_\beta\hat{P}_\mu|0\rangle &= -g_S t^a\partial_\mu\partial_\beta a^a_\alpha(x)|_{x=0} \\
&= -g_S t^a\frac{1}{3}(D_\beta f_{a\mu\alpha} + D_\mu f_{a\beta\alpha})|_{x=0}\,,
\end{aligned}
\tag{B.9}
$$

$$
\begin{aligned}
&\int d^4x\langle x|\hat{P}_\alpha\hat{P}_\beta\hat{P}_\mu\hat{P}_\nu|0\rangle \\
&\quad= g_S t^a\int d^4x\langle x|(i\partial_\nu\partial_\mu\partial_\beta\hat{a}^a_\alpha - g_S t^b\partial_\mu\hat{a}^a_\alpha\partial_\nu\hat{a}^b_\beta - g_S t^b\partial_\nu\hat{a}^a_\alpha\partial_\mu\hat{a}^b_\beta - g_S t^c\partial_\beta\hat{a}^a_\alpha\partial_\nu\hat{a}^c_\mu)|0\rangle \\
&\quad= \frac{i}{8}g_S D_{(\nu}D_\mu t^a f^a_{\beta)\alpha}|_{x=0} - \frac{g_S^2}{4}t^a t^b(f^a_{\mu\alpha}f^b_{\nu\beta} + f^a_{\nu\alpha}f^b_{\mu\beta} + f^a_{\beta\alpha}f^b_{\nu\mu})|_{x=0}\,,
\end{aligned}
\tag{B.10}
$$

$$\int d^4x\langle x|\hat{f}_{\mu\nu}\hat{P}_\alpha|0\rangle = -iD_\alpha f_{\mu\nu}|_{x=0} \tag{B.11}$$

$$\int d^4x\langle x|\hat{P}_\alpha\hat{f}_{\mu\nu}\hat{P}_\beta|0\rangle = \frac{i}{2}g_S t^a f^a_{\alpha\beta}f_{\mu\nu}|_{x=0}\,, \tag{B.12}$$

$$\int d^4x\langle x|\hat{f}_{\mu\nu}\hat{P}_\alpha\hat{P}_\beta|0\rangle = \frac{i}{2}g_S t^a f^a_{\alpha\beta}f_{\mu\nu}|_{x=0} - D_\beta D_\alpha f_{\mu\nu}\,, \tag{B.13}$$

where parentheses between Lorentz indices represent symmetrization without normalization factor of $1/n!$. Beyond the usual commutation relations of gauge–covariant derivatives, to obtain these results the following identities were used:

$$
\begin{aligned}
&\int d^4x\langle x|\hat{p}_\mu\ldots|0\rangle = \langle q=0|\hat{p}_\mu\ldots|0\rangle = 0\,, \\
&\int d^4x\langle x|\ldots\hat{a}^a_\mu|0\rangle \longrightarrow a^a_\mu(0) = 0\,.
\end{aligned}
\tag{B.14}
$$

Inserting these matrix elements ((B.7)–(B.13)) and the expansion (B.6) in (B.5), the gluon propagator reads:

$$\begin{aligned} D_{F,\mu\nu}^{c'c}(q) = & \frac{-i}{q^2}g_{\mu\nu} + 2ig_S\frac{f_{\mu\nu}}{q^4} - 4\frac{g_S}{q^6}q_\alpha D^\alpha f_{\mu\nu} + g_S\frac{2}{3}\frac{g_{\mu\nu}}{q^6}q_\alpha D^\beta f_{a\beta\alpha} + i\frac{2g_S}{q^8}g_{\mu\nu}q^\alpha q^\beta D_\beta D^{\mu'} f_{\mu'\alpha} \\ & + 2i\frac{g_S}{q^6}D^2 f_{\mu\nu} - \frac{8i}{q^8}g_S q_\alpha q_\beta D^\beta D^\alpha f_{\mu\nu} + i\frac{g_S^2}{2}\frac{g_{\mu\nu}}{q^6}f_{\alpha\mu'}f^{\mu'\alpha} + i\frac{g_S^2}{q^8}g_{\mu\nu}q^\alpha q^\beta f_{\ \beta}^{\mu'} f_{\mu'\alpha} \\ & - 4i\frac{g_S^2}{q^6}f_{\mu\mu'}f^{\mu'}_{\ \ \nu}\,, \end{aligned} \tag{B.15}$$

which concludes our computation of the gluon propagator.

B.3 Basis change from (2.52) to (2.7)

In section 2.4 we presented a master formula from [35] for the unrenormalized Wilson coefficients of operator $S_{i,\mu\nu}$ with one cut quark line and up to one soft gluon or photon insertion. Such formula is not written in terms of the original operators $S_{i,\mu\nu}$ but rather in terms of new operators which are built from background quark fields, Dirac matrices and covariant derivatives. The transformation relations between such new operators and the original ones $S_{i,\mu\nu}$ were presented but not justified. The purpose of this appendix is to describe the computation of those transformation relations.

Let us start with the only non–trivial matrix element with one covariant derivative:

$$\begin{aligned} \langle\overline{\Psi}D^\nu\gamma^\alpha\gamma_5\Psi\rangle &= \frac{1}{2}\langle\overline{\Psi}(\not{D}\gamma^\nu + \gamma^\nu\not{D})\gamma^\alpha\gamma_5\Psi\rangle \\ &= -im_f\frac{1}{2}\langle\overline{\Psi}\gamma^\nu\gamma^\alpha\gamma_5\Psi\rangle + \frac{1}{2}\langle\overline{\Psi}\gamma^\nu(2D^\alpha - im_f\gamma^\alpha)\gamma_5\Psi\rangle \\ &= -im_f\langle\overline{\Psi}\gamma^\nu\gamma^\alpha\gamma_5\Psi\rangle + \langle\overline{\Psi}D^\alpha\gamma^\nu\gamma_5\Psi\rangle\,, \end{aligned} \tag{B.16}$$

where we have used 1) the quark equations of motion to replace covariant derivatives for quark masses and 2) the fact that soft matrix elements of total derivatives vanish, which allows us to reverse the direction of covariant derivatives. Since all these matrix elements must be proportional to either $F_{\mu\nu}$ or its dual tensor, then we are interested in its antisymmetric part with respect to ν, α. Therefore we have:

$$\begin{aligned} \langle\overline{\Psi}D^{[\nu}\gamma^{\alpha]}\gamma_5\Psi\rangle &= -\frac{m_f}{2}\langle\overline{\Psi}\sigma^{\nu\alpha}\gamma_5\Psi\rangle \\ &= -i\frac{m_f}{4}\epsilon^{\nu\alpha\tau\rho}\langle\overline{\Psi}\sigma_{\tau\rho}\Psi\rangle \\ &= -i\frac{m_f}{4}\epsilon^{\nu\alpha\tau\rho}X_2^S\langle ee_f F_{\tau\rho}\rangle \end{aligned} \tag{B.17}$$

and in the second line we have used an identity of the product of Dirac matrices from [131].[1]

[1] Note that in [131] the author defines $\gamma_5 \equiv \gamma_0\gamma_1\gamma_2\gamma_3$ instead of the more standard definition $\gamma_5 \equiv i\gamma_0\gamma_1\gamma_2\gamma_3$ that is used in [35] and in this work.

With respect to matrix elements of operators with two covariant derivatives we have:

$$\begin{aligned}\langle\overline{\Psi}D^{\nu_1}D^{\nu_2}\Psi\rangle &= \frac{1}{2}\langle\overline{\Psi}(-ig_S G^{a\nu_1\nu_2}t^a - iee_f F^{\nu_1\nu_2})\Psi\rangle \\ &= -\frac{i}{2}\Big(X_5^S - X_3^S\Big)\langle ee_f F^{\nu_1\nu_2}\rangle\ .\end{aligned} \tag{B.18}$$

Note that we have used that $[D^\mu, D^\nu] = -i(g_S t^a G^{a\mu\nu} + ee_f F^{\mu\nu})$ which is in line with the definition of the covariant derivatives that was done in chapter 2.

The next term with two covariant derivatives is:

$$\begin{aligned}\langle\overline{\Psi}D^{\nu_1}D^{\nu_2}\gamma_5\Psi\rangle &= -\frac{i}{2}\langle\overline{\Psi}(g_S t^a G^{a\nu_1\nu_2} + ee_f F^{\nu_1\nu_2})\gamma_5\Psi\rangle \\ &= \frac{i}{8}\epsilon^{\nu_1\nu_2\alpha\beta}\epsilon_{\alpha\beta\tau\rho}\langle\overline{\Psi}g_S t^a G^{a\tau\rho}\gamma_5\Psi\rangle \\ &= -\frac{X_4^S}{4}\epsilon^{\nu_1\nu_2\alpha\beta}\langle ee_f F_{\alpha\beta}\rangle\ .\end{aligned} \tag{B.19}$$

Note that we have neglected the $F^{\nu_1\nu_2}$ contribution due to its parity.

The last element with two covariant derivatives is $\langle\overline{\Psi}D^{\nu_1}D^{\nu_2}\sigma^{\alpha\beta}\Psi\rangle$. The antisymmetric part with respect to ν_1, ν_2 is proportional to the field–strength tensors that have odd C–parity. Since the part $\overline{\Psi}\sigma^{\alpha\beta}\Psi$ also has odd C–parity, this part of the operator has a net even C–parity and therefore its one–photon matrix element vanishes. Therefore the tensor structure of the matrix element must be:

$$\begin{aligned}\langle\overline{\Psi}D^{\nu_1}D^{\nu_2}\sigma^{\alpha\beta}\Psi\rangle &= A_1 g^{\nu_1\nu_2}\langle ee_f F^{\alpha\beta}\rangle \\ &+ ee_f A_2\Big(g^{\nu_1\alpha}\langle F^{\nu_2\beta}\rangle + g^{\nu_2\alpha}\langle F^{\nu_1\beta}\rangle - g^{\nu_1\beta}\langle F^{\nu_2\alpha}\rangle - g^{\nu_2\beta}\langle F^{\nu_1\alpha}\rangle\Big)\ .\end{aligned} \tag{B.20}$$

To find the form factors A_i we need two equations which we find by contracting pairs of Lorentz indices. Let us start with:

$$\begin{aligned}\langle\overline{\Psi}D^2\sigma^{\alpha\beta}\Psi\rangle &= 4(A_1 + A_2)\langle ee_f F^{\alpha\beta}\rangle \\ &= \langle\overline{\Psi}(\not{D}\not{D} + \frac{i}{2}[D_\mu, D_\nu]\sigma^{\mu\nu})\sigma^{\alpha\beta}\Psi\rangle \\ &= -m_f^2 X_2^S\langle ee_f F^{\alpha\beta}\rangle \\ &+ \frac{1}{2}\langle\overline{\Psi}(g_S t^a G^a_{\mu\nu} + ee_f F_{\mu\nu})\Big(g^{\mu\alpha}g^{\nu\beta} - g^{\mu\beta}g^{\nu\alpha} + i\epsilon^{\mu\nu\alpha\beta}\gamma_5\Big)\Psi\rangle \\ &= \Big(-m_f^2 X_2^S + X_5^S - X_3^S - X_4^S\Big)\langle ee_f F^{\alpha\beta}\rangle\ ,\end{aligned} \tag{B.21}$$

where we have used an identity from [131] for the product $\sigma^{\mu\nu}\sigma^{\alpha\beta}$. We have also discarded some elements because of their C–parity by the same arguments that we used for the previous matrix element. The other independent equation can be found by contracting ν_2 and α:

$$\begin{aligned}\langle\overline{\Psi}D^{\nu_1}D_\alpha\sigma^{\alpha\beta}\Psi\rangle &= (A_1 + 4A_2)\langle ee_f F^{\nu_1\beta}\rangle \\ &= \frac{i}{2}\langle\overline{\Psi}D^{\nu_1}(\not{D}\gamma^\beta + im_f\gamma^\beta)\Psi\rangle \\ &= \frac{1}{2}\langle\overline{\Psi}\Big(m_f\gamma^\beta D^{\nu_1} + \gamma^\rho\gamma^\beta(g_S t^a G^{a\nu_1}_{\ \ \rho} + eF^{\nu_1}_{\ \ \rho})\Big)\Psi\rangle - \frac{m_f}{2}\langle\overline{\Psi}D^{\nu_1}\gamma^\beta\Psi\rangle \\ &= \frac{1}{2}(X_5^S - X_3^S)\langle ee_f F^{\nu_1\beta}\rangle\ .\end{aligned} \tag{B.22}$$

Solving this system of two equations for A_1 and A_2 we find the relations cited in chapter 2:

$$\begin{aligned} A_1 &= \frac{1}{3}\Big(- m_f^2 X_2^S - X_S^4 + \frac{1}{2}(X_5^S - X_3^S)\Big) \\ A_2 &= \frac{1}{12}(m_f^2 X_2^S + X_S^4 + X_5^S - X_3^S)\ . \end{aligned} \tag{B.23}$$

There are two non–trivial matrix elements with three covariant derivatives. The first one that we consider is $\langle\overline{\Psi}D^{\nu_1}D^{\nu_2}D^{\nu_3}\gamma^\alpha\Psi\rangle$. Let us first see that it is antisymmetric with respect to ν_1 and ν_3. We can conclude this by noting that its symmetric part is even under charge conjugation:

$$\begin{aligned} \langle\overline{\Psi}D^{\{\nu_1}D^{\nu_2}D^{\nu_3\}}\gamma^\alpha\Psi\rangle \longrightarrow &\langle(D^{\{\nu_1}D^{\nu_2}D^{\nu_3\}}\overline{\Psi})\gamma^\alpha\Psi\rangle(-1) \\ &\langle\overline{\Psi}D^{\{\nu_3}D^{\nu_2}D^{\nu_1\}}\gamma^\alpha\Psi\rangle\ , \end{aligned} \tag{B.24}$$

where in the last step we were able to change the direction of the covariant derivatives by introducing a minus sign owing to the fact that soft matrix elements of total covariant derivatives vanish. Thus we can conclude:

$$\begin{aligned} \frac{1}{ee_f}\langle\overline{\Psi}D^{\nu_1}D^{\nu_2}D^{\nu_3}\gamma^\alpha\Psi\rangle = &A_3(g^{\nu_1\nu_2}\langle F^{\nu_3\alpha}\rangle - g^{\nu_2\nu_3}\langle F^{\nu_1\alpha}\rangle) \\ &+ A_4(g^{\nu_1\alpha}\langle F^{\nu_2\nu_3}\rangle + g^{\nu_3\alpha}\langle F^{\nu_1\nu_2}\rangle) + A_5 g^{\nu_2\alpha}\langle F^{\nu_1\nu_3}\rangle\ . \end{aligned} \tag{B.25}$$

For this matrix element we will have to contract three pairs of indices and solve the corresponding three–equation system. Let us start with ν_3 and α:

$$\begin{aligned} \langle\overline{\Psi}D^{\nu_1}D^{\nu_2}D_\tau\gamma^\tau\Psi\rangle &= \Big(- A_3 + 3A_4 + A_5\Big)\langle ee_f F^{\nu_1\nu_2}\rangle \\ &= -\frac{m_f}{2}\Big(X_5^S - X_3^S\Big)\langle ee_f F^{\nu_1\nu_2}\rangle \\ &= \langle\overline{\Psi}D_\tau D^{\nu_1}D^{\nu_2}\gamma^\tau\Psi\rangle\ . \end{aligned} \tag{B.26}$$

For ν_2 and α we have:

$$\begin{aligned} \langle\overline{\Psi}D^{\nu_1}D_\tau D^{\nu_3}\gamma^\tau\Psi\rangle &= \Big(- 2A_3 + 2A_4 + 4A_5\Big)\langle ee_f F^{\nu_1\nu_3}\rangle \\ &= -\frac{m_f}{2}\Big(X_5^S - X_3^S\Big)\langle ee_f F^{\nu_1\nu_3}\rangle - \langle\overline{\Psi}D^{\nu_1}G_\tau{}^{\nu_3}\gamma^\tau\Psi\rangle - i\langle\overline{\Psi}D^{\nu_1}ee_f F_\tau{}^{\nu_3}\gamma^\tau\Psi\rangle \\ &= \frac{1}{2}\left(- \frac{3}{2}m_f X_5^S + m_f X_3^S + \frac{1}{2}X_7^S\right)\langle ee_f F^{\nu_1\nu_3}\rangle\ , \end{aligned} \tag{B.27}$$

where we have used that:

$$\langle\overline{\Psi}D^{\nu_1}ee_f F_\tau{}^{\nu_3}\gamma^\tau\Psi\rangle = -i\frac{m_f X_5^S}{4}\langle ee_f F^{\nu_1\nu_3}\rangle\ . \tag{B.28}$$

We can continue with ν_1 and ν_2:

$$\begin{aligned}
\langle\overline{\Psi}D_\tau D^\tau D^{\nu_3}\gamma^\alpha\Psi\rangle &= \Big(3A_3 - A_4 - A_5\Big)\langle ee_f F^{\nu_3\alpha}\rangle \\
&= -\frac{i}{2}\langle\overline{\Psi}G_{\mu\nu}\sigma^{\mu\nu}D^{\nu_3}\gamma^\alpha\Psi\rangle + \frac{1}{2}\langle\overline{\Psi}ee_f F_{\mu\nu}\sigma^{\mu\nu}D^{\nu_3}\gamma^\alpha\Psi\rangle \\
&= \frac{1}{2}\langle\overline{\Psi}(-2G^\alpha{}_\nu\gamma^\nu + iG_{\mu\nu}\epsilon^{\mu\nu\alpha\tau}\gamma_\tau\gamma_5)D^{\nu_3}\Psi\rangle \\
&+ \frac{1}{2}\langle\overline{\Psi}ee_f(-2iF^\alpha{}_\nu\gamma^\nu - F_{\mu\nu}\epsilon^{\mu\nu\alpha\tau}\gamma_\tau\gamma_5)D^{\nu_3}\Psi\rangle \\
&= \frac{X_7^S}{4}\langle ee_f F^{\nu_3\alpha}\rangle + \langle\overline{\Psi}\,\overline{G}^{\alpha\tau}\gamma_\tau\gamma_5 D^{\nu_3}\Psi\rangle \\
&+ \frac{m_f X_5^S}{4}\langle ee_f F^{\nu_3\alpha}\rangle - \frac{1}{2}ee_f F_{\mu\nu}\epsilon^{\mu\nu\alpha\tau}\langle\overline{\Psi}\gamma_\tau\gamma_5 D^{\nu_3}\Psi\rangle \\
&= \Big(\frac{X_7^S}{4} - \frac{X_{8,1}^S}{2} - \frac{X_4^S}{2} + \frac{m_f X_5^S}{4}\Big)\langle ee_f F^{\nu_3\alpha}\rangle\,,
\end{aligned} \tag{B.29}$$

where we have used that:

$$\langle\overline{\Psi}\,\overline{G}^{\alpha\tau}\gamma_\tau\gamma_5 D^{\nu_3}\Psi\rangle = -\frac{X_{8,1}^S}{2}\langle ee_f F^{\nu_3\alpha}\rangle - \frac{X_4^S}{2}\langle ee_f F^{\nu_3\alpha}\rangle\,. \tag{B.30}$$

Solving the system of three equations one finds:

$$\begin{aligned}
A_3 &= \frac{1}{24}\Big(-5X_{8,1}^S + 2X_7^S - 5m_f X_4^S + 2m_f X_3^S\Big)\,, \\
A_4 &= \frac{1}{24}\Big(-5X_{8,1}^S + X_7^S - 3m_f X_5^S - m_f X_4^S + 4m_f X_3^S\Big)\,, \\
A_5 &= \frac{1}{24}\Big(-2X_{8,1}^S - X_7^S - 3m_f X_5^S - 2m_f X_4^S + 2m_f X_3^S\Big)\,.
\end{aligned} \tag{B.31}$$

Appendix C

Triangle scalar loop integrals in arbitrary dimensions

In chapter 3 we quoted the result of [123] for scalar triangle loop integrals in arbitrary space–time dimensions (3.65) with unit propagator powers, $J_3^{(d)}$. In this appendix we complete the definition of relevant quantities that we used and present the results in a way that clearly shows the appearance of logarithms and ultraviolet singularities.

First, let us define the Cayley determinant S_3:

$$S_3 = \begin{vmatrix} 2m_1^2 & -p_1^2+m_1^2+m_2^2 & -p_3^2+m_1^2+m_3^2 \\ -p_1^2+m_1^2+m_2^2 & 2m_2^2 & -p_2^2+m_2^2+m_3^2 \\ -p_3^2+m_1^2+m_3^2 & -p_2^2+m_2^2+m_3^2 & 2m_3^2 \end{vmatrix} . \tag{C.1}$$

In the same fashion we define the Cayley determinants S_{ij} of self–energy integrals, which are obtained by suppressing one of the three propagators in the triangle:

$$S_{ij} = \begin{vmatrix} 2m_i^2 & -p_i^2+m_i^2+m_j^2 \\ -p_i^2+m_i^2+m_j^2 & 2m_j^2 \end{vmatrix} = -\lambda_-(p_i^2, m_i^2, m_j^2) . \tag{C.2}$$

Similarly for the Gram determinants we have:

$$\begin{aligned} G_3 &= -8 \begin{vmatrix} p_1^2 & p_1\cdot p_2 \\ p_1\cdot p_2 & p_2^2 \end{vmatrix} = 2\lambda_-(p_1^2, p_2^2, p_3^2) , \\ G_{12} &= -4p_1^2 , \qquad G_{13} = -4p_3^2 , \qquad G_{23} = -4p_2^2 , \end{aligned} \tag{C.3}$$

where $p_3 = -p_1 - p_2$. Finally we have $M_3 = S_3/G_3$ and $M_{ij} = S_{ij}/S_3$.

Now let us define x_k:

$$x_1 = 1 - \frac{D - E\beta + 2(C - B\beta)}{2(1-\beta)(C-B\beta)} , \qquad x_2 = 1 + \frac{D - E\beta}{2(C-B\beta)} , \qquad x_3 = -\frac{D-E\beta}{2\beta(C-B\beta)} , \tag{C.4}$$

where

$$\begin{aligned} A &= p_1^2 , \qquad B = p_3^2 , \qquad C = -p_1\cdot p_3 , \qquad D = -(p_1^2 + m_1^2 - m_2^2) , \\ E &= -(p_3^2 + m_1^2 - m_3^2) , \qquad F = m_1^2 , \qquad \beta = \frac{C + \sqrt{C^2 - AB}}{B} . \end{aligned} \tag{C.5}$$

x_{ij} and x_k fulfill the following relevant identities:

$$p_i^2 x_{ij}^2 = m_i^2 - M_{ij} \,, \qquad p_i^2 (x_k - x_{ij})^2 = M_3 - M_{ij} \,. \tag{C.6}$$

Finally, we will present the formulas for the case $d = 4 + 2k - 2\epsilon$ with $k \in \mathbb{N}$, which are relevant for our computation. Keeping full ϵ dependence we have:

$$\begin{aligned}
&J_3^{(4+2k)} \times \frac{(4\pi)^{2+k} \lambda_-^{1/2}(p_1^2, p_2^2, p_3^2)}{i(4\pi)^\epsilon} \\
&\quad = \Gamma(-k+\epsilon)\Big(M_3^k \Big(\frac{\mu^2}{M_3}\Big)^\epsilon - M_{ij}^k \Big(\frac{\mu^2}{M_{ij}}\Big)^\epsilon \Big) \sum_{n_1=1} \frac{1}{n_1} \left(- \frac{x_{ij}}{x_k - x_{ij}} \right)^{n_1} \\
&\quad - M_{ij}^k \Big(\frac{\mu^2}{M_{ij}}\Big)^\epsilon \left[\sum_{\substack{n_1=1 \\ n_2=1}}^{n_2=k} \frac{\Gamma\big(-k+n_2+\epsilon\big)}{(n_1+2n_2)n_2!} \left(- \frac{x_{ij}}{x_k - x_{ij}} \right)^{n_1} \left(- \frac{p_i^2 x_{ij}^2}{M_{ij}} \right)^{n_2} \right. \\
&\qquad \left. + \sum_{\substack{n_1=1 \\ n_2=k+1}} \frac{\Gamma\big(-k+n_2\big)}{(n_1+2n_2)n_2!} \left(- \frac{x_{ij}}{x_k - x_{ij}} \right)^{n_1} \left(- \frac{p_i^2 x_{ij}^2}{M_{ij}} \right)^{n_2} \right] \\
&\quad - \Big\{ x_{ij} \to 1 - x_{ij} \;\; ; \;\; x_k \to 1 - x_k \Big\} \,.
\end{aligned} \tag{C.7}$$

Note that we neglected the infinitesimal term $i\epsilon$ that gives the Feynman prescription, because it is not relevant in the deep space–like region that we are interested in. Nevertheless, it can be easily reinstated by replacing $M_{ij} \to M_{ij} - i\epsilon$ and $M_3 \to M_3 - i\epsilon$. Taking the limit $\epsilon \to 0$ we have:

$$\begin{aligned}
&J_3^{(d)} \times \frac{(4\pi)^{2+k} \lambda_-^{1/2}}{i} \\
&\quad = \frac{(-1)^k}{k!} \left\{ M_3^k \Big(\frac{1}{\hat{\epsilon}} + \ln\Big\{ \frac{\mu^2}{M_3} \Big\} \Big) - M_{ij}^k \Big(\frac{1}{\hat{\epsilon}} + \ln\Big\{ \frac{\mu^2}{M_{ij}} \Big\} \Big) \right\} \sum_{n_1=1} \frac{1}{n_1} \left(- \frac{x_{ij}}{x_k - x_{ij}} \right)^{n_1} \\
&\quad + \frac{(-1)^k}{k!} \sum_{j=1}^{k} \frac{1}{j} \Big(M_3^k - M_{ij}^k \Big) \sum_{n_1=1} \frac{1}{n_1} \left(- \frac{x_{ij}}{x_k - x_{ij}} \right)^{n_1} \\
&\quad - M_{ij}^k \Big(\frac{1}{\hat{\epsilon}} + \ln\Big\{ \frac{\mu^2}{M_{ij}} \Big\} \Big) \left[\sum_{\substack{n_1=1 \\ n_2=1}}^{n_2=k} \frac{(-1)^{k-n_2}}{(n_1+2n_2)(k-n_2)!n_2!} \left(- \frac{x_{ij}}{x_k - x_{ij}} \right)^{n_1} \left(- \frac{p_i^2 x_{ij}^2}{M_{ij}} \right)^{n_2} \right. \\
&\quad - M_{ij}^k \left[\sum_{\substack{n_1=1 \\ n_2=1}}^{n_2=k} \frac{1}{(n_1+2n_2)n_2!} \left(- \frac{x_{ij}}{x_k - x_{ij}} \right)^{n_1} \left(- \frac{p_i^2 x_{ij}^2}{M_{ij}} \right)^{n_2} \frac{(-1)^{k-n_2}}{(k-n_2)!} \sum_{j=1}^{k-n_2} \frac{1}{j} \right. \\
&\qquad \left. \left. + \sum_{\substack{n_1=1 \\ n_2=k+1}} \frac{\Gamma\big(-k+n_2\big)}{(n_1+2n_2)n_2!} \left(- \frac{x_{ij}}{x_k - x_{ij}} \right)^{n_1} \left(- \frac{p_i^2 x_{ij}^2}{M_{ij}} \right)^{n_2} \right] \right. \\
&\quad - \Big\{ x_{ij} \to 1 - x_{ij} \;\; ; \;\; x_k \to 1 - x_k \Big\} \,,
\end{aligned}$$

where a sum over the three permutations $(i,j,k) \to (1,2,3) \to (2,3,1) \to (3,1,2)$ is implied. μ is the renormalization scale. The singular terms $1/\hat{\epsilon}$ vanish and dependence on μ disappears when powers of the propagators get high enough via derivatives with respect to the masses.

Bibliography

[1] D. Hanneke, S. Hoogerheide, and G. Gabrielse. In: Physical Review A 83.052122 (2011).

[2] D. Hanneke, S. Fogwell, and G. Gabrielse. In: Physical Review A 100.120801 (2008).

[3] T. Aoyama, T. Kinoshita, and M.Nio. In: Physical Review D 97.036001 (2018).

[4] G. W. Bennet et al. In: Physical Review D 73.072003 (2006).

[5] B.Abi et al. In: Physical Review Letters 126.141801 (2021).

[6] T. Aoyama et al. In: Physics Reports 887 (2020), pp. 1–166.

[7] G. Colangelo et al. In: (2022). arXiv:2203.15810 [hep-ph]. URL: https://doi.org/10.48550/arXiv.2203.15810.

[8] J. Grange et al. In: (2015). arXiv:1501.06858 [physics.ins-det]. URL: https://doi.org/10.48550/arXiv.1501.06858.

[9] S. J. Brodsky and E. de Rafael. In: Physical Review 168.1620 (1968).

[10] B. E. Lautrup and E. de Rafael. In: Physical Review 174.1835 (1968).

[11] V.L. Ivanov et al. In: ArXiv 2008.05548 (2020).

[12] E. V. Abakumovaa, M. N. Achasova, and V. E. Blinova. In: Nuclear Instruments and Methods 651 (2011), pp. 21–29.

[13] F. Ambrosino et al. In: Physical Letters B 670.285 (2009).

[14] B. Aubert et al. In: Physical Review Letters 103.231801 (2009).

[15] R. Alemany, M. Davier, and A. Hoecker. In: European Physical Journal C2.123 (1998).

[16] C. M. Carloni Calame et al. In: Physical Letters B 325 (2015), p. 746.

[17] G. Abbiendi et al. In: European Physical Journal C 139 (2017), p. 77.

[18] P. Banerjee et al. In: European Physical Journal C 80.591 (2020).

[19] Sz. Borsanyi et al. In: Nature 593 (2021), pp. 51–55.

[20] Alexei Bazavov et al. In: (2023). arXiv:2301.08274 [hep-lat]. URL: https://doi.org/10.48550/arXiv.2301.08274.

[21] E. De Rafael. In: Inference Review 6.3 (2021). URL: https://inference-review.com/article/muons-and-new-physics.

[22] G. Colangelo, M.Hoferichter, M. Procura, et al. In: JHEP 74 (2015).

[23] G. Colangelo, M. Hoferichter, M. Procura, et al. In: JHEP 161 (2017).

[24] M. Hoferichter et al. In: Physical Review Letters 121.112002 (2018).

[25] G. Colangelo et al. In: Physical Review Letters 118.232001 (2017).

[26] M. Hayakawa, T. Kinoshita, and A. I. Sanda. In: Physical Review Letters 75.790 (1995).

[27] J. Bijnens, E. de Rafael, and H. Zheng. "Low-Energy Behaviour of Two-Point Functions of Quark Currents". In: Zeitschrift für Physik C Particles and Fields 62 (1994), pp. 437–454.

[28] G. Colangelo, M.Hoferichter, M. Procura, et al. In: JHEP 91 (2014).

[29] Johan Bijnens et al. In: JHEP 2003.0304 (2003). arXiv:hep-ph/0304222. URL: https://doi.org/10.1088/1126-6708/2003/04/055.

[30] M. Knecht and A. Nyffeler. In: The European Physical Journal C 21 (2001). arXiv:hep-ph/0106034, 659—678. URL: https://doi.org/10.1007/s100520100755.

[31] G. Colangelo et al. In: Physical Review D 101.051501 (2020). arXiv:1910.11881 [hep-ph]. URL: https://doi.org/10.1103/PhysRevD.101.051501.

[32] Gilberto Colangelo et al. In: JHEP 2020.101 (2020). arXiv:1910.13432 [hep-ph]. URL: https://doi.org/10.1007/JHEP03%282020%29101.

[33] Gilberto Colangelo et al. In: The European Physical Journal C 81.702 (2021). arXiv:2106.13222 [hep-ph]. URL: https://doi.org/10.1140/epjc/s10052-021-09513-x.

[34] J. Bijnens, N. Hermansson-Truedsson, and A. Rodriguez-Sanchez. In: Physical Letters B 798.134994 (2019). arXiv:1908.03331 [hep-ph].

[35] J. Bijnens et al. In: Nuclear and Particle Physics Proceedings 312-317 (2020), pp. 180–184.

[36] J. Bijnens, N. Hermansson-Truedsson, and A. Rodríguez-Sánchez. In: Journal of High Energy Physics 04.240 (2021). arXiv:2101.09169v2 [hep-ph]. URL: https://doi.org/10.1007/JHEP04%282021%29240.

[37] V. Shtabovenko, R. Mertig, and F. Orellana. In: Computer Physics Communications 256.107478 (2020). arXiv:2001.04407.

[38] V. Shtabovenko, R. Mertig, and F. Orellana. In: Computer Physics Communications 207 (2016). arXiv:1601.01167, pp. 432–444.

[39] R. Mertig, M. Böhm, and A. Denner. In: Computer Physics Communications 64.3 (1991), pp. 345–359. URL: https://doi.org/10.1016/0010-4655(91)90130-D.

[40] B. Ananthanarayan et al. In: Physical Review Letters 127.151601 (2021). arXiv:2012.15108 [hep-th]. URL: https://doi.org/10.1103/PhysRevLett.127.151601.

[41] A. I. Davydychev. In: Physics Letters B 263.1 (1991), pp. 107–111. URL: https://doi.org/10.1016/0370-2693(91)91715-8.

[42] A. I. Davydychev. In: Journal of Mathematical Physics 32.1052 (1991). URL: doi:10.1063/1.529383.

[43] Stanley J. Brodsky and J. D. Sullivan. In: Physical Review 156.5 (1967), pp. 1644–1647.

[44] Janis Aldins, Stanley J. Brodsky, and Toichiro Kinoshita. In: Physical Review D 1.8 (1970).

[45] Marc Knecht and Nyffeler Andreas. In: Physical Review D 65.073034 (2002).

[46] Fred Jegerlehner. STMP – The Anomalous Magnetic Moment of the Muon. Vol. 274. Springer, 2017.

[47] F. E. Low. In: Physical Review 110.4 (1958), pp. 974–977.

[48] T. Blum et al. In: Physical Review Letters 124.132002 (2020). arXiv:1911.08123 [hep-lat].

[49] E.-H. Chao et al. In: European Physical Journal C 81.651 (2021). arXiv:2104.02632 [hep-lat].

[50] V. Pascalutsa, V. Pauk, and M. Vanderhaeghen. In: Physical Review D 85.116001 (2012). 1204.0740.

[51] V. Pauk and M. Vanderhaeghen. In: Physical Review D 90.11 (2014).

[52] J. Green et al. In: Physical Review Letters 115.222003 (2015). 1507.01577.

[53] I. Danilkin and M. Vanderhaeghen. In: Physical Review D 95.014019 (2017). 1611.04646.

[54] F. Hagelstein and V. Pascalutsa. In: Physical Review Letters 120.072002 (2018). 1710.04571.

[55] M. Peskin and D. Schroeder. An introduction to quantum field theory. Addison–Wesley Publishing Company, 1995.

[56] M. Sugawara and A. Kanazawa. In: Physical Review 123.1895 (1961). URL: https://doi.org/10.1103/PhysRev.123.1895.

[57] S. Mandelstam. In: Physical Review 112.4 (1958).

[58] Robert Karplus and Maurice Neuman. In: Physical Review 80.3 (1950), pp. 380–385.

[59] W. Bardeen and W. Tung. In: Physical Review 173.5 (1968), pp. 1423–1433.

[60] R. Tarrach. In: Nuov. Cim. A 28 (1975), 409—422. URL: https://doi.org/10.1007/BF02894857.

[61] Harry Bateman et al. Higher Trascendental Functions – Volume 1. McGraw–Hill, 1953.

[62] James D. Bjorken. In: Journal of Mathematical Physics 5.2 (1964), pp. 192–198.

[63] (Particle Data Group) R. L. Workman et al. In: Progress of Theoretical and Experimental Physics 2022.083C01 (2022).

[64] P. Masjuan and P. Sanchez-Puertas. In: Physical Review Letters D95.054026 (2017). arXiv:1701.05829 [hep-ph].

[65] M. Hoferichter et al. In: European Physical Journal C74.3180 (2014).

[66] M. Hoferichter et al. In: JHEP 10.141 (2018). arXiv:1808.04823 [hep-ph].

[67] G. A. Baker. Essentials of Padé Approximants. First. New York: Academic Press, 1975.

[68] P. Masjuan and S. Peris. In: Physical Review Letters B686.307 (2010). arXiv:0903.0294 [hep-ph].

[69] C. Hanhart et al. In: European Physical Journal C73.2668 (2013). arXiv:1307.5654 [hep-ph], Erratum: Eur. Phys. J. C75, 242 (2015).

[70] C.-W. Xiao et al. In: European Physical Journal C81.1002 (2021). arXiv:1509.02194 [hep-ph].

[71] Simon Holz et al. In: European Physical Journal C82.434 (2022). arXiv:2202.05846 [hep-ph].

[72] A. D. Martin and T. D. Spearman. Elementary Particle Theory. North Holland Publishing Company, 1970.

[73] I. Danilkin, O. Deineka, and M. Vanderhaeghen. In: Physical Review Letters D96.114018 (2017). arXiv:1709.08595 [hep-ph].

[74] O. Deineka, I. Danilkin, and M. Vanderhaeghen. In: European Physical Journal Web Conference 199.02005 (2019). arXiv:1808.04117 [hep-ph].

[75] V. Pauk and M. Vanderhaeghen. In: European Physical Journal C74.3008 (2014). arXiv:1401.0832 [hep-ph].

[76] I. Danilkin and M. Vanderhaeghen. In: Physical Review D 95.014019 (2017). arXiv:1611.04646 [hep-ph].

[77] M. Knecht et al. In: Physical Review Letters B787.111 (2018). arXiv:1808.03848 [hep-ph].

[78] R. N. Cahn. In: Physical Review Letters D35.3342 (1987).

[79] R. N. Cahn. In: Physical Review Letters D37.833 (1988).

[80] [L3 Collaboration] P. Achard et al. In: Physical Review Letters B526.269 (2002).

[81] [L3 Collaboration] P. Achard et al. In: JHEP 0703.018 (2007).

[82] P. Roig and P. Sanchez-Puertas. In: Physical Review D 101.074019 (2020). arXiv:1910.02881 [hep-ph].

[83] Gernot Eichmann et al. In: (2014). arXiv:1411.7876v2 [hep-ph].

[84] G. P. Lepage and S. J. Brodsky. In: Physics Letters B 87.359 (1979).

[85] G. P. Lepage and S. J. Brodsky. In: Physical Review D 22.2157 (1980).

[86] V. A. Nesterenko and A. V. Radyushkin. In: Soviet Journal of Nuclear Physics 38.284 (1983).

[87] V. A. Novikov et al. In: Nuclear Physics B 237.3 (1984), pp. 525–550.

[88] A. S. Gorsky. In: Soviet Journal of Nuclear Physics 46.537 (1987).

[89] A. V. Manohar. In: Physics Letters B 244.101 (1990).

[90] M. Hoferichter et al. In: JHEP 10.141 (2018). arXiv:1808.04823 [hep-ph].

[91] M. Hoferichter et al. In: Physical Review Letters 121.112002 (2018). arXiv:1805.01471 [hep-ph].

[92] Kenneth Wilson. In: Physical Review 179.1499 (1969).

[93] Steven Weinberg. The Quantum Theory of Fields. Cambridge University Press, 1996.

[94] B. L. Ioffe and A. V. Smilga. In: Nuclear Physics B 232 (1984), pp. 109–142. URL: doi:10.1016/0550-3213(84)90364-X.

[95] A. Czarnecki, W. J. Marciano, and A. Vainshtein. In: Physical Review D 67.073006 (2003). arXiv:hep-ph/0212229.

[96] V. A. Novikov et al. In: Fortschritte der Physik 32.11 (1984), pp. 585–622.

[97] M. A. Shifman, A. I Vainshtein, and V. I. Zakharov. In: Nuclear Physics B 147 (1979), pp. 385–518.

[98] M. A. Shifman et al. In: Physics Letters B 77.1 (1978), pp. 80–83. URL: https://doi.org/10.1016/0370-2693(78)90206-X.

[99] V. Fock. In: Physikalische Zeitschrift der Sowjetunion 12 (1937), pp. 404–425.

[100] M. A. Shifman. In: Nuclear Physics B173.1 (1980), pp. 13–31.

[101] R. Strichartz. A guide to distribution theory and Fourier transform. World Scientific Publishing Company, 2003.

[102] L. F. Abbott. In: Acta Physica Polonica B13.1–2 (1981). https://www.actaphys.uj.edu.pl/R/13/1/33/pdf, pp. 33–50.

[103] Y. Aoki et al. In: The European Physical Journal C 82.869 (2022). arXiv:2111.09849v2 [hep-lat].

[104] H. Kluberg-Stern and J. B. Zuber. In: Physical Review D 12.2 (1975), pp. 467–481. URL: https://doi.org/10.1103/PhysRevD.12.467.

[105] H. Kluberg-Stern and J. B. Zuber. In: Physical Review D 12.2 (1975), pp. 482–488. URL: https://doi.org/10.1103/PhysRevD.12.482.

[106] H. Kluberg-Stern and J. B. Zuber. In: Physical Review D 12.10 (1975), pp. 3159–3180. URL: https://doi.org/10.1103/PhysRevD.12.3159.

[107] Giampiero Passarino and Martinus Veltman. In: Nuclear Physics B 160.1 (1979), pp. 151–207. URL: https://doi.org/10.1016/0550-3213(79)90234-7.

[108] R. Keith Ellis et al. In: Physics Reports 518.4–5 (2012), pp. 141–250. URL: https://doi.org/10.1016/j.physrep.2012.01.008.

[109] Dima Bardin and Giampiero Passarino.
The Standard Model in the Making: Precision Study of the Elecroweak Interactions.
Clarendon Press, Oxford, 1999.

[110] É. É. Boos and A. I. Davydychev. In: Theoretical and Mathematical Physics 89 (1991), 1052—1064. URL: https://doi.org/10.1007/BF01016805.

[111] Sumit Banik and Samuel Friot. In: (2022). arXiv:2212.11839 [hep-ph]. URL: https://doi.org/10.48550/arXiv.2212.11839.

[112] O. N. Zhdanov and A. K. Tsikh. In: Siberian Mathematical Journal 39.2 (1998), pp. 245–260. URL: https://doi.org/10.1007/BF02677509.

[113] Oleg Igorevich Marichev. Methods for Computing Integrals of Special Functions.
Minsk, 1978.

[114] Henri Skoda and Jean-Marie Trepreau, eds.
Aspects of Mathematics: Contributions to Complex Analysis and Analytic Geometry.
Vol. E26. Springer, 1994, pp. 233–241.

[115] Kasper J. Larsen and Robbert Rietkerk. In: Computer Physics Communications 222 (2018). arXiv:1701.01040 [hep-th], pp. 250–262. URL: https://doi.org/10.1016/j.cpc.2017.08.025.

[116] P. Griffiths and J. Harris. Principles of algebraic geometry. John Wiley and Sons, 1978.

[117] M. Passare, A .K. Tsikh, and A. A. Cheshel. In: Theoretical and Mathematical Physics 109 (1996), 1544—1555. URL: https://doi.org/10.1007/BF02073871.

[118] E. W. Barnes. In: Proceedings of the London Mathematical Society s2-5 (1907), pp. 59–116.

[119] H. M. Srivastava and Per W. Karlsson. Multiple Gaussian Hypergeometric Series. John Wiley and Sons, 1985.

[120] J. Horn. In: Mathematische Annalen 34 (1889), 544—600. URL: https://doi.org/10.1007/BF01443681.

[121] Samuel Friot and David Greynat. In: Journal of Mathematical Physics 53.023508 (2012). arXiv:1107.0328 [math-ph]. URL: https://doi.org/10.1063/1.3679686.

[122] A. K. Tsikh.
Translations of Mathematical Monographs: Multidimensional Residues and Their Applications.
Vol. 103. American Mathematical Society, 1992.

[123] Khiem Hong Phan and Dzung Tri Tran. In:
Progress of Theoretical and Experimental Physics 2019.6 (2019). arXiv:1904.07430 [hep-ph]. URL: https://doi.org/10.1093/ptep/ptz050.

[124] Lucy Joan Slater. Generalized Hypergeometric Functions. Cambridge University Press, 1966.

[125] K. Melnikov and A. Vainshtein. In: Physical Review D 70.113006 (2004). arXiv:hep-ph/0312226. URL: https://doi.org/10.1103/PhysRevD.70.113006.

[126] Luigi Cappiello et al. In: Physical Review D 102.016009 (2020). arXiv:1912.02779 [hep-ph]. URL: https://doi.org/10.1103/PhysRevD.102.016009.

[127] Josef Leutgeb and Anton Rebhan. In: Physical Review D 101.114015 (2020). arXiv:1912.01596 [hep-ph]. URL: https://doi.org/10.1103/PhysRevD.101.114015.

[128] Johan Bijnens, Nils Hermansson-Truedsson, and Antonio Rodríguez-Sánchez. In: (2022). arXiv:2211.17183 [hep-ph]. URL: https://doi.org/10.48550/arXiv.2211.17183.

[129] Johan Bijnens, Nils Hermansson-Truedsson, and Antonio Rodríguez-Sánchez. In: EPJ Web of Conferences 274.06010 (2022). arXiv:2211.04068 [hep-ph]. URL: https://doi.org/10.1051/epjconf/202227406010.

[130] E. V. Shuryak and A. I. Vainshtein. In: Nuclear Physics B 201.1 (1982), pp. 141–158. URL: https://doi.org/10.1016/0550-3213(82)90377-7.

[131] A. J. Macfarlane. In: Communications in Mathematical Physics 2 (1966), pp. 133–146. URL: https://doi.org/10.1007/BF01773348.